POLITECNICO DI MILANO
DEPARTMENT OF ENERGY
DOCTORAL PROGRAMME IN ELECTRICAL ENGINEERING

ADVANCED STATE ESTIMATION IN DISTRIBUTION SYSTEMS

Doctoral Dissertation of:
Milos Subasic

Supervisor:
Prof. Cristian Bovo

Tutor:
Prof. Cristian Bovo

The Chair of the Doctoral Program:
Prof. Alberto Berizzi

2011-2014 – XXVII cycle

Acknowledgements

Firstly, I would like to thank to Prof. Alberto Berizzi for having a faith in my capabilities and giving me an opportunity to study and develop myself as a researcher during doctorate at Politecnico di Milano. I would also like to express the gratitude for his immediate help and advices in many stressful situations.
Secondly, my deep gratitude goes to my supervisor, Prof. Cristian Bovo for his sincere interest in my development and close attention he gave to my work and for having faith in me even when I wasn't sure about my capabilities. I wish also to thank him for enabling me to take part in the development of big project with the industry during my PhD. Without his guidance, ideas and expertize, I wouldn't be where I am now.
Finally, big thanks go to my older colleague, Valentin Ilea, for every-day involvement in my growth as a researcher and all the advices, help and support he gave me. His expertize was an inspiration for me and it tackled me to improve myself.

I would like to express my deepest gratitude for the support and love of my family. Growing up in a family of teachers and engineers is a great privilege. I can never thank my parents and grandparents enough for their encouragement and love. Individual attention from my mother, Gordana, an expert in early childhood education, was an enormous advantage. I am also grateful for the love and encouragement of my grandmother, Nadežda, whose teaching and literature knowledge was instrumental to my education. My gratitude also goes to my other grandmother, Nevenka, whose fighting through life and diligence was an inspiration for me. As a second-generation power engineer, I am proud to follow in the footsteps of my father, Zoran.
My father's power engineering background and his encouragement for learning math, physics and science provided a strong foundation for educational success. Love and encouragement of my grandfather, high school teacher, was a constant source of support throughout my education. He is fondly remembered and greatly missed. I am further thankful for the camaraderie and support of my brother, Nikola, who is also studying engineering.

Abstract

This research is composed of two major topics; first, the development of the State Estimation function for distribution systems and second, on of Measurement Equipment Placement for the sake of improvement of observability of distribution network.

The traditional vertically integrated structure of the electric utility has been deregulated in recent years particularly by adopting the competitive market paradigm in many countries around the world. The market-governed electrical business and the Renewable Energy Sources (RES) have changed significantly the power flows in distribution networks.

On the other side, the evolution of the distribution systems seen through the remarkable expansion of dispersed generation plants connected to the medium and low voltage network is one of the main challenges. The growth of the dispersed generation is causing a profound change of the distribution systems in the technical, legal and regulatory aspects; most likely the Distribution System Operators (DSOs) will more and more take, on local dimensions, tasks and responsibilities of the role assigned on a national scale to the operator of the electricity transmission network. In other words, the DSO will become a sort of a "local dispatcher" and will involve its real/passive customers in activities related to the network management and optimization. This, obviously, requires a deep review of the regulatory framework.

In this sense, definition of "Smart Grid", now usually in use, appears reduced as it focuses only on the appearance of the network, while it is more appropriate to speak about "Smart Distribution System" (SDS), extending the involvement also to network users. Among the various initiatives that the distributor must undertake in order to adapt the methods of planning, management and analysis of operation of the network, acquisition of dedicated tools and the related infrastructure plays a crucial role.

Most distributed energy resources (DER) can be disposed in the distribution network and to be accessible to provide network support, DER must co-ordinate with the rest of the power system without affecting other costumers. The capability of DER to provision ancillary services will depend on factors such as DER location and number of resources integrated to the grid. Most of the benefits relying on ancillary services will be directly dependent upon the location whereas as the penetration of DER increases, it will impact not only the distribution system capacity restraints but the voltage and frequency stability of the interconnected DER units.

From the infrastructural point of view, there is a clear need of

enhancing the observability of the network, now generally limited to the HV/MV substation and the preparation of appropriate channels of communication with the users.

Software tools evolution includes the enhancements of the SCADA side for managing the new devices and information coming from the network on one side. In addition, a new family of software applications is being developed to support in both real-time operation and the planning phase.

At this point, the specific software tools for both real-time management and planning of the distribution network need to be developed. To implement these, the developer has to have in mind all the above stated limitations and challenges of modern systems. This thesis will provide tools for improvement of the observability of the distribution systems and optimal planning of network for the same cause.

Contents

List of Figures

List of Tables

CHAPTER 1

1. Introduction

1.1 Motivation

Widespread electrification has been classified as one of the greatest engineering achievements of the 20th century by the National Academy of Engineering [1]. As electrical energy systems are closely connected to most aspects of modern society, electric service interruptions are extremely burdensome and expensive; a 2006 study estimated that the national annual cost of power interruptions in Italy is € 267.8 million [2]. Improving electric system reliability is therefore a major research emphasis.

Grid operators must ensure reliable electric service and preventing blackouts. That requires supplying consumers' load demands while remaining within both physical and engineering constraints of the network and connected facilities. As for many engineering systems, operating in a secure region far from potential failure points (i.e., operation with sufficient stability margins) is desired for maintaining reliability. This is particularly important in electric power systems due to the inherent uncertainty resulting from, for instance, uncontrollable customer load demands, uncertain system parameters, and the potential for unexpected outages of generation and transmission facilities.

Inability to maintain sufficient stability margins may result in uncontrolled operation, potentially leading to voltage collapse and wide-scale blackouts, as occurred in the September 2003 blackout in Italy that affected 57 million people nationwide and had estimated cost of € 120 million [3].

Not only reliability, but also economic operation of electrical power systems is a major concern of power system engineers. To emphasize the importance of the economic operation of power systems, following numbers of the power distribution in Europe should be considered [126]:

- € 400 billion of investments by 2020;
- 2 400 electricity distribution companies;
- 260 million connected customers, of which 99% are residential customers

and small businesses;

- 240 000 people are employed;
- 2 700 TWh of energy distributed.

Fig. 1.1 offers some more numbers regarding distribution systems of Europe explaining how huge electrical business is and by that further emphasizing the importance of economic operation of systems and size of the market.

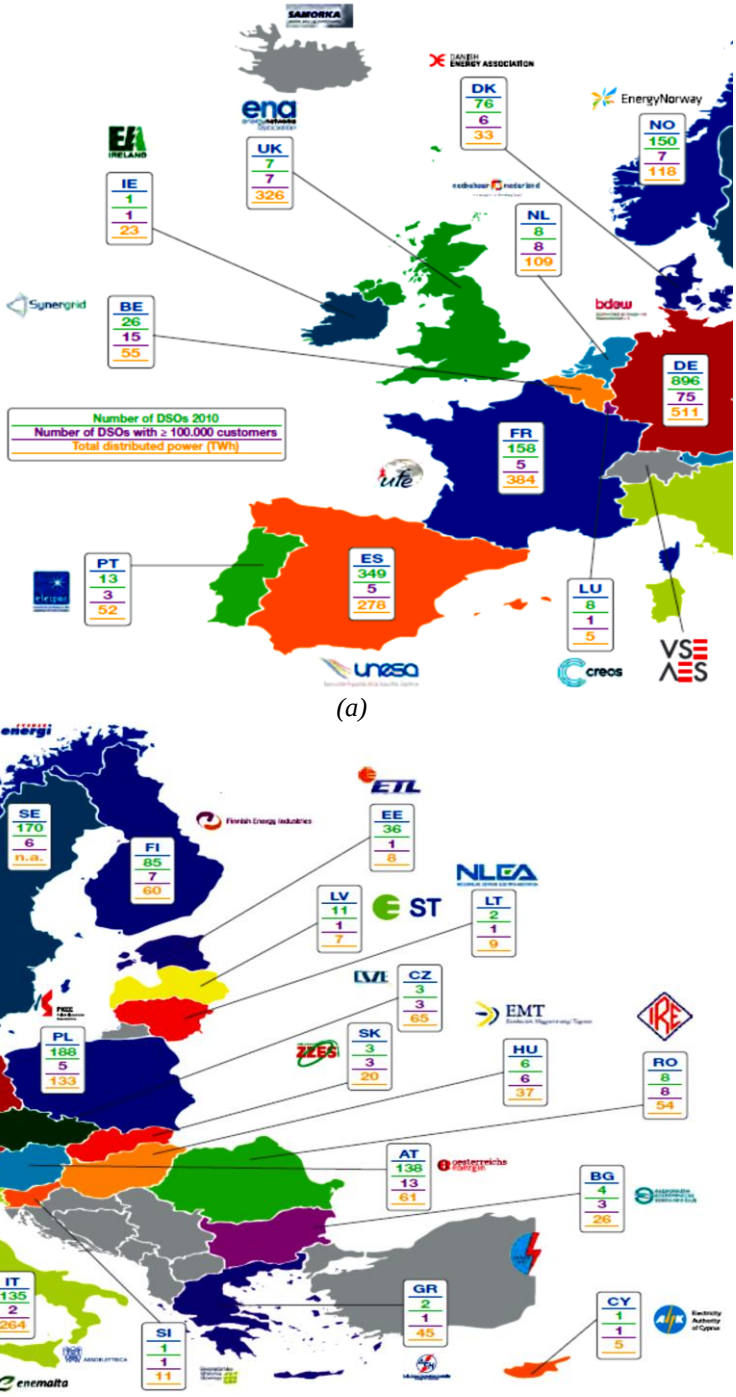

Figure 1.1: *Distribution systems of Europe in numbers (a) left portion and (b) right portion*

To concretize to nation level, with the large size of the power system industry in Italy (as one measure of industry size, electric industry revenues of

Enel, Italian electrical utility company, were € 80.5 billion in 2013 [4]), improvements in power system economics have the potential for significant impacts.

Many aspects of electric power systems are optimized to reduce costs and enable the management of the network in automated manner. However, physical and organizational issues related to modern power systems unable this. Historically, power systems have been vertically governed systems with clearly distinctive subsystems – generation, transmission and distribution. Distribution Networks (DNs) have been planned, designed, and operated as passive systems i.e. systems with no generation. The recent large growth of dispersed generators (DG) in the DNs represents a major challenge: the distribution companies have to start behaving as a local DSO similarly to the Transmission System Operators (TSOs). In other words, the Distribution Company will become a sort of "local dispatcher" and will involve its real/passive customers in activities related to the network management and optimization. Thus, a key element in the future DNs will be achieving and maintaining the observability of the network to provide inputs to various DSO functions such as voltage and power flow control.

In this sense, the DSO must undertake various initiatives in order to adapt the methods of planning, management and analysis of operation of the network to the new context. For all of this to be possible, it is mandatory for the DSO to possess a thorough real-time knowledge of the system state. The solution at hand would be the use of the least square based SE techniques used for a very long time by the TSOs. However, the percentage of investments into measurement equipment is much more reduced than the increase of DG penetration and the situation is very similar to the past: a limited set of measurements in the primary substations and sometimes in secondary substations are available. Moreover, the equipment is mostly old and the precision class is inappropriate for classical state estimation as it was installed for other purposes, (e.g. input signal for the protection systems). Then, the measurements are not synchronized but averaged and collected at different moments. On the other hand, it is not physically possible to install measurement equipment in many buses of a real DN as they are buried welded junctions between various cables. All these make impossible the application of classical SE techniques adopted for the transmission system, as there is no sufficient redundancy, synchronization and statistical characterization of the available information.

Thus, the application of a complete state-estimation technique similar to the ones used by the TSOs is impossible. However, many approaches tend to use the traditional least square methods by introducing a large number of pseudo-measurements for loads and generators. But in real DNs, the loads and generators profiles are estimated profiles based on the past yearly energy consumption. This means that there is no statistical information available about them so it is impossible to correctly use them as pseudo-measurements in a least square approach.

Hence, it is necessary to design innovative techniques to improve as much as possible the observability of the DS. Such approaches need to be robust and computationally fast as they should run on-line under a single control center on many different DNs with hundreds of buses. This dissertation discusses the research about the State Estimation (SE) function in DNs that tackles the

problem of network observability and therefore represents the core function for managing power systems.

Improvement of the observability of the DN in a way to obtain as accurate as possible representation of the network state give promising results but its impact is still not sufficient with the perspective of further penetration of DGs and increased need to make automatic control actions. So, even though DSOs are reluctant to do so because of the expenses, investments into the new measurement equipment are the matter of necessity. The measurement equipment should be placed optimally throughout the network to ensure the best possible attainable observability with the least possible number of new measurement locations to diminish the expenses.

The problem of the determination of the best locations of the measurement equipment for state estimation is known as the problem of Optimal Measurement Equipment Placement (OMEP). With every additional instrument, assessment of state is improved, but there are economical and physical boundaries related to the number of additional equipment: it is necessary to find the minimum number of additional instruments that, when placed in optimal locations, enable maximal network observability.

Therefore, the attention of the dissertation is directed as well towards the OMEP function, which aim is to improve the observability of the DN and thus further improve the results obtained by SE algorithm.

1.2 Organization

This dissertation is organized around two major themes: 1) State Estimation function in DN that is used for improvement of observability of Distribution Systems (DSs) and 2) Optimization of Measurement Placement function which is a planner function, helping DSOs to optimally plan new network or improvement of the existing one by introducing new measurement equipment in certain points of the network.

Chapter 2 provides the description of Active Distribution System Management paradigm, analyzing in detail the changes in modern DS regarding DG penetration and key changes in DN of today. This chapter explains why the development of new DMS is necessary and where is the crucial space for the research developed in this dissertation in modern power systems.

Chapter 3 formulates the classical State Estimation function, offering the mathematical model and fields of implementation. It also explains how distribution systems are different from the transmission ones and why they require different approach regarding State Estimation function.

Chapter 4 presents the State Estimation in Distribution Network approach that has been developed during the PhD research by Departmental R&D group. Detailed description of the problem, methodology and mathematical system is provided. An innovative approach is proposed: it consists in minimizing the sum of the squares of the differences between measured and estimated values of the quantities provided by the measurement equipment present in the system. The proposed technique is based on the Interior Point method. The benefits of the approach in terms of observability improvement are illustrated by simulations involving realistic MV distribution system models. The results presented in the paper represent a part of the INGRID 2

project, which is the product of the collaboration among Politecnico di Milano, SIEMENS SpA and Università degli Studi di Milano and represents a tool developed to answer the above mention needs of the Distribution System Operator (DSO).

Chapter 5 introduces and develops the idea of General OMEP problem. The aim of the proposed methodology is to improve the observability of the DN. In obtaining the results, innovative evolutionary technique was used in its two forms of coding – integer and binary. Also, different approaches regarding the evolution process have been exploited. The chapter presents these different approaches and compares the results obtained to determine the best one. Also, the comparisons and the benefits of the approaches are illustrated by simulations involving realistic MV distribution system models. In continuance, multi-objective OMEP model is developed and discussed enabling its further exploitation due to vast DSOs requirements. This type of OMEP was named Advanced OMEP and it involves adaptations of objective function (OF) of the problem in order to adapt to the previously mentioned requirements.

Chapter 6 summarizes the developments and discusses future work. Proposed areas of future work include OMEP function further utilization and general design strategy of measurement placement throughout DNs.

Chapter 8 is appendix of the dissertation offering bibliographical references, data of the test network, etc.

1.3 Contributions

The contributions of this dissertation can be organized in two major areas: 1) modelling, computational and industrial advances of SE function developed specifically for the specific nature of DNs 2) theoretical, computational and industrial advances of developed OMEP function.

The main modelling contribution of SE function is its innovative and complete approach for DN observability improvement that does not rely on a methodology developed for transmission networks. The second modelling contribution lies in its mathematical model specially designed for DN that takes into account many limitations of today's DSs. Also, developed SE solution is capable of adaptation to different types of DNs and available realistic low quality measurement equipment so it can operate in its non-optimization or optimization module. Model is made in a way that it can bypass the improbabilities introduced by realistic DG and still obtain high level of observability.

The developed approach is computationally advanced and fast. It is designed to accept complex inputs and process them, giving the result at the time frames completely suitable for on-line operations.

As the consequence, this software solution is suitable for broad applicability in electrical industry and as a matter of fact, it is already running on a number of pilot projects all over Italy. As its model is made in a way it can process different type of network inputs, it is a necessary part of Distribution Management System (DMS) software as it enables much needed knowledge about DSs in order for DSO to make control actions.

The first theoretical contribution of OMEP lays within its pioneering approach for solution of this type of problem. The algorithm is completely functional for planning of realistic DS. Tests on the large number of networks, case scenarios, different configurations and inputs also offer the theoretical design strategy of measurement equipment placement in generalized DN. Further on, an implementation of evolutionary technique for this type of a problem has proven to be very successful and promising also for other similar types of problems.

Taking into account that this is a planning problem, computational time was not an immensely important issue, but developers made sure that time consumption is still optimal and even with the larger DNs (hundreds of buses), problem was converging within satisfactory time frame.

The potential for industrial exploitation of the OMEP solution is huge. This function will be in a very near future essential for planning of new DNs or improvement of the existing ones. As the economic criterion is behind any decision made in electrical industry and every decision is quite expensive, this software solution can provide much needed information to DSOs and/or investors. Exactly its modular and easily adjustable nature offers the possibility to DSOs to investigate different criteria and objectives that are valuable in making a decision and enforce these into the software solutions as an input. This software solution can serve to significantly improve the observability of the DN with the limitation of imposed economic constraints.

CHAPTER 2

2. Active Distribution System Management

The expansion of decentralized and intermittent renewable generation capacities introduces new challenges to ensuring the reliability and quality of power supply. Most of these new generators (both in number and capacity) are being connected to distribution networks – which is a trend that will continue in the coming years.

This situation has profound implications for DSOs. Until recently, DSOs designed and operated distribution networks through a top-down approach. Predictable flows in the electricity network did not require extensive management and monitoring tools.

But this model is changing. Higher shares of dispersed energy sources lead to unpredictable network flows, greater variations in voltage, and different network reactive power characteristics. Local grid constraints can occur more frequently, adversely affecting the quality of supply. On the other side, DSOs are expected to continue to operate their networks in a secure way and to provide high-quality service to their customers.

Distribution management will allow grids to integrate Dispersed Energy Resources (DER) efficiently by leveraging the inherent characteristics of this type of generation. The growth of DER requires changes to how distribution networks are planned and operated. Bi-directional flows need to be taken into account: they must be monitored, simulated and managed.

The chapter sets out implications for the tasks of system operators (TSOs and DSOs) and DG/RES operators and outlines options for system planning and development, system operation, and information exchange, thereby opening the door for further analysis. It focuses on outstanding technical issues and necessary operational requirements and calls for adequate regulatory mechanisms that would pave the way for these solutions.

2.1 Integration of Distributed Generation: A Key Challenge for DSOs

DER includes dispersed/decentralized generation (DG) and distributed energy storage (DES). With the EU on its way to meeting a 20% target for RES in total energy consumption by 2020, the share of electricity supply from RES is on the rise. Intermittent RES like solar and wind add an additional variable to the system that will require more flexibility from generation (including RES) and demand and investments in network infrastructure. Such intermittent RES will be connected largely to European distribution systems. At the same time, electrification of transport will be needed to further decarbonize the economy. For a significant deployment of electric vehicles by 2050, Europe needs to target a 10% share of electric vehicles by 2020. These vehicles will need to be charged through the electrical system. Together with the electrification of heating and cooling, these trends will contribute to further evolution of European power systems.

2.1.1 Distributed Generation: Facts and Figures

Dispersed/decentralized generation (DG) are generating plants connected to the DN, often with small to medium installed capacities, as well as medium to larger renewable generation units. Due to high "numbers", they are important compared to the "size" of the DN. In addition to meeting on-site needs, they export the excess electricity to the market via the local distribution network. DG is often operated by smaller power producers or so-called prosumers.

Unlike centralized generation, which is dispatched in a market frame under the technical supervision of TSOs, small DG is often fully controlled by the owners themselves. The technologies include engines, wind turbines, fuel cells and photovoltaic (PV) systems and all micro-generation technologies. In addition to intermittent RES, an important share of DG is made up of combined heat and power generation (CHP), based on either renewables (biomass) or fossil fuels. A portion of the electricity produced is used on site, and any remainder is fed into the grid. By contrast, in case of CHP the generated heat is always used locally, as heat transport is costly and entails relatively large losses. Table 2.1 provides an overview of generation types usually connected at different distribution voltage levels.

Table 2.1: Common voltage connection levels for different types of DG/RES

Usual connection voltage level	Generation technology
HV (usually 38-150 kV)	Large industrial CHP Large-scale hydro Offshore and onshore wind parks Large PV
MV (usually 10-36 kV)	Onshore wind parks Medium-scale hydro Small industrial CHP Tidal wave systems Solar, thermal and geothermal systems Large PV
LV (<1 kV)	Small individual PV, Small-scale hydro, Micro CHP, Micro wind

The following examples demonstrate that a move from simple DG connection to DG integration is a must already today in some countries. As illustrated in Fig. 2.1, in Galicia, Spain, the installed capacity of DG connected to the distribution networks of Union Fenosa Distribución (2,203 MW) represents 120% of the area's total peak demand (1,842 MW) [5].

	Installed Capacity (MW)	Percentage (%)
CHP (Natural Gas)	166,9	7,6
Rest CHP	319,4	14,5
Wind Power	1.369,5	62,1
Photovoltaic (PV)	10,3	0,5
Hydro	306,1	13,9
Other Renewables	31,4	1,4
TOTAL Generation	2.203,6	100

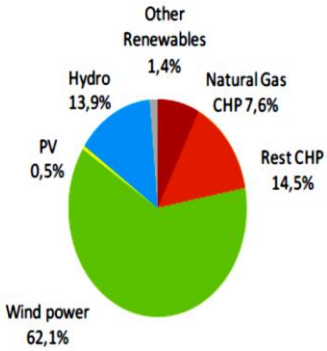

	Max. Hourly Average capacity (MW)
Galicia Demand	1.842

Figure 2.1: *Distributed generation installed capacity and peak demand in Galicia, Spain [5]*

In the regional distribution network in the south of Germany (see Figure 2.2), the installed capacity of intermittent renewable DG already represents a large percentage of the peak load. In many places, the DG output of distribution networks already exceeds local load – sometimes by multiple times. From the TSO point of view, the DSO network then looks like 'a large generator' in periods with high RES production [6].

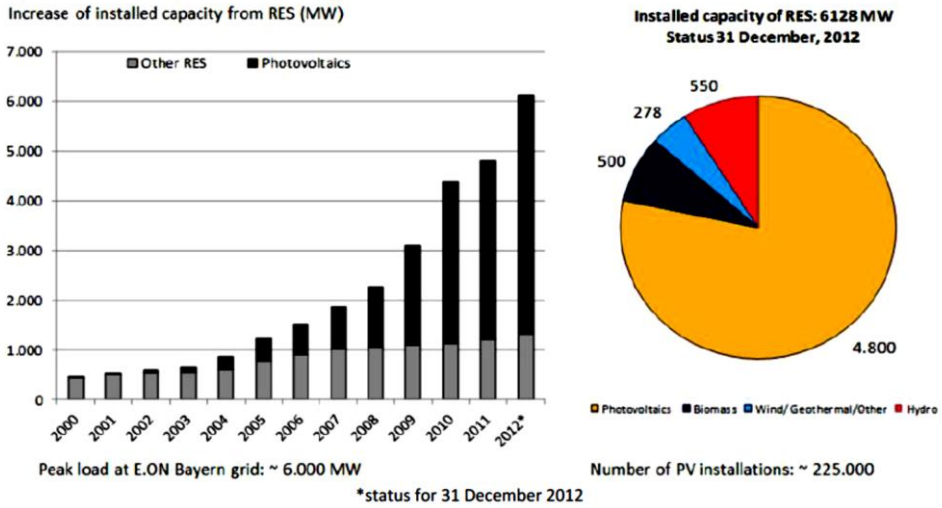

Figure 2.2: *Installed capacity of photovoltaic installations in the E.ON Bayern grid*

In 2014, 20 GW of PV were connected to Italian distribution grids (Enel Distribuzione), with additional 10GW of wind generation. It is the highest yearly increase in distributed generation connected to the grid worldwide [131].

In northwest Ireland with a peak demand of 160 MW, 307.75 MW of distributed wind generation are already connected to the distribution system in 2013, and a further 186 MW are contracted or planned. Beyond this, another 640 MW of applications have been submitted [132].

2.1.2 Key Challenges for Current Distribution Networks

In theory, due to its proximity to the loads, dispersed generation should contribute to the security of supply, power quality, reduction of transmission and distribution peak load and congestion, avoidance of network overcapacity, reduced need for long distance transmission, postponement of network investments and reduction in distribution grid losses (via supplying real power to the load and managing voltage and reactive power in the grid).

In reality, integrating dispersed generation into DN represents a capacity challenge due to DG production profiles, location and firmness. DG is not always located close to load and DG production is mostly non-dispatchable (cannot control its own output). Therefore, production does not always stand in parallel with demand (stochastic regime) and DG does not necessarily generate when the distribution network is constrained. In addition, power injections to higher voltage levels need to be considered where the local capacity exceeds local load. This poses important challenges for both DN development and operation [7].

2.1.2.1 Network reinforcement

The ability of DG to produce electricity close to the point of consumption mitigates the need to use network capacity for transport over longer distances during certain hours. However, the need to design the DN for peak load remains undiminished and the overall network cost may even increase. For example, peak residential demand frequently corresponds to moments of no

PV production. Figure 2.3 shows the situation in the southern Italian region of Puglia. It indicates the incredible increase in the power installed and energy produced from PVs in recent years and the subsequent evolution of power flows at the connection point between the transmission network and the distribution network. As the peak load corresponds to literally zero PV production, there is no reduction in investment ("netting" generation and demand) [4].

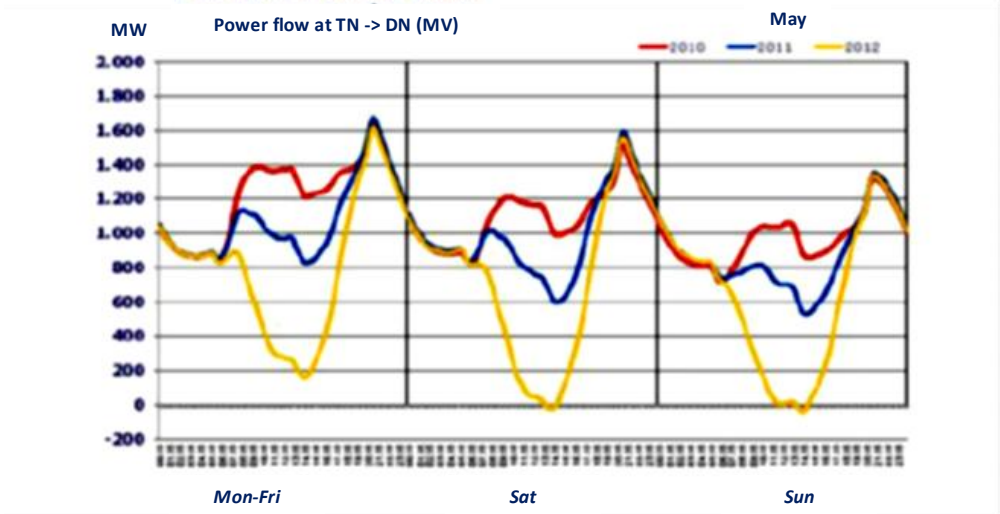

Figure 2.3: *Power flows between transmission and distribution network in Italy, 2010- 2012 (Source: Enel Distribuzione)*

Generally speaking, DNs have to be prepared for all possible combinations of production and load situations. They are designed for a peak load that often only occurs for a few hours per year, in what this dissertation refers to as the fit-and-forget approach. Even constraints of short duration trigger grid adaptations (e.g. reinforcement). DNs have always been designed in this way, but with DG, the utilization rate of network assets declines even more.

Network connection studies and schemes for generators are designed to guarantee that under normal operation all capacity can be injected at any time of the year. The current European regulatory framework provides for priority and guaranteed network access for electricity from RES (Art. 16 of RES Directive 2009/28/EC) and RES-based CHP (Art. 14 of the new Energy Efficiency Directive 2012/27/EC). RES-E is mostly connected on a firm/permanent network access basis (but cannot be considered as firm for such design purposes). Generation and load of equivalent sizes imply different design criteria as e.g. wind and PV has lower diversity than load. In addition, wider cables to lower the voltage might be needed. Overall, this can lead to higher reinforcement cost and thus a rise in CAPital EXpenditure (CAPEX)[1] for DSOs and/or higher connection costs for DG developers.

[1] CAPEX - Funds used by a company to acquire or upgrade physical assets such as property, industrial buildings or equipment. This type of outlay is made by companies to maintain or increase the scope of their operations. These expenditures can include everything from repairing a roof to building a brand new factory.

The contribution of DG to the deferral of network investments holds true only for a relatively small amount and size of DG and for predictable and controllable primary sources [8],[9].

The lead time needed to realize generation investment is usually shorter than that for grid reinforcement. Article 25.7 of Directive 2009/72/EC requires DSOs to take into account DER and conventional assets when planning their networks. This may be complicated when applications for connection are submitted at short notice and DSOs receive no information on connection to private networks. Situations will occur when DSOs have large amounts of DER connected to their network and the resulting net demand seen further up the system hierarchy is lowered. Virtual saturation – a situation when the entire capacity is reserved by plants queuing for connection that may not eventually materialize – may also occur as generator plans cannot be firm before the final investment decision. However, even in the cases when the project is not built, it occupies an idle capacity which may lead new grid capacity requests to face increased costs if case network reinforcements are needed. Temporary lack of network capacity may result in 'queuing' and long waiting times, delaying grid connection of new generators [10].

The situation is similar in case of grid losses (related costs are part of DSOs' OPerational Expenditure (OPEX[1])). Figure 2.4 shows that with a low share of DG these losses drop, but once there are large injections of DG into the DN and load flows over the network, grid losses tend to increase. DG can reduce network costs in transport levels but requires higher costs in the level to which it is connected [11].

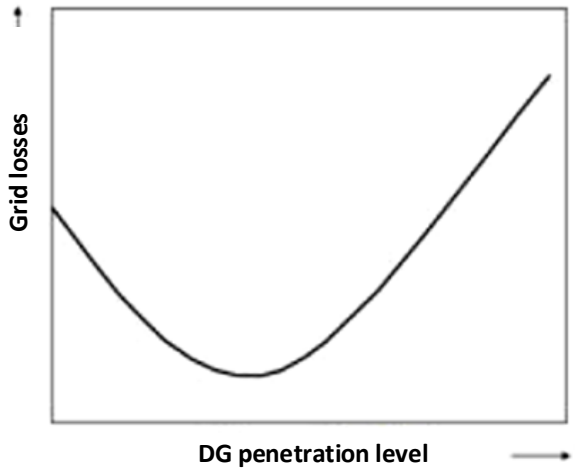

Figure 2.4: *Relation between the degree of DG penetration and grid losses*

2.1.2.2 Distribution Network Operation

Dispersed generation, in particular intermittent RES, represents a challenge not only for system balancing, but also for local network operation.

[1]OPEX - A category of expenditure that a business incurs as a result of performing its normal business operations. One of the typical responsibilities that management must contend with is determining how low operating expenses can be reduced without significantly affecting the firm's ability to compete with its competitors.

The security and hosting capacity of the DS is determined by voltage (statutory limits for the maximum and minimum voltage ensure that voltage is kept within the proper margins and is never close to the technical limits of the grid) and the physical current limits of the network (thermal rates of lines, cables, transformers that determine the possible power flow).

DS can be driven out of its defined legal and/or physical operating boundaries due to one or both of the following:

- Voltage variations: Injection of real power leads to voltage profile modifications. Voltage increase (overvoltage) is the most common issue at the connection point for DG units and the relevant grid area. Reversed power flows (flows from distribution to transmission) occur when DG production exceeds local load. The more local production exceeds local demand, the stronger the impact on voltage profiles. Figure 2.5 illustrates such situations [12].

  DSOs may have difficulties in maintaining the voltage profile at the customer connection points, in particular on LV level, as real voltage control is not in place. In most countries, monitoring of grid values is not present and most dispersed generators are not equipped to participate in system management – no active contribution of generation to network operation is expected. As a result, operational system security may be endangered and security of facilities (both customers' installations and the network as such) put at risk.

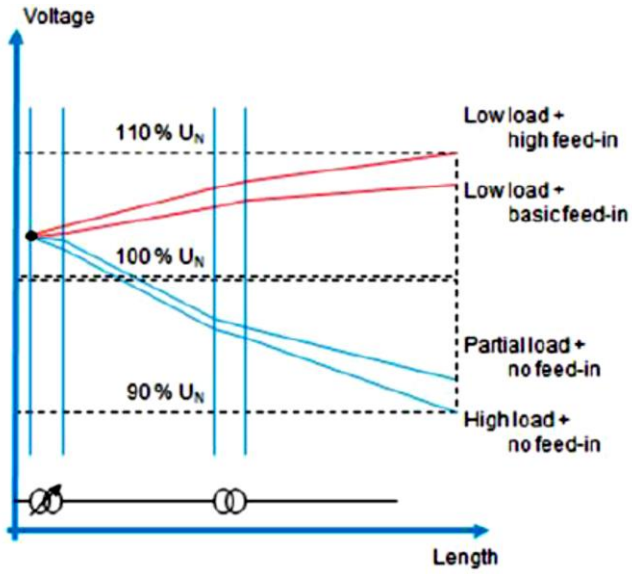

Figure 2.5: *Instability in distribution system*

- Congestions: When excessive DG feed-in pushes the system beyond its physical capacity limits, congestions may occur in distribution networks:

$$P_G - P_L > P_{max} \tag{2.1}$$

where:

P_G total generated power of the system;
P_L total consumption of the system;
P_{max} physical capability limit of the system.

This may lead to necessary emergency actions to interrupt/constrain off generation feed-in or supply. A similar situation can occur in case of excessive demand on the system (P_L - P_G> P_{max}). This could apply to high load originated e.g. by charging of electric vehicles, heat pumps and electrical HVAC (heating ventilation and air-conditioning).

Generation curtailment is used in cases of system security related events (i.e. congestion or voltage rise). The regulatory basis for generation curtailment in such emergency situations differs across Europe. In some countries (e.g. in Italy, Spain, Ireland), the control of DG curtailment is de facto in TSO hands: the DSO can ask the TSO, who is able to control real power of DG above a certain installed capacity, to constrain DG if there is a local problem. As the TSO is not able to monitor DN conditions (voltage, flows), DSOs can only react to DG actions [15]. This can result in deteriorating continuity on the distribution system which will impact both demand customers and DG.

In systems with a high penetration of DG, both types of unsecure situations already occur today. As a result, DSOs with high shares of DG in their grids already face challenges in meeting some of their responsibilities. These challenges are expected to become more frequent, depending on the different types of connected resources, their geographic location and the voltage level of the connection.

- Active network and reversed power flow: The introduction of DG on to the DN impacts upon power flows, voltage conditions and fault current levels [133]. These impacts can be positive, such as reduction of voltages sags and release of additional network capacity, but can negatively impact on the protection systems. DG introduces additional sources of fault current, which may increase the total fault level within the network, while possibly altering the magnitude and direction of fault currents measured by the protection systems. The contribution of one single DG is normally relatively insignificant, but the aggregate contribution of many DG units can lead to a number of problems such as: blinding, false tripping and loss of grading.

To summarize, the key challenges for DSOs include:

- Increased need for network reinforcement to accommodate new DG connections:
  - Network operators are expected to provide an unconditional firm connection which may cause delays or increase costs for connecting dispersed generation;
  - Increased complexity for extension (including permitting procedures) and maintenance of the grid may require temporary limitation for connection of the end customers.
- Problems with operation of the distribution grid:
  - Local power quality/operational problems, in particular variations in voltage but also fault levels and system perturbations like harmonics or flickers;
  - Rising local congestions when flows exceed the existing maximum

capacity, which may result in interruptions of generation feed-in or supply;
- Longer restoration times after network failure due to an increased number and severity of such faults.

Current DSO responsibilities are the following:

- *Distribution planning, system development, connection & provision of network capacity*
  DSOs are in charge of developing their network. They design new lines and substations and ensure that they are delivered or that existing ones are reinforced to enable connection of load and decentralized power production. Depending on the size of a DG/RES & DER system, DSOs may require a new connection at a particular voltage level. They are obliged to provide third party access to all end customers and provide network users with all information they need for efficient access and use of the distribution system. They may refuse access to the grid only when they can prove that they lack the necessary network capacity (Art. 32 of Directive 2009/72/EC).
- *Distribution network operation/management and support in system operation*
  DSOs maintain the system security and quality of service in DNs. This includes control, monitoring and supervision, as well as scheduled and non-scheduled outage management. DSOs are responsible for operations directly involving their own customers. They support the TSOs, who are typically in charge of overall system security, when necessary in a predefined manner, either automatically or manually (e.g. through load shedding in emergency situations). A common basis for these rules is now being set in the EU-wide network codes (operational security, balancing, congestion management, etc.).
- *Power flow management: Ensuring high reliability and quality in their networks*
  - Continuity and capacity: DSOs are subject to technical performance requirements for quality of service including continuity of supply (commonly assessed by zonal indexes such as average duration of interruptions per customer per year (SAIDI) and average number of interruptions per customer per year (SAIFI) or individual indexes like number and duration of interruptions) and power quality laid out in national law, standards and grid codes. They are also responsible for voltage quality in distribution networks (maintaining voltage fluctuations on the system within given limits). In planning, the DSO ensures that networks are designed to maintain these standards regardless of power flow conditions. However in cases of network faults, planned outages or other erroneous events, the DSO must undertake switching actions so that adequate supply quality is maintained. Up until now, this has been rather static, increasingly automation or remote switching will need to be undertaken to ensure near real-time fault isolation and restoration of supply.
  - Voltage and reactive power: Voltage quality is impacted by the electrical installations of connected network users. Thus the task of

the DSO in ensuring voltage quality must account also for the actions of network users, adding complexity and the need for both real-time measurement and mitigating resources (i.e. on-load voltage control) and strict network connection criteria. European standard EN 50160 specifies that the maximum and minimum voltage at each service connection point must allow an undisturbed operation of all connected devices. Voltage at each connection should thus be in the range of ± 10% of the rated voltage under normal operating conditions. In some countries, compliance with these or other specified national voltage quality requirements that can be even more restrictive represents part of DSOs' contractual obligations and quality regulation. In some countries, network operators are required to compensate customers in case the overall voltage quality limits are breached.

2.1.2.3 Traditional Design of Distribution Networks

The fundamental topological design of traditional distribution grids has not changed much over the past decades. Up until recently, DSOs have distributed energy and designed their grids on a top-down basis.

Under the paradigm "networks follow demand", their primary role was to deliver energy flowing in one direction, from the transmission substation down to end users. This approach makes use of very few monitoring equipment and is suitable for distribution networks with predictable flows.

Because of the different development of electrification, distribution networks characteristics differ from country to country. Voltage rate levels are usually distinguished as LV, MV or HV. As shown in Figure 2.6, the level of supervision, control and simulation in HV distribution networks is close to that of TSOs in their networks. MV and LV networks are mostly rather passive – here DSOs lack network visibility and control. The lower the monitoring level are, the lower the operational flexibility is.

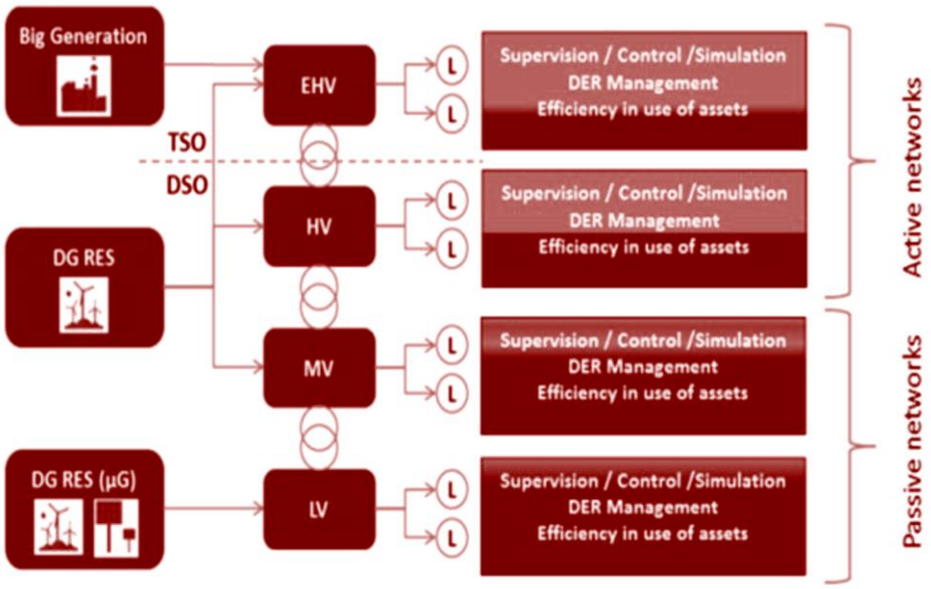

Figure 2.6: *Current DSO network*

Traditional distribution networks have different characteristics in topology (meshed or radial), operation type (meshed or radial), number of assets and customers, operational flexibility and monitoring level:

- *HV networks* (also called sub-transmission) are very similar to transmission networks. The topological design of the grid is meshed and may be operated as radial or meshed depending on the situation. HV networks are operated in a similar way all around Europe: N-1 or N-2 contingency criteria are usually used for rural and urban areas, respectively. The monitoring level at HV is very high. DSOs operating HV grids are able to supervise and control the HV network from the control room centers.
- *MV distribution networks* significantly differ in their characteristics with respect to urban and rural grids. Mostly, meshed topology is used that can be operated either as meshed (closed loop) or radial (open loop). In some countries or depending on the network type in a region, MV operation may always be radial. A high density of loads and relatively high demand typically causes high equipment load factors (transformers, cables) for urban areas. Rural areas are characterized by larger geographical coverage and lower load density and thus longer lines, high network impedances and lower equipment load factors. The proportion of European MV networks with remote monitoring, control and automated protection/fault sectionalization is currently low but increasing by necessity.
- LV networks are usually radially operated. Similar to MV networks, urban and rural LV networks have different characteristics. The proportion of LV monitoring and control is typically even lower than in MV. Measurements usually rely on aggregated information from substations and are only available with a significant time lag. Profile information will not be available.

2.2 Active Distribution Networks

Once DG in distribution networks surpasses a particular level, building distribution networks able to supply all load & DG within the existing quality of service requirements will frequently be too expensive and inefficient. For example, in many places the network would only be constrained for few hours per year. In addition, the security of supply and quality of service problems will no longer be limited to specific situations.

Integrating the high amount of existing and projected DG and, later, other DER will require new Information and Communication Technology (ICT) solutions and an evolution of the regulatory framework for both network operators and users. Network planning and operation methodologies need to be revised to take the new solutions into account.

2.2.1 Key Building Blocks

There is no unique solution because DNs are rather heterogeneous in terms of grid equipment and DG density at different voltage levels. Every DN

should be assessed individually in terms of its network structure (e.g. customers and connected generators) and public infrastructures (e.g. load and population density). Nevertheless, the needed development towards future distribution systems which meet the needs of all customers can be described in the three schematic steps pictured below (Fig. 2.7): from (1) passive network via (2) reactive network integration to (3) active system management.

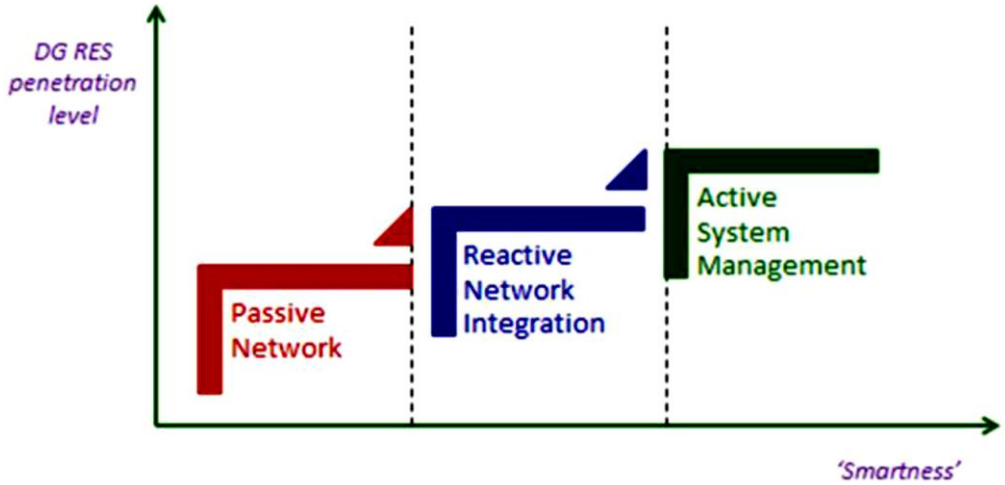

Figure 2.7: *Three-Step Evolution of Distribution Systems [134]*

1. **Passive distribution networks make use of the so-called "fit and forget" approach [134].** This approach indicates resolving all issues at the planning stage, which may lead to an oversized network. DSOs provide firm capacity (firm grid connection and access) that may not be fully used anymore due to local consumption of the electricity produced by DG. This approach has the advantage of requiring low flexibility, control and supervision, but is possible to implement only for a network with very low DER penetration. Once DER penetration rises, the system cannot be designed to cater for all contingencies without very significant investment in basic network infrastructure, making this approach less economical.
2. **Reactive network integration is often characterized by the "only operation" approach.** This approach is used today in some countries with a high share of DG. The regulation requires connecting as much DG as possible with no restrictions. Congestions (or other grid problems) are solved at the operation stage by restricting both load and generation. This solution could restrict DG injections during many hours per year and lead to negative business case for DG if they are not remunerated for the restrictions [134]. Already today, some pioneering countries in this field with high DG penetration levels can be considered as having reached the interim "reactive network integration" stage at which DSOs solve problems once they occur (largely only in operation).
3. **The active approach would allow for interaction between planning, access & connection and operational timeframes. Different levels of connection firmness and real-time flexibility can reduce investment needs.** The existing hosting capacity of the distribution network can be used more optimally if other options including ICT, connection &

operational requirements that guarantee adequate performance of DER towards the system (i.e. via grid codes) and market-based procurement of ancillary services from DER are considered [134]. Operational planning of DNs (similar to that at transmission level) would be in place in networks with high DER shares in order to incentivize dispatch in a way that is compatible with the network. Improved network capacity planning and congestion management at distribution level at different times and locations will be required to maximize the level of generation which is injected in the most economical way for all parties, while maintaining network stability. DSOs must have tools for overseeing maintenance of network standards. Additionally they should have the possibility to buy flexibility from DG and load in order to optimize network availability in the most economic manner or to manage network conditions which are outside the contracted connection of the customers. DSOs should have the possibility to buy flexibility from DG and load on so-called "flexibility platforms" in order to solve grid constraints. The network reinforcement could be deferred until the moment when it becomes more cost-effective than the on-going cost of procuring services from DER [13]. Interactions between DSOs, TSOs and market actors at different stages are depicted in Figure 2.8:

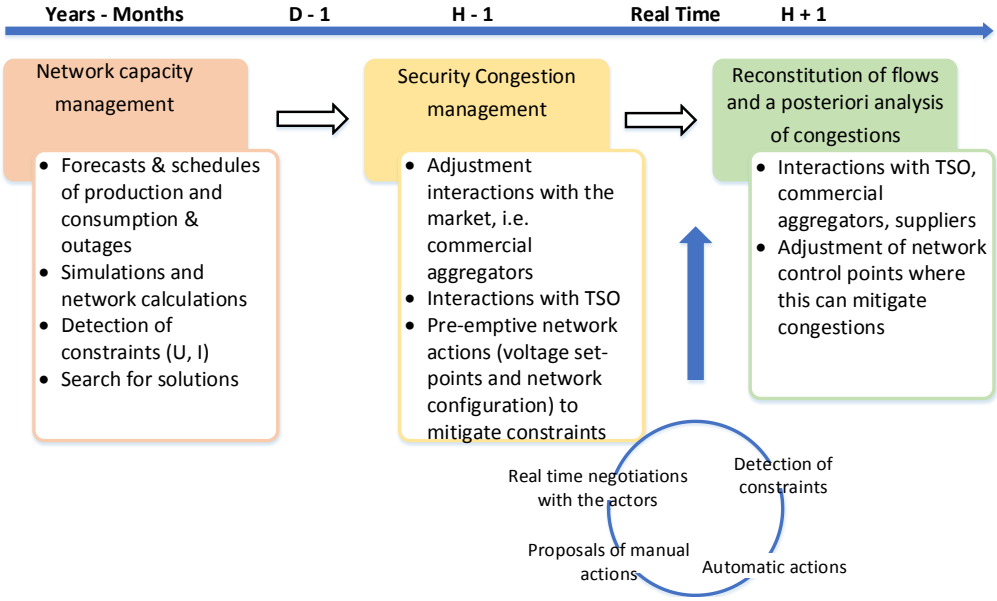

Figure 2.8: *DSO interactions with markets & TSO at different time frames [134]*

Using the active system management approach would enable maximal integration of DER, making the most of the existing grid while enabling DSOs to fulfil the security standards and enabling DER to find the right conditions for their business plan in the most cost-effective way. Table 2.2 highlights the key features of each phase, broken down into the different "layers": development & planning, operations, information exchange and technical development. The subsequent sections of the chapter discuss the active system management approach within the individual layers in detail.

Table 2.2: Three-Step Evolution of Distribution Systems in detail [134]

Layer		Passive DN	Re-active DN integration	Active DS management
Network development (planning, connection & access)		Fit and forget approach: everything "solved" at the planning stage	Only operation approach: connection with no restrictions and solutions at the operations stage *Or* Fit and forget approach	*Combined planning and operational solutions:* Active capacity and loss management through commercial interaction with market actors selling flexibility services
Network operation		Low monitoring & control of DG RES, often only by the TSO Missing rules & services for DG contribution to quality of service, security of supply & firmness	Emergency generation curtailment by DSO Active voltage control distribution networks. Grid codes for DG to meet connection criteria and be able of voltage based control and reactive power contribution	Connection and access criteria combined with operation tools to manage DER Flexibility support from DSO to TSO and from TSO to DSO when required New system services for DSOs arranged via commercial ancillary services and grid codes.
Information exchange		Little information exchange from TSOs/DER to DSOs (small DER do not send information)	High-level information exchange from TSOs/DER to DSOs	Structured and organized off-line and where needed real-time information exchange (standardized interfaces with DER required)
Technical development	Network	Limited monitoring & control capabilities (usually only HV) Conventional SCADA for HV network and DMS/OMS for MV and LV	Increased monitoring and control at HV & MV via telecommunications SCADA/DMS/OMS with the measurement of certain new DG	Increased monitoring, simulation and control down to LV via telecommunications Advanced Distribution Management Systems13 for DSOs/ SCADA and Distribution Management System (DMS)
	DER	DG often not prepared for power factor control Storage & EV not developed	Enhanced DG protection systems/ inverters enabling voltage & reactive power control	Configurable settings: e.g. protection / fault ride through settings, voltage droop Presence of storage & EVs

2.2.2 Distribution Network Development, Planning, Access and Connection

2.2.2.1 Coordinated Network Development

DSOs should be able to plan their grids well in advance to prevent bottlenecks in the most cost-effective way. Data acquired within DN monitoring and information exchange with TSOs and distributed energy resources could be very beneficial in this respect.

In addition, every connection request should be analyzed and considered in the planning process in order to maximize the utilization of the existing network. According to the traditional regulatory approach to connection requests analysis currently applied in most countries, the network operator performs an individual analysis and provides an individual solution to each connection. The first connections may use the available capacity of the existing network. But once there is an increased demand for new DG connections in the same area and the available network capacity is limited, this approach is not always optimal from the overall cost and network development perspective.

One way to tackle this issue is to allow for coordination of all relevant actors, including network operators, investors and local authorities in the analysis of connection requests. One of the examples is the approach made in Spain [14]. To rationalize the RES expansion and optimize the available energy resources, some Spanish regions created so-called "Evacuation Boards". They are characterized by a coordinated grid connection request process. RES installation plans are deployed and coordinated between the administration, RES investors and transmission and distribution system operators. In these evacuation boards the TSO or DSO do not receive individual requests; they are collected by the Regional Administration and after a validation process submitted for an aggregated analysis to be made together by the DSO & TSO. The positive impact of the new networks for consumption (extra capacity for consumers) is also considered. In addition to the cost-sharing mechanism (proportionally to the capacity assigned to each RES project), the covenants for the development of such infrastructures contain the necessary guarantees, payment and execution terms. Benefits of this approach include overall minimized costs of network development and project, reduction of project risks thanks to the possibility to correctly analyze both the costs and timetables needed for the different RES penetration scenarios, and reduced time for acquiring all necessary administrative permits.

Coordination between TSOs and DSOs is likely to play a particular role. Whilst in some cases modifications required by DSOs from TSOs or vice versa do not considerably affect the capabilities of one or the other to maintain their network performance, the impact may be substantial in other cases. For example, when the HV or EHV (extreme-high voltage) network is saturated, connection of generation to the MV network cannot be planned without taking into account the conditions at HV network. An optimal network development is also a key to minimize losses in the electrical system. Transmission or distribution network conditions which require regular (or conditional) exchange of information between TSOs and DSOs should be

defined. Standard reciprocal data exchange arrangements about the expected development of generation/load at the different voltage levels and about the network reinforcements needed at the TSO level, not directly related to the lower voltage planning activities, should be put in place.

2.2.2.2 Connection

For proper integration into the network, distributed generation needs to fulfil minimum technical criteria: the equipment and its protective relays must be able to resist voltage dips and prevent islanding and there should be separate metering for production and consumption. DG should also be subjected to the same costs as other generators, including adequate connection fees. DSOs must know what is on-line when they are working to prevent accidents. Therefore, they should have a possibility to verify compliance with requirements. DG should thus "be registered" with the DSO, and remote disconnection by the DSO to prevent damage to facilities of other clients while maneuvering should be technically possible under conditions defined by regulation. To secure safe operation of the distribution grid, DSOs should also be able to define control schemes and settings for generators connected to their grids, in coordination with the TSO where necessary in order to ensure compliance with overall system requirements.

2.2.3 Active Distribution Network Operation

Dispersed generation should be incentivized to sell their production into the electricity market. Aggregation of DG in form of so-called Virtual Power Plants (VPPs), flexible loads and possibly decentralized storage is expected to play an important role in facilitating access of small customers to the market and addressing the uncertainty of availability and providing enhanced capability to manage the risk of not being able to meet the contracted scheduled output. The aggregator role could also be taken up by electricity service companies (ESCO) or suppliers. The aggregator is to provide an interface between DER and other market actors and system operators. In addition, DG should be obliged to meet scheduling, nomination and balancing obligations as other power generators do, including payment of balancing charges. DG should also be responsible for their imbalances on equal terms with other Balancing Responsible Parties. It is highly beneficial for system stability and cost reduction if variable RES technologies are incentivized to reduce forecast errors and to minimize imbalances in the market and take up necessary responsibilities towards the system as other generation technologies do [15].

The network plays an important service role of supporting the market. Operational barriers may arise, characterized by one or more violations of the physical, operational, or policy constraints under which the grid operates in the normal state or under contingency cases. They are transient – associated with a specified point in time. As such, they may be detected before or during the day-ahead, the hour-ahead markets or during real-time system operation. In order to facilitate secure network operation and smooth functioning of the future market with high DER penetration, DSOs need to become active

operators of their networks. This means that they need adequate tools to operate their networks. In order to facilitate this, they need to know the state of the network in each time. In addition, network users need to actively participate in network usage optimization. In this way, the possible above mentioned violations can be eliminated.

2.2.3.1 DSO System Services

Active DSOs should be allowed to coordinate the offering of new system services, as required by the new Energy Efficiency Directive (Art 15.1 of 2012/27/EC) while ensuring the security, integrity and quality of supply in their networks. The DSO is best placed to facilitate this mechanism as the data need to be gathered at substation level and in-depth knowledge of the grid layout and its behavior is required. Moreover, the DSO has a legal responsibility to ensure that such technical constraints are mitigated.

The blue area in Figure 2.9 schematically outlines the stages in the electricity market in which the network operators do not interfere, but act as mere behind-the-scene facilitators. The green area depicts the system services that are to be administrated by network operators (for both transmission and distribution system needs). Such system services could be defined in grid codes (voltage and reactive power contribution) or procured as ancillary services from DER within a transparent and non-discriminatory regulatory framework.

Today, ancillary services are procured by the TSO, largely from large power producers, to manage the system as whole. In near future, flexibility platforms where flexibility is offered (usually via aggregators) to DSOs for relieving congestion in their networks but also to TSOs to provide balancing and dispatching in transmission grids will play an important role, in particular for close to real-time flexibility.

Italy is one of the pioneering countries in promoting standards for procurements of generating resources for ancillary services, with special referral to the dispersed uncontrollable generation. Document 354/2013/R/eel provides the guideline for such an action [16]. There is a persistent action to make the most of the technological development that is happening in these years. Therefore, the units for production of electrical energy from renewable sources and energy storage systems (whether in electrochemical battery, hydraulic, compressed air, etc.) must promote, in relation to the conditions of economic efficiency of these technological developments, a system in which all networks gradually become smart, in relation to the conditions of development of DG. Gradually, all plants need to become eligible to provide network services. This is in relation to the possibility that the various technologies are subjects to the charges for the supply of those network services that are not able to provide at the moment. In general, it is the entire electrical system that must become "smarter" and which must be able to operate in order to exploit in the most efficient performance of each of the technologies of use of the sources of energy available.

Such a system will make more efficient use of DG, and the development of ancillary services in DNs such that distributed generation can actively participate in the management of the power system. This seems necessary in a

context where an increasing share of the hourly load is met by the distributed generation that does not provide the same network services and amending the profile of the residual load daily (that is covered by the significant production units) to the point reset it in a few hours, and in some areas.

The regulatory action conducted so far has enabled undoubtedly important steps forward, bringing Italy between the countries at the forefront of integration of non-programmable renewable and dispersed generation. This corresponds to the primary interest of Italy, which boasts one of the highest degrees of penetration of these systems.

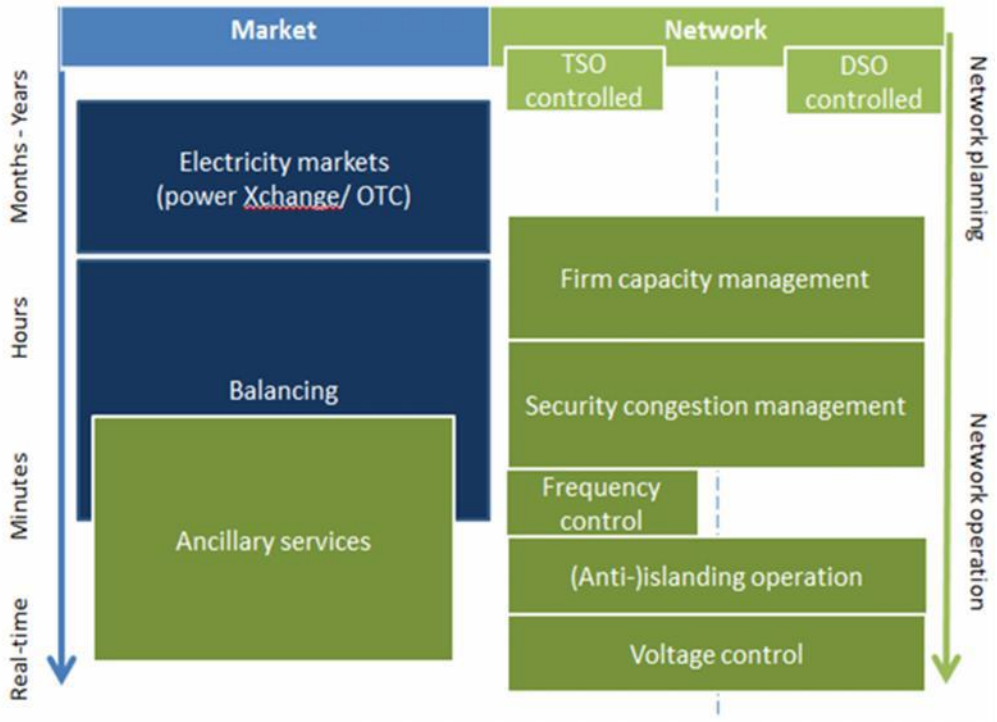

Figure 2.9: *Market and network operations [134]*

Distribution congestion

Security congestion management would be used to solve the technical constraints at distribution level close to real-time in the alert state. In these defined cases, the DSO could deviate from the merit order, but ex-post justification and compensation should be provided. This could be executed by pre-agreed contracts for instance. The DSO should then pay the "up regulating" cost elsewhere in the system, and should remunerate the downward cost to the local generator that is constrained off in his grid (including the missed income from the support scheme and the costs of keeping balanced position).

Emergencies

Emergency tools including direct load management (load shedding) and emergency DG curtailment should be used only in well-defined emergency states/once the contracted options are exhausted. When the grid stability is at risk, DSOs should be able to act physically to control and constrain off both local consumption and production (as is already the case in some countries –

e.g. Germany or Sweden). Priority access rules should not restrict network operators' ability to flexibly respond to emergency situations.

Any action on DN users requested by the TSO should be agreed with the DSO as system operators. TSOs should not act on any individual DER connected to the DS. Any direct order from the TSO to DER embedded in distribution networks targeted to safeguard operation of the system will be executed by the DSO, not the TSO.

2.2.3.2 Information Exchange

Today, DSOs have don't possess systems installed for acquiring data from DG of smaller size in particular. In some cases, the TSO receives information from DG in real time while DSOs do not have real-time access to this information. There is not usually an operational exchange between the TSO and the DSO.

In the future, a well-structured and organized information exchange between relevant actors will be necessary to operate the distribution network with high DG penetration in real-time or close to real time (Fig. 2.10). This form of information exchange will be used for DSO planning and asset management purposes (to optimize network capacity and availability in the most economic manner) while ensuring that all customers feel the absolute minimum impact of DG on power quality and continuity. It is the first and potentially most effective step which can be taken to reduce the cost of DG connection and integration [17].

At the transmission level, generators already send schedules to the TSO for system balance purposes and to guarantee that their realization is technically possible. In systems with high DG penetration, the DSO will need information about DG forecast, schedules and active dispatch to improve their visibility and to assist with real-time or close to real-time management of the distribution network including local network constraints. DSOs should have managed access to communication and monitoring assets of DG to collect information that will be necessary for operation of their networks. The granularity of the data exchange will depend on the size of the generating unit. The necessary information should be then exchanged between the DSO and the TSO (in both directions). DSOs should provide the TSO with information on active power that the TSO needs to facilitate secure system operation. DSOs operating sub-transmission networks may also require TSO information in real time.

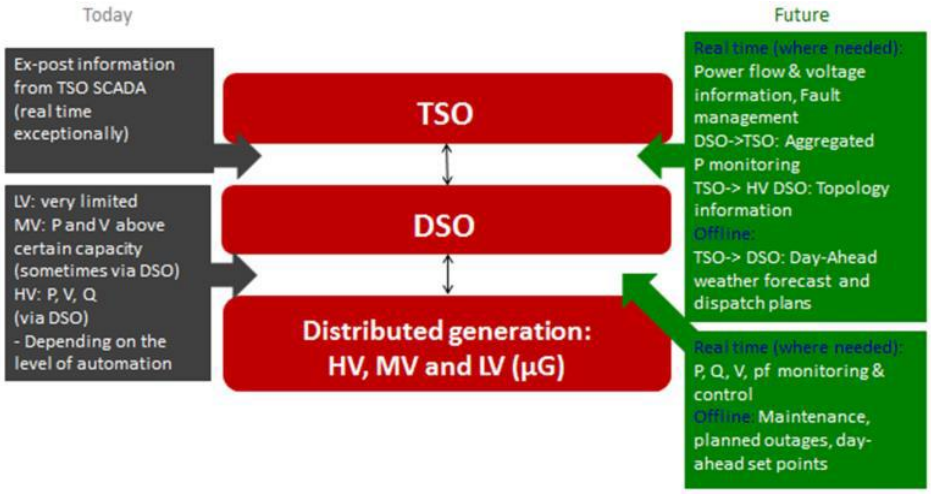

Figure 2.10: *Information Exchange Today and in the Future [17]*

In addition, the participation of DG and load connected to the distribution grid in TSO balancing markets could create constraints in the distribution grid should be taken into account. Generators and flexible loads connected to the distribution grid should be able to also provide these ancillary services for system balancing and transmission system congestion management purposes. Aggregators may be able to achieve certain changes in the demand and in the generation of the consumers and producers in their portfolio, in order to offer services to system operators. However, the issue that an area managed by an aggregator may not correspond to the distribution network responsibility area (forecasts and schedules are delivered at a portfolio level for a bidding zone) needs to be addressed. In these situations, the DSO needs to ensure that this activation does not interfere with security of supply in its own network. Similarly, actions by the DSO to solve constraints could affect the system balance.

Appropriate methodologies and processes should be defined in order to ensure that market schedules are not in conflict with network operation or that transmission and distribution network operation are not in conflict with one another (e.g. TSO asking for a modification which would violate distribution system security standards). Enhanced monitoring and control strategies for distribution networks will need to be deployed.

2.2.3.3 Voltage Control

As outlined previously, system voltage needs to be maintained within a security standard range. Voltage control is a system service managed by network operators in order to maintain voltage in their networks within limits and to minimize the reactive power flows and consequently, technical losses. While generation/load balance is carried out at system level by the TSO, voltage control of the distribution grid requires the involvement of the DSO.

The traditional approach to voltage control includes reinforcing the grid or installing preventative measures. Voltage control has been traditionally done by transformers (using on and off load tap changers) and capacitor banks that inject reactive power into the grid (see Table 2.3). The DSO fixes a set

point and prepares scenarios/ranges for different voltages within which the voltage must be maintained.

Table 2.3: Voltage control in current distribution networks

HV	• Usually power transformers with on-load tap changers • Capacitors frequently used to control the voltage
MV	• No analogue values in secondary substations obtained in real time (typically analogue values only at MV feeders) • MV networks connected to HV through a power transformer with on-load tap changer Capacitors can be commonly found also in these substations to improve the power factor • Voltage set points specified at MV substation busbars
LV	• MV/LV transformers may be fixed ratio (i.e. have not tap changers) or have off-load tap changers, manually controlled. Taps selected to compensate the effect of MV voltage drops at LV levels (passive approach). • These tap-changers operate only a few times during transformers lifetime • Sometimes capacitors are installed in consumer facilities to meet power factor regulations • New controllable MV/LV transformers are emerging but expensive

As the penetration of DG in networks increases, it is no longer possible to ensure sustained system security without some dynamic resources, including reactive power compensation and active voltage control. The DSO's role in ensuring not only that adequate network capacity is available for all connected customers (demand and load) under all conditions, but also in managing voltage and reactive power flows on distribution networks is becoming more complex.

Two technical considerations for voltage control in distribution networks include:

1. With high DG penetration, active power becomes a significant driver for voltages changes in MV and LV networks (the kW-V effect is more significant than the kVAr-V effect). The lower the distribution voltage level, the higher this effect [18].
2. In MV and LV networks, the active power effect may not be always neutralized by the reactive power injections/withdrawals available in the system. To regulate voltage, DSO should be able to control reactive power and in some cases also active power.

In high-voltage networks, DSOs will be able to maintain the voltage within the security standards if they have the means to manage reactive power flows. Real power will not cause voltage deviation under normal operation. On the other hand, at medium and low voltage levels, real power changes due to DG feed-in cause voltage rises (especially in cables) [18]. Distributed generation changes voltage triangle design and as a result, both scenarios with and without DG have to be considered. Reactive power may help compensate the real power effect but may not be sufficient to neutralize it.

As reactive power cannot be transported over long distances and as many regions with high DG penetration (thus voltage control challenges) have no conventional sources of reactive power, managing voltage on a local or sub-regional basis could be the most economically viable solution for the entire

electricity system. For these purposes, the DSO should be able to sectionalize its networks, to actively interact with DG to request supply voltage control and reactive dispatch or to exploit active demand services over the distribution network to solve operational problems. Clear interface conditions and an agreed operational framework at the interface between TSO and DSO are also necessary (including parameters for TSO-DSO interface nodes).

Innovative approaches to voltage control should be explored. Experiences from several European countries show that compensation at the TSO-DSO connection point may not be flexible enough in case of emergency. The increasing DG penetration requires continuous adaption of the capacities at the connection points [135]. Voltage control requires a system approach that would include minimizing system losses, optimizing network investments and coordinating the necessary operational windows and control actions between the individual TSO and DSO, with particular attention to cases of emergency.

Solutions on the network side and on the network users' side should be considered:

Network contribution

There are cases where HV voltage control cannot be achieved in a manner which maintains both transmission and distribution security without additional reactive power resources on the network. Investments in new analytical, control and monitoring expertise and facilities in MV and LV (like power electronics, real time supervision) may be required. For example, satellite cables with large diameters could drastically reduce voltage rise within the grid [19]. Alternatively, voltage controlled MV/LV transformers can be installed in order to decouple the voltage rise within the MV and the LV networks caused by RES feed-in. These innovative network techniques would need to be considered and allowed within regulation.

Combination of both solutions

A combination of both solutions may be used. Studies show that in some situations even a contribution by distributed generation will not be able to maintain the voltage within limits [20]. Both to minimize any impact (real power generation) on DG and to ensure that TSO-DSO interface standards can be maintained for system stability, it may thus be necessary that additional reactive resources are installed in DNs. The contribution of the system operators or DG to these resources must be reflective of the particular network issue being addressed and the beneficiaries of the installation. It may also be necessary in future for DG which will displace reactive power resources to also contribute to the reactive power facilities on its hosting networks so as to maximize its potential to deliver real power. This is already the case with larger (industrial) demand facilities that are required to follow strict power factor regulations. Where this solution is considered the most cost-effective, generators should be required to comply with minimum connection & operational requirements necessary for managing distribution network stability. On the other hand, DG contribution to loss minimization may be compensated on a commercial basis.

Reduction of real power that might be technically necessary to manage the network voltage and avoid complete generation disconnection should be

used only when other solutions have been exhausted. Congestion management would apply in this case, with emergency DG curtailment only if necessary.
So, the recommendations are the following:

- Active DSOs should be allowed to coordinate the offering of new system services. Such system services could be procured as ancillary services from DER or defined in grid codes (voltage and reactive power contribution);
- Flexibility platforms where flexibility is offered (either directly by larger DG/load or via aggregators which group a large number of DG and loads) to DSOs (but also to TSOs to provide balancing and redispatching in transmission grids) could play an important role for close to real-time flexibility in particular;
- DSOs should be included in the information exchange about:
  - planned location/connection/clustering of contracted customers (aggregators);
  - forecasts and schedules necessary for dealing with local grid constraints;

  Appropriate methodologies and tools for these purposes should be developed;
- Voltage control requires a system approach considering transmission and distribution networks. Coordination between DSO and TSO at the interface point should aim at reactive power optimization and minimizing system investments and losses;
- DG contribution to voltage control, probably in combination with network solutions, is likely to play an important role in keeping DNs stable. Where this solution proves to be the most cost-effective one, generators connected to the DN above a certain capacity should be required to have reactive power capabilities in line with those for transmission connected RES, adapted to the connection level and capacity.

2.2.4 Technical Development: Towards Flexible Distribution Systems

With a rising share of DER, monitoring, control strategies and advanced protection systems in MV and LV distribution networks will have to develop in order to enable DSOs to:

- Determine and forecast grid capacity and bottlenecks;
- Supervise and control power flows and voltage in their networks;
- Enable the new operations at the distribution level (including non-discrimination and effective real-time grid capacity monitoring and management of injections/withdrawals);
- Enable congestion management and voltage control procedure in distribution networks;
- Enhance the distribution grid hosting capability.

This solution should not be taken up in isolation from other options such as services from DERs to help manage the DS mentioned above. The route to the future energy system will incorporate both aspects. The most economically efficient solution will depend on the topology, load and generation profiles

within a given DS. A two-level approach might be adopted: larger DG (with a defined installed capacity and level of connection) could be monitored and tele-controlled while other DER may not be dispatchable and should be forecast and monitored by the DSO on an aggregated basis at the substation level.

Technology options for development of the abovementioned options are outlined in Table 2.4. In addition, new design ideas such as "satellite cables" and dynamic line rating (DLR) are being tested. With DLR, real-time information, for example the temperature of the conductor or the wind speed, can be used to calculate a temporary rating of a line, thus allowing more power to flow. This technology increases the utilization of the line and also allows more RES to be integrated than if static ratings were used. Smart meters will provide relevant monitoring functionalities, such as real-time local voltage and load data that will be of high importance in DN management processes and systems.

Table 2.4: Technology options for distribution network development

Function	Medium Voltage	Low Voltage
Monitoring	Current, voltage, fault passage indicators and other sensors	Centralization of information via secondary substations
Control	Remotely controllable reclosers, switches automated protection / fault sectionalization – remote monitored fault detectors Voltage or power factor set points to DGs	Controllable MV/LV transformers (with centralized or decentralized sensors)

2.3 Implications for Regulation and Market Design

The transition towards more active DNs requires the development of technology as well as requirements for both network operators and network users to contribute to system security. Appropriate commercial and regulatory frameworks need to be put in place.

As mentioned above, the new Energy Efficiency Directive (Art 15.1 of 2012/27/EC) provides a good baseline for setting up system services at distribution level that will allow for an energy efficient use of infrastructure. Its appropriate implementation is thus crucial.

In addition, regulation and a flexibility market model should be further developed to address the following issues:

- Principles and methods for defining system states within the so-called 'traffic lights concept': boundaries between the green, yellow (procurement of flexibility from markets) and red zones (emergency state with non-commercial services) should be defined depending on physical operating boundaries of a system, including methodologies of how they will be monitored, calculated and audited.
- Regulations for governing the most cost-efficient solutions: Regulatory mechanisms for governing, when the investment delaying is more cost-effective than active distribution approach, should be elaborated, for

example in order to ensure that network development occurs when excursions to the yellow and red operating states become too frequent. Active system management will affect the amount and structure of operational expenditure and would replace some CAPEX with OPEX. DSOs should be able to look at the business case for both the investment solution (CAPEX) and the service-based solution (OPEX), or a mixture of the two, and decide which is preferable. Adoption of a regulatory mechanism is necessary to integrate this approach in the grid fee calculation. DSOs need to be provided with adequate remuneration for the most adequate solution: investment or active system management tools including procurement of flexibility services from network users.

- New roles and relationships between different actors in the market: In particular, the role of flexibility providers (to be taken up by aggregators/suppliers/ESCOs) and the relationship between these flexibility providers and network operators, suppliers, the balance responsible party (BRP) and the local customer/local producer should be addressed.
- Interaction between the DSO and the market: How will the DSO have visibility of what is happening on the market side that may impact on the DSO network and cause constraints in the short or long term? For example, a flexibility provider may have a contract to provide reserves to the TSO, but needs to use the DS to which its resources are connected to deliver this service. However, a bottleneck on the DS may prevent this delivery. These technical aspects of flexibility markets require further investigation.
- Measurement/determination of "non-produced" and "non-consumed" energy is an important related issue: unlike consumed and produced energy, saying how much a generator has "not produced" when he reduced his production on demand of e.g. an aggregator is rather difficult, and appropriate methodologies have to be developed and implemented. Knowledge of the initial schedule is important in this respect.
- Revision of planning guidelines for distribution network development: Revision of these rules should be reconsidered in order to account for ancillary services that the DSO can procure. Are deterministic security standards such as the *N*-1 criterion appropriate or should they move to being more probabilistic and based on reasonable risk of expected energy not served in order to maintain high reliability while minimizing over-investment in redundant capacity?
- Establishment of contingency assessment and outage management (organization and coordination of outages) rules for DNs and their users.

2.4 Conclusions

1. Secure and cost-effective integration of DER requires a rethink of how distribution grids are planned and operated

Distribution networks are currently coping with the rapid increases in decentralized RES feed-in that Europe is experiencing. Decentralized feed-in of RES has already started to outstrip local demand in some European

regions. This growth can be quite rapid, as the increased feed-in often occurs in rural areas with little demand. Building sources of production close to consumption does not reduce DN cost. The network still has to be designed to supply maximum demand for situations when there is no DG production. In addition, operation of such a system becomes more complex. Once the share of decentralized RES passes a certain point, it overburdens the local distribution grid. DSOs are therefore increasingly facing voltage problems and grid congestions.

2. DSOs need tools that allow them to become real system operators

DSOs are responsible for developing their grids efficiently and providing quality of service for end customers. But in order to satisfy these responsibilities in the changing context of DER/DG, DSOs need adequate new tools. On one side, advanced software solutions are necessary for managing the DN in optimized way. Then, system services at the distribution level are key in this respect. Such services include the participation of decentralized generators in voltage and reactive power management, distribution network capacity management and congestion management, and information exchange between TSOs, DSOs and DER.

Distribution network capacity management involves taking services from DER into account in the planning stage to optimize investments and ensure that infrastructure is only extended when it is more cost-efficient than procuring services from DER.

3. Optimizing DER management through flexibility services should be explored

Traditional methods of grid expansion reinforce the network so that it may bear maximum feed-in from distributed generation. However, such maximum capacity is only required for a short period of time each year. While this approach will remain important, it may therefore not always be the most optimal and cost-effective solution – not least because new lines often face problems of public acceptance.

New solutions must be developed to enhance the hosting capacity of the distribution grid; minimizing situations when DG feed-in has to be reduced or new connections have to be denied. Such solutions include new network technologies and design concepts, the contribution of generation to system performance, and access to flexibility services provided by DG operators, storage and demand response. Their flexibility could be procured on a competitive basis via flexibility platforms and be offered to DSOs, but also to TSOs as a way of managing redispatching issues in transmission grids. They should be used whenever it is most efficient.

4. One-size-does-not-fit-all: different distribution networks require different solutions

While best practice sharing is desirable, the most economically efficient solution will depend on the topology, demand and generation profiles within a given distribution system. The route to the future energy system will probably incorporate aspects of each of the above mentioned solutions. The regulatory

framework should grant DSOs enough flexibility to determine the most appropriate solution for their network. Methods of prioritizing and selecting the most cost-effective solutions should be further investigated.

5. Coordination among all relevant stakeholders is the key

A system-wide approach to DG and network development is needed. For instance, all stakeholders must be involved in analyzing grid connection requests. This will lower the costs of network development and connection while reducing connection waiting times for new users compared to business as usual.

6. Take into account lessons learnt from smart grid demonstration projects

Europe already has experience of smart grid demonstration projects worth more than €5.5 billion [21]. The future large-scale deployment of smart grids should reflect best practices from these projects and already implemented solutions. European network codes are currently being designed and will include requirements for distribution network users. They should take into account latest improvements on the ground and not close the door to the implementation of new, proven innovation in distribution networks. Standardization plays a key role in facilitating these solutions.

7. Tap into the potential of aggregation

Aggregators will act as possible middlemen for many small DG and load customers, offering the flexibility options they buy from their clients to TSOs and DSOs. A market model should be developed to unlock the potential of such aggregation and new roles and relationships between new and existing actors should be defined. This will enable demand, DG and storage resources to participate in the markets for energy and ancillary services.

8. Equip DSOs with the tools they need to ensure quality of service and to facilitate the market

Establishment of system services at distribution level calls for adequate supporting tools that allow DSOs to operate their networks in a "more active" way. Such tools should include access to technical data and further development of the ICT systems essential for operational control of the grid**.**

It is the basic task of DSOs to guarantee security in their grids and to support the security of the system as a whole. They are also in the best position to plan and manage the new opportunities and risks related to the grid. They should thus act as facilitators for flexibility platforms which will allow generators, suppliers and consumers to offer network services either directly or via aggregators.

DSOs are also best suited to manage operational data of distribution network users and pass it to TSOs in an appropriate form and in the cost-effective manner if needed.

The flexibility market and European rules for system operation should not be designed in isolation. Technical and commercial data will become more interrelated. Operational rules have an impact on market rules. EU network codes that redefine operational and balancing rules will have implications for

procurement of flexibility services from DG, decentralized storage and flexible loads and should therefore be designed to facilitate it.

9. Review connection and access regimes for distributed energy resources

A review of grid access regimes, including priority and guaranteed grid access for renewables is becoming increasingly necessary. Currently such rules prevent grid and market operators from implementing cost-effective solutions to avoid grid congestion. Instead, they trigger inefficient investments in grid extension based on rare situations.

Variable network access contracts or alternatives involving close to real-time operation might be part of the solution. They would allow for limiting DG injection by the grid operator based on an agreement with the producer concerned, who would be remunerated, or at the initiative of the producer on the basis of market prices and/or local flexibility mechanisms.

Priority access rules for DER also should not prevent network operators from responding flexibly to emergency situations.

10. Design regulation to include network solutions beyond simple "investment in copper"

DSO regulation should be adjusted to encourage the transformation of DNs into actively managed DSs wherever this is the most economical solution. Faced with new challenges posed by DER, DSOs could design and operate their networks more efficiently if national regulation defines cost-efficiency more broadly. The expected replacement of part of CAPEX by OPEX should be taken into account and DSOs should be provided with an adequate reward for CAPEX and improved evaluation of OPEX. DSOs should receive an adequate rate of return on their network investments without time delay.

In addition, the current approach to network development should be reconsidered: DSOs should be able to take into account DER and conventional assets when planning their networks (as required by Article 25.7 of Directive 2009/72/EC).

CHAPTER 3

3. Classical State Estimation

3.1 Introduction

Power systems are operated by system operators from the area control centers. The main goal of the system operator is to maintain the system in the normal secure state as the operating conditions vary during the daily operation. Accomplishing this goal requires continuous monitoring of the system conditions, identification of the operating state and determination of the necessary preventive or corrective actions in case the system state is found to be *insecure*. This sequence of actions is referred to as the security analysis of the system.

The first stop of security analysis is to monitor the current state of the system. This involves acquisition of measurements from all parts of the system and then processing them in order to determine the system state. The measurements may be both of analog and digital (on/off status of devices) type. Substations are equipped with devices called remote terminal units (RTU) which collect various types of measurements from the field and are responsible for transmitting them to the control center. More recently, the so-called intelligent electronic devices (IED) are replacing or complementing the existing RTUs. It is possible to have a mixture of these devices connected to a local area network (LAN) along with a SCADA front end computer, which supports the communication of the collected measurements to the host computer at the control center. The SCADA host computer at the control center receives measurements from all the monitored substations' SCADA systems via one of many possible types of communication links such as fiber optics, satellite, power line connection (PLC), etc.

Measurements received at the control center will include line and transformer power flows, bus voltage and line current magnitudes, generator outputs, loads, circuit breaker and switch status information, transformer tap positions, and switchable capacitor bank values. These raw data and measurements are processed by the state estimator in order to filter the

measurement noise and detect gross errors. State estimator solution will provide an optimal estimate of the system state based on the available measurements and on the assumed system model. This will then be passed on to all the energy management system (EMS) application functions such as the contingency analysis, automatic generation control, load forecasting and optimal power now, etc. The same information will also be available via a LAN connection to the corporate offices where other planning and analysis functions can be executed off-line.

Static state estimation refers to the procedure of obtaining the voltage phasors at all of the system buses at a given point in time. This can be achieved by direct means which involve very accurate synchronized phasor measurements of all bus voltages in the system. However, such an approach would be very vulnerable to measurement errors or telemetry failures. Instead, state estimation procedure makes use of a set of redundant measurements in order to filter out such errors and find an optimal estimate. The measurements may include not only the conventional power and voltage measurements, but also those others such as the current magnitude or synchronized voltage phasor measurements as well. Simultaneous measurement of quantities at different parts of the system is practically impossible; hence a certain amount of time skew between measurements is commonly tolerated. This tolerance is justified due to the slowly varying operating conditions of the power systems under normal operating conditions.

The definition of the system state usually includes the steady state bus voltage phasors only. This implies that the network topology and parameters are perfectly known. However, errors in the network parameters or topology do exist occasionally, due to various reasons such as unreported outages, transmission line sags on hot days, etc.

The foregoing concerns were first recognized and subsequently addressed by Fred Schweppe, who proposed the idea of state estimation in power systems [22],[23],[24]. Introduction of the state estimation function broadened the capabilities of the SCADA system computers, leading to the establishment of the EMS, which would now be equipped with, among other application functions, an on-line State Estimator (SE) [25].

3.2 Power System Static State Estimation

3.2.1 Nonlinear Measurement Model

A power system with *N* buses is considered, where *m* quantities are measured and whose topology and parameters are known. Under these conditions, if the complex bus voltages are known, it is possible to determine any power flow in the transmission network and/or any bus power injection. This is the reason why the complex bus voltages are named state variables of the power system.

The set of m measurements taken along the electrical network and the measurement errors are related through the following model [26]:

$$\mathbf{z} = \mathbf{z}_0 + \boldsymbol{\eta} \tag{3.1}$$

where, **z** is a (m × 1) vector of the measurements; $\mathbf{z}_0$ is a (m × 1) vector of the actual measurements, which is a function of the actual power system state and $\boldsymbol{\eta}$ is a (m × 1) random vector which models the measurement errors (inaccuracy of the meters, errors of transformers as measurement instruments, communication errors, effects of analog-digital conversion, etc.).

The actual values of state variables of the power system, and consequently the actual value of the measured quantities, are unknown. In order to estimate the power network state, it is necessary to make certain assumptions about the measurement model and using the relationship between the measurements and the estimated states. With respect to the measurements, it is observed that all meters have an error whose magnitude is related to its accuracy level. Under normal circumstances, the magnitude of this error is situated within a tolerable range and does not deteriorate the measurement. In addition, the error of a meter does not affect the measurement taken by another meter. For this reason, it is assumed that the vector of measurement errors has a Gaussian (normal) distribution $E(\eta)$, with zero mean and a covariance matrix R, which is analytically expressed as:

$$E(\boldsymbol{\eta}) = 0 \quad E(\boldsymbol{\eta}\boldsymbol{\eta}^t) = \mathbf{R} \tag{3.2}$$

where **R** is a diagonal matrix, indicating that measurement errors are not inter-related. The diagonal elements of this matrix are the variances of the measurement errors, which are usually expressed as a function of the full scale value of meters.

The actual values of the measurements and the actual states are related by:

$$\mathbf{z}_0 = \mathbf{h}(\mathbf{x}) \tag{3.3}$$

where **h**(**x**) is a vector composed of *m* nonlinear functions of the system state, based on Kirchhoff's and Ohm's laws and **x** is the vector of power system states, which for a power system with *N* buses is a $n = 2N - 1$ column vector (only the reference angle is not included in the vector of system states). Under these assumptions the measurement model of Eq. (3.1) is re-written as:

$$\begin{gathered} \mathbf{z} = \mathbf{h}(\mathbf{x}) + \boldsymbol{\eta} \\ E(\boldsymbol{\eta}) = 0; \quad E(\boldsymbol{\eta}\boldsymbol{\eta}^t) = \mathbf{R} \end{gathered} \tag{3.4}$$

The measurements typically include real and reactive power flows in the transmission, real and reactive power injections in the buses, and voltage magnitudes. The magnitude of the current in transmission lines could also be monitored, but this practice is not the usual in HV transmission systems. Another important aspect is related to the number and location of the measurements in the electrical network. The degree of redundancy of the measurement set is denoted by ρ and defined as:

$$\rho \triangleq \frac{m}{n} = \frac{m}{2N - 1}$$

Observe that a necessary (but not sufficient) condition to estimate the state of the power system is: $m \geq n$, or $\rho \geq 1.0$. In addition to a good

redundancy (ρ > 1.5, for example), it is required that the measurements are distributed properly in the electrical network, because this facilitates both the state estimation itself and the detection and identification of gross errors.

Finally, in addition to the set of tele-measurements obtained via SCADA, some components of the vector of measured quantities z can be the so-called pseudo-measurements; that is, information from other sources (studies of load forecasting or results of previous estimates, for example) stored in a static database. The variances of these measurements must reflect the degree of uncertainty associated with them, which in general is greater than that associated with the normal measurements.

3.2.2 Weighted least squares method

The formulation of the Power System State Estimation (PSSE) based on the Weighted Least Squares (WLS) approach consists of estimating the state $\hat{\mathbf{x}}$ by minimizing the unconstrained objective function:

$$J(\hat{\mathbf{x}}) = [\mathbf{z} - \mathbf{h}(\hat{\mathbf{x}})]^t \mathbf{R}^{-1} [\mathbf{z} - \mathbf{h}(\hat{\mathbf{x}})] = \sum_{i=1}^{m} R_{ii}^{-1} [z_i - h_i(\hat{\mathrm{x}})]^2 \tag{3.5}$$

with respect to $\hat{\mathbf{x}}$.

Bearing in mind the measurement model given by Eq. (3.4), in the problem stated by Eq. (3.5), the quantity:

$$\mathbf{r} = \mathbf{z} - \mathbf{h}(\hat{\mathbf{x}})$$

represents the *vector of measurement residuals*. It is computed as the difference between the value effectively measured and the value computed with the estimated state. Therefore, the target is to calculate the vector $\hat{\mathrm{x}}$ which minimizes the sum of the squared residuals, weighted by the inverse of the variances of the measurement errors. The weighting factors represented by the inverse matrix **R** indicate that the greater the uncertainty with respect to the measurement, the smaller the weight (or importance) assigned to the measurement. That is, the measurements of lower variance receive greater weight than those which have greater uncertainty, and therefore have a greater influence on the solution of the optimization problem. The optimization process will naturally tend to assign higher residuals (in magnitude) to the less accurate measurements.

Figure 3.1 illustrates geometrically the formulation of the least squares problem. A set of points (t_1, Z_1), (t_2, Z_2), (t_3, Z_3) and (t_4, Z_4) is given, through which a straight line must be drawn. Due to the impossibility of the straight line to pass simultaneously by these four points, it is necessary to formulate a problem in which the sum of the absolute differences between the values Z_i available and the corresponding points where the straight will pass, named residuals and denoted by r_1, r_2, r_3 and r_4, is minimized.

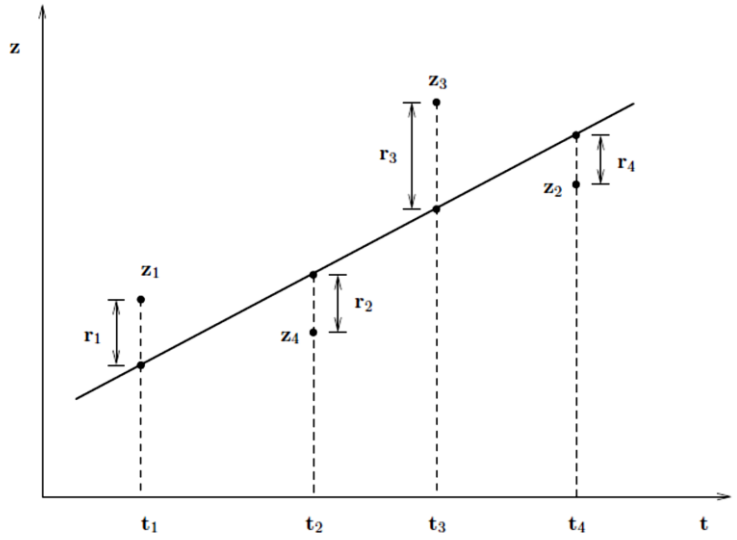

Figure 3.1: *Linear regression - geometrical illustration*

3.3 Gauss-Newton Method

The PSSE can be formulated as a weighted least squares problem expressed as:

$$\min_{\hat{\mathbf{x}}} J(\hat{\mathbf{x}}) = [\mathbf{z} - \mathbf{h}(\hat{\mathbf{x}})]^t \mathbf{R}^{-1} [\mathbf{z} - \mathbf{h}(\hat{\mathbf{x}})] \tag{3.6}$$

where **x** is the vector of state variables, **z** is the vector of measurements and **R** is the covariance matrix of the measurement errors.

The optimality condition for the problem stated by Eq. (3.6) is expressed by:

$$\left.\frac{\partial J}{\partial x}\right|_{\mathbf{x}=\hat{\mathbf{x}}} = 0 \Rightarrow \mathbf{H}^t(\hat{\mathbf{x}})\mathbf{R}^{-1}[\mathbf{z} - \mathbf{h}(\hat{\mathbf{x}})] = 0 \tag{3.7}$$

where $\mathbf{H}(\hat{\mathbf{x}}) = \left.\frac{\partial \mathrm{h}(\mathbf{x})}{\partial \mathbf{x}}\right|_{\mathbf{x}=\hat{\mathbf{x}}}$ is the matrix of first derivatives of the non-linear functions **h**(**x**), calculated at the point $\hat{\mathbf{x}}$. Despite the minimization of the function expressed by Eq. (3.6) does not involve constraints, the search for the solution of the least squares problem presents considerable difficulty. The index to be optimized is a quadratic function, expressed in terms of a vector of non-linear equations relating the state variables and the measurements. Additionally, Eq. (3.7), which represents the optimality conditions, has no closed solution and therefore requires the use of iterative methods. Several numerical methods could be applied to solve a problem of this type. However, the quadratic nature of the objective function and the absence of constraints make this optimization problem appropriate to the solution by the Newton's method, described in following subchapter.

3.3.1 Linearization of the Measurement Model

The application of iterative methods to solve the non-linear optimization problem expressed by Eq. (3.6) requires the current estimate of the state vector to be updated with successive corrections given by:

$$\hat{\mathbf{x}}^{k+1} = \hat{\mathbf{x}}^{k} + \Delta\mathbf{x} \tag{3.8}$$

In order to determine the increment $\Delta\mathbf{x}$ of Eq. (3.8), the linearization of $\mathbf{h}(\mathbf{x})$ around the point $\hat{\mathbf{x}}^{k}$, in the direction $(\mathbf{x} - \hat{\mathbf{x}}^{k})$, should be considered:

$$\mathbf{h}(\hat{\mathbf{x}}^{k} + \Delta\mathbf{x}) \approx \mathbf{h}(\hat{\mathbf{x}}^{k}) + \mathbf{H}(\hat{\mathbf{x}}^{k})(\mathbf{x} - \hat{\mathbf{x}}^{k}) \tag{3.9}$$

where all terms have been previously defined.

The replacement of this equation in $\mathbf{z} = \mathbf{h}(\mathbf{x}) + \boldsymbol{\eta}$ provides:

$$\mathbf{z} - \mathbf{h}(\hat{\mathbf{x}}^{k}) = \mathbf{H}(\hat{\mathbf{x}}^{k})(\mathbf{x} - \hat{\mathbf{x}}^{k}) + \boldsymbol{\eta}$$

which stands for the linearized measurement model and whose compact form is given by:

$$\Delta\mathbf{z} = \mathbf{H}(\hat{\mathbf{x}}^{k})\Delta\mathbf{x} + \boldsymbol{\eta}$$
$$E(\boldsymbol{\eta}) = 0; \quad E(\boldsymbol{\eta}\boldsymbol{\eta}^{t}) = \mathbf{R}$$

where $\Delta\mathbf{z} = \mathbf{z} - \mathbf{h}(\hat{\mathbf{x}}^{k})$ is the vector of measurement residuals and $\Delta\mathbf{x} = (\mathbf{x} - \hat{\mathbf{x}}^{k})$.

In terms of the linearized measurement model, the objective function of the least squares problem of Eq. (3.6) is expressed as:

$$J(\Delta\mathbf{x}) = [\Delta\mathbf{z} - \mathbf{H}(\hat{\mathbf{x}}^{k})\Delta\mathbf{x}]^{t}\mathbf{R}^{-1}[\Delta\mathbf{z} - \mathbf{H}(\hat{\mathbf{x}}^{k})\Delta\mathbf{x}]$$

and the corresponding optimality condition is given by:

$$\left.\frac{\partial J}{\partial \Delta\mathbf{x}}\right|_{\mathbf{x}=\hat{\mathbf{x}}^{k}} = 0 \Longrightarrow \mathbf{H}^{\mathrm{t}}(\hat{\mathbf{x}}^{k})\mathbf{R}^{-1}[\Delta\mathbf{z} - \mathbf{H}(\hat{\mathbf{x}}^{k})\Delta\mathbf{x}] = 0$$

Or alternatively:

$$[\mathbf{H}^{\mathrm{t}}(\hat{\mathrm{x}}^{k})\mathbf{R}^{-1}\mathbf{H}(\hat{\mathrm{x}}^{k})]\Delta\mathrm{x} = \mathbf{H}^{\mathrm{t}}(\hat{\mathrm{x}}^{k})\mathbf{R}^{-1}\Delta\mathrm{z} \tag{3.10}$$

The expression (3.10) is called Gauss Normal Equation and represents the linear system to be solved at each iteration for the determination of the increment $\Delta\mathbf{x}$ of the state vector. This correction can also be determined by using the Gauss-Newton iterative method. In this case, the function $J(\mathbf{x})$ of Eq. (3.6) is expanded in Taylor series, around the point $\hat{\mathbf{x}}^{k}$, along the direction $\Delta\mathbf{x}$, to the second order term, that is:

$$J(\hat{\mathbf{x}}^k + \Delta\mathbf{x}) = J(\hat{\mathbf{x}}^k) + \left.\frac{\partial J(\mathbf{x})^t}{\partial \mathbf{x}}\right|_{\mathbf{x}=\hat{\mathbf{x}}^k} \Delta\mathbf{x} + \frac{1}{2}\Delta\mathbf{x}^t \left.\frac{\partial^2 J(\mathbf{x})}{\partial \mathbf{x}^2}\right|_{\mathbf{x}=\hat{\mathbf{x}}^k} \Delta\mathbf{x}$$

where: $\left.\frac{\partial J(\mathbf{x})}{\partial \mathbf{x}}\right|_{\mathbf{x}=\hat{\mathbf{x}}^k}$ and $\left.\frac{\partial^2 J(\mathbf{x})}{\partial \mathbf{x}^2}\right|_{\mathbf{x}=\hat{\mathbf{x}}^k}$ are respectively the vector of first derivatives and the matrix of second derivatives of the function $J(\mathbf{x})$ with respect to $\mathbf{x}$, calculated in point that represents the current estimate $\hat{\mathbf{x}}^k$.

The minimum of the function $J(\hat{\mathbf{x}}^k + \Delta\mathbf{x})$ is obtained by differentiating this function with respect to $\Delta\mathbf{x}$ and making the result equal to zero, that is:

$$\frac{\partial J}{\partial(\Delta\mathbf{x})} = \left.\frac{\partial J(\mathbf{x})^t}{\partial \mathbf{x}}\right|_{\mathbf{x}=\hat{\mathbf{x}}^k} + \left.\frac{\partial^2 J(\mathbf{x})}{\partial \mathbf{x}^2}\right|_{\mathbf{x}=\hat{\mathbf{x}}^k} \Delta\mathbf{x} = 0$$

or alternatively:

$$\left.\frac{\partial^2 J(\mathbf{x})}{\partial \mathbf{x}^2}\right|_{\mathbf{x}=\hat{\mathbf{x}}^k} \Delta\mathbf{x} = -\left.\frac{\partial J(\mathbf{x})^t}{\partial \mathbf{x}}\right|_{\mathbf{x}=\hat{\mathbf{x}}^k} \tag{3.11}$$

The gradient vector $\left.\frac{\partial J(\mathbf{x})}{\partial \mathbf{x}}\right|_{\mathbf{x}=\hat{\mathbf{x}}^k}$ is given by:

$$\begin{aligned} \left.\frac{\partial J(\mathbf{x})}{\partial \mathbf{x}}\right|_{\mathbf{x}=\hat{\mathbf{x}}^k} &= \left.\left(\frac{\partial\{[\mathbf{z}-\mathbf{h}(\hat{\mathbf{x}})]^t \mathbf{R}^{-1}[\mathbf{z}-\mathbf{h}(\hat{\mathbf{x}})]\}}{\partial \mathbf{x}}\right)\right|_{\mathbf{x}=\hat{\mathbf{x}}^k} = \\ &= -2\left(\frac{\partial \mathbf{h}(\mathbf{x})}{\partial \mathbf{x}}\right)^t \Bigg|_{\mathbf{x}=\hat{\mathbf{x}}^k} \mathbf{R}^{-1}[\mathbf{z}-\mathbf{h}(\hat{\mathbf{x}})]\big|_{\mathbf{x}=\hat{\mathbf{x}}^k} \\ &= -2\mathbf{H}(\hat{\mathbf{x}}^k)^t \mathbf{R}^{-1}\Delta\mathbf{z} \end{aligned} \tag{3.12}$$

where $\mathbf{H}(\hat{\mathbf{x}}^k)$ and $\Delta\mathbf{z}$ were previously defined.

The application of the same procedure to compute the matrix of second derivatives of J(x) provides:

$$\left.\frac{\partial^2 J(\mathbf{x})}{\partial \mathbf{x}^2}\right|_{\mathbf{x}=\hat{\mathbf{x}}^k} = \left.\frac{\partial}{\partial \mathbf{x}}\left[-2\left(\frac{\partial \mathbf{h}(\mathbf{x})}{\partial \mathbf{x}}\right)\mathbf{R}^{-1}[\mathbf{z}-\mathbf{h}(\hat{\mathbf{x}})]\right]\right|_{\mathbf{x}=\hat{\mathbf{x}}^k}$$

Supposing that in the neighborhood of the solution the variations of the matrix H(x) are negligible, that is:

$$\mathbf{H}(\mathbf{x}) = \frac{\partial \mathbf{h}(\mathbf{x})}{\partial \mathbf{x}} \approx constant$$

then:

$$\left.\frac{\partial^2 J(\mathbf{x})}{\partial \mathbf{x}^2}\right|_{\mathbf{x}=\hat{\mathbf{x}}^k} \approx 2\mathbf{H}^t(\hat{\mathbf{x}}^k)\mathbf{R}^{-1}\mathbf{H}(\hat{\mathbf{x}}^k)$$

such that Eq. (3.11) is rewritten as:

$$\mathbf{H}^t(\hat{\mathrm{x}}^k)\mathbf{R}^{-1}\mathbf{H}(\hat{\mathrm{x}}^k)\,\Delta\mathrm{x} = \mathbf{H}^t(\hat{\mathrm{x}}^k)\mathbf{R}^{-1}\Delta\mathrm{z} \tag{3.13}$$

which is the same expression obtained with the linearized measurement model.

3.3.2 Computational Aspects

The matrix **R** of Eq. (3.13) is diagonal. For this reason, the product matrix ($\mathbf{H}^t\mathbf{R}^{-1}\mathbf{H}$), named Gain or Information matrix, is approximately twice more dense than the matrix **H**. Additionally, the matrix **H** is sparse and thus the information matrix has a number of non-zero elements which allows the use of sparse techniques. In addition, this matrix is symmetrical in structure and numerical values and positive semidefinite, which facilitates their factorization [27].

The elements of the Jacobian matrix $\mathbf{H}(\hat{\mathbf{x}}^k)$ are obtained by deriving the expressions of $\mathbf{h}(\mathbf{x})$ with respect to the state vector x. Despite the simplicity of these derivatives, the calculation of their numerical values demands a reasonable computational effort, since it is performed repeatedly during the iterations.

The iterative process starts at an initial estimate $\hat{\mathbf{x}}^0$ and computes increments in the state variables $\Delta\hat{\mathbf{x}}$ by solving the linear system of Eq. (3.13) at each iteration. The state vector is updated according to Eq. (3.8), until the convergence criterion is satisfied, that is:

$$\max|\Delta\hat{x}_i| \leq \varepsilon \tag{3.14}$$

where ε is a pre-specified tolerance. This criterion indicates that the iterative process is finished when the magnitude of adjustments in the state variables is negligible. Another important aspect of the problem represented by the normal equation (3.13) is that it has a tendency to numerical ill-conditioning. This can be verified by analyzing the number of conditioning of the matrix of information. The spectral conditioning number of a matrix **C** is defined as:

$$Cond(\mathbf{C}) = \frac{\sigma_M}{\sigma_m} \tag{3.15}$$

where σ_M and σ_m are respectively the maximum and the minimum eigenvalues of matrix **C**.

The index Cond (**C**) provides a measurement of how small disturbances in matrix **C** affect the solution of the linear system $\mathbf{Cx} = \mathbf{b}$. With respect to the Gauss Normal equation it can be proved that:

$$Cond(\mathbf{H}^t\mathbf{H}) = (Cond(\mathbf{H}))^2$$

that is, if **H** is numerically ill-conditioned, matrix $\mathbf{H}^t\mathbf{H}$ will have a worse numerical conditioning.

The linear system of Eq. (3.13) can be solved by applying the method of Cholesky and the 2nd method of Tinney (also known as minimum degree algorithm). The procedure for obtaining the solution of the normal equation can be summarized in the following steps:

- Decompose the information matrix $\mathbf{A} = [\mathbf{H}^t\mathbf{R}^{-1}\mathbf{H}]$ (symmetrical and positive definite), via Cholesky method, in $\mathbf{A} = \mathbf{L}^t\mathbf{L}$
- Perform inverse substitution in the linear system $\mathbf{L}^t\mathbf{y} = \mathbf{b}$, to obtain $\mathbf{y}$ (where $\mathbf{b} = \mathbf{H}^t\mathbf{R}^{-1}\Delta\mathbf{z}$), and direct substitution in the linear system $\mathbf{L}\Delta\mathbf{x} = \mathbf{y}$ to obtain $\mathbf{x}$.

Since the structure of the information matrix is not modified during the iterative process, the ordering and the structure of matrix A can be determined only once, which speeds up the computational process, since the solution method is iterative and requires multiple solutions of the normal equation.

3.3.3 Algorithm

The state estimation through Gauss-Newton method can be summarized in the following sequence of steps:

1. determine the structure of the Jacobian matrix $\mathbf{H}(\mathbf{x})$ and information matrix $[\mathbf{H}^t\mathbf{R}^{-1}\mathbf{H}]$ and the ordering scheme of the information matrix;
2. specify an initial estimate for the state variables vector $\hat{\mathbf{x}}^0$;
3. calculate the numerical values of $\mathbf{H}(\hat{\mathbf{x}}^k)$, $\mathbf{H}^t(\hat{\mathbf{x}}^k)\mathbf{R}^{-1}\mathbf{H}(\hat{\mathbf{x}}^k)$, $\Delta\mathbf{z} = \mathbf{z} - \mathbf{h}(\hat{\mathbf{x}}^k)$ and $\mathbf{b} = \mathbf{H}^t(\hat{\mathbf{x}}^k)\mathbf{R}^{-1}\Delta\mathbf{z}$;
4. factorize the information matrix $[\mathbf{H}^t\mathbf{R}^{-1}\mathbf{H}] = \mathbf{L}\mathbf{L}^t$;
5. solve the linear system $\mathbf{L}\mathbf{L}^t\Delta\mathbf{x}^k = \mathbf{b}$;
6. update the state variables vector $\hat{\mathbf{x}}^{k+1} = \hat{\mathbf{x}}^k + \Delta\mathbf{x}^k$
7. check convergence: if $\max|\Delta\hat{x}_i| \leq \varepsilon$ (generally $\varepsilon = 10^{-4}\ pu$), compute the power flows in the transmission lines and the power injections and finish the iterative process.
8. make $k = k + 1$ and return to step 3;

It is noted that in the last iterations of the iterative process the changes in the numerical values of the matrix $\mathbf{H}$ are practically negligible, which allows you to keep this matrix constant during some iterations. This strategy reduces the computational effort demanded by the iterative process, provided that in the final iterations only the calculation of $\Delta\mathbf{z} = \mathbf{h}\left(\hat{\mathbf{x}}^{(k)}\right) - \mathbf{z}$ and $\mathbf{b} = \mathbf{H}^t(\hat{\mathbf{x}}^k)\mathbf{R}^{-1}\Delta\mathbf{z}$ is required.

3.3.3 Decoupled Estimators

The decoupled estimators are based on the same approximations of the fast decoupled power flow. The main characteristics of these estimators are the exploration of the $P\delta - QV$ decoupling and the use of constant matrices (information matrix $\mathbf{H}^t(\hat{\mathbf{x}})\mathbf{R}^{-1}\mathbf{H}(\hat{\mathbf{x}})$ and/or Jacobian matrix $\mathbf{H}$) [28].

To show how the decoupling $P\delta - QV$ can be explored in the state estimation algorithms, suppose that the vector of measurements is partitioned as:

$$\mathbf{z} = \begin{bmatrix}\mathbf{z}_P \\ \mathbf{z}_Q\end{bmatrix} = \begin{bmatrix}\mathbf{t} \\ \mathbf{p} \\ \mathbf{u} \\ \mathbf{q} \\ \mathbf{V}\end{bmatrix}$$

where, $\mathbf{z}_P$ corresponds to **p** and **t**, which are the vector of the real power injection and real power flow measurements, respectively; and $\mathbf{z}_Q$ corresponds to **u**, **q** and **V**, which represent the vectors of the reactive power injection, reactive power flow, and voltage magnitude measurements.

By adopting a similar partition to the non-linear functions that relate the measurements to the states and to the measurement errors, the measurement model can be expressed as:

$$\begin{bmatrix}\mathbf{z}_P\\ \mathbf{z}_Q\end{bmatrix} = \begin{bmatrix}\mathbf{h}(\mathbf{x})_P\\ \mathbf{h}(\mathbf{x})_Q\end{bmatrix} + \begin{bmatrix}\boldsymbol{\eta}_P\\ \boldsymbol{\eta}_Q\end{bmatrix}$$

with:

$$E\left\{\begin{bmatrix}\boldsymbol{\eta}_P\\ \boldsymbol{\eta}_Q\end{bmatrix}\right\} = 0 \quad E\left\{\begin{bmatrix}\boldsymbol{\eta}_P\\ \boldsymbol{\eta}_Q\end{bmatrix}\begin{bmatrix}\boldsymbol{\eta}_P\\ \boldsymbol{\eta}_Q\end{bmatrix}^t\right\} = \begin{bmatrix}\mathbf{R}_P & 0\\ 0 & \mathbf{R}_Q\end{bmatrix}$$

where, $\mathbf{h}(\mathbf{x})_P$, $\mathbf{h}(\mathbf{x})_Q$, $\boldsymbol{\eta}_P$ and $\boldsymbol{\eta}_Q$ are the vectors of non-linear functions and the vectors of the measurement errors corresponding to the real and reactive measurements, respectively; $\mathbf{R}_P$ and $\mathbf{R}_Q$ represent the sub-matrices of covariance measurement errors associated with the real and reactive measurements, respectively. The Jacobian matrix of the non-linear functions $\mathbf{h}(\mathbf{x})_P$ and $\mathbf{h}(\mathbf{x})_Q$, corresponding to this non-linear measurement model can be written as:

$$\mathbf{H}(\mathrm{V},\delta) = \begin{bmatrix}\mathbf{H}_{P\delta} & \mathbf{H}_{PV}\\ \mathbf{H}_{Q\delta} & \mathbf{H}_{QV}\end{bmatrix} \tag{3.16}$$

where $\mathbf{H}_{P\delta} = \frac{\partial \mathbf{h}(\mathbf{x})_P}{\partial \boldsymbol{\delta}}$ and $\mathbf{H}_{PV} = \frac{\partial \mathbf{h}(\mathbf{x})_P}{\partial \mathbf{V}}$ are the sub-matrices of first derivatives of the functions $\mathbf{h}(\mathbf{x})_P$ (related to the real measurements) with respect to the angle and magnitude of the complex bus voltages; and $\mathbf{H}_{Q\delta} = \frac{\partial \mathbf{h}(\mathbf{x})_Q}{\partial \boldsymbol{\delta}}$ and $\mathbf{H}_{PV} = \frac{\partial \mathbf{h}(\mathbf{x})_Q}{\partial \mathbf{V}}$ are the sub-matrices of first derivatives of the functions $\mathbf{h}(\mathbf{x})_Q$ (related to the reactive measurements) with respect to the angle and magnitude of the complex bus voltages.

According to the previous partitioning, the information matrix $[\mathbf{H}^t\mathbf{R}^{-1}\mathbf{H}]$ can be rewritten as:

$$\begin{bmatrix}\mathbf{H}_{P\delta}^{\boldsymbol{t}} & \mathbf{H}_{Q\delta}^{\boldsymbol{t}}\\ \mathbf{H}_{PV}^{\boldsymbol{t}} & \mathbf{H}_{QV}^{\boldsymbol{t}}\end{bmatrix}\begin{bmatrix}\mathbf{R}_P & 0\\ 0 & \mathbf{R}_Q\end{bmatrix}\begin{bmatrix}\mathbf{H}_{P\delta} & \mathbf{H}_{PV}\\ \mathbf{H}_{Q\delta} & \mathbf{H}_{QV}\end{bmatrix}$$

such that, the matrix product indicated in the last equation provides:

$$\begin{bmatrix}\mathbf{H}_{P\delta}^{\boldsymbol{t}}\mathbf{R}_P^{-1}\mathbf{H}_{P\delta} + \mathbf{H}_{Q\delta}^{\boldsymbol{t}}\mathbf{R}_Q^{-1}\mathbf{H}_{Q\delta} & \mathbf{H}_{P\delta}^{\boldsymbol{t}}\mathbf{R}_P^{-1}\mathbf{H}_{PV} + \mathbf{H}_{Q\delta}^{\boldsymbol{t}}\mathbf{R}_Q^{-1}\mathbf{H}_{QV}\\ \mathbf{H}_{PV}^{\boldsymbol{t}}\mathbf{R}_P^{-1}\mathbf{H}_{P\delta} + \mathbf{H}_{QV}^{\boldsymbol{t}}\mathbf{R}_Q^{-1}\mathbf{H}_{Q\delta} & \mathbf{H}_{PV}^{\boldsymbol{t}}\mathbf{R}_P^{-1}\mathbf{H}_{PV} + \mathbf{H}_{QV}^{\boldsymbol{t}}\mathbf{R}_Q^{-1}\mathbf{H}_{QV}\end{bmatrix}$$

or in a compact form:

$$\begin{bmatrix}\mathbf{A}_{P\delta} & \mathbf{A}_{PV}\\ \mathbf{A}_{Q\delta} & \mathbf{A}_{QV}\end{bmatrix}$$

where:

$$\mathbf{A}_{P\delta} = \mathbf{H}_{P\delta}^{\boldsymbol{t}}\mathbf{R}_P^{-1}\mathbf{H}_{P\delta} + \mathbf{H}_{Q\delta}^{\boldsymbol{t}}\mathbf{R}_Q^{-1}\mathbf{H}_{Q\delta}$$
$$\mathbf{A}_{PV} = \mathbf{H}_{P\delta}^{\boldsymbol{t}}\mathbf{R}_P^{-1}\mathbf{H}_{PV} + \mathbf{H}_{Q\delta}^{\boldsymbol{t}}\mathbf{R}_Q^{-1}\mathbf{H}_{QV}$$
$$\mathbf{A}_{Q\delta} = \mathbf{H}_{PV}^{\boldsymbol{t}}\mathbf{R}_P^{-1}\mathbf{H}_{P\delta} + \mathbf{H}_{QV}^{\boldsymbol{t}}\mathbf{R}_Q^{-1}\mathbf{H}_{Q\delta}$$
$$\mathbf{A}_{QV} = \mathbf{H}_{PV}^{\boldsymbol{t}}\mathbf{R}_P^{-1}\mathbf{H}_{PV} + \mathbf{H}_{QV}^{\boldsymbol{t}}\mathbf{R}_Q^{-1}\mathbf{H}_{QV}$$

Generally, the transmission lines of the power systems with voltage magnitude level greater than 69 kV have a high ratio $\frac{\mathrm{X}}{\mathrm{R}}$ [137], such that the submatrices $\mathbf{H}_{P\delta}$ and $\mathbf{H}_{QV}$ are predominant over $\mathbf{H}_{PV}$ and $\mathbf{H}_{Q\delta}$. Similarly, the submatrices $\mathbf{A}_{P\delta}$ and $\mathbf{A}_{QV}$ are predominant over $\mathbf{A}_{PV}$ and $\mathbf{A}_{Q\delta}$. The exploration of these features is the basis for the development of two types of decoupled state estimators described as follows.

3.3.3.1 Decoupling of the algorithm

The state estimator based on the decoupling in the algorithm adopts the following two approximations of the information matrix:

- sub-matrices $\mathbf{A}_{P\delta}$ and $\mathbf{A}_{QV}$ are computed for the voltage flat profile, that is, $V_i = 1.0\ p.u.$ and $\delta_i = 0°$ for all the buses;
- sub-matrices $\mathbf{A}_{PV}$ and $\mathbf{A}_{Q\delta}$ are neglected.

With these assumptions, the state estimator is represented by the equation:

$$\begin{bmatrix}\mathbf{A}_{P\delta} & 0\\ 0 & \mathbf{A}_{QV}\end{bmatrix}\begin{bmatrix}\Delta\boldsymbol{\delta}\\ \Delta\mathbf{V}\end{bmatrix} = \begin{bmatrix}\mathbf{H}_{P\delta}^{\boldsymbol{t}} & \mathbf{H}_{Q\delta}^{\boldsymbol{t}}\\ \mathbf{H}_{PV}^{\boldsymbol{t}} & \mathbf{H}_{QV}^{\boldsymbol{t}}\end{bmatrix}\mathbf{R}^{-1}[\mathbf{z} - \mathbf{h}(\boldsymbol{\delta}, \mathbf{V})] \tag{3.17}$$

The iterations of this algorithm are performed as follows:

- 1/2 iteration: calculation of the increment $\Delta\boldsymbol{\delta}$:

$$\mathbf{A}_{P\delta}\Delta\boldsymbol{\delta} = \left[\mathbf{H}_{P\delta}^{\boldsymbol{t}}\left(\boldsymbol{\delta}^k, \mathbf{V}^k\right) \mid \mathbf{H}_{Q\delta}^{\boldsymbol{t}}\left(\boldsymbol{\delta}^k, \mathbf{V}^k\right)\right]\mathbf{R}^{-1}[\mathbf{z} - \mathbf{h}(\boldsymbol{\delta}^k, \mathbf{V}^k)] \tag{3.18}$$

$$\boldsymbol{\delta}^{k+1} = \boldsymbol{\delta}^k + \Delta\boldsymbol{\delta} \tag{3.19}$$

- 1/2 iteration: calculation of the increment $\Delta\mathrm{V}$:

$$\mathbf{A}_{QV}\Delta\mathbf{V} = \left[\mathbf{H}_{PV}^{\boldsymbol{t}}\left(\boldsymbol{\delta}^{k+1}, \mathbf{V}^k\right) \mid \mathbf{H}_{QV}^{\boldsymbol{t}}\left(\boldsymbol{\delta}^{k+1}, \mathbf{V}^k\right)\right]\mathbf{R}^{-1}[\mathbf{z} - \mathbf{h}(\boldsymbol{\delta}^{k+1}, \mathbf{V}^k)] \tag{3.20}$$

$$\mathbf{V}^{\boldsymbol{k+1}} = \mathbf{V}^{\boldsymbol{k}} + \Delta\mathbf{V} \tag{3.21}$$

The estimator decoupled in the algorithm converges to the same solution that would be obtained without exploring the decoupling, only the number of iterations is modified, that is, the approximations made in the information matrix only affect the convergence of the iterative process without changing the final solution.

3.3.3.2 Decoupling of the Model

In this case, the approximations are adopted in the Jacobian matrix H, that is:

- the Jacobian matrix is calculated for V = 1.0 *p.u.* and δ = 0° for all buses;
- sub-matrices $\mathbf{H}_{PV}$ and $\mathbf{H}_{Q\delta}$ are neglected;
- the series resistance of the transmission lines are neglected in the computation of the sub-matrix $\mathbf{H}_{P\delta}$.

With these approximations, matrix $\mathbf{H}(\mathbf{V}, \boldsymbol{\delta})$ is expressed as:

$$\mathbf{H}(\mathbf{V}, \boldsymbol{\delta}) = \begin{bmatrix} \mathbf{H}_{P\delta} & 0 \\ 0 & \mathbf{H}_{QV} \end{bmatrix} \tag{3.22}$$

and the iterations of this algorithm are performed as follows:

- 1/2 iteration: computation of the increment $\Delta\boldsymbol{\delta}$:

$$\mathbf{A}'_{P\delta}\Delta\boldsymbol{\delta} = \mathbf{H}_{P\delta}^{t}\mathbf{R}_{P}^{-1}[\mathbf{z}_P - \mathbf{h}_P(\boldsymbol{\delta}^k, \mathbf{V}^k)] \tag{3.23}$$

$$\boldsymbol{\delta}^{k+1} = \boldsymbol{\delta}^k + \Delta\boldsymbol{\delta} \tag{3.24}$$

- 1/2 iteration: computation of the increment $\Delta\mathbf{V}$:

$$\mathbf{A}'_{QV}\Delta\mathbf{V} = \mathbf{H}_{QV}^{t}\mathbf{R}_{Q}^{-1}[\mathbf{z}_Q - \mathbf{h}_Q(\boldsymbol{\delta}^{k+1}, \mathbf{V}^k)] \tag{3.25}$$

$$\mathbf{V}^{k+1} = \mathbf{V}^k + \Delta\mathbf{V} \tag{3.26}$$

where the sub-matrices $\mathbf{A}'_{P\delta}$ and $\mathbf{A}'_{QV}$ are computed by taking into account only $\mathbf{H}_{P\delta}$, $\mathbf{R}_P$, $\mathbf{H}_{QV}$ and $\mathbf{R}_Q$ respectively, that is:

$$\mathbf{A}'_{P\delta} = \mathbf{H}_{P\delta}^{t}\mathbf{R}_{P}^{-1}\mathbf{H}_{P\delta}$$
$$\mathbf{A}'_{QV} = \mathbf{H}_{QV}^{t}\mathbf{R}_{Q}^{-1}\mathbf{H}_{QV}$$

The approximations used in estimator decoupled in the model can change the final solution. However, these changes tend to be negligible if the level of magnitude of system voltage is sufficiently high (EHV for example).

3.4 Bad Data Processing

In the context of the PSSE, gross measurements are those with a degree of inaccuracy much larger than it is supposed in the measurement model. These bad data result from errors in the communication devices, inaccurate meters, modelling of pseudo-measurements etc. The presence of errors in the set of measurements processed by the state estimator obviously damages the estimates. Since the estimator based on the least squares formulation minimizes the weighted sum of the squared residuals, the residuals with large magnitudes associated with the gross measurements will have a large effect on the final estimates of the state variables. The data more evidently

erroneous are rejected during the pre-filtering process, which verifies if the measurements are within certain limits, performing tests based on the comparison of redundant measurements. Among the several tests performed in the stage of pre-processing, the following can be cited:

- comparison of the measurement with its nominal value;
- comparison of the measurement of a data set with the measurements of the previous (stored) data set;
- consistency tests based on Kirchhoff's laws, comparisons between the measurements at both ends of a circuit, checking on the status of the keys/circuit breakers, etc.

Despite the fact that this process facilitates both the state estimation itself as well as the detection and identification of gross measurements, pre-filtering tests are not capable of detecting errors of magnitude between 3 and 10 standard deviations. This normally requires more elaborate techniques. In this chapter, we present the procedures most commonly used to detect the existence and identify the gross measurements, such that they can be removed or replaced by pseudo-measurements.

3.4.1 Bad Data Detection

The techniques for the detection and identification of gross errors presented in this subchapter are based on the analysis of the measurement residuals or a function of these variables. The reason for this choice is that the residual provide useful information about possible violations of the assumptions made with respect to the measurement model. As previously defined, the m × 1-vector of measurement residuals is given by:

$$\mathbf{r} = \mathbf{z} - \hat{\mathbf{z}} \tag{3.27}$$

where, $\mathbf{z}$ is the measurement vector and $\hat{\mathbf{z}}$ is the vector of the measurements computed with the estimated state.

The difference shown in Eq. (3.27) can be interpreted as an estimate for the measurement errors vector (on whose mean and variance certain assumptions were stated when formulating the measurement model). In the absence of errors, residual, or certain function residuals, will tend to confirm these assumptions. Otherwise, it can be inferred that measurements with gross errors were processed. In addition, the analysis of the individual residuals must lead to the identification of the gross measurements. This section describes a procedure for detecting errors based on a function of the measurement residuals. To establish the procedure for the bad data detection, it must be recalled that the vector of measurement errors is supposed have normal distribution, with zero mean and diagonal covariance matrix. This specification allows developing a procedure for the detection of bad data based on the measurement residuals. The natural candidate for a process of this type would be an individual test on the value of the residuals, in order to check whether any of them violates the assumptions made with respect to the measurement model. This technique, however, requires the use of the covariance matrix of the measurement residuals, whose determination is

computationally expensive. Considering that the bad data processing is performed on line after each SE, it is concluded that the individual examination of residual would not be a computationally efficient technique for simple detection of gross measurements. Even so, if the presence of these measurements is detected, a possible methodology for the identification of gross errors is based on the covariance matrix of the measurement residuals, as will be subsequently shown. The computational difficulties associated with the individual analysis of the measurement residuals lead to the search for a test based on an observable function of the residuals, whose behavior in the presence and in the absence of gross errors is clearly distinct. The weighted sum of the squared residuals is a function that satisfies this condition, that is, if there are gross measurements in the measurement set, $J(\hat{\mathbf{x}})$ tends to assume higher values than when such measurements are absent. Thus, taking as a basis the value of the weighted sum of the squared residuals, some conclusion can be stated about the presence of errors. Since both the residual and the weighted sum of the squared residuals are random variables it is reasonable to establish a type of detection test based on the statistical properties of these variables. The analytical formulation of the detection process errors is based on a statistical hypotheses test for which the following settings are required:

- Statistical hypothesis: assumption about the probabilistic distribution of one or a set of random variables;
- Basic hypothesis (*Null hypothesis*), H_0: main hypothesis;
- Alternative hypothesis, H_1: complement of the basic hypothesis H_0, that is, if H_0 is false, H_1 is true, and vice-versa;
- Hypothesis test: procedure to decide if the hypothesis H_0 must be accepted or rejected.

The Hypothesis Test theory defines two types of errors:

- Type I Error: rejection of the basic hypothesis H_0 when it is true;
- Type II Error: acceptance of the basic hypothesis H_0 when it is false.

The false alarm probability, denoted α, is the probability of having a type I error (α is considered the significance level of the test). Similarly, β represents the probability of error type II. The quantity $(1-\beta)$ represents the probability of the basic assumption H_0 to be rejected when it is false. This quantity is called power function of the hypothesis test. The application of the hypothesis test consists of reducing as much as possible the probability of false alarm α and the probability of error type II β. For this reason, fixed α in pre-specified in a low value (between 0.01 and 0.1, for example) and the power function $(1-\beta)$ is maximized over all the alternatives. This requires an observable function of the random variables, which behaves differently under the conditions of basic and alternative assumptions. This difference in behavior is used to design the test. For example, suppose that S is a statistical function that tends to assume lower values when the basic assumption is true than when it is false. From a probability of false alarm α fixed at a small value and the probability density function of the variables in this study, a threshold K can be determined, so that the test will be positive if $S > K$ and negative otherwise. Then it is considered that the test results have a significance level

of (100×α). In the case of PSSE, for the application of the test of Hypotheses assumed that:

- the vector of measurement errors has normal distribution with zero mean and covariance matrix **R** diagonal;
- the structure and the parameters of the network are known;
- the measurement model is linearized at a point close the solution.

Under these conditions, the weighted sum of the squared residual has a chi-square distribution (denoted χ^2) with $m-n$ degrees of freedom, where m and n are respectively the number of measurements and the number of states. Fig. 3.2 shows the probability density function of the chi-square distribution with eight degrees of freedom. Note that this function is defined only for positive values, and it is asymmetrical. In the presence of gross errors, the previous assumptions become false and the weighted sum of the squared residual does not present the chi-square distribution, tending to assume high values.

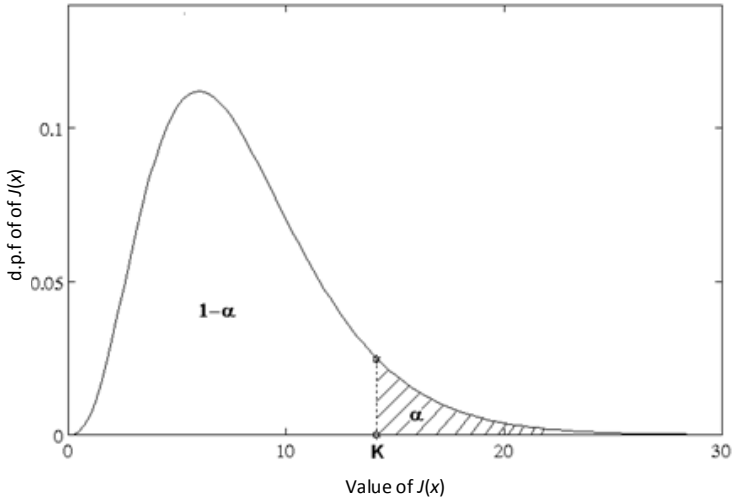

Figure 3.2: *Chi-squared probability density function with 8 degrees of freedom*

In terms of the previously mentioned assumptions, the problem of detecting errors is established in accordance with the following hypothesis test:

- basic assumption H_0: the weighted sum of the squared residuals $J(\hat{\mathbf{x}})$ presents the χ^2 distribution;
- alternative hypothesis, H_1: the basic assumption is false.

Based on the probability of false alarm, it is possible to establish a threshold K, such that:

$$P(J(\hat{\mathrm{x}}) > K \mid J(\hat{\mathrm{x}}) \text{ presents the distribution } \chi^2) = \alpha \qquad (3.28)$$

where $P(a > b|c)$ represents the probability that a is greater than b assuming that c is true.

As shown in Fig. 3.2, the probability α and its complement $(1-\alpha)$ may be interpreted as areas under the curve of density probability function of $J(\hat{\mathbf{x}})$. Note that the specification of α determines uniquely the threshold K, that is:

$$K = \chi^2_{m-n;1-\alpha} \tag{3.29}$$

where $\chi^2_{m-n;1-\alpha}$ denotes the percentile $(1-\alpha)$ of the χ^2-distribution with $(m-n)$ degrees of freedom. In summary, the test for the error detection based on the weighted sum of the squared residuals consists in comparing the value of $J(\hat{\mathbf{x}})$ with the value K, obtained from the cumulative χ^2 distribution with $(m - n)$ degrees of freedom and probability of false alarm equal to α. If $J(\hat{\mathbf{x}}) > K$, then there is evidence that there are gross measurements in the measurement set. If the number of degrees of freedom becomes high (in practice, greater than 30), which occurs frequently in the case of PSSE, the χ^2 distribution tends to behave as a Gaussian distribution with mean $(m - n)$ and variance $2(m - n)$. This is illustrated in Fig. 3.3, which verifies that, as the number of degrees of freedom ℓ increases, the curve will tend to symmetry with respect to the average.

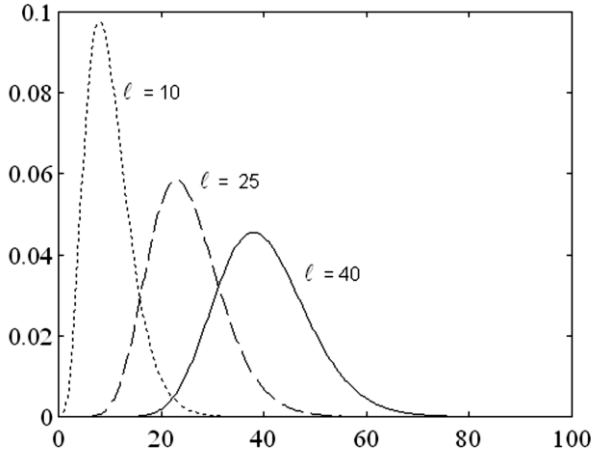

Figure 3.3: *Density probability function of the χ^2 distribution is 3 degrees of freedom [138]*

For values of ℓ higher than 30, it is possible to demonstrate that the quantity:

$$\frac{J(\hat{\mathbf{x}}) - (m-n)}{\sqrt{2(m-n)}} \tag{3.30}$$

tends to the standard normal distribution, so that the percentiles of this distribution can be used instead of those obtained from the χ^2 distribution to determine K. In this case K is expressed analytically as:

$$\Phi\left(\frac{K-(m-n)}{\sqrt{2(M-N)}}\right) = 1-\alpha \tag{3.31}$$

where $\Phi(\cdot)$ is the cumulative standard normal distribution. The test for the bad data detection can be summarized in the following steps:

- calculate the weighted sum of the squared residuals $J(\hat{\mathrm{x}})$ after the state estimation;
- compare $J(\hat{\mathbf{x}})$ with the threshold K, obtained (a) the $\chi 2$ distribution with $(m - n)$ degrees of freedom and probability of false alarm α or, from the standard normal distribution if $(m - n) > 30$, by Eq. (3.31):

- if $J(\hat{\mathbf{x}}) > K$, it is concluded that there is at least one bad data in the measurement set;
- if $J(\hat{\mathbf{x}}) \leq K$, it is concluded that there is no bad data in the measurement set.

3.4.2 Bad Data Identification

Based on the results of the bad data detection test, two alternatives can be taken. If the test does not indicate the existence of such measurements, the estimation process is finished. Otherwise, the gross measurements must be identified, which requires the individual examination of measurement residuals. If there is only a single gross measurement, a possible strategy of identification could be based on the determination of maximum residual, with the expectation that this would correspond to the gross measurements. However, this is not necessarily true, because meters of different types have different accuracy levels, such that the variances of the measurements can be significantly affected. In addition, there is the possibility that the residual are correlated, so that the effect of a gross error associated with a measurement can spread over the residual of other quantities. These difficulties are overcome by using the *Method of Maximum Normalized Residuals* [28],[29].

3.4.3 Multiple Bad Data Processing

The simplest case of bad data processing is that of a single gross measurement. The identification procedure most often used is the one in which it is assumed that the gross measurement is that corresponding to the maximum normalized measurement residual (in magnitude), after being verified the presence of bad data in the measurement set. Further about this problem can be found in literature [30].

However, more realistic and more frequent situations are not those relative to the existence of a simple gross error (GE). On the contrary, practical situations are characterized by the occurrence of multiple gross measurements, interactive or not. In the case of multiple non-interactive errors, the application of a generalized *Method of Maximum Normalized Residuals* may be sufficient to correctly identify the gross measurements [31]. In case of multiple interactive bad data, this generalization can be non-effective, producing results which are not consistent with the reality. This happens because the residuals are linear combinations of the measurement errors. Therefore, there is not, necessarily, a unique correspondence between the residual with larger magnitudes and the larger measurement errors, and for this reason the gross measurements may not be those relating to maximum normalized residuals.

There are numerous ways to process the multiple bad data. One of those, *Identification by elimination*, corresponds to an extension of the procedure adopted in the case of simple gross errors for the case of multiple gross errors [32]. The second one, *Identification based on hypothesis test*, is based on set of suspect measurements selected in the measurement set, and applies procedures based on hypothesis tests to refine this set [33].

3.5 Observability Analysis

The problem of observability of power systems consists essentially in determining whether the measurements that compose a given set provide sufficient information for the SE of the power system. The analysis of observability is particularly important during the real time operation of the power system, because its results can determine changes in the procedures for estimating the state variables.

In the case of deficiency of the measurement set for example, the observability analysis must provide subsidies for, in a subsequent step, proceeding to the estimation of states of the observable components (islands) of the power system. Alternatively, it is possible to establish procedures for allocating appropriate pseudo-measurements which, once added to the deficient measurement set, will allow the recovery of the observability of the system as a whole.

Another important by-product of the analysis of observability is the determination of critical measurements and critical pairs. Their correct identification is important both to indicate points of reinforcement of the measurement set and to the processing of gross errors.

The routines for determination of observability are also useful as a tool for design of the measurement set. In this case, it must guarantee the achievement of reliable estimates even if some measurements are lost during the power system operation, due to the failure of the data transmission system or by the elimination resulting from the processing of gross errors. The tests of observability can be used to evaluate the measurement set and indicate where these must be reinforced, through the addition of new measurements.

3.5.1 Concepts and Solution Method

Consider a measurement set M of a power system for state estimation purposes. It is assumed that the measurements are real and reactive power injections in the buses, real and reactive power flows in the transmission lines and bus voltage magnitude. The concept of power system observability is formally expressed by the following definition:

Definition 3.1 *A power system is observable, from the point of view of the static state estimation, with respect to a given set of measurements M if the state variables of the power system (magnitudes and angles of the bus voltages) may be determined by processing the measurements of M through a state estimator. Otherwise, the power system is considered non-observable with respect to M.*

The definition above, although clear, it is not operational for the purposes of observability analysis. For this reason, it is necessary to characterize the concept of observability in terms of certain matrices and graphs associated with the network topology and the measurement set, which will be introduced as follows.

As previously seen, the weighted least squares approach provides an estimate for the increments $\Delta\mathbf{x}$, obtained through the minimization of the objective function:

$$J(\Delta\mathbf{x}) = [\Delta\mathbf{z} - \mathbf{H}\Delta\mathbf{x}]^t\mathbf{R}^{-1}[\Delta\mathbf{z} - \mathbf{H}\Delta\mathbf{x}] \tag{3.32}$$

where, for the sake of simplicity, the argument of H(.) has been eliminated. The final solution of the state estimation problem states is obtained through an iterative procedure in which $\Delta\mathbf{x}$ is calculated at each iteration by solving the so-called *Gauss normal equation*:

$$\mathbf{G}\Delta\mathrm{x} = \mathbf{H}^t\mathbf{R}^{-1}\Delta\mathbf{z} \tag{3.33}$$

where:

$$\mathbf{G} = \mathbf{H}^t\mathbf{R}^{-1}\mathbf{H} \tag{3.34}$$

is the information or gain matrix defined in subchapter 3.2.

From the definition introduced earlier in this section, it is clear the relationship between the observability and the features of the matrix **G**. In fact, aiming at solving the normal equation, it is necessary that the information matrix **G** is non-singular. Given that the covariance matrix of the errors of measurement **R** is generally supposed diagonal and non-singular, which implies that the Jacobian matrix **H** must have full rank, that is, as *m*>*n*, the rank of **H** must be equal to *n*. Therefore, it is necessary to have at least a subset of *M* composed by *n* measurements, such that the *n* corresponding rows of the Jacobian matrix are linearly independent. This leads to the definitions of observability presented as follows.

Definition 3.2 *A power system is algebraically observable with respect to a set of measurements M, if the Jacobian matrix **H** has rank equal to n, which is the dimension of the vector of state variables x.*

According to this definition, the algebraic observability depends on the operation point used for the linearization of the measurement model. Reference [34] assumes that this operation point is the flat bus voltage profile (magnitudes and angles of all bus voltages equal to 1.0 *p.u.* and 0.0 rad, respectively), in addition to the decoupled approximation for **H** proposed by [23]. In spite of a power system being algebraically observable, it is possible that during the iterative solution process, numerical problems eventually prevent the convergence, due to the poor conditioning of the matrix H or due to the actual state being too far away from the initial estimates. To take this fact into account, it introduces the following definition:

Definition 3.3 *A power system is numerically observable with respect to M if the estimates for all states can be obtained through iterative solution starting from initial state estimates equal to 1.0 p.u. for the magnitudes and 0.0 rad for the angles of the bus voltages.*

Therefore, it can be inferred that although the numerical observability implies in algebraic observability, the reciprocal is in general not true. Testing the numerical observability is equivalent to solve the problem of static state estimation from the flat voltage profile, for a given measurement set M. The methods based on triangular factorization proposed in [35] are in reality the

verification of the numerical observability, which are already implemented in the proper solution process of the normal equation. Another possible test for analyzing the power system observability could be the calculation (in floating-point) of the rank of the Jacobian matrix, which would provide information about the algebraic observability. Although several algorithms suitable for calculating the rank of an array are available [36], the cpu time required for this purpose is not compatible with real-time applications. In addition, they do not indicate the points of the power network at which the measurement set might require reinforcement, nor about observable islands.

Clements-Wollenberg method was the first specifically developed method for the analysis of the topological observability, based on the network topology and the location of the measurements, and therefore not using calculations in floating point. It is a heuristic method, which is based on principles drawn from the experience in the analysis of electrical networks [37]. In spite of its undeniable appeal to physical understanding of the problem of observability, the method of Clements-Wollenberg is essentially heuristic. Consequently, the method provides conservative results in some cases, that is, the power network can be classified as non-observable when the power system is in reality observable. The method for observability analysis presented as follows supplies the deficiencies of the algorithm of Clements and Wollenberg, being supported by a more solid theoretical foundation.

3.5.2 Topological Observability

3.5.2.1 P – δ and Q – V observability

The introduction of the notions of the observability P − δ and the observability Q − V, which are important for the investigation of topological observability, implies the decomposition of the problem into two sub-problems. This decoupling is similar to that used in formulation of the fast decoupled power flow problem. It recognizes that the measurements of real power convey a greater quantity of information about the voltage angles. Conversely, reactive power measurements provide more information about the voltage magnitude. Taking into account the P − δ/Q − V decoupling and assuming that the relationship reactance/resistance of the series impedances of the transmission lines is much greater than 1.0, the following model of decoupled measurement is developed [136]:

$$\mathbf{z}_P = \mathbf{H}_P \boldsymbol{\delta} + \boldsymbol{\eta}_P \tag{3.35}$$

$$\mathbf{z}_Q = \mathbf{H}_Q \boldsymbol{V} + +\mathbf{k} + \boldsymbol{\eta}_Q \tag{3.36}$$

The vector $\mathbf{z}_P$ is composed by measurements of real power injections and flows, and the vector $\mathbf{z}_Q$ contains the measurements of voltage magnitude, reactive power injections and flows. The corresponding measurement errors are represented by $\boldsymbol{\eta}_P$ and $\boldsymbol{\eta}_Q$. Vector $\mathbf{k}$ can be obtained from reference [136].

The vectors $\boldsymbol{\delta}$ and $\mathbf{V}$ contains $N - 1$ bus voltage angles and N bus voltage magnitudes, respectively. The constant vector $\mathbf{k}$ depends on the shunt admittances of the transmission lines. Finally, the matrices $\mathbf{H}_P$ and $\mathbf{H}_Q$ depend

basically on the measurement set, the topology of the electrical network and the series admittances of the transmission lines. From Eqs. (3.35) and (3.36), one can state that:

Definition 3.4 *A power system composed by N buses is P−δ/Q−V) algebraically observable with respect to the real (reactive) measurement sets, if and only if the rank of the matrix* $\mathbf{H}_P$ *(*$\mathbf{H}_Q$*) is equal to N − 1 (N).*

If there is no parity between the real and reactive measurement sets, the problems of P − δ and Q − V observability must be analyzed separately. A difficulty that arises in this case is the asymmetry introduced by the measurements of voltage magnitude, without similar on sub-problem P − δ. However, this type of measurement can be replaced by reactive power flow measurement in a fictitious transmission line, connecting the bus where measurement of the voltage magnitude is taken to a reference bus [38],[39]. Therefore, in general, any algorithm for analysis of observability should be executed twice for the same system. However, the measurement sets used in practice normally present the measurements of power injection and power flow taken in pairs real/reactive. If the voltage magnitude measurement is considered only in the reference bus, the conclusions about the observability P − δ and Q − V can be obtained from a single application of the algorithm of observability. Without loss of generality, this chapter considers that the measurements of power injections and flows are taken in pairs.

3.5.2.2 Algorithm

This subchapter deals with a combinatory algorithm for the determination of topological observability. The algorithm in question is derived from the work described in [40]. The method is based on the formulation of the problem of topological observability in terms of *graph of the system measurement*, *Z*, associated with a given measurement set *M*, whose vertices and edges are defined as follows:

1. The vertices of *Z* are the same vertices of the graph of network;
2. If the flow in the line *i−j* is measured, then the vertices *i* and *j* in *Z* are connected by an edge that will be associated with that measure of edge flow (flow);
3. If the injection in bus *i* is measured, the vertex *i* in *Z* will be connected to each of its adjacent vertices by edges that will all be associated with the measurement of the power injection (edges of injection).

The graph of measurement contains, therefore, all the possible edges that may be associated with the measurements on *M*. Once this subgraph is determined, the problem of topological observability analysis may be thus enunciated: investigate the existence of a spanning tree in graph of measurements, considering the constraint that this tree may not contain more than one edge associated to a given measure.

A tree with these characteristics is clearly an observable spanning tree of the graph of the network associated with the M. The proposed algorithm is able to find such tree whenever it exists, as well as detects promptly the cases in which it does not exist.

3.5.2.3 Measures of Magnitude of Voltage

If the parity between real and reactive measurements is not verified, the problems of observability $P - \delta$ and $Q - V$ must be analyzed separately. In addition, the presence of multiple measurements of voltage magnitude in the system must be properly taken into account, because these measurements significantly influence the analysis of observability $Q - V$. Van Cutsen and Gailly [38] showed that the voltage measurements can be represented (in which concerns the analysis of topological observability only) by reactive flow in a transmission line, with a fictitious unitary susceptance, connecting the bus where the voltage is measured to the earth. It becomes necessary therefore to include an additional bus representing the reference, so that from the point of view of observability $Q - V$, the network becomes contain N + 1 buses. Consequently, an observable spanning tree for analysis $Q - V$ should contain N branches. To illustrate the effect of voltage measurements in the analysis of observability $Q - V$, consider the Fig. 3.4, which represents an electrical network in which only reactive measurements (q, u and v) are represented. Note that only the power injections and power flows do not guarantee the $Q - V$ observability. However, the voltage measurements allow you to find a spanning tree that includes observable in the land, which is shown in Fig. 3.4.

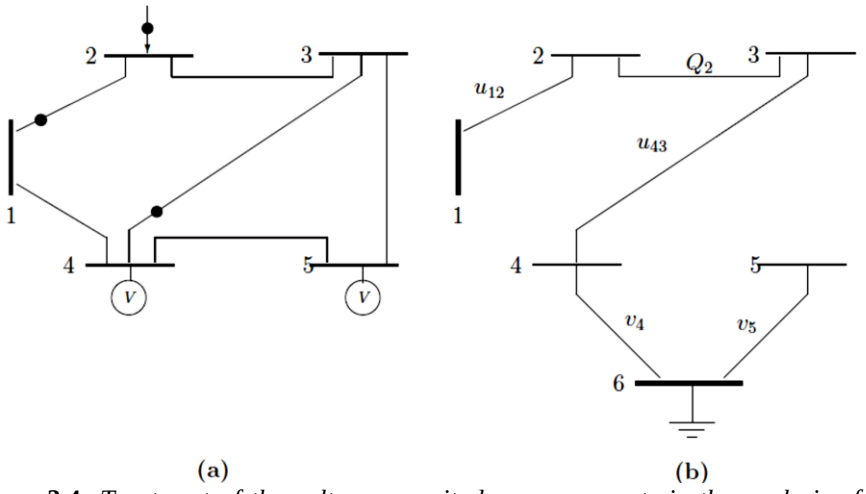

Figure 3.4: *Treatment of the voltage magnitude measurements in the analysis of the Q−V observability*

Finally, it appears that the method described above for the representation of voltage measurements in the analysis of observability is consistent with the fact that widely known that, even when the measurements of power are made to pairs real/reactive, there is need to have at least a voltage magnitude measurement to estimate the states. In fact, only in this case is that if one can connect the observable ground in the spanning tree analysis of observability $Q - V$.

3.6 Conclusions

The state estimation determines the best estimate of the current power system states, usually including the voltage phasors, transformer tap positions and circuit breaker status, given the stream of telemetry that has been collected from the system's sensors, current network model and information from other data sources. In the modern control centers, estimates are used as the major input for many grid supervision applications. Thus, state estimator is commonly referred as the "boarding ticket" to many other power system monitoring and control applications. The role of the state estimation in modern power system control center is illustrated in Fig. 3.5.

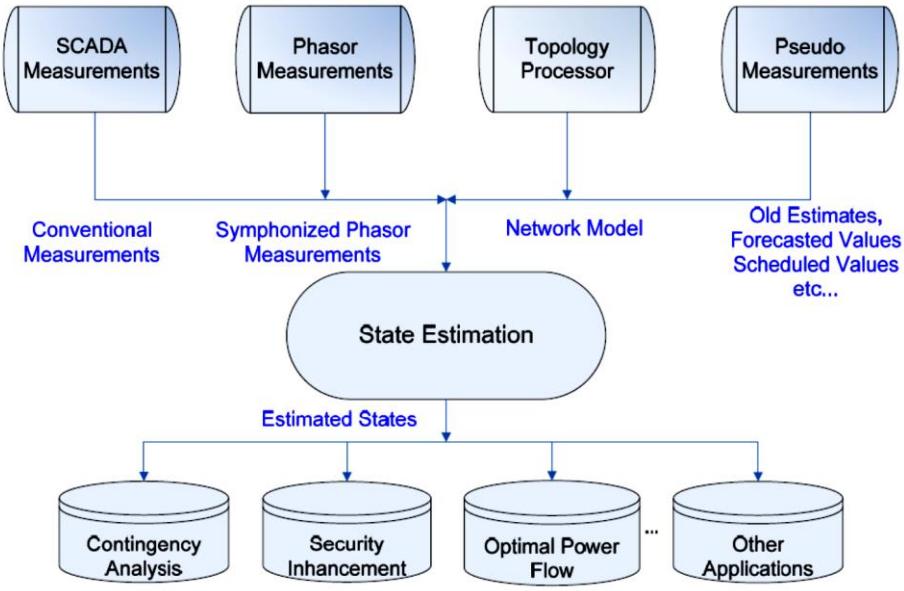

Figure 3.5: *Role of State Estimation in power system control and operation*

Power systems have three operation states: normal state, restorative state and emergency state. To maintain the power system in the normal secure state is the main goal of the power system operation. State estimation is a tool through which the grid operating states can be captured. In most power grids, state estimation is intensively used for static security assessment.

The method of this assessment is to monitor the state of the system and estimate the system state, identify the restorative and emergency state and make appropriate function to bring the power system back to normal state. Specifically, the contingency analysis is conducted to ensure that the power system is operated in normal state. Furthermore, it is used to identify the security state of the system and make corresponding action to prevent insecure grid operation. Besides, measurements are used as the input of state estimation and topology processor. While the estimate conducted for the power system, the state of the power system is identified. Then, there will be control actions to put the emergency state and restorative state of power system back to normal state. If the state of the power system is normal, there will also be a contingency analysis to identify if the power system is secure. When the power system is in insecure state, preventive action will put the

system back to normal secure state, which is the ideal state of the power system.

The SE solution determines the optimal estimate of the system state, which is composed of complex bus voltages in the entire power system. The estimates based on the network model and the gathered measurements from the system. Moreover, state estimation provides the best estimates for all the line flows, loads, transformer taps, and generator outputs. The typical functions of state estimation are topology processor, observability analysis, state estimation solution, bad data processing and parameters and structural error processing. Firstly, the topology processor gathers status for the circuit breakers and switches, and produces the one-line diagram of the system. Secondly, Observability analysis determines if a state estimation solution for the entire system can be obtained by the available set of measurements and the identified network topology. Besides, it could identify the unobservable branches and the observable islands in the system if any exist. Thirdly, bad data processing detects the existence of gross errors in the measurement set. It identifies and eliminates bad measurements provided that there is enough redundancy in the measurement configuration. Lastly, parameter and structural error processing estimates various network parameters, such as transmission line model parameters, transformer tap changer parameters, shunt capacitor or reactor parameters using the measurements as known values. Besides this functionality, structural errors in the network configuration as the erroneous breaker status can be identified provided that there is enough measurement redundancy.

CHAPTER 4

4. Distribution System State Estimation

4.1 Introduction and Motivation

High penetration of DG is currently limited by the passive operating methods of DN. Automatic Voltage Control (AVC) with current compounding applied to distribution transformers usually assumes a simple R+jX or Z∠θ network model which, combined with radial power flow, allows the AVC system to maintain the voltage of the network within limits. When DNs become real, this network and load model no longer applies. With the export of power from the generating station a voltage difference is often created. The resultant voltage rise along the feeder from the substation to the DG can cause the feeder voltage to exceed its upper limit [41].

The DG has to provide ancillary services (to solve local and global issues – frequency, reserve, voltage regulation, congestion management). Therefore the DS will assume the role of DSO. Premise of this is the knowledge of the network. For this reason, SE applied to DN is a main tool to improve the effects of DG penetration as an improved knowledge of the network condition, or state, is required. Usually, at distribution level, insufficient measurements are taken to allow satisfactory control, so measurement is extended through the use of SE techniques.

As previously elaborated, SE has been widely used on TNs to assess the network operating conditions given a set of redundant measurements. Since not only the redundancy cannot be obtained, but also the number of measurement equipment is limited in DNs, distribution SE algorithms in most of the approaches use a large number of load pseudo-measurements.

When transferring the techniques of SE to DNs, there are additional aspects that must be considered. They focus on the causes of ill-conditioning of the gain matrix **G**, which can lead to poor convergence, or non-convergence, of the iterative state estimator.

Following issues regarding SE must be analyzed when designing the Distribution System State Estimation (DSSE):

- **Pseudo-measurements.** The distribution state estimator is expected to have a large number of load pseudo-measurements or to use some other innovative technique. Authors in [42] suggest that this may cause problems of instability due to increased poor conditioning of the gain matrix.
- **Network Impedances.** Adjacent long and short lines (i.e. large and small impedances) are also a source of ill-conditioning [43]. The authors proposed an orthogonal decomposition method. This feature of SE can be expected to have an effect where there are very low impedance lines coupling busses.
- **Virtual Measurements.** The combination of measurements with very large and very small weighting factors leads to ill-conditioning of the gain matrix **G** [44]. The use of equality constraints to fix known values, e.g. zero injection at a non-load bus, can improve numerical stability.
- **Scaling.** Poor scaling of measurement values has been identified as another cause of ill-conditioning of the gain matrix [45]. While this is satisfactory for Transmission System State Estimation (TSSE), the above suggests that for distribution state estimate on the base should be reduced.

Adding to the complexity of the problem is the existence of the significant differences in the characteristics of typical DNs compared to typical TNs that are summarized in the Table 4.1 below [46]:

Table 4.1: Technology options for DN development

Characteristics	Transmission	Distribution
Topology	Generally extensively meshed and must be analyzed as a whole	Generally many independent substations, each supplying several radial feeders. Can be analyzed as multiple independent islands
Phase unbalance	The degree of unbalance is generally sufficiently small that it can be ignored and only positive sequence analyzed	The degree of unbalance may be quite large and each phase should be in that case considered independently
SCADA Measurements	A high percentage of devices have measurements. Significant part of the network has measurement redundancy and is mathematically observable	Generally has many more load points than measurements. Practically speaking, there is usually no measurement redundancy and, considering SCADA measurements only, is highly unobservable
Network Size vs Investments	A typical network size ranges from few hundred busses to one or two thousand	A typical network size ranges from 10 000 to 100 000 electrical nodes

Finally, apart from the already described physical and technological characteristics of DNs, increased penetration of DGs is leaving multiple prints in operational issues of DNs. It is necessary to briefly describe the changes that DG is inducing in modern systems which points out once again the importance of DSSE.

4.1.1 The Impact of Dispersed Generation on Distributed Networks

DG is playing an increasing role in the electric power system of todays. DG is by definition limited in size (roughly 10 MW or less) [47] and interconnected at the substation, distribution feeder or customer load levels. DG technologies include photovoltaics, wind turbines, fuel cells, small and micro sized turbine packages, stirling-engine based generators, and internal combustion engine-generators. These technologies have already entered in a period of rapid expansion and commercialization. With so much new DG being installed, it is critical to assess the power system impacts accurately so that these units can be applied in a manner that avoids causing degradation of power quality, reliability, and control of the utility system [47].

The introduction of generation sources on the DS can significantly impact the flow of power and voltage conditions at customers and utility equipment. These impacts may manifest themselves either positively or negatively depending on the DS operating characteristics and the DG characteristics. Positive impacts are generally called “system support benefits” and include:

- Voltage support and improved power quality;
- Loss reduction;
- Transmission and distribution capacity release;
- Deferments of new or upgraded transmission and distribution infrastructure;
- Improved utility system reliability.

Achieving the above benefits is in practice much more difficult than it is often realized. The DG sources must be reliable, dispatchable, of the proper size and at the proper locations. They must also meet various other operating criteria. Since many DGs will not be utility owned or will be variable energy sources such as solar and wind, there is no guarantee that these conditions will be satisfied and that the full system support benefits will be realized. In fact, power system operations may be adversely impacted by the introduction of DG if certain minimum standards for control, installation and placement are not maintained. This subchapter is focusing on the voltage quality, loss reduction and reliability factors associated with DG.

4.1.1.1 Voltage Regulation and Losses

Radial DSs are normally regulated using load-tap-changing transformers at substations, supplementary line regulators on feeders, and switched capacitors on feeders. Voltage regulation practice is based on radial power flows from the substation to the loads while DG sometimes introduces reversed power flows that interfere with the effectiveness of standard voltage regulation practice.

If a DG unit is applied just downstream of a voltage regulator or on-load tap changing (LTC) transformer that is using considerable line drop compensation, then the regulation controls will be unable to properly measure feeder demand (Fig. 4.2). With DG, the voltage becomes lower on the feeder. In this case, the voltage is reduced because the DG reduces the observed load at the line drop compensator control. This can confuse the regulator into setting a voltage lower than is required to maintain adequate service levels at the tail end of the feeder. This is the opposite effect of "voltage support", a commonly touted benefit of DG.

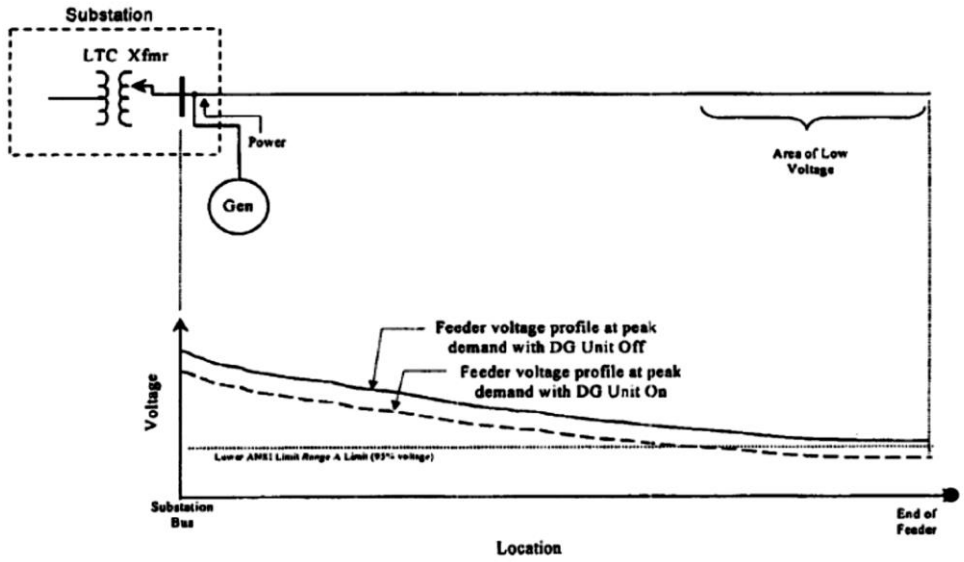

Figure 4.1: *Voltage profiles with and without DG [47]*

DG may also result in high voltage at some electric customers. For example, a small residential DG system that shares a common distribution transformer with several other residences may raise the voltage on the secondary enough to cause high voltage at these customers. The presence of the DG may introduce reverse power flow to counteract this normal voltage drop, perhaps even raising voltage somewhat, and the service voltage may actually be higher at the customer services than on the primary side of the distribution transformer.

The preceding examples have shown ways that both high and low service voltage can occur due to the incompatibility of DG with the radial power flow based voltage regulation approach used on most utility systems. As a result, the DG influence on voltage for any potential application should always be assessed to insure that no customers will be adversely impacted.

In essentially all cases, the impact on the feeder will be negligible for any individual residential scale DG unit (<10 kW) [47]. However, when the aggregate capacity of many small units deployed reaches a critical threshold or when the capacity of a single unit is large enough, then the knowledge of the network state and voltage regulation studies are desirable to insure that the feeder voltage will be maintained within appropriate limits. The aggregate DG capacity threshold, for which studies become appropriate, depends on many factors. DG will also impact losses on the feeder. DG units should be placed at optimal locations where they provide the best reduction in feeder losses. In

that manner it would be planned and called distributed generation. However, DG is installed where there are customers. The connection point is generally the nearest point to the network. This is why it is referred as dispersed.

4.1.1.2 Voltage Flicker

DG may cause noticeable voltage flicker. Flicker can be either a simple issue or a complex issue as far as its analysis and mitigation are concerned. From the simple perspective, it can be the result of starting a machine (e.g. induction generator) or step changes in DG output which result in a significant voltage change on the feeder. If a generator starts**,** or its output fluctuates frequently enough, flicker of lighting loads may be noticeable to customers.

Mitigation approaches include reduced voltage starts on induction generators as well as speed matching. Synchronous generators might require tighter synchronization and voltage matching. A less technical approach to reduce flicker involves placing constraints on when and how often DG operators may start and change the output of DG systems. In the case of wind and solar energy systems, the outputs will fluctuate significantly as the sun and wind intensity change.

Determination of the risk of flicker problems due to basic generator starting conditions or output fluctuations is fairly straightforward using the flicker curve approach, particularly if the rate of these fluctuations is well defined, the fluctuations are "step" changes and there are no complex dynamic interactions of equipment. The dynamic behavior of machines and their interactions with upstream voltage regulators and generators can complicate matters considerably. For example, it is possible for output fluctuations of a DG (even smoother ones from solar or wind systems) to cause hunting of an upstream regulator and, while the DG fluctuations alone may not create visible flicker, the hunting regulator may create visible flicker. Thus, flicker can involve factors beyond simply starting and stopping of generation machines or their basic fluctuations. Dealing with these interactions requires an analysis that is far beyond the ordinary voltage drop calculation performed for generator starting.

4.1.1.3 Harmonics

Many generating like wind power plants or PV units are connected to the grid via inverter. The inverters are the main contributors to the insertion of the harmonics in the grid. Although the contribution of a single converter might seem insignificant because of the power of the DG it is connected to, contribution of many units can insert big distortion. Nowadays, inverters are designed with IGBT (Insulated Gate Bipolar Transistor) technology that use pulse width modulation to generate the injected "pure" sinusoidal wave. This new technology produces a cleaner output with fewer harmonic that should satisfy the IEEE 1547-2003 standards [139]. Rotating generators such as synchronous generators can be another source of harmonics. Depending on the design of the generator windings (pitch of the coils), core non-linearity, grounding and other factors, significant harmonics can occur. The grounding arrangement of the generator and step-up transformer will play a major role in

limiting the feeder penetration of harmonics. Arrangements can be selected to block or reduce third harmonic injection to the utility system. This would tend to confine it to the DG site only.

For larger DG units or cases involving complex harmonic problems, measurements and modeling of the system harmonics may be required to assess conditions. Any analysis should consider the impact of DG currents on the background utility voltage distortion levels. The limits for utility voltage distortion are 5% for total harmonic distortion (THD) and 3% for any individual harmonic [47].

4.1.1.4 Impact on Short Circuit Levels

Studies of the impact of DG on the network faults current indicate that DG may invalidate overcurrent protection. DG may affect the operation of existing DNs by providing flows of fault currents which were not expected when the protection was originally designed. In practice, the presence of DG may result in increased fault currents which depend on capacity, penetration, technology, interface of the DG, and system voltage prior to the fault.

The fault contribution from a single small DG unit is not large, however, the aggregate contributions of many small units, or a few large units, can alter the short circuit levels enough to cause fuse-breaker miscoordination. This could affect the reliability and safety of the DS [47].

For inverters, the fault contributions will depend on the maximum current level and duration for which the inverter manufacturer's current limiter is set to respond. For most induction generators, the significant current would only last a few cycles and would be determined by dividing the pre-fault voltage by the transient reactance of the machine. Even though a period of few cycles is a short time, it is long enough to impact fuse-breaker coordination and breaker duties in some cases.

The current contribution from DG units is enough to impact fuse coordination in some cases, especially in weaker parts of the system. The contributions will decrease with the increase of generator's distance from the fault. The configuration and impedance of the DG site step-up transformer will also play a role.

4.1.1.5 Grounding and Transformer Interface

DG must be applied with a transformer configuration and grounding arrangement compatible with the utility system to which it is to be connected. Otherwise, voltage swells and over-voltages may be imposed on the utility system that damage utility or customer equipment.

Use of a DG source that does not appear as an effectively grounded source connected to such systems may lead to over-voltages during line to ground faults on the utility system. This condition is especially dangerous if a generation island develops and continues to serve a group of customers on a faulted DS [47].

To avoid problems, all DG sources on multi-grounded neutral systems that are large enough to sustain an island should present themselves to the utility system as an effectively grounded source. If they do not, they should

use appropriate protective relaying to detect primary side ground fault over-voltages and quickly trip off-line (instantaneous trip).

4.1.1.6 Islanding

Islanding occurs when the DG (or group of DGs) continues to energize a portion of the utility system that has been separated from the main utility system. Islanding can occur only if the generator(s) can self-excite and sustain the load in the islanded section. In most cases it is not desirable for a DG to island with any part of the utility system because this can lead to safety and power quality problems that will affect the utility system and loads. Islanding also increases the likelihood that DG sources may be allowed to subject the island to out of range voltage and frequency conditions during its existence. And it can pose a serious safety threat during downed conductors and utility repair operations since the public and utility workers may be exposed to circuits that otherwise would be de-energized. Finally, islanding can hinder service restoration by requiring line crews to spend extra time disabling the island conditions. This will impact reliability indices such as SAIDI.

To prevent islanding, a DG unit operating in parallel with the utility system should in a timely manner sense a significant voltage sag or discontinuity of service on the utility side and disconnect from the system.

Voltage and frequency relays are used as a means of anti-island protection. In most cases, if a generator becomes islanded, it will not be able to satisfy the sudden change in its load without a significant change in voltage and/or frequency and the relays will trip the unit off-line. This type of anti-islanding protection is called “passive.” Passive protection can be deceived if the generator is able to carry the load of the island without a substantial change in voltage or frequency so, as a further safeguard; many smaller inverters today also use what is called “active” anti-islanding protection. One common “active” approach is for the inverter to be “tuned” to operate while islanded at a frequency other than nominal value [47]**.**

Since islanding can cause severe voltage quality and reliability problems, the proper use and setting of anti-islanding controls is one of the more important issues for DG installations. Of course, for this action to take place, the network operator must, in every moment, be aware of the state of the DN.

Today, the way to avoid unwanted islanding is to disconnect the DG through the interface breakers, operated by minimum/maximum voltage/frequency relays, i.e., by local information only.

This requirement results in restrictive protection settings which, in many cases, determine the unsuitable breaker operation e.g., due to instability conditions of the electrical system. In such cases, the DG could be shed when it is necessary to stabilize the system [145]. The only way to overcome this problem is to set up an adequate communication system between the distributor substation and the DG.

4.1.1.7 Intentional Islanding for Reliability

The implementation of DG can increase reliability of electric service if units are configured to provide “backup-islands” during upstream utility

source outages. To be effective this requires reliable DG units and careful coordination of utility sectionalizing and protection equipment [47].

A DG assigned to carry the island must be able to restart and pick up the island load after the switch has opened. Power flow analysis of island scenarios must be performed to insure that proper voltage regulation is maintained and to establish that the DG can handle inrush during "starting" of the island. The DG unit must be able to follow load during islanded operation and the switch will need to sense if a fault current has occurred downstream of the switch location and send a signal to block islanding if a fault has occurred within the island zone. When utility power is restored on the utility side, the switch must not close unless the utility and "island" are tightly in synchronism. This requires measuring the voltage on both sides of the switch and transmitting that information to the DG unit supporting the island so that it can "synchronize" with the utility and allow reconnection.

4.1.1.8 Bidirectional Power Flow and Protection System

The presence of DG connected to DNs changes the typical operating conditions. In particular, the inversion of the PF on the MV/LV transformers could occur. In the passive DNs, the power flows typically from MV to LV systems, and the protection systems are based on this assumption. When the power produced by the DG is higher than that power required by the local loads, the LV network seen from the MV side could be considered as a generating unit connected to the MV system. The frequency of this situation will increase with high RES penetration [144].

The protection systems currently in operation in the LV networks are not able to handle bidirectional PFs: in the presence of bidirectional PFs, they are likely to behave unsuitably in the selection of the fault point. This can result in unwanted islanding of a portion of the LV system, supplied by the DG, which could be not acceptable for safety reasons.

4.1.1.9 Hosting Capacity

As already underlined, the increase in DG penetration may have an adverse influence on several power quality parameters and, in a wider perspective, a direct impact on the management and control of distribution grids, and finally, on the whole power system security. To quantify the impact of increasing penetration of DG on the power system, the Hosting Capacity (HC) approach was developed. The basis of this approach is a clear understanding of the technical requirements that the customer places on the system (i.e. quality and reliability) and the requirements that the system operator may place on individual customers to guarantee reliable and high-quality operation of the system. By definition, HC is the maximum DG penetration at which the power system operates satisfactorily and it is determined by comparing some performance indices with predefined bounds, which are selected in order to represent the limit of secure operation of the power system [141]. The performance indices are calculated as a function of the DG penetration level, and the HC is the DG penetration level at which at least one performance index reaches upper/lower bound.

Technical rule EN 50160 [142] introduces some reference terms that could be adapted in order to set the performance indices limit, however, especially with respect to power quality issues, it lacks a common accepted approach. An overview of the state-of-the-art on power quality indices can be found in [143].

From all previously stated, it is obvious that DSSE with other functions of modern DMS are having a huge importance in DNs even now and this trend will only increase in the future. Together with the already described circumstances of active DNs that rely on DSSE in Chapter 2 of this dissertation, here will be briefly underlined some of the other key features of this function.

Optimal operation of DNs comprises of the economics, quality and reliability of distributed energy. One of the most important tools that enable optimal operation of DNs in all its features is monitoring of the system and DSSE is the software tool that enables it. Knowing the state of the DNs is a base to other DS control functions:

- real time reliability system and reconfiguration network for reliability improvement;
- VAR management in the DNs for minimizing the losses;
- reconfiguration of the network for optimal power flow;
- fault management in the DNs for the reduction of customers' interruption duration;
- short time load forecasting in DN;
- energy management and load management of the DNs.

Nowadays, DSSE is a field of a significant scientific interest and many authors have been dealing with this subject. As already pointed out, many approaches have been based on the adaptation of Transmission System State Estimation (TSSE) to DN environment. Following subchapter addresses some of the key developments in the field of DSSE.

4.2 Bibliography review

Since the pioneering work of F.C. Schweppe in 1970 [48], SE has become a key function in supervisory control and planning of electric power grids. It serves to monitor the state of the grid and enables energy management systems (EMS) to perform various important control and planning tasks such as establishing near real-time network models for the grid, optimizing power flows, and bad data detection/analysis. Another example of the utility of SE is the SE-based reliability/security assessment deployed to analyze contingencies and determine necessary corrective actions against possible failures in the power systems.

In view of the ongoing development of a "smarter" grid, more research on SE is needed to meet the challenges that the envisioned smart grid functionalities present. Among others, environmental compliance, energy conservation, and improved dependability, reliability, and security will impose additional constraints on SE and require improved performance in

terms of response time and robustness [49]. In this subchapter, a brief survey drown out from extensive bibliography research of SE developed technologies will be provided and also examined the challenges and opportunities presented by the evolution of the legacy grid into a smarter grid.

Research presented by M. E. Baran and A. W. Kelley in [50] bring the first steps towards development of DSSE. In conventional operation of a DS, there is very little real-time information available to monitor the system; the voltage and the power supplied to the feeders at the substation are usually the only realtime measurements available to DSOs at distribution control centers. However, more extensive real-time monitoring and control is needed for effective operation of the system and for good quality of service to the customers. In addition to monitoring and control of switches and control devices, detailed real-time load data is needed for real-time monitoring and control purposes. Unfortunately, this data is not currently available and historical data about the customer loads is used to forecast the loads [51]. Obviously, the accuracy of historical data may not be good enough for real-time applications.

Since it is not possible to measure every quantity and telemeter it to the control center, only a limited number of real-time measurements will be available at the control center. Then the problem becomes determining the operating point of the system as accurately as possible based on these limited measurements.

When there are only a few measurements, power flow analysis can be used to obtain an approximate solution by scaling the forecasted loads such that the power flow results match the measurements. To improve the accuracy of load data, however, more real-time measurements are needed so that the validity of the forecasted load data can be checked and corrected if necessary. Authors proposed using of SE for this purpose.

The main function of SE is to minimize the errors and inconsistencies that may exist in data. A state estimator can "smooth out" small errors in meter readings, detect and identify gross measurement errors, and "fill-in" meter readings that have failed due to communication failures [52].

The main point of reference [50] is to develop a SE method that can be used in monitoring of a distribution feeder in real-time. The authors relied strongly on classical TSSE approach with adjustments taking into account the specific nature of DNs like representation of feeders and deficiency of real-time measurements. Three-phase approach has been utilized in this research.

An investigation of the measurement functions will reveal that all the functions, except the one corresponding to the voltage magnitude measurement, are nonlinear functions of state variables. These functions are more complex than the single-phase case, since they not only contain product terms between neighboring nodes, but also cross product terms between phases. This indicates that the Jacobian **H** corresponding to the measurement equations will not be constant (i.e., the elements of Jacobian will depend on state variables, **x**). However, it is very desirable to have a constant Jacobian for computational efficiency, since then the normal equations will be easier to construct and solve iteratively. For this purpose, authors tried to approximate the Jacobian by simplifying its elements.

For SE to be effective, a minimum amount of real-time data is necessary. In this research, the power supplied to the feeders and voltage measurements at the substation are the only real-time measurements available at distribution level. Some feeders may have a few branch current or power measurements also. Considering the data required for power flow analysis as the minimum data, and taking distribution transformer primaries as load points, this real-time data is not enough for SE. Therefore, authors propose to use historical load data to forecast the loads since it is an approach commonly used by utilities. These forecasted data are used as pseudo-measurements, measurements that are less accurate than actual measurements, to supplement for the real-time data available for SE.

The minimum data assumed to be available will satisfy the so-called topological observability when it is applied on a per-phase basis. However, the mutual terms in three-phase analysis and current magnitude measurements may require the check for numerical observability which corresponds to the gain matrix being non-singular. Numerical observability can be checked during the LDU factorization of the gain matrix, **G**; if any of the pivots become very small then this is an indication that the gain matrix may be singular, hence the system may not be observable.

Results indicate that SE with limited measurements improves the accuracy of the load only marginally when the forecasted load data is properly scaled. In continuance, results indicate that SE has good convergence characteristics even with very limited measurements. Test results also indicate that SE can improve the forecasted load data by using real-time measurements. However, the effectiveness of SE mainly depends on the accuracy of the forecasted loads when there are only limited real-time measurements. It is also observed that power flow measurements are more effective in bad data identification than current measurements. It is the hope of these authors that as more real-time measurements become available at distribution level, SE will be used for feeder monitoring as widely as it is used for monitoring of TNs today.

The development of the DSSE was further tackled by the same authors in [53]. The main focus of this research was to develop a computationally efficient SE method that is tailored for monitoring of distribution feeders in real-time. A branch-current-based three-phase SE method was developed. The method can handle radial and weakly meshed feeders which may have a few loops created by closing some normally-open tie or line switches. The method is computationally more efficient and more insensitive to line parameters than the conventional node-voltage-based SE methods. This improvement mainly comes from the fact that the branch current formulation decouples the SE problem into three sub-problems, one for each phase. Furthermore, a simple rule based feeder network reduction method is proposed in this research to further improve the computational efficiency of SE without sacrificing accuracy.

The branch-current-based SE method, like conventional node-voltage-based SE methods, is based on the weighted least square (WLS) approach. Rather than using the node voltages as the system state, the proposed method uses the branch currents and solves the following WLS problem to obtain an estimate of the system operating point defined by the system state x:

$$\min_{\mathbf{x}} J(\mathbf{x}) = \sum_{i=1}^{m} w_i (z_i - h_i(x))^2 = [\mathbf{z} - \mathbf{h}(\mathbf{x})]^{\mathrm{T}} \mathrm{W} [\mathbf{z} - \mathbf{h}(\mathbf{x})] \qquad (4.1)$$

where w_i and $h_i(x)$ represent the weight and the measurement function associated with measurement z_i, respectively. For the solution of this problem, the conventional iterative method is adapted by solving the normal equations at each iteration.

One of the main challenges in implementing this approach for SE in distribution feeders is incorporating the unbalanced nature of distribution feeders into the problem. Other challenges are the lack of enough real-time measurements and the fact that most of the available measurements are branch current magnitude measurements which are not usually included in the conventional SE methods.

In general, main feeders are three-phase, however, some laterals can be two-phase or single-phase. The lines are usually short and untransposed. Loads can be three-phase, two-phase or single-phase (like residential customers). Therefore, it is desirable to use a three phase model as also recommended for power flow analysis of feeders.

To use branch currents as state variables in SE, authors determined the measurement functions, $h_i(x)$ for each measurement z_i first. If all the measurements were of complex branch currents and node injection currents, then the measurement functions would be linear.

Two types of power measurements are assumed to be available: actual power flow measurements and pseudo load measurements obtained from the load forecast data. These power measurements are converted into equivalent current measurements that are calculated at each iteration by using the available voltage estimates.

Voltage measurements (if there are any) will be ignored, except the voltage measurement at the substation bus which is taken as the reference bus. This is based on the observation that the voltage measurements do not have a significant effect on SE results provided that the system is observable.

Now using current measurements, actual and/or equivalent, SE problem given by Eq. (4.1) needs to be solved to estimate all the branch currents. However, it should be noted that the objective function is separable on a phase basis, since the measurement functions for measurements on a given phase are functions of the branch currents of that phase only. Hence, one can decompose Eq. (4.1) into three sub-problems, one for each phase $\varphi = 1,2,3$. The current only SE problem for phase φ is:

$$\begin{aligned} \min_{\mathbf{I}} J(\mathbf{I}) = & \sum_{i=1}^{ms} w_i \{ (I_{ri}^m - h_{ri}^m(\mathbf{I}_r))^2 + (I_{xi}^m - h_{xi}^m(\mathbf{I}_x))^2 \} \\ & + \sum_{i=1}^{mc} w_i (I_i^m - h_{ci}(\mathbf{I}))^2 \end{aligned} \qquad (4.2)$$

where:

I vector of state variables, in this approach branch currents;

I_{ri}^{m} equivalent current measurement of the real power measurement;
I_{xi}^{m} equivalent current measurement of the reactive power measurement;
$h_{ri}^{m}(\mathbf{I}_r)$ measurement function of the real part of the equivalent current measurement;
$h_{xi}^{m}(\mathbf{I}_x)$ measurement function of the imaginary part of the equivalent current measurement;
I_{i}^{m} current measurement;
$h_{ci}(\mathbf{I})$ measurement function of branch current magnitude measurement;

The two summation terms in the objective function are for the power and the current measurements.

The current only SE problem given by Eq. (4.2) is solved together with the voltage update procedure *forward sweep* to obtain the SE solution. This iterative process involves the following steps at each iteration *k*:

Step 1. Given the node voltages V^{k-l}, convert power measurements into equivalent current measurements.
Step 2. Use current measurements to obtain an estimate of branch currents $\hat{\mathbf{x}}_{\varphi}^{k} = \left[\hat{\mathbf{I}}_{r,\varphi}^{k}\ \hat{\mathbf{I}}_{x,\varphi}^{k}\right]$ by solving the current only SE problem given by Eq. (4.2) for each phase $\varphi = 1,2,3$.
Step 3. Given the branch currents, update the node voltage $\mathbf{V}^{k}$ by the forward sweep procedure.
Step 4. Check for convergence; if two successive updates of branch currents are less than a convergence tolerance, stop, otherwise go to step 1.

Test results indicate that the method has superior performance compared to the conventional node-voltage-based methods both in terms of computation speed and memory requirements. The method is specially tailored for weakly meshed DSs which are radial or have a few loops. Another advantage of the method is its insensitivity to line parameters, which improves both its convergence and bad data handling performance. Finally, it is shown that the proposed feeder reduction method is very effective in improving the computation speed and filtering properties of the method without sacrificing accuracy.

Research of C. N. Lu, J. H. Teng and W. H. E. Liu [54] is another three-phase DSSE approach. Authors point out that, due to the requirements of filtering measurement data and having real-time system states for on-line operation, the need for a DSSE is more than justified.

In addition to the network data, DSO also needs a set of redundant measurements to obtain an estimate of the system states. In a fully automated system the measurements are sufficient for SE. However, in the current stage of distribution system automation (DSA), the number of meters installed in the system is low and may not be sufficient for SE, i.e. the system may not be completely observable. In order to obtain an SE under this condition, techniques have to be developed to provide additional data (i.e. pseudo-measurements) to the estimator.

Authors mitigate the problem of redundancy by introducing speial three-phase SE algorithm based on normal equation method. A new rectangular form SE based on current instead of power, is introduced. The proposed

algorithm can be used to handle many types of measurements. It is applicable to the current magnitude measurements that are often found in the distribution sysrem telemetry. The three-phase network models and mathematical formulation of the method are described in this paper.

Authors point out that historical data are available and can be utilized to forecast the loadings of feeders and distribution transformers. These data are treated as pseudo-measurements. Loads in a DS are usually classified as three general types of customers. they are the residential, industrial and commercial customers. Typical load pattern or daily load curve of each type of customer can be obtained by electric load synthesis or load survey technique [55]. The load composition of each distribution transformer can be calculated according to the energy consumption of all customers served by the transformer. By using the load patterns and the derived load composition, an hourly load of distribution transformer can be estimated and used as a pseudo-measurement.

Authors use similar model as the one presented in reference [53] - SE formulation based on current instead of power. The proposed formulation can handle all types of measurements. In each iteration of SE, power measurements are converted into their equivalent currents. The authors also make a similar observation regarding the observability and how to obtain it.

The measurement data are simulated by using a three-phase power flow solution. Noise is added to each measurement and weights of measurements are given. Noise is added randomly to the actual and pseudo-measurements and is at the ranges of ±10% and ±30% respectively. Two different weights are given to the measurements, one for the actual measurements and the other one for the pseudo-measurements. The weights are 1/3 and 1/50 respectively.

Since measurement noise is included randomly in the measurements, ±10% and ±30% respectively, for actual and pseudo-measurements, the final SE solutions will not be the same as the power flow solution. The results of research indicated that even with only the pseudo-measurements, the proposed algorithm can provide an SE solution. However, due to the low accuracy of the pseudo-measurements, the solution is bad when we compare it with the base case power flow solution. This estimated solution can be improved by adding real-time measurements to the measurement set.

Test results of this research have shown that the proposed rectangular form current based formulatuon is a suitable choice for the DSSE. Authors conclude that more investigation is required in order to determine other techniques that may faciliate the performance and accuracy requirements of the DSSE.

Ke Li in [56] introduces the concept of stochastic results of DSSE and a detailed analysis. Author points out that due to the large number of customers, it is impractical to monitor distribution systems in real-time at every customer location. A practical DSSE scheme must be based on substation measurements, few critical circuit measurements and a large number of customer load estimates. A DSE should be a three-phase model to represent the unbalance phase load and phase configuration, instead of the single phase model in TSSE.

The DSSE study also requires an appropriate load model in order to represent each customer or group of customers, which can include a mixture of residential, commercial and industrial load. Due to the uncertain behavior

of customer loads, each load can not be represented by a deterministic quantity. The customer load can be represented by pseudo-measurement, an expected value with an associated deviation. The limited real-time measurements and numerous customer loads of the lower voltage level in DS dramatically increase the uncertainties of system states; therefore, the traditional deterministic model of distribution power flow studies could lead to incorrect results.

The proposed DSSE model requires the information of the DS configuration, real-time measurements and customer load pseudo-measurements. The system configuration information illustrates the connections of circuits and buses of the power DS as well as the switch status. Real-time measurements include the real and reactive power flow, bus voltage magnitudes, and the line current magnitudes. Customer load pseudo-measurements are obtained from the knowledge of the customers. The authors also uses LWS approach to solve DSSE.

The bus load errors vary from 20% to 50% with different type of customers. For instance, the industrial type load (particularly with larger customers) can be estimated more accurately so it has lower variance. The residential type load is diflicult to be estimated so the higher variances can be selected. The commercial type load is generally between the above two type loads.

The standard deviations of customer load pseudo-measurements and real-time measurements are two of the system parameters affecting the system state deviations. Figure 4.2 depicts the influence on the system critical voltage at bus 5 of the test from this research due to the changing the customer load pseudo-measurement errors from 10% to 50%. The bus voltage deviation appears to be a linear function of the customer load pseudo-measurements according to this figure. It can be concluded how increasing the load measurement accuracy will improve the estimated deviations of the bus voltage.

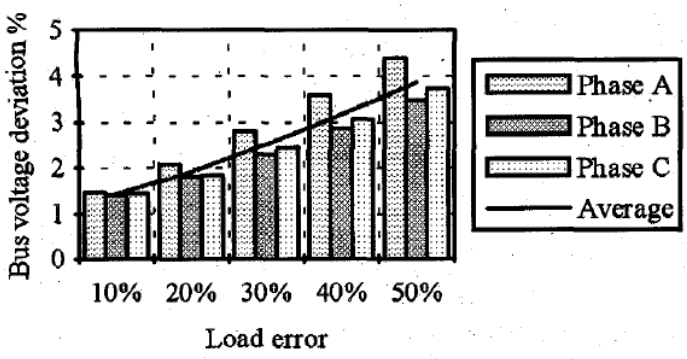

Figure 4.2: *Voltage Deviation vs. Load error at critical bus of the DN [56]*

The results of this research lead to the conclusion that the change of real-time measurement deviation has little influence on the bus farther away from the substation, but a large influence at the bus near the substation. To improve the voltage deviation at the voltage critical bus, the method of increasing measurement accuracy for customer load is a better choice.

The additional real-time measurements will improve the estimating accuracy. Generally, it is more economical to install the bus voltage

measurement as opposed to a line measurement to decrease the estimated deviation of the bus voltage magnitude.

The research of A. P. S. Meliopoulos and F. Zhang in [57] provides an estimate of the total electric load for each distribution circuit without the requirement of knowledge of the individual loads along the circuit. Authors noted that the use of low weights for historical data is meaningless if these data represent critical measurements. These methods require extensive field tuning to achieve reasonable performance. The distributed nature of loads in a DS, i.e. distributed load, deserves special attention. The proper implementation of DMS functions requires the knowledge of the distributed load [58]. A SCADA system which measures all the components of the distributed load may be prohibitively expensive. For this reason, authors of the paper propose a method which estimates the total electric load from measurements placed at strategic points along the DS without knowledge of the individual loads along the circuit. This structure and approach does not exclude measurements of individual electric loads, i.e. large industrial customers or other key load components.

Authors form their research on three-phase power flow model for DS and then DSSE is formulated based on WLS approach followed by an extension of the traditional topological observability analysis method and quantitative measures to asses the performance of the SE method. This paper introduces the methodology of phasor measurement units (PMUs). A conceptual view of the system using PMUs is depicted in Figure 4.3. The figure illustrates the use of the Global Positioning System (GPS) as an absolute time reference. As an example, the figure shows a PMU which is capable of communicating with the GPS to provide an absolute time reference with a nominal accuracy of 1 microsecond. Subsequently, a synchroruzing signal is transmitted via radio to all data acquisition systems (DAS) which may be dispersed throughout a DS.

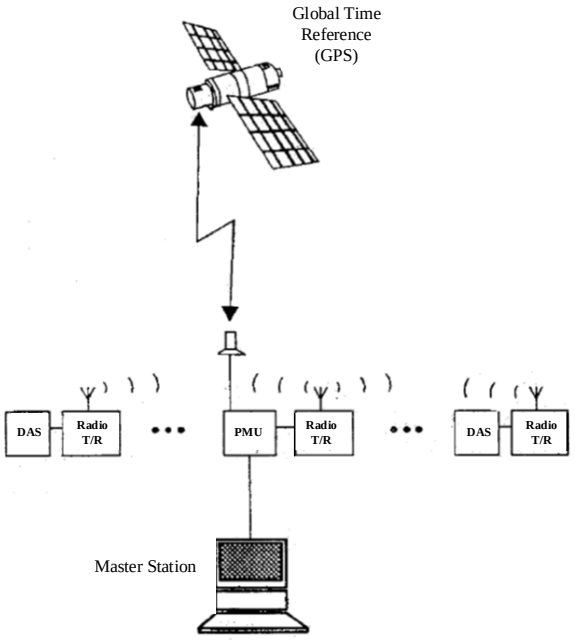

Figure 4.3: *Concept of performing synchronized measurements for DS [57]*

In any SE problem, the question of observability is very important. For DS observability analysis, the conventional topological method [34] cannot be used directly because the definition of system state is not the same as in the traditional sense and not all buses are three phase buses. Existing topological observability algorithms, with small modifications, are used for the part of the system which satisfies the following measurement selection condition:

- the voltage measurement is selected such that if there is a voltage measurement for one of the phases of a bus, then there is a voltage measurement for all other phases of the bus;
- the current measurement is selected such that if there is a current measurement for one of the phases of a transmission or distribution line, then there is a current measurement for all other phases of the transmission or distribution line.

Authors note that while the voltage state variables exhibit very small errors, the load current state variables exhibit substantially larger errors. It is important to note here that the use of uniformly distributed measurement error substantially contributes to these large errors. The results suggest that improvements in estimating the electric load require improvements in the accuracy of the measurement system.

The research developed in [59] is aimed towards development of robust three-phase SE. Its extension to observability analysis and bad data processing is also discussed. Method uses forward and backward propagation scheme to estimate line flows, node voltages and loads at each node, based on the measured quantities.

Author points out that conventional state estimation methods based on least square method technique may fail to give solution to the DSSE in many cases due to ill-conditioned gain matrix and Jacobian matrices. Also these methods are applicable to system with lower number of nodes and lower *r/x* ratio of lines and computationally are not efficient. In this paper a new formulation and solution algorithm for solving SE is proposed for three-phase unbalanced DSs. In the proposed technique, the observability routine decides if the measurement set is suficient to allow the computation of the SE. Bad measurement data are detected, eliminated and replaced by pseudo or calculated values.

The algorithm developed for this research checks the measurement values. If the measurements are not available, then the values are either calculated or pseudo-measurements are provided. Selections of pseudo-measurements, filling of missing data, providing appropriate weightage are the functions of the observability analysis algorithm. Backward propagation is used to calculate branch currents, branch flows and average of calculated and measured branch flows providing weights. During the iterative process the bad data is detected and replaced by pseudo or calculated values.

Bad data processor detects the presence of bad data (gross error) in the measurement set. After bad data is detected, it identifies which measurements are erroneous. These are eliminated from the set of measurements to be utilized for the SE and suitable values are replaced. In this approach, the difference between the measured and calculated values are calculated during

each state estimator iterative process. These difference values are monitored and reduced as the iterations advanced. Due to presence of bad measurements, some of these values may persist to be significant. After reasonable number of iterations (say 4 or 5), if these values corresponding to some measurements exceeds a pre-specified threshold value (say T_z = 0,1), these are suspected to be bad measurements. These measurements are replaced by the calculated values or pseudo-measurements and the state estimation iterative process is continued.

At the end of research, author concludes that the algorithm based on forward and backward propagation is suitable for unbalanced three-phase radial DNs. The new methodology has been tested to analyze practical DNs having higher *r*/*x* ratio of lines. The proposed method has worked well regardless of the feeder *r/x* ratio while the conventional WLS method failed to give a solution in most of the cases.

Finally, in [60] authors point out that the DSSE literature is either based on the probabilistic power flowor direct adaptation of TSSE algorithms (particularly WLS). The issue of measurement inadequacy is addressed through pseudo-measurements that are stochastic in nature. However, the performance of the SE algorithms under the stochastic behaviour of pseudo-measurements is not addressed in the DSSE literature.

The work presented in this paper investigated the existing TSSE techniques and algorithms and assessed their suitability to the DSSE problem. Furthermore, the statistical measures utilised in this paper mainly depend on the probability distribution of the measurements and not on the line model of the network.

Authors claim that in DS, measurements are predominantly of pseudo type, which are statistical in nature, so the performance of a SE should be based on some statistical measures. Various statistical measures such as bias, consistency and quality have been adopted for assessing the effectiveness of SE in other technology areas such as target tracking [61].

Authors note that various algorithms have been suggested for TSSE. All these algorithms work well in TSs because there is high redundancy in the measurements. However, in DSs, because of sparsity of measurements, there is less or no redundancy in the measurements. Hence, when these algorithms are exposed to DS they start showing their limitations. For example, in TSs, weighted least absolute value estimator (WLAV) [62] eliminates bad data out of redundant measurements, but in DSs it fails to work because it treats every pseudo-measurement as bad data and there is no redundancy to eliminate these pseudomeasurements. Apart from this method, authors tested classical WLS approach already explained in more details in Chapter 3 of this disseration. Third classical method that is tested in this research is Schweppe Huber generalized M (SHGM) estimator [63].

Three types of measurements were taken into consideration. The telemetered measurements were utilised as real measurements. Zero injections with a very low variance (10^{-8}) were modelled as virtual measurements. Loads were modelled as pseudo-measurements. Various scenarios considering the errors in real measurements as 1% and 3%, whereas 20% and 50% in pseudo measurements were examined. The range of errors in pseudo-measurements was chosen on the basis of errors in load estimates of various classes of

customers, like industrial, domestic and commercial. The loads of the industrial customers can be estimated more accurately than the domestic and commercial, thus they have less error. On the other hand, loads of domestic customers are difficult to estimate, hence they have large error. The error in commercial load estimates lies between the two, which was reported in previous findings. It was also taken into consideration that with this choice of range, the maximum demand limits at various buses are not violated and the condition of linear approximation is valid.

Test shown that WLS shows consistent results in all test cases. On the other hand, WLAV is inconsistent in all the cases. It is interesting to note that SHGM is inconsistent for small errors in pseudo-measurements and consistent for large errors in pseudo-measurements. The reason is that the measurement set considered for study is predominantly comprised of the pseudo-measurements, and large error in pseudo-measurements increases the measurement variance.

The statistical criteria discussed in this paper depend on the characteristics of the distribution of measurement errors. The results presented are based on the assumption that the measurement errors are normally distributed. Under this assumption, the WLS satisfies the statistical criteria and hence was found to be the suitable solver for the DSSE. However, this may not be true if the measurement errors are not normally distributed. For instance if the errors follow the Laplace distribution [64], the WLAV estimator gives better performance than WLS and SHGM. The reason for this is that the WLAV is consistent with the Laplace distribution and maximisation of log-likelihood of the Laplace density function results in the WLAV formulation.

In reality, different probabilistic load distributions exist in the DSs and no standard distribution can fit all of them. Furthermore, the large size of the DN having various probability distributions at different buses makes accommodating them in a single SE impractical. A more practical approach is to model the actual probability distributions as a mixture of several Gaussian distributions (Figure 4.4) and apply the WLS state estimator which is consistent with the normal distribution.

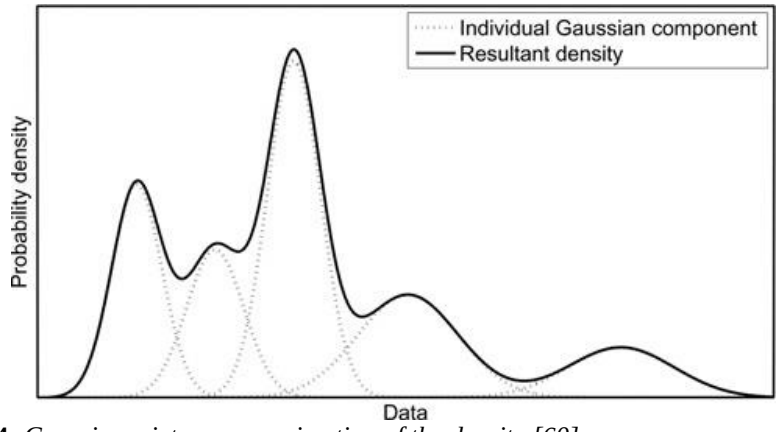

Figure 4.4: *Gaussian mixture approximation of the density [60]*

The performance evaluation of SE techniques shows that the existing solution methodology of WLAV and SHGM cannot be applied to the DSs. In order to obtain the consistent and good quality estimate, significant

modifications are required in these algorithms. WLS gives consistent and better quality performance when applied to DSs. Hence, authors found out that out of the three approaches, WLS is the most suitable solver for the DSSE problem. The WLS works well if the noise characteristics are known. In the absence of this knowledge, either the WLS needs to be modified or a new class of algorithms needs to be introduced.

4.2.1 Critical review of the proposed bibliography

As one can see for the stated brief bibliography review, many researchers have addressed the issues of DN observability and State Estimation (SE) proposing different approaches. Many approaches, such as in [50],[53]-[56] tend to use the traditional least square methods by introducing a large number of pseudo-measurements for loads and generators. But in real DNs the loads and generators profiles are determined based on the annual energy consumption from the previous years [65]. This means that there is no statistical information available so it is impossible to correctly use them as pseudo-measurements.

Introducing a large number of pseudo-measurements is meaningless if these represent critical measurements. Trying to achieve the minimum redundancy by adding the large number of pseudo-measurements will deteriorate the quality of SE applied to DN. Some approaches, such as in [57] propose using the Phasor Measurement Units (PMUs), but this type of equipment is expensive and most of the DSOs do not use it. Last, a three or multi-phase approach [50],[53],[54],[56]-[59] is not applicable for real MV grids: the loads are generally balanced and the cables parameters (especially mutual coupling) are not known [65]. Results stated in [53] are based on the exclusion of voltage measurements and this is justified by the fact this type of measurements don't have significant effect on SE results provided that the system is observable. However, DS is not observable.

Hence, it is necessary to design suitable innovative techniques to improve as much as possible the observability of the DN. The aim of the proceeding subchapters of this chapter is to provide these techniques for DSSE.

4.3 Distribution System State Estimation

The evolution of DSs sees in the remarkable expansion of the DG plants connected to the medium and low voltage networks one of the main challenge. The growth of DG will cause a profound change of the DS in the technical, legal and regulatory aspects; most likely the distribution company will more and more undertake, on local scale, tasks and responsibilities of the role assigned on a national scale to the operator of the electricity transmission network, becoming thus a DSO. In other words, the distribution company will become a sort of "local dispatcher" and will involve its active/passive customers in activities related to the network management and optimization; obviously, this requires a deep review of the regulatory framework.

In this sense, the DSO must undertake various initiatives in order to adapt the methods of planning, management and analysis of operation of the network. For all of this to be possible it is mandatory for the DSO to possess a

thorough real-time knowledge of the system state. The solution at hand would be the use of the least square based SE techniques used for a very long time by the TSOs. However, in nowadays DSs, the pace of investments into measurement equipment is much more reduced than the increase of DG penetration and the situation is very similar to the past when the DS were passive. Thus, only a limited set of measurements in the primary substations and, sometimes, in some secondary substations are available. Then, the equipment is mostly old and the precision class is inappropriate for applying state estimation as it was installed for other purposes, (e.g. input signal for the protection systems). All these factors make the DS lack of redundancy or, in other words, to have sub-unitary redundancy. Moreover, the data acquisition process of these measurements is qualitatively poor: the measurements are not always synchronized but averaged and collected in different moments so, is very hard to statistically characterize them.

Thus, the application of a complete SE technique similar to the ones used by the TSOs is impossible. However, many approaches, as already explained, tend to use the traditional least square methods by introducing a large number of pseudo-measurements for loads and generators. Nevertheless, in real DSs, the loads and generators profiles are estimated profiles based on the past yearly energy consumption. This means that there is no statistical information available about them, so it is impossible to correctly use them as pseudo-measurements in a least square approach.

Hence, it is necessary to design innovative techniques to improve as much as possible the observability of the DS. Such approaches need to be robust and computationally fast as they should run on-line for many networks. In this chapter, various approaches that depend on the available measurements in the DS were exposed. The degree of their complexity increases with the number of available measurements. As mentioned in the Chapter 1, INGRID project, which was specifically developed for automated control software package for DSO, comprises SE function [66] which will be developed in details in the following subchapters.

4.3.1 Available Information

The information currently available to the DSO is of two types (Fig. 4.5): (*i*) estimated load and generation profiles and (*ii*) a set of measurements at the primary substation level and, sometimes, at the secondary substation level. In what regards the first category, the real and reactive power demand (P_L^0, Q_L^0) and the generation (P_G^0, Q_G^0) profiles are known through an appropriate processing of the historical data that gives "standard" curves for various loads and generators based on the annual energy consumption. This information is far from being accurate which implies that in the majority of cases the PF results obtained using these data are not consistent with the actual operation and hence no decision regarding the control and management of the DS can be taken.

However, every 10-15 minutes, a set of measurements in the primary substation of the DS is available as averaged values over the considered period of time (Fig. 4.5):

- voltage magnitude at the HV busbar (V_{HV}^m);

- voltage magnitude at the MV busbars (V_{MV1}^{m} and V_{MV2}^{m});
- real and reactive power crossing the secondary winding of the transformers and the corresponding direction ($P_{T,r/q}^{m}, Q_{T,r/q}^{m}$)[1];
- current magnitude in the secondary winding of the transformers ($I_{T,r/q}^{m}$);
- current magnitude on each MV feeder directly connected to the MV busbars ($I_{f,i/k}^{m}$).

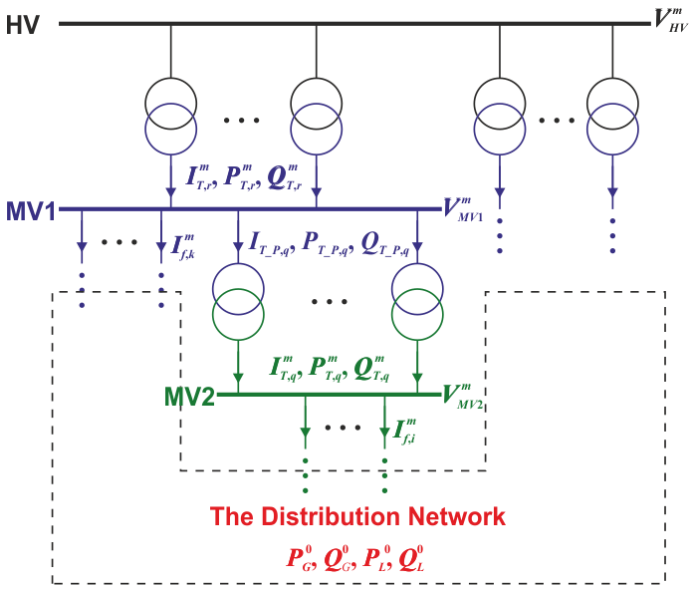

Figure 4.5: *Available information in a primary substation of a DS grid*

In addition, in some DS, also a set of measurements in the secondary substations is available (Fig. 4.6):

- voltage magnitude at MV busbars ($V^{\mathbf{m}}$);
- real and reactive power flows at the to or from buses of the connected feeders in the secondary substations ($P_{ft}^{\mathbf{m}}, Q_{ft}^{\mathbf{m}}, P_{tf}^{\mathbf{m}}, Q_{tf}^{\mathbf{m}}$);
- current magnitudes at the to or from buses of the connected feeders in the secondary substations ($I_{ft}^{\mathbf{m}}, I_{tf}^{\mathbf{m}}$);
- the real and reactive power demanded by the loads ($P_L^{\mathbf{m}}, Q_L^{\mathbf{m}}$) and the generator production ($P_G^{\mathbf{m}}, Q_G^{\mathbf{m}}$).

[1] In order to compactly describe the variables of identical meaning but different indices, instead of writing e.g. $P_{T,r}^{m}$ and $P_{T,q}^{m}$, it was chosen to write $P_{T,r/q}^{m}$. This is true also for the other appropriate variables.

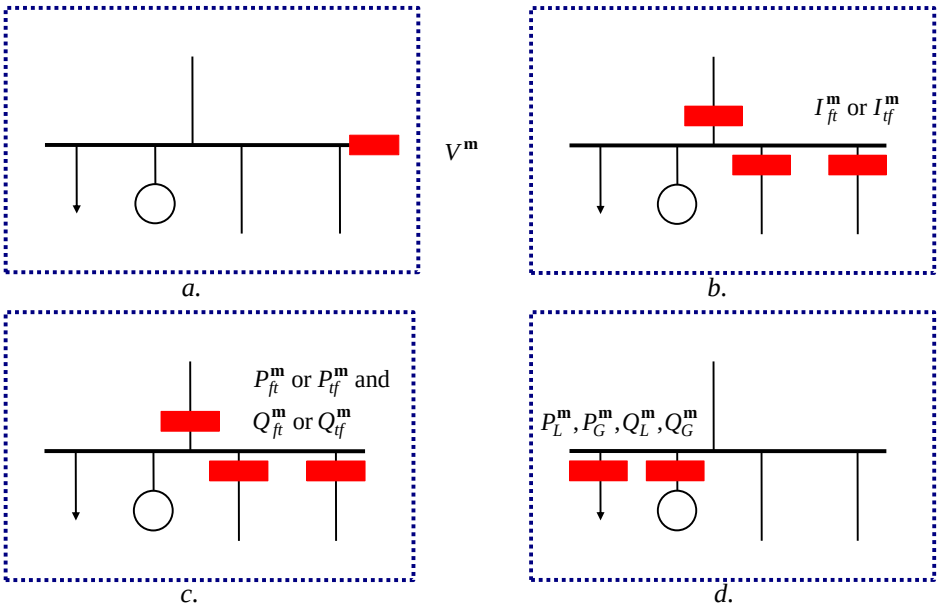

Figure 4.6: *Available information in secondary substations of a DS grid: a. Voltage measurements; b. Line current measurements; c. Line real and reactive power flow measurements; d. Load and generation measurements*

Unfortunately, the DNs are large power systems and the number of available measurements is very low compared to the total number of state variables in the network. Hence, it is impossible to apply the well-known SE algorithms used by the TSO as the network has no redundancy. An additional argument is given by the impossibility to statistically characterize the available load and generator standard profiles: it is not known how far or near each available profile is to the real profile. Thus, the only possibility is to develop new techniques to improve the network observability. These, depending on the number of measurements, can be from simpler and computationally fast, to more complex. From this point of view, two major approaches have been developed: (*i*) a simplified state estimation (SSE) approach which regards DS where only the measures in the primary substation are known and (*ii*) an advance state estimation (ASE) approach where also the measurements in the secondary substations are present.

4.3.2 Simplified State Estimation (SSE) Function

The procedure was designed considering only the measurements in the primary substations (Fig. 4.5) together with historical load and generation profiles which allowed very simple and fast computations, neglecting the PF equations. Changing the load and generation profiles such that the estimates given by PF match the measurement is equivalent to finding the real and reactive power that is injected or absorbed by the feeder. Therefore, network can be simplified on a level of primary substation and feeders' equivalents and hence, PF equations are not necessary.

4.3.2.1 General Approach

If only the measurements in the primary substations are known (see Fig. 4.5), the only possibility is to adjust the available standard profiles such that a

PF computation delivers a set of results that matches the available measurements. In this regard, it can be generally proceed as follows [67],[68]:

1) adjust the tap ratio of the HV/MV transformers according to the available measurements;
2) perform a PF using the historical and actual profiles and the HV bus as the slack bus ($V_{slack} = V_{HV}^{m}$) to obtain the initial currents and powers absorbed by the feeders ($I_{f,i/k}^{0}, P_{f,i/k}^{0}, Q_{f,i/k}^{0}$); the initial power losses in the feeders ($P_{loss\_f,i/k}^{0}, Q_{loss\_f,i/k}^{0}$) and MV1/MV2 transformers ($P_{loss\_T,q}^{0}, Q_{loss\_T,q}^{0}$); the initial voltages at the substation MV busbars ($V_{MV1}^{0}$and V_{MV2}^{0}) and the initial currents and powers flowing through the transformers ($I_{T,i/k}^{0}$ and $P_{T,i/k}^{0}, Q_{T,i/k}^{0}$) (Fig. 4.5);
3) substitute the DN feeders with equivalent loads ($P_{f,i/k}$ and $Q_{f,i/k}$) and adjust them to $P_{f,i/k}^{est}$ and $Q_{f,i/k}^{est}$ such that the variables in the primary substation match the measurements. Of course, as the feeders can be active, these equivalent loads can also have negative values;
4) modify the generation and load profiles to $P_{L}^{est}, Q_{L}^{est}, P_{G}^{est}, Q_{G}^{est}$ such to obtain $P_{f,i/k}^{est}$ and $Q_{f,i/k}^{est}$, then perform a new PF to obtain the estimated values of the measured quantities. If the errors between the estimates and the measurements are not well contained, go back to point 2). Otherwise, retain as the final load/generation profiles.

To correctly modify the generation and load profiles it is necessary to accurately estimate the power losses in the feeders corresponding to the new profile. Since the power losses are proportional to the square of the current a good approximation of the power losses in the feeders was found to be:

$$\begin{aligned} P_{loss\_f,i/k}^{est} &= c_{P,i/k}^{2} \cdot P_{loss\_f,i/k}^{0} \\ Q_{loss\_f,i/k}^{est} &= c_{P,i/k}^{2} \cdot Q_{loss\_f,i/k}^{0} \end{aligned} \tag{4.3}$$

where c_P is the power coefficient, computed as:

$$c_{P,i/k} = V_{MV2,1}^{m} \cdot I_{f,i/k}^{m} / V_{MV2,1}^{0} \cdot I_{f,i/k}^{0} \tag{4.4}$$

Finally, an important assumption on which the algorithms from this dissertation rely is that once the current and power estimates match the measurements, also the resulting voltages estimates will automatically match the measurements. The hypothesis is valid as the primary substation is analogous to a very small radial network were the slack voltage and the loads are known. This assumption validates the approximation of Eq. (4.3) and allows the proposed procedures to focus only on the current and power measurements.

While the second step of the above procedure is obvious, steps 1), 3) and 4) will be developed in the former subchapter. The core of the above methodology is given by step 3) for which two algorithms can be defined: one, very fast, based on simple computations and another one, computationally slower, based on optimization techniques. Both approaches

have their advantages and disadvantages and they are both going to be exposed in the following subchapters.

4.3.2.2 Tap Ratio Computation

To solve the PF problem, it is necessary to define many input data: real and reactive power required by the loads and produced by each generating unit, the topology of the network, the electrical data of each component and the magnitude of voltage of the HV busbar of the primary station. Another important information is the tap changer position of the HV/MV transformer.

Generally, for this type of device, 20 different positions are available, but, due to technical limitation there is not the possibility to communicate the position of the tap changer. In particular, the bit number available to code the position is very limited. Therefore, it is essential to define a procedure able to compute the tap change position of the transformer; otherwise, the PF results could be significantly different from the real values.

To overcome this problem, a specific procedure, invoked before the SE function, has been developed. It permits to compute the tap change position for 2 o 3 winding transformer starting from the measured data obtained in real time.

4.3.2.2.1 2-Winding transformer

The 2-Winding transformer is represented according to the circuit scheme reported in Fig. 4.5. To compute the tap changer position, the following data is necessary:

- the real and reactive power at the MV level of the transformer;
- the voltage magnitude at both HV and MV level.

Using this information, it is possible to apply the Boucherot theorem starting from the voltage magnitude of MV busbar (section A in Fig. 4.7) to compute the voltage of section B. Then, using the information about the magnitude voltage of HV busbar (section C) it is possible to compute the tap change ratio with the following equation:

$$k = V_C / V_B \tag{4.5}$$

Obviously, in order to apply this procedure, it is mandatory to know the values of the real and reactive power given by the transformer to the MV network. Without this information, it is not possible to compute the tap change ratio.

Moreover, the numerical result given by this procedure is influenced by the measure errors that affect the input data.

A particular situation can occur when the measurement data is given at section C (Fig. 4.7).

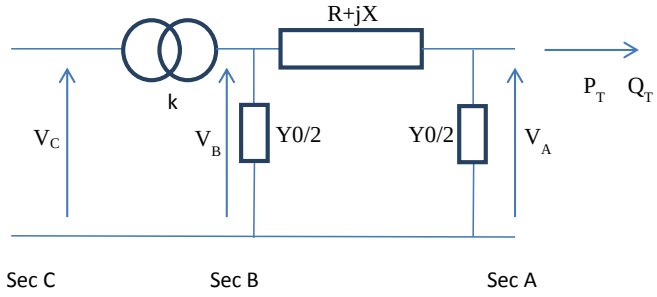

Figure 4.7: *2-Winding transformer model*

In this case, it is necessary to perform an iterative Boucherot following the steps:

1. Based on the initial value of the tap, compute a first estimate for the voltage in section B, V_B^0 , according to the above equation;
2. Perform Boucherot to determine V_A^k, where k is the index of current iteration;
3. Compute the error between V_A^k and the measured value V_A^m: $\Delta V^k = V_A^m - V_A^k$;
4. If $\Delta V^k > tol$ then update the voltage in section B as: $V_B^{k+1} = V_B^k + \Delta V^k$ and redo steps 2-4;
5. If $\Delta V^k \leq tol$ then compute the correct value of the tap ratio as:

$$k = V_C^m / V_B^m \tag{4.6}$$

The iterative procedure was tested for various stressed situations and proved to be delivering very good results within insignificant computation time.

4.3.2.2.2 3-Winding Transformer

The procedure developed for the 2-Winding transformer is not directly applicable to 3-Winding transformer. 3-Winding transformer is represented in according with Fig. 4.8; therefore it is necessary to compute two tap change ration. For example, for an HV/MV1/MV2 transformer, the two tap rations are respectively between HV/MV1 and HV/MV2.

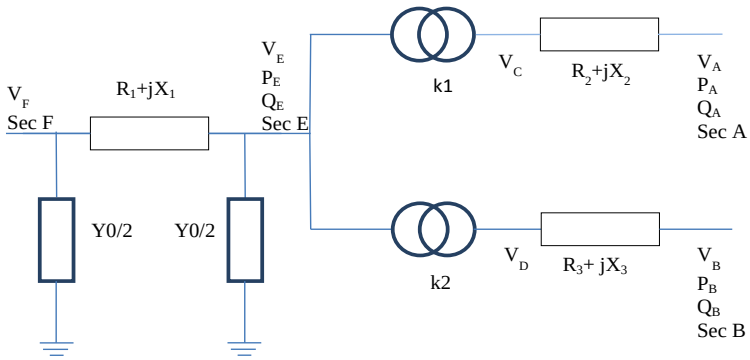

Figure 4.8: *3-Winding transformer model*

Also, in this case, the following data are necessary to compute the values of the two tap ratios, k_1 and k_2:

- the real and reactive power at the both MV levels of the transformer;
- the voltage magnitude at HV, MV1 and MV2.

In according with the symbols used in Fig. 4.7, k_1 and k_2 are given by the following equation:

$$\begin{aligned} k_1 &= V_E/V_C \\ k_2 &= V_E/V_D \end{aligned} \tag{4.7}$$

Therefore, it is necessary to compute the following magnitude voltages: V_C, V_D and V_E. Starting from the section A and applying the theorem of Boucherot, it is possible to compute the value of V_C. The same is true for section B and D.

Then, V_E should be computed. In this case, it is possible to compute P_E and Q_E applying the balance equation for real and reactive power at this section taking into account that k_1 and k_2 represent an ideal transformer:

$$\begin{aligned} P_E &= P_C + P_D \\ Q_E &= Q_C + Q_D \end{aligned} \tag{4.8}$$

Now, it is possible to use the information given by the voltage magnitude of section F to implement an interactive Boucherot procedure. In other words, it is possible to assign to V_E an initial value ($V_E^0 = 1$ in per unit) and applying Boucherot from section E to section F, it is possible to compute V_F and compare this value with the voltage measured in real time, V_{F_meas}:

$$\Delta V = V_F^m - V_F \tag{4.9}$$

Then, V_E is update in according to the following equation:

$$V_E^{k+1} = V_E^k - \Delta V^k \tag{4.10}$$

After that, it is possible to repeat the procedure until ΔV is lower or equal to a given tolerance (i.e. $1 \cdot 10^{-7}$ in p.u.). Finally, adopting the V_E given by this procedure, k_1 and k_2 are computed. The time required to execute this interactive procedure is negligible.

4.3.2.3 Losses approximation formula

Subchapter 4.3.2.1 reports that in order to correctly modify the generation and load profiles, it is necessary to accurately estimate the power losses in the feeders corresponding to the new profile. An approximation of the power losses in the feeders was offered. At this point, the justification of the proposed approximation is given.

To avoid the computation of the PF to get the exact value of the losses, it is required to be able to obtain a good approximation with the available information (initial value of the losses, $P^0_{loss\_f,i/k}, Q^0_{loss\_f,i/k}$, initial apparent power absorbed by the feeder, available measurements, etc.). Power losses are

made up from two components – longitudinal losses that are proportional to the square of the current absorbed by the feeder and shunt losses that are proportional to the square of the voltage. Taking this into consideration, the change in losses from a known initial point to another unknown point in terms of PF results was roughly estimated by considering it equal to the square of the apparent power ratio between these operating points and Eq. (4.3) was derived. In this way, both longitudinal and shunt losses have been incorporated without the need to compute time-consuming PFs during the convergence of the state estimation algorithm.

This claim is proven by testing it on feeders with various topologies and load/generation characteristics. The data for some tested the feeders is given in Table 4.2.

Table 4.2: Approximation of losses – test feeders data

Feeder	A	B	C	D
No. buses	14	28	90	20
$A^0_{f,i/k}$ [kVA]	1080.71	852.06	1114.54	385.01
$P^0_{loss\_f,i/k}$ [kW]	3.39	1.00	20.42	0.98
$P^0_{loss\_f,i/k}/A^0_{f,i/k}$ [%]	0.31	0.12	1.83	0.25

Table reports 4 feeders of different lengths, different number of buses and ratios between load and generation. Apparent powers absorbed by the feeders, their real power loss and ratio between power loss and feeder's apparent power is also reported for the initial point.

Further, tests were run to evaluate the quality of estimation for the real power losses as follows: with the initial PF, exact $A^0_{f,i/k}$ and $P^0_{loss\_f,i/k}$ have been obtained. Then loads and generation in each bus of the feeder were modified in order to obtain higher value of $A^0_{f,i/k}$ (approximately 10%, 20%, … higher value). Another PF was run to get the exact value of the new $A_{f,i/k}$ and $P_{loss\_f,i/k}$. Using the Eqs. (4.3) and (4.4), the factor c_{p_f} and estimation of the losses were computed and then the estimation was compared with the exact value of the losses obtained by PF – the relative error in estimation was obtained (ε). The results are summarized in Fig. 4.9.

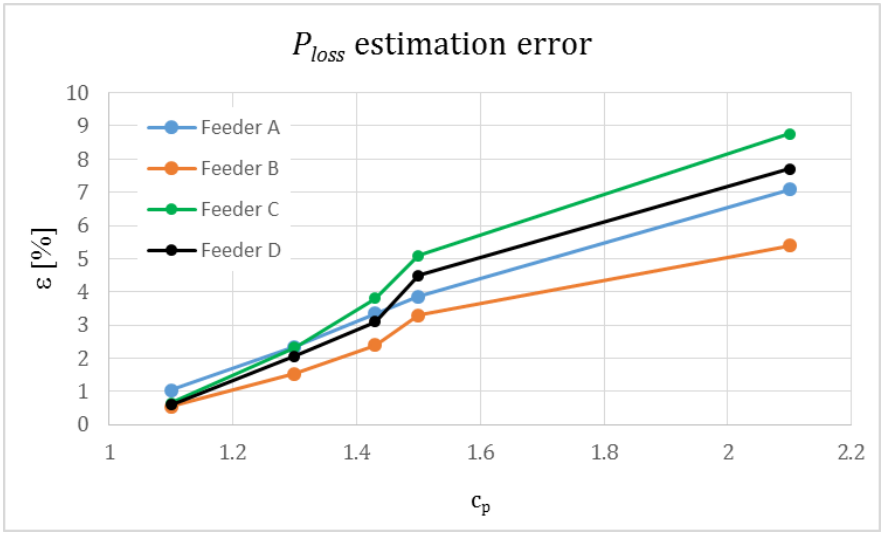

Figure 4.9: *Losses approximation*

As it can be seen, when the increase of the apparent power change is below 60 % of the initial (c_{p_f} up to 1.6), the error is well contained (a few percent), which means that the approximation is very good. With larger value of c_{p_f} like 2 or 2.2, the error is around 9% but this also does not pose a significant problem: the values of the losses in the feeder represents a small % of the total load of the feeder (see Table 4.2) so even if their estimation is not the best, but still good, the total impact on the power absorbed by the feeder is minimized. In the very rare case the estimation is not satisfactory, performing a new estimation starting from an updated load/generation profile which gives a value of $A^0_{f,i/k}$ nearer to the measured quantities will solve the problem.

Analogous tests were also carried to evaluate the estimation of the reactive power losses. The obtained results were identical to the real power losses results, so the same conclusions can be derived.

4.3.2.4 The Non-Optimized Approach to Compute $P^{est}_{f,i/k}$ and $Q^{est}_{f,i/k}$

The computations required in the third step of the SSE can be performed without PFs on the entire grid, which considerably reduces the computation time. In this subchapter, a very fast method consisting in simple computations that modify the equivalent feeder loads such that the estimated quantities gradually match the available measurements is presented. The procedure consists in gradually adjusting the feeders equivalent loads such that the derived estimated quantities are gradually matched with the measurements. This involves three steps that will be further developed:

1. Align the feeders current magnitudes with the measured quantities;
2. Correct the phase errors of the transformers currents such that the estimates match the measured quantities in the transformers;
3. Alter the estimates of the current feeders such that a suitable trade-off regarding all the measurement errors is found.

Referring to Fig. 4.4, steps 1-3 are first independently applied for each of the MV2 buses to find $I^{est}_{f,i}, P^{est}_{f,i}, Q^{est}_{f,i}, I^{est}_{T,q}, P^{est}_{T,q}, Q^{est}_{T,q}$. At this point, the currents and powers in the primary of the MV1/MV2 transformers, $I^{est}_{T\_P,q}, P^{est}_{T\_P,q}, Q^{est}_{T\_P,q}$ are computed and matched with the real quantities. Thus, they can be considered measurements and subtracted from the measured currents and powers of the HV/MV1 transformers to obtain $I^{m'}_{T,r}, P^{m'}_{T,r}, Q^{m'}_{T,r}$. Using these equivalent measures, steps 1) – 3) are applied for each MV1 bus to estimate the rest of the remaining quantities, i.e. $I^{est}_{f,k}, P^{est}_{f,k}, Q^{est}_{f,k}, I^{est}_{T,r}, P^{est}_{T,r}, Q^{est}_{T,r}$.

In the following, steps 1-3 are shown considering a generic MV bus where 4 feeders and a step-up transformer are connected (Fig. 4.10).

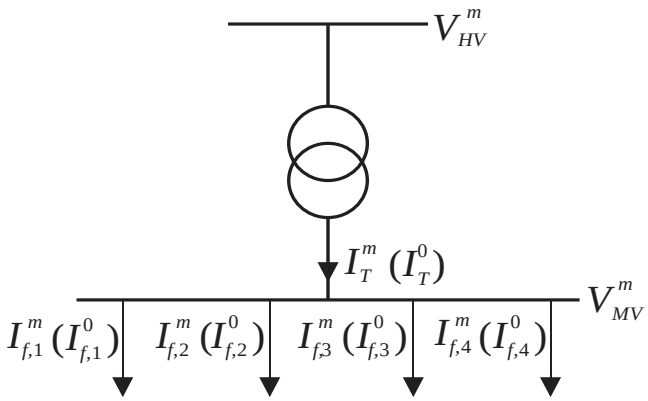

Figure 4.10: *Generic 4-feeders DN*

4.3.2.4.1 Aligning the Current Magnitudes – the c_p Factor

Considering our assumptions, a typical situation is depicted in Fig. 4.11 where a network of four feeders was assumed.

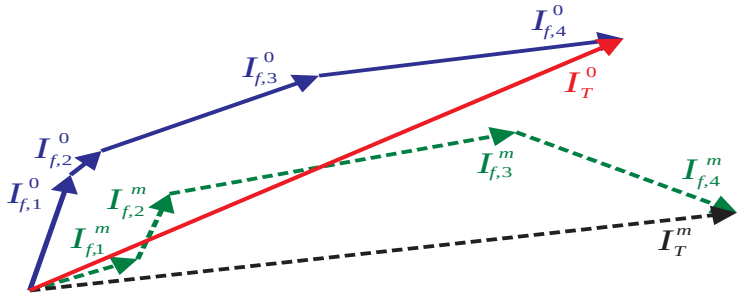

Figure 4.11: *SSE application on a four feeders DN: initial data*

According to the available data, only the vectors $I_{T,r/q}^{m}, I_{T,r/q}^{0}$ and $I_{f,i/k}^{m}$ will be completely known (magnitude and phase) while for the vectors $I_{f,i/k}^{m}$ only the magnitudes will be known. Referring to the generic case (Fig. 4.10) and under these circumstances, assuming a small power factor deviation for the feeders, the only thing that can be done is to modify, under constant power factor, the load and generation profile such that $I_{f,k}^{est} = I_{f,k}^{m}$. This is translated in modifying each individual real and reactive power of load and generator by $I_{f,k}^{m}/I_{f,k}^{0}$. This will result in the vectors $I_{f,k}^{est}$ and $I_{T,r}^{est}$ as shown in Fig. 4.12.

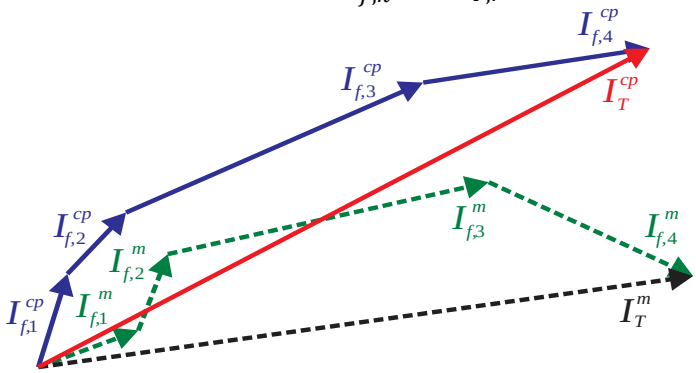

Figure 4.12: *SSE application on a four feeders DN: step one*

This is achieved through the first step where PF will be computed with the initial data and the HV bus as the slack bus with $V_{HV} = V_{HV}^{m}$. As a result of

former computation, all the relevant quantities of the system such as $V_{MV}^0, I_{f,i/k}^0, P_{loss\_f,i/k}^0$ will be obtained. These quantities represent the starting point for later computations.

In order to distinguish between physical measured value of a certain quantity and the actual value of the non-measured quantity, different subscripts are used: *m* for the former and *act* for the later one. Assuming that $cos\varphi_f = const$, the actual and initial apparent powers absorbed by feeder *i* or *k* are:

$$A_{f,i/k}^{act} = \frac{\sum_{l \in load\_f,i/k} P_{L,l}^{act} + P_{loss\_f,i/k}^{act}}{cos\varphi_f} = \sqrt{3} V_{MV}^m I_f^m \tag{4.11}$$

$$A_{f,i/k}^{0} = \frac{\sum_{l \in load\_f,i/k} P_{L,l}^{0} + P_{loss\_f,i/k}^{0}}{cos\varphi_f} = \sqrt{3} V_{MV}^0 I_f^0 \tag{4.12}$$

where:

$\sum_{l \in load\_f,i/k} P_{L,l}^{act}$ total actual real power of the load pertaining to feeder *i* or *k*;

$P_{loss\_f,i/k}^{act}$ actual losses pertaining to the feeder *i* or *k*;

$\sum_{l \in load\_f,i/k} P_{L,l}^{0}$ total initial real power of the load pertaining to feeder *i* or *k*;

$P_{loss\_f,i/k}^{0}$ initial losses pertaining to the feeder *i* or *k*;

Dividing the quantities given by Eq. (4.11) and Eq. (4.12), c_{p_f} for each feeder *i* or *k* is computed:

$$c_{p_f} = \frac{\sum_{l \in load\_f,i/k} P_{L,l}^{act} + P_{loss\_f,i/k}^{act}}{\sum_{l \in load\_f,i/k} P_{L,l}^{0} + P_{loss\_f,i/k}^{0}} = \frac{V_{MV}^m I_f^m}{V_{MV}^0 I_f^0} \tag{4.13}$$

Now, by updating initial variables, feeder powers are obtained:

$$\begin{aligned} P_f^{c_p} &= c_{p_f} \cdot P_f^0 \\ Q_f^{c_p} &= c_{p_f} \cdot Q_f^0 \end{aligned} \tag{4.14}$$

4.3.2.4.2 Phase Correction and Power Flow Inversion Check

At this point, the currents in the inputs of the feeders have been aligned in magnitude, i.e. $I_{f,i/k}^{est} \simeq I_{f,i/k}^m$, but there can be a noticeable phase error between the vectors I_T^{est} and I_T^m. This error can be easily minimized by shifting the angle of each $I_{f,i/k}^{est}$ vector with the respective phase error, i.e. with $\angle(I_T^{est}, I_T^m)$. In our particular generic case the situation is depicted in Fig. 4.13.

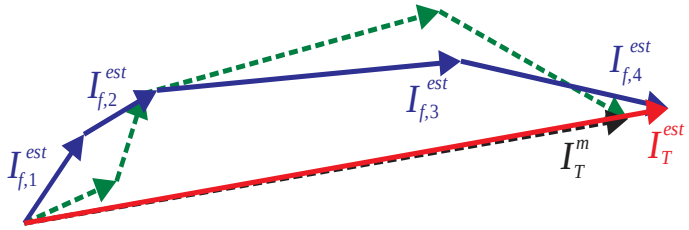

Figure 4.13: *SSE application on a four feeders DN: final step*

However, one more problem needs to be faced. Taking into account that modern DNs are no longer passive, PF inversion in some feeders can occur. By PF inversion, the difference of power signs between the initial PF and the actual/real situation in the filed which can induce larger errors in the estimation is considered. This is, of course, due to the effect of DG spread throughout the grid.

The grid is not supplied with many measurements. As a matter of fact, on distribution feeder only current magnitude measurement are present. That means that information about the flow of energy is not known. State estimator must be supplied with a mechanism to recognize possible flow inversion so that mistakes in estimation are bypassed.

If, for example, the situation with four distribution feeders from which two (feeder 2 and feeder 4) are capable of producing energy is observed, the following scenarios can occur:

$$\begin{cases} P_{f,1} + P_{f,2} + P_{f,3} + P_{f,4} = P_{T,1} \\ P_{f,1} - P_{f,2} + P_{f,3} + P_{f,4} = P_{T,2} \\ P_{f,1} + P_{f,2} + P_{f,3} - P_{f,4} = P_{T,3} \\ P_{f,1} - P_{f,2} + P_{f,3} - P_{f,4} = P_{T,4} \end{cases} \tag{4.15}$$

Four different summations of feeder real powers and hence four different possible P_T are obtained. Now by defining matrix B that contains the signs of feeders' real powers (Eq. 4.15) can be expressed in matrix form:

$$\begin{bmatrix} 1 & 1 & 1 & 1 \\ 1 & -1 & 1 & 1 \\ 1 & 1 & 1 & -1 \\ 1 & -1 & 1 & -1 \end{bmatrix} \times \begin{bmatrix} P_{f,1} \\ P_{f,2} \\ P_{f,3} \\ P_{f,4} \end{bmatrix} = \boldsymbol{B} \cdot \boldsymbol{P}_f = \begin{bmatrix} P_{T,1} \\ P_{T,2} \\ P_{T,3} \\ P_{T,4} \end{bmatrix}$$

As it was already stated, these scenarios create different phase angles situations, so procedure for updating phase angles must be imbedded into flow inversion procedure. The reader should also take into account that both scenarios for real and reactive powers were considered which means that for each P scenario n of Q scenarios exist. By combining all of the stated scenarios, the best one is selected. Here for the sake of simplicity, only P scenarios will be described. Q scenarios are executed in the same manner.

First, initial feeder and measured transformer phase angles must be computed as follows:

$$\begin{aligned} \varphi_f^0 &= \angle(P_{f,i/k}^0 + jQ_{f,i/k}^0) \\ \varphi_T^m &= \angle(P_T^m + jQ_T^m) \end{aligned} \tag{4.16}$$

Then, from already computed values of $P_{f,i/k}^0$ and $Q_{f,i/k}^0$, $A_{f,i/k}^{c_p}$ can be obtained in the following manner:

$$A_{f,i/k}^{c_p} = \sqrt{\left(c_{p_f} P_{f,i/k}^0\right)^2 + j\left(c_{p_f} Q_{f,i/k}^0\right)^2} \tag{4.17}$$

Using matrix $\boldsymbol{B}$ for a certain case, P_T can be obtained as follows:

$$P_T = \boldsymbol{B} \cdot P_f^{c_p} \tag{4.18}$$

Next, using the loop, all the rows of matrix $\boldsymbol{B}$ will be examined, computing the following:

$$\varphi_T^{est} = \angle(P_T + jQ_T) \tag{4.19}$$

Using Eqs. (4.16) and (4.19) phase error $\Delta\varphi_{f,i/k}$ can be acquired:

$$\Delta\varphi_{f,i/k} = \varphi_T^m - \varphi_T^{est} \tag{4.20}$$

Now, as already mentioned, new estimate of feeder's phase angle will be obtained using this phase error $\Delta\varphi_{f,i/k}$:

$$\varphi_{f,i/k}^{est} = \varphi_{f,i/k}^0 + \Delta\varphi_{f,i/k} \tag{4.21}$$

Using Eq. (4.21), new estimates of real and reactive powers can be computed as following:

$$\begin{aligned} P_{f,i/k}^{est} &= A_f^{c_p} \cdot \cos(\varphi_{f,i/k}^{est}) \\ Q_{f,i/k}^{est} &= A_f^{c_p} \cdot \sin(\varphi_{f,i/k}^{est}) \end{aligned} \tag{4.22}$$

Corrected values of real and reactive transformer's powers can be obtained using Eq. (4.22):

$$\begin{aligned} P_T^{cor} &= \sum_{i/k=1}^{n_f} P_{f,i/k}^{est} \\ Q_T^{cor} &= \sum_{i/k=1}^{n_f} Q_{f,i/k}^{est} \end{aligned} \tag{4.23}$$

where:
n_f number of feeders supplied by the considered transformer.

At the end of the loop, by combining *P* and *Q* scenarios as already stated, errors of real and reactive power of the transformer can be acquired using Eq. (4.23) and the measured values:

$$\begin{aligned} \Delta P_T &= P_T^m - P_T^{cor} \\ \Delta Q_T &= Q_T^m - Q_T^{cor} \end{aligned} \tag{4.24}$$

Finally, the scenario with the smallest error given by Eq. (4.24) is chosen and the flow direction is set according to that scenario.

4.3.2.4.3 Power Residual Manipulation

Next step in improving state estimation requires certain compromises. As an effect of our hypothesis that $I_{f,i/k}^{est} \simeq I_{f,i/k}^{m}$, errors on feeders will be almost zero. These vectors are not equal because in the above equations the estimation of the losses is used. While for feeders almost perfect estimation can be obtained, errors on the transformers quantities can be noticeable. Now it is the time to distribute the errors from the transformers to the feeders.

If feeder's estimates tolerance is set to 1%, for example, great improvement of transformer's estimates can be obtained.

The procedure starts with defining transformer errors of real and reactive power estimates. First it is necessary to compute new transformer power estimate in respect with the powers obtained in the previous step of the process:

$$\begin{aligned} P_T^{est'} &= \sum_{i/k=1}^{n_f} P_{f,i/k}^{est} \\ Q_T^{est'} &= \sum_{i/k=1}^{n_{feeders}} Q_{f,i/k}^{est} \end{aligned} \tag{4.25}$$

Then, using Eq. (4.25) and measured values of the measured transformer powers, the errors $\Delta P_T'$ and $\Delta Q_T'$ are computed:

$$\begin{aligned} \Delta P_T' &= P_T^m - P_T^{est'} \\ \Delta Q_T' &= P_T^m - Q_T^{est'} \end{aligned} \tag{4.26}$$

The idea is to distribute the errors $\Delta P_T'$ and $\Delta Q_T'$ on feeders as much as possible taking into account the tolerance mentioned before. This will be done using the vectors $\Delta P_{f,i/k}$ and $\Delta Q_{f,i/k}$ that are bounded by the "capacity" of the feeder as follows:

$$\begin{aligned} \Delta P_{f,k} &= \frac{\left|P_{f,i/k}^{est}\right|}{\sum_{k=1}^{n_f} P_{f,i/k}^{est}} \Delta P_T' \\ \Delta Q_{f,k} &= \frac{\left|Q_{f,i/k}^{est}\right|}{\sum_{k=1}^{n_f} Q_{f,i/k}^{est}} \Delta Q_T' \end{aligned} \tag{4.27}$$

where $k = 1, \dots, n_f$.

In this way, power errors on each feeder have been set according to their "capacity", or to be more precise, their sharing in the total amount of real and reactive power.

The strategy was to diminish first the error on the reactive power as much as possible and then to "push" the rest to the real power error estimates. It will be seen later in results provided that greater improvements were obtained in this way.

Procedure is taking into account all the situations regarding the sign of the real and reactive powers of feeders ($P_{f,i/k} \leq 0, P_{f,i/k} \geq 0, Q_{f,i/k} \leq 0, Q_{f,i/k} \geq 0$) and also respective amounts of power propagated from transformer ($\Delta P_{f,i/k} \leq 0, \Delta P_{f,i/k} \geq 0, \Delta Q_{f,i/k} \leq 0, \Delta Q_{f,i/k} \geq 0$).

Thus, depending on the case, the real and reactive power limits are depicted according to Fig. 4.14 (two circles depict lower and upper feeders' apparent power bound, $0.99A_{f,i/k}$ and $1.01A_{f,i/k}$ respectively):

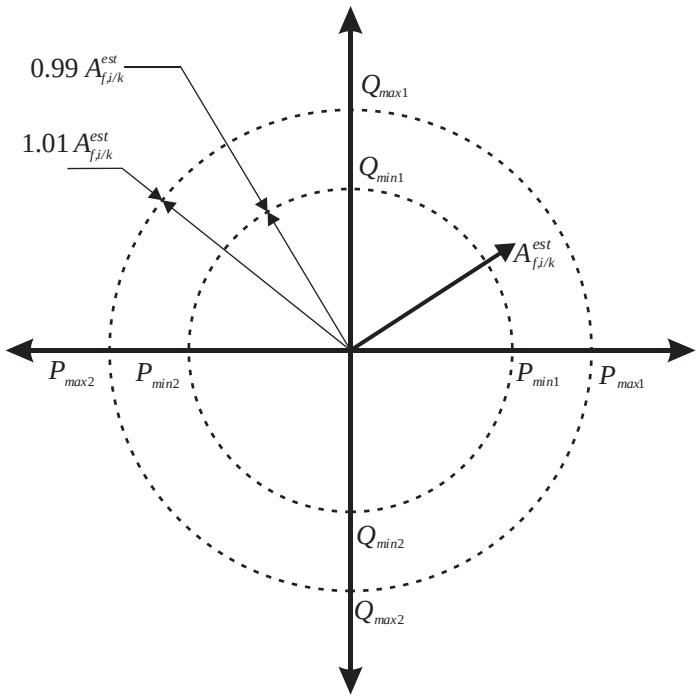

Figure 4.14: *Upper and lower boundaries*

To illustrate the procedure, the example where both $P^{est}_{f,i/k}$ and $Q^{est}_{f,i/k}$ are positive will be considered, with $\Delta Q^{est}_{f,i/k} > 0$ and $\Delta P^{est}_{f,i/k} < 0$. Procedure first tries to set as much as it can of reactive power residual $\Delta Q^{est}_{f,i/k}$ and as $\Delta Q^{est}_{f,i/k} + \Delta Q_{res} < \Delta Q^{max}_{f,i/k}$, it has enough "space" to allocate it. ΔQ_{res} denotes power residual from operations with the previous feeder. Once $\Delta Q^{est}_{f,i/k}$ is allocated, $\Delta P^{est}_{f,i/k}$ can also be allocated, completely or partially. As $\Delta P^{est}_{f,i/k} < 0$, if $\Delta P^{est}_{f,i/k} + \Delta P_{res} < \Delta P^{min}_{f,i/k}$, only part of it can be allocated, the rest is stored in ΔP_{res} and will be transferred to the operations with next feeder. If

$\Delta P_{f,i/k}^{est} + \Delta P_{res} > \Delta P_{f,i/k}^{min}$, the entire $\Delta P_{f,i/k}^{est}$ will be allocated with $\Delta P_{res} = 0$. This is shown in Fig. 4.15.

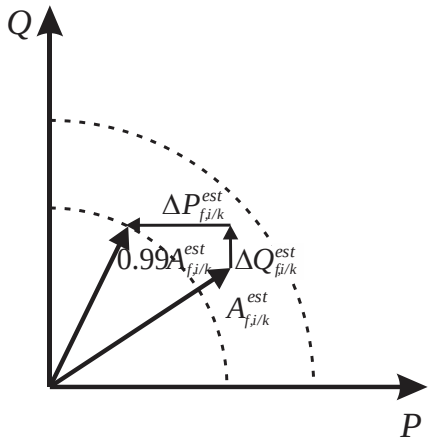

Figure 4.15: *Residual manipulation*

4.3.2.5 The Optimization Approach to Compute $P_{f,i/k}^{est}$ and $Q_{f,i/k}^{est}$

The above method is computationally very fast but its success requires the initial phases of the feeder currents to be in the vicinity of the real values. If they are not, even if the measurements are errorless, the vector sum of the feeder currents estimates will be significantly different from the real one and applying the power residual manipulation step from the previous procedure will not solve the problem. Thus, the final results may contain significant errors.

This problem will appear mainly when DG is installed in the feeders of the DN: while the loads tend to have the same power factor as in the standard profiles, the DG is usually operated at unitary power factor and any error in the estimation of the generated real power can alter significantly the power factor of the feeder. Of course, the errors increase with the penetration level of the DG. This limitation can be substantially improved if the approach is changed to an optimization problem that forces the state variables to match the corresponding measurements. For this, the alignment condition between estimates and measurements are considered:

$$x_k^{est} - x_k^m = 0 \tag{4.28}$$

where k = 1,…, N stands for the index of the N available measurements; x_k^{est} are the estimates of the state variables and x_k^m are the values of the measurements.

Due to the measurement errors, condition given by Eq. (4.28) cannot be realized. Instead, the errors between the estimates and the measurements can be minimized by solving the following quadratic optimization problem:

$$\min \sum_{k=1}^{N} \alpha_k^2 \quad \text{subject to: } x_k - x_k^m + \alpha_k = 0, k = 1, \dots, N \tag{4.29}$$

$$f(\mathbf{x}) = 0$$
$$g(\mathbf{x}) \leq 0$$

where $\mathbf{x} = [x_1 \dots x_k]^T$, α_k are the slack variables standing for the absolute error between the *k*-th state variable, x_k, and the *k*-th measurement.

In the above model, first set of constraints will force the state variables to fit the associated measurements while the following sets of constraint $f(\mathbf{x})$ and $g(\mathbf{x})$ represents various technical constraints in the primary substations of the DS.

When defining the optimization problem according to (4.29), the measured currents through the transformers can be neglected: once the powers and the voltage estimates in the transformers are matched with the measurements, also the corresponding currents will be automatically matched. Moreover, considering the assumption previously made, also the voltage measurements can be neglected and the measured magnitude of the apparent powers absorbed by the feeders, $A_{f,i}$ and $A_{f,k}$, can be derived from the voltage and current measurements. Thus, an optimization problem where only the states associated with the power measurements need to be fit is obtained. The objective function can thus be written as:

$$\min \sum_{r=1}^{N_{T1}} \alpha_{PT,r}^2 + \sum_{r=1}^{N_{T1}} \alpha_{QT,r}^2 + \sum_{k=1}^{N_{f1}} \alpha_{Af,k}^2 + \sum_{q=1}^{N_{T2}} \alpha_{PT,q}^2 + \sum_{q=1}^{N_{T2}} \alpha_{QT,q}^2 + \sum_{i=1}^{N_{f2}} \alpha_{Af,i}^2 \tag{4.30}$$

where:

N_{T1} the number of HV/MV$_1$ transformers;
N_{T2} the number of MV1/MV2 transformers;
N_{f1} the number of feeders connected to the MV1 buses;
N_{f2} the number of feeders connected to the MV2 buses;
$\alpha_{PT,r/q}$ the slack variables associated to $P_{T,r/q}^m$;
$\alpha_{QT,r/q}$ the slack variables associated to $Q_{T,r/q}^m$;
$\alpha_{Af,k,i}$ the slack variable associated to the measured magnitude of the apparent powers absorbed by the feeders connected to the MV1 and MV2 buses, respectively.

The above objective function is subject to various constraints of both types. The following can be written regarding the measurements in the transformers and feeders connected to the MV1 buses:

$$\begin{aligned} P_{T,r} - P_{T,r}^m + \alpha_{PT,r} &= 0 \\ Q_{T,r} - Q_{T,r}^m + \alpha_{QT,r} &= 0 \\ A_{f,k} - A_{f,k}^m + \alpha_{Af,k} &= 0 \end{aligned} \tag{4.31}$$

where $P_{T,r}$, $Q_{T,r}$ and $A_{f,k}$ are the state variables associated with the $P_{T,r}^m$, $Q_{T,r}^m$ and $A_{f,k}^m$ measurements, and $A_{f,k}^m$ is computed as:

$$A_{f,k}^{m} = \sqrt{3} V_{MV1}^{m} \cdot I_{f,k}^{m} \tag{4.32}$$

In addition, the MV1 feeder equivalent loads, $P_{f,k}$ and $Q_{f,k}$, and the real and reactive powers in the primary of the MV1/MV2 transformers need to be aligned with the corresponding apparent powers:

$$\begin{aligned} P_{f,k}^{2} + Q_{f,k}^{2} - A_{f,k}^{2} = 0 \\ P_{T\_P,q}^{2} + Q_{T\_P,q}^{2} - A_{T\_P,q}^{2} = 0 \end{aligned} \tag{4.33}$$

where $P_{T\_P,q}$, $Q_{T\_P,q}$ and $A_{T\_P,q}$ are the real, reactive and apparent powers in the primary of the MV1/MV2 transformers, respectively (see Fig. 4.5).

In order to completely describe the MV1 buses, constraints regarding the real and reactive power balance at these buses are added to the model:

$$\begin{aligned} \sum_{k=1}^{N_{f1}} P_{f,k} + \sum_{q=1}^{N_{T2}} P_{T\_P,q} + \sum_{r=1}^{N_{T1}} P_{T,r} = 0 \\ \sum_{k=1}^{N_{f1}} Q_{f,k} + \sum_{q=1}^{N_{T2}} Q_{T\_P,q} + \sum_{r=1}^{N_{T1}} Q_{T,r} = 0 \end{aligned} \tag{4.34}$$

In analogy with the MV1 buses constraints given by Eqs. (4.31) – (4.34), a set of constraints for the MV2 buses can be defined as:

$$P_{T,q} - P_{T,q}^{m} + \alpha_{PT,q} = 0 \tag{4.35}$$

$$Q_{T,q} - Q_{T,q}^{m} + \alpha_{QT,q} = 0$$

$$A_{f,i} - A_{f,i}^{m} + \alpha_{Af,i} = 0$$

$$P_{f,i}^{2} + Q_{f,i}^{2} - A_{f,i}^{2} = 0 \tag{4.36}$$

$$\begin{aligned} \sum_{i=1}^{N_{f2}} P_{f,i} + \sum_{q=1}^{N_{T2}} P_{T,q} = 0 \\ \sum_{i=1}^{N_{f2}} Q_{f,i} + \sum_{q=1}^{N_{T2}} Q_{T,q} = 0 \end{aligned} \tag{4.37}$$

where $P_{T,q}$, $Q_{T,q}$ and $A_{f,i}$ are the state variables associated with the $P_{T,q}^{m}$, $Q_{T,q}^{m}$ and $A_{f,q}^{m}$ measurements. $A_{f,q}^{m}$ is computed as:

$$A_{f,q}^{m} = \sqrt{3} V_{MV2}^{m} \cdot I_{f,i}^{m} \tag{4.38}$$

Finally, for the model to be consistent, it is necessary to define a set of constraints that link the MV2 buses variables to the MV1 buses variables. These are the power balance equations between the primary and the secondary windings of the MV1/MV2 transformers:

$$\begin{aligned} P_{T\_P,q} - P_{T,q} - P_{loss\_T,q} - P_{sh\_loss\_T,q} = 0 \\ Q_{T\_P,q} - Q_{T,q} - Q_{loss\_T,q} - Q_{sh\_loss\_T,q} = 0 \end{aligned} \tag{4.39}$$

where $P_{loss\_T,q}$ and $Q_{loss\_T,q}$ are the real and reactive power losses along the MV1/MV2 transformers, respectively; while $P_{sh\_loss\_T,q}$ and $Q_{sh\_loss\_T,q}$ are the real and reactive power losses in the shunt elements of the MV1/MV2 transformers, respectively.

To compute $P_{loss\_T,q}$ and $Q_{loss\_T,q}$ a formulation similar to Eq. (4.3) can be used, these time the defined equations are exact as they involve a single network element:

$$\begin{aligned} P_{loss\_T,q} = \left(\frac{A_{T\_p,q}}{A^0_{T\_p,q}}\right)^2 \cdot P^0_{loss\_T,q} \\ P_{loss\_T,q} = \left(\frac{A_{T\_p,q}}{A^0_{T\_p,q}}\right)^2 \cdot P^0_{loss\_T,q} \end{aligned} \tag{4.40}$$

The shunt losses mainly depend on the square of the voltage and, considering the adopted hypothesis regarding the voltages, these losses can be considered constant quantities given by:

$$\begin{aligned} P_{sh\_loss\_T,q} = \left(\frac{V^m_{MV1}}{V^0_{MV1}}\right)^2 \cdot P^0_{sh\_loss\_T,q} \\ Q_{sh\_loss\_T,q} = \left(\frac{V^m_{MV1}}{V^0_{MV1}}\right)^2 \cdot Q^0_{sh\_loss\_T,q} \end{aligned} \tag{4.41}$$

In order to assure that the optimization problem converges to a realistic operating point, the control variables need to be lower and upper bounded. For this optimization problem various limits are defined such to fulfill the technical requirements of the analyzed system. Thus, these limits are defined considering: the capability limits of the installed generators, the capacitive currents of the feeders, the maximum currents of the branches connected to the primary substation and the direction of the power flows as suggested by the corresponding measurements. Feeder power limits, therefore, are:

$$\begin{aligned} -\sum P^{max}_g \le P_f \le 1.5 \cdot \left|A^{max}_f\right| \\ -\sum Q^{max}_g - Q_{cables} \le Q_f \le 1.5 \cdot \left|A^{max}_f\right| \\ 0 \le A_f \le 1.5 \cdot \left|A^{max}_f\right| \end{aligned} \tag{4.42}$$

Generally, upper bound is defined by maximal thermal current ($A^{max}_f = \sqrt{3} V I^{max}_f$) of the feeder. But, in this case, the point is on the SE, so cases with powers exceeding maximal values can occur, this bound has numerical nature (augmentation of 50%).

As P_f is absorbed power, lower bound is given by the maximum generation capability of the feeder with appropriate sign. Lower bound of Q_f

is composed of two terms. The first one corresponds to the maximum generation capability of the feeder with appropriate sign, while the other takes into account estimated reactive power of the network when it is empty. As it is injected power, the sign is negative. Minimal value for A_f is 0.

Real and reactive power flows through transformers are limited as follows:

$$\begin{aligned} 0.5P_T^m \le P_T \le 1.5P_T^m \\ 0.5Q_T^m \le Q_T \le 1.5Q_T^m \end{aligned} \tag{4.43}$$

Upper and lower limits of transformer power flows are given by large bands (±50%) of the measurement errors.

Moreover, large limits are defined for the slack variables as there is no knowledge about the quality of the measurements so they are actually free variables, but they are minimized in objective function. Upper and lower limits for slack variables are in per unit as follows:

$$-10 \le \alpha \le 10 \tag{4.44}$$

4.3.2.6 Load and Generation Profiles Update

After completing the procedures for improving the SE and obtaining the estimates for the feeder equivalent loads, the loads and generation profiles need to be updated such that a new PF will turn the estimated quantities. For this, the total quantity to be split to each feeder's loads and generators is:

$$\begin{aligned} \Delta P_{f,i/k}^{tot} &= P_{f,i/k}^{est} - P_{f,i/k}^0 - (c_{P_f}^2 - 1) \cdot P_{loss\_f,i/k}^0 \\ \Delta Q_{f,i/k}^{tot} &= Q_{f,i/k}^{est} - Q_{f,i/k}^0 - \left(c_{P_f}^2 - 1\right) \cdot Q_{loss\_f,i/k}^0 - \left(\frac{V_{MV}^m}{V_{MV}^0}\right)^2 \cdot Q_{sh\_los\_f,i/k}^0 \end{aligned} \tag{4.45}$$

In this equation $P_{f,i/k}^{est}$ denotes the estimate of feeder's real power obtained using proposed procedures, $P_{f,i/k}^0$ denotes initial power of the feeder, $P_{loss\_f,i/k}^0$ are the initial real power losses in the feeders. The same can be said regarding the reactive powers adding that $Q_{sh\_los\_f,i/k}^0$ is the initial power produced by the shunt capacitance of the feeders.

Now updating the load and generation profiles can start.

First, the total quantity of real power to be assigned to loads and generators will be computed as:

$$\begin{aligned} \Delta P_{L\_tot\_f,i/k} &= \frac{\sum_{l \in load\_f,i/k} P_{L,l}^0}{\sum_{l \in load\_f,i/k} P_{L,l}^0 + \sum_{g \in gen\_f,i/k} P_{G,g}^0} \Delta P_{f,i/k}^{tot} \\ \Delta P_{G\_tot\_f,i/k} &= -\frac{\sum_{g \in gen\_f,i/k} P_{G,g}^0}{\sum_{l \in load\_f,i/k} P_{L,l}^0 + \sum_{g \in gen\_f,i/k} P_{G,g}^0} \Delta P_{f,i/k}^{tot} \end{aligned} \tag{4.46}$$

where $\sum_{l \in load\_f,i/k} P_{L,l}^0$ presents the total initial real power of the loads pertaining to feeder *i* or *k*; and $\sum_{l \in load\_f,i/k} P_{L,l}^0 + \sum_{g \in gen\_f,i/k} P_{G,g}^0$ is the total initial real power. $\sum_{g \in gen\_f,i/k} P_{G,g}^0$ represents the total initial real power of

the generators pertaining to feeder *i* or *k*; The minus sign comes from the premise that $P_{f,i/k} = \sum P_{L,i/k} - \sum P_{G,i/k}$.

Next, $\Delta P_{G\_tot\_f,i/k}$ will be assigned to each generator in the feeder according to the sign of $\Delta P_{G\_tot\_f,i/k}$ and the capability of each generator:

1. $\Delta P_{G\_tot\_f,i/k} > 0$ and $\Delta P_{G\_tot\_f,i/k} > \sum\left(P^{max}_{G\_f,i/k} - P^{0}_{G\_f,i/k}\right)$:

$$\begin{aligned} P^{est}_{G\_f,i/k} &= P^{max}_{G\_f,i/k} \\ \Delta P_{L\_res\_f,i/k} &= -(\Delta P_{G\_tot\_f,i/k} - \sum P^{max}_{G\_f,i/k}) \end{aligned} \tag{4.47}$$

To be noted that we forced $P^{est}_{G\_f,i/k}$ to the maximum value, but as $\Delta P_{G\_tot\_f,i/k}$ is higher, there will be some residual left, $\Delta P_{L\_res\_f,i/k}$ which will be later assigned to the loads. As a result, $\Delta P_{L\_tot\_f,i/k}$ will be updated in following manner: $\Delta P_{L\_tot\_f,i/k} = \Delta P_{L\_tot\_f,i/k} + \Delta P_{L\_res\_f,i/k}$.

2. $\Delta P_{G\_tot\_f,i/k} < 0$ and $\left|\Delta P_{G\_tot\_f,i/k}\right| > \sum\left(P^{0}_{G\_f,i/k} - P^{min}_{G\_f,i/k}\right)$:

$$\begin{aligned} P^{est}_{G\_f,i/k} &= P^{min}_{G\_f,i/k} \\ \Delta P_{L\_res\_f,i/k} &= -(\sum P^{min}_{G\_f,i/k} - \Delta P_{G\_tot\_f,i/k}) \end{aligned} \tag{4.48}$$

3. $\Delta P_{G\_tot\_f,i/k} > 0$ and $\Delta P_{G\_tot\_f,i/k} \leq \sum\left(P^{max}_{G\_f,i/k} - P^{0}_{G\_f,i/k}\right)$:
   In this case $P^{est}_{G\_f,i/k}$ is computed such that ΔP_{G_tot} is distributed according to the capability of each generator with respect to the total available regulation band:

$$P^{est}_{G\_f,i/k} = P^{0}_{G\_f,i/k} + \frac{P^{max}_{G\_f,i/k} - P^{0}_{G\_f,i/k}}{\sum\left(P^{max}_{G\_f,i/k} - P^{0}_{G\_f,i/k}\right)} \Delta P_{G\_tot\_f,i/k} \tag{4.49}$$

Next, $\Delta P_{L\_tot\_f,i/k}$ can be assigned to each individual load according to:

$$P^{est}_{L\_f,i/k} = P^{0}_{L\_f,i/k} + \frac{P^{0}_{L\_f,i/k}}{\sum P^{0}_{L\_f,i/k}} \Delta P_{L\_tot\_f,i/k} \tag{4.50}$$

As for the real powers, the total quantity of real power to be assigned to loads and generators will be computed as:

$$\begin{aligned} \Delta Q_{L\_tot\_f,i/k} &= \frac{\sum_{l \in load\_f,i/k} Q^{0}_{L,l}}{\sum_{l \in load\_f,i/k} Q^{0}_{L,l} + \sum_{g \in gen\_f,i/k} Q^{0}_{G,g}} \Delta Q^{tot}_{f,i/k} \\ \Delta Q_{G\_tot\_f,i/k} &= -\frac{\sum_{g \in gen\_f,i/k} Q^{0}_{G,g}}{\sum_{l \in load\_f,i/k} Q^{0}_{L,l} + \sum_{g \in gen\_f,i/k} Q^{0}_{G,g}} \Delta Q^{tot}_{f,i/k} \end{aligned} \tag{4.51}$$

where $\sum_{l \in load\_f,i/k} Q^{0}_{L,l}$ presents the total initial reactive power of the loads pertaining to feeder *i* or *k*; and $\sum_{l \in load\_f,i/k} Q^{0}_{L,l} + \sum_{g \in gen\_f,i/k} Q^{0}_{G,g}$ is the total initial reactive power. $\sum_{g \in gen\_f,i/k} Q^{0}_{G,g}$ represents the total initial reactive

power of the generators pertaining to feeder *i* or *k*; The minus sign comes from the premise that $Q_{f,i/k} = \sum Q_{L,i/k} - \sum Q_{G,i/k}$.

Next, $\Delta Q_{G\_tot\_f,i/k}$ will be assigned to each generator in the feeder according to the sign of $\Delta Q_{G\_tot\_f,i/k}$ and the capability of each generator:

4. $\Delta Q_{G\_tot\_f,i/k} > 0$ and $\Delta Q_{G\_tot\_f,i/k} > \sum\left(Q^{max}_{G\_f,i/k} - Q^{0}_{G\_f,i/k}\right)$:

$$\begin{aligned} Q^{est}_{G\_f,i/k} &= Q^{max}_{G\_f,i/k} \\ \Delta Q_{L\_res\_f,i/k} &= -(\Delta Q_{G\_tot\_f,i/k} - \sum Q^{max}_{G\_f,i/k}) \end{aligned} \tag{4.52}$$

To be noted that we forced $Q^{est}_{G\_f,i/k}$ to the maximum value, but as $\Delta Q_{G\_tot\_f,i/k}$ is higher, there will be some residual left, $\Delta Q_{L\_res\_f,i/k}$ which will be later assigned to the loads. As a result, $\Delta Q_{L\_tot\_f,i/k}$ will be updated in following manner: $\Delta Q_{L\_tot\_f,i/k} = \Delta Q_{L\_tot\_f,i/k} + \Delta Q_{L\_res\_f,i/k}$.

5. $\Delta Q_{G\_tot\_f,i/k} < 0$ and $\left|\Delta Q_{G\_tot\_f,i/k}\right| > \sum\left(Q^{0}_{G\_f,i/k} - Q^{min}_{G\_f,i/k}\right)$:

$$\begin{aligned} Q^{est}_{G\_f,i/k} &= Q^{min}_{G\_f,i/k} \\ \Delta Q_{L\_res\_f,i/k} &= -(\sum Q^{min}_{G\_f,i/k} - \Delta Q_{G\_tot\_f,i/k}) \end{aligned} \tag{4.53}$$

6. $\Delta Q_{G\_tot\_f,i/k} > 0$ and $\Delta Q_{G\_tot\_f,i/k} \leq \sum\left(Q^{max}_{G\_f,i/k} - Q^{0}_{G\_f,i/k}\right)$:
   In this case $Q^{est}_{G\_f,i/k}$ is computed such that ΔQ_{G_tot} is distributed according to the capability of each generator with respect to the total available regulation band:

$$Q^{est}_{G\_f,i/k} = Q^{0}_{G\_f,i/k} + \frac{Q^{max}_{G\_f,i/k} - Q^{0}_{G\_f,i/k}}{\sum\left(Q^{max}_{G\_f,i/k} - Q^{0}_{G\_f,i/k}\right)} \Delta Q_{G\_tot\_f,i/k} \tag{4.54}$$

Next, $\Delta Q_{L\_tot\_f,i/k}$ can be assigned to each individual load according to:

$$Q^{est}_{L\_f,i/k} = Q^{0}_{L\_f,i/k} + \frac{Q^{0}_{L\_f,i/k}}{\sum Q^{0}_{L\_f,i/k}} \Delta Q_{L\_tot\_f,i/k} \tag{4.55}$$

4.3.3 Simplified State Estimation Simulation Results

4.3.3.1 The non-optimized approach to compute $P^{est}_{f,i/k}$ and $Q^{est}_{f,i/k}$

4.3.3.1.1 Performance analysis of each step of the non-optimized approach

Some results of the non-optimized SSE will be presented here to clarify the advantages it offers and how much of the improvement is achieved step by step.

The performance of the SSE algorithm is analyzed by applying each step of the defined procedure. The test network contains 154 buses and 155

branches and the primary substation consists of two parallel HV/MV transformers feeding 4 distribution feeders, among which the third has installed generators. In order to test the procedure, 1000 sets of measurements were created starting from standard profiles as follows: (*i*) the load/generation profiles were randomly varied according to a specified uncertainty, then (*ii*) the PF was performed and the set of measures extracted. Then, the SSE was run starting from the standard data and the set of measures. The tests are carried out assuming a load and generation profiles uncertainty of 40% and an uncertainty of the power factor of each component of 5%. Test DN is shown in Fig (4.16):

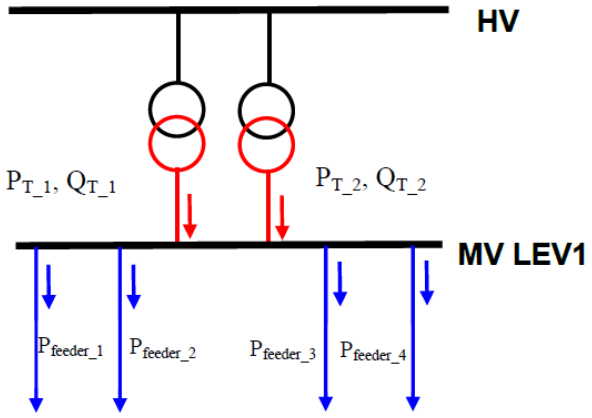

Figure 4.16: *Test DN*

First set of tables (Table 4.3) presents the results of estimator just with using the c_p factor, without phase correction nor residual manipulation.

Table 4.3: Estimation results after using c_p factor

Error [%]	P_{T1}	P_{T2}
AVERAGE	1.72E+00	1.72E+00
MIN	5.42E-03	5.42E-03
MAX	4.51E+00	4.51E+00
STD DEVIATION	1.08E+00	1.08E+00

Error [%]	Q_{T1}	Q_{T2}
AVERAGE	2.26E+00	2.26E+00
MIN	1.26E-03	1.26E-03
MAX	6.99E+00	6.99E+00
STD DEVIATION	1.47E+00	1.47E+00

Error [%]	$I_{feederMT1}$	$I_{feederMT2}$	$I_{feederMT3}$	$I_{feederMT4}$
AVERAGE	5.80E-04	5.77E-03	5.79E-03	5.64E-03
MIN	6.05E-06	1.69E-05	5.63E-06	4.45E-06
MAX	1.81E-02	1.82E-02	1.78E-02	1.97E-02
STD DEVIATION	3.94E-03	3.92E-03	3.93E-03	3.98E-03

The following set of tables (Table 4.4) refers to results obtained by using c_p factor and phase correction procedure.

Table 4.4: Estimation results after using c_p factor and phase correction

Error [%]	P_{T1}	P_{T2}
AVERAGE	2.41E-01	2.41E-01
MIN	3.64E-04	3.64E-04
MAX	6.58E-01	6.58E-01
STD DEVIATION	1.49E-01	1.49E-01

Error [%]	Q_{T1}	Q_{T2}
AVERAGE	2.41E-01	2.41E-01
MIN	9.64E-04	9.64E-04
MAX	6.59E-01	6.59E-01
STD DEVIATION	1.49E-01	1.49E-01

Error [%]	$I_{feederMT1}$	$I_{feederMT2}$	$I_{feederMT3}$	$I_{feederMT4}$
AVERAGE	6.91E-04	7.33E-04	1.08E-03	2.62E-03
MIN	3.00E-06	7.36E-07	1.04E-06	1.98E-06
MAX	2.33E-03	2.67E-03	3.86E-03	1.05E-02
STD DEVIATION	4.52E-04	5.00E-04	7.79E-04	1.92E-03

The last set of tables (Table 4.5) refers to results obtained using complete solution offered by the SSE.

Table 4.5: Estimation results after completion of SSE

Error [%]	P_{T1}	P_{T2}
AVERAGE	4.08E-02	4.08E-02
MIN	1.61E-05	1.61E-05
MAX	1.25E-01	1.25E-01
STD DEVIATION	2.75E-03	2.75E-03

Error [%]	Q_{T1}	Q_{T2}
AVERAGE	9.03E-03	9.03E-03
MIN	2.21E-05	2.21E-05
MAX	2.87E-02	2.87E-02
STD DEVIATION	6.09E-03	6.09E-03

Error [%]	$I_{feederMT1}$	$I_{feederMT2}$	$I_{feederMT3}$	$I_{feederMT4}$
AVERAGE	2.40E-01	2.41E-01	2.40E-02	2.53E-01
MIN	2.04E-04	7.97E-05	2.34E-04	5.98E-04
MAX	6.53E-01	6.55E-01	6.54E-01	6.91E-01
STD DEVIATION	1.49E-01	1.49E-01	1.49E-01	1.57E-01

As seen in first set of tables, both average and maximal errors of feeders' current estimates are very small and this is due to the fact that $I^{est}_{feeder,k} \simeq I^{m}_{feeder,k}$. The error, however, is not null because losses of feeders are estimated, not known values, as stated before. The errors of the transformers' estimates present the main problem. By aligning the current magnitudes, the estimation was not very successful. That's why phase correction procedure with power flow inversion detection was introduced. It is obvious from the second set of tables that improvement gained this way is considerable. For example, in the first set of tables, maximal errors on real and reactive power estimates of the transformers are 4.51% and 6.99% respectively. After phase correction procedure with power flow inversion detection, these have been reduced to 0.658% and 0.659% respectively. Also, reader can see that outstanding improvement has been achieved regarding average errors on the transformers in this step, decrease from 1.72% to 0.241% regarding real power, and from 2.26% to 0.241% regarding reactive power.

To further improve the estimation and reduce errors even more, we have introduced power residual manipulation. After this, maximal errors on real and reactive power estimates of the transformers were 0.125% and 0.029% respectively. Taking into account that after aligning the current magnitudes procedure they were 4.51% and 6.99% respectively, this presents remarkable result. Regarding average errors, improvements have also been gained, from 0.241% to 0.041% for real power and from 0.241% to 0.009% for reactive power. But, as a result of using power residual manipulation procedure, feeders' current errors have been increased to maximal of 0.691%, but in any case it remains small.

4.3.3.1.2 Performance and limitations of the non-optimized approach

Following results refer to performance of proposed DSSE in different network scenarios.

First set of data refers to load power uncertainty of 40% for each load randomly, and also power factor uncertainty of 5% for each load randomly which can be observed as "normal" state of the network operation, at its normal operation boundary. Thousand simulations have been run.

Results will be given for two types of generation in the third feeder – generation of 50 kW in comparison with 225 kW of consumption and 550 kW of generation with 225 kW of consumption. This is done to show how generation in DN induces larger errors in estimation. For each set of data, the results will be presented without and with procedure of residuals manipulation.

- Case 1: feeder 3 – load 225 kW, generation 50 kW - normal operation (Table 4.6 and Table 4.7)

Table 4.6: Case 1: without residual manipulation – normal operation

Error [%]	P_{T1}	P_{T2}
AVERAGE	2.44E-01	2.44E-01
MIN	1.16E-03	1.16E-03
MAX	7.28E-01	7.28E-01
STD DEVIATION	1.51E-01	1.51E-01

Error [%]	Q_{T1}	Q_{T2}
AVERAGE	2.45E-01	2.45E-01
MIN	5.18E-04	5.18E-04
MAX	7.26E-01	7.26E-01
STD DEVIATION	1.51E-01	1.51E-01

Error [%]	V_{MV}
AVERAGE	7.03E-04
MIN	1.83E-06
MAX	2.28E-03
STD DEVIATION	4.62E-04

Error [%]	I_{T1}	I_{T2}
AVERAGE	2.46E-01	2.46E-01
MIN	9.53E-04	9.53E-04
MAX	7.28E-01	7.28E-01
STD DEVIATION	1.51E-01	1.51E-01

Error [%]	$I_{feederMT1}$	$I_{feederMT2}$	$I_{feederMT3}$	$I_{feederMT4}$
AVERAGE	7.03E-04	7.49E-04	9.13E-04	2.74E-03
MIN	1.82E-06	2.33E-06	5.30E-06	6.09E-06
MAX	2.30E-03	2.73E-03	3.86E-03	1.17E-02
STD DEVIATION	4.62E-04	5.11E-04	6.72E-04	1.93E-03

Table 4.7: Case 1: with residual manipulation – normal operation

Error [%]	P_{T1}	P_{T2}
AVERAGE	6.02E-03	6.02E-03
MIN	1.61E-06	1.61E-06
MAX	2.23E-02	2.23E-02
STD DEVIATION	3.94E-03	3.94E-03

Error [%]	Q_{T1}	Q_{T2}
AVERAGE	6.02E-03	6.02E-03
MIN	1.61E-06	1.61E-06
MAX	2.23E-02	2.23E-02
STD DEVIATION	3.94E-03	3.94E-03

Error [%]	V_{MV}
AVERAGE	2.48E-05
MIN	4.54E-08
MAX	7.69E-05
STD DEVIATION	1.56E-05

Error [%]	I_{T1}	I_{T2}
AVERAGE	6.02E-03	6.02E-03
MIN	1.61E-06	1.61E-06
MAX	2.23E-02	2.23E-02
STD DEVIATION	3.94E-03	3.94E-03

Error [%]	$I_{feederMT1}$	$I_{feederMT2}$	$I_{feederMT3}$	$I_{feederMT4}$
AVERAGE	2.45E-01	2.45E-01	2.44E-02	2.58E-01
MIN	8.66E-04	7.90E-04	6.43E-05	1.37E-03
MAX	7.24E-01	7.26E-01	7.23E-01	7.70E-01
STD DEVIATION	1.50E-01	1.50E-01	1.50E-01	1.59E-01

It can be easily seen that even without using residual manipulation procedure, results obtained are below 1% for average but also maximal error on transformer and feeder estimates. Of courses, results obtained by using this procedure are of better quality but it's practical use will be more pronounced with larger amount of generation. Also, it can be observed that feeders' current estimates are worse in later table, as already explained.

- Case 2: feeder 3 – load 225 kW, generation 550 kW - normal operation (Table 4.8 and Table 4.9)

Table 4.8: Case 2: without residual manipulation – normal operation

Error [%]	P_{T1}	P_{T2}
AVERAGE	1.44E+00	1.44E+00
MIN	8.06E-04	8.06E-04
MAX	6.93E+00	6.93E+00
STD DEVIATION	1.15E+00	1.15E+00

Error [%]	Q_{T1}	Q_{T2}
AVERAGE	1.44E+00	1.44E+00
MIN	1.72E-04	1.72E-04
MAX	6.93E+00	6.93E+00
STD DEVIATION	1.55E+00	1.55E+00

Error [%]	V_{MV}
AVERAGE	3.93E-04
MIN	2.85E-07
MAX	1.69E-02
STD DEVIATION	2.96E-03

Error [%]	I_{T1}	I_{T2}
AVERAGE	1.45E+00	1.45E+00
MIN	4.46E-04	4.46E-04
MAX	6.95E+00	6.95E+00
STD DEVIATION	1.16E+00	1.16E+00

Error [%]	$I_{feederMT1}$	$I_{feederMT2}$	$I_{feederMT3}$	$I_{feederMT4}$
AVERAGE	3.93E-03	3.93E-03	6.17E-03	4.47E-03
MIN	3.56E-07	3.07E-06	4.51E-06	3.38E-06
MAX	1.69E-02	1.70E-02	2.51E-02	1.83E-02
STD DEVIATION	2.96E-03	2.96E-03	4.69E-03	3.46E-03

Table 4.9: Case 2: with residual manipulation – normal operation

Error [%]	P_{T1}	P_{T2}
AVERAGE	6.94E-01	6.94E-01
MIN	7.52E-06	7.52E-06
MAX	6.89E+00	6.89E+00
STD DEVIATION	1.07E+00	1.07E+00

Error [%]	Q_{T1}	Q_{T2}
AVERAGE	1.57E-01	1.57E-01
MIN	6.22E-05	6.22E-05
MAX	3.49E+00	3.49E+00
STD DEVIATION	3.72E-01	3.72E-01

Error [%]	V_{MV}
AVERAGE	4.41E-04
MIN	8.11E-08
MAX	9.84E-03
STD DEVIATION	1.03E-03

Error [%]	I_{T1}	I_{T2}
AVERAGE	3.93E-01	3.93E-01
MIN	3.72E-05	3.72E-05
MAX	4.64E+00	4.64E+00
STD DEVIATION	6.79E-01	6.79E-01

Error [%]	$I_{feederMT1}$	$I_{feederMT2}$	$I_{feederMT3}$	$I_{feederMT4}$
AVERAGE	7.44E-01	7.46E-01	2.40E-02	2.53E-01
MIN	1.69E-03	1.79E-03	2.34E-04	5.98E-04
MAX	1.00E+00	1.00E+00	1.01E+00	1.07E+00
STD DEVIATION	3.27E-01	3.27E-01	3.32E-01	3.52E-01

Case 2 introduces significant amount of generation in the third feeder and, as the effect of that, one can see that errors on all the estimates have grown significantly. As an effect of using proposed procedure of residual manipulation, errors on reactive power of the transformers have been decreased for roughly 3.5% which is an considerable amount (maximal value), but as a result of that not much could be done regarding real power. It can be also observed that average values, however, are good because they decreased from 1.44% to 0.694% for real and 0.157% for reactive power.

Second set of data refer to load power uncertainty of 80% for each load randomly, and also power factor uncertainty of 10% for each load randomly which can be observed as very bad initial data. Thousand simulations have been run.

Results will be given for two types of generation in the third feeder – generation of 50 kW in comparison with 225 kW of consumption and 550 kW of generation with 225 kW of consumption. This is done to show how generation in distribution network induces larger errors in estimation. For each set of data, presented will be the results without and with procedure of residuals manipulation.

- Case 3: feeder 3 – load 225 kW, generation 50 kW - disturbed operation (Table 4.10 and Table 4.11)

Table 4.10: Case 3: without residual manipulation – disturbed operation

Error [%]	P_{T1}	P_{T2}
AVERAGE	5.00E-01	5.00E-01
MIN	1.18E-03	1.18E-03
MAX	1.74E+00	1.74E+00
STD DEVIATION	3.48E-01	3.48E-01

Error [%]	Q_{T1}	Q_{T2}
AVERAGE	5.00E-01	5.00E-01
MIN	1.33E-03	1.33E-03
MAX	1.74E+00	1.74E+00
STD DEVIATION	3.48E-01	3.48E-01

Error [%]	V_{MV}
AVERAGE	1.48E-03
MIN	1.33E-06
MAX	7.38E-03
STD DEVIATION	1.22E-03

Error [%]	I_{T1}	I_{T2}
AVERAGE	5.02E-01	5.02E-01
MIN	1.08E-03	1.08E-03
MAX	1.75E+00	1.75E+00
STD DEVIATION	3.49E-01	3.49E-01

Error [%]	$I_{feederMT1}$	$I_{feederMT2}$	$I_{feederMT3}$	$I_{feederMT4}$
AVERAGE	1.48E-03	1.62E-03	2.00E-03	5.56E-03
MIN	2.14E-06	5.81E-06	7.66E-06	1.26E-06
MAX	7.39E-03	8.36E-03	7.96E-03	2.55E-02
STD DEVIATION	1.22E-03	1.40E-03	1.49E-03	4.28E-03

Table 4.11: Case 3: with residual manipulation – disturbed operation

Error [%]	P_{T1}	P_{T2}
AVERAGE	4.05E-02	4.05E-02
MIN	9.79E-06	9.79E-06
MAX	1.26E+00	1.26E+00
STD DEVIATION	1.33E-03	1.33E-03

Error [%]	Q_{T1}	Q_{T2}
AVERAGE	1.90E-02	1.90E-02
MIN	2.03E-05	2.03E-05
MAX	8.37E-02	8.37E-02
STD DEVIATION	1.49E-02	1.49E-02

Error [%]	V_{MV}
AVERAGE	4.42E-05
MIN	7.24E-08
MAX	1.76E-04
STD DEVIATION	2.92E-05

Error [%]	I_{T1}	I_{T2}
AVERAGE	2.78E-03	2.78E-03
MIN	6.71E-06	6.71E-06
MAX	7.29E-01	7.29E-01
STD DEVIATION	7.17E-02	7.17E-02

Error [%]	$I_{feederMT1}$	$I_{feederMT2}$	$I_{feederMT3}$	$I_{feederMT4}$
AVERAGE	4.78E-01	4.79E-01	4.78E-01	5.00E-01
MIN	1.07E-04	2.12E-04	4.57E-04	5.23E-04
MAX	1.00E+00	1.00E+00	1.00E+00	1.07E+00
STD DEVIATION	3.02E-01	3.03E-01	3.02E-01	3.19E-01

It can be seen that in this case as a result of increased uncertainty in both power of the load and power factor, results are much worse than in Case 1. Although average errors of transformers' estimates stay below 1%, maximal error on transformers' real power is little above this border. Other results are good.

This set of results present the actual limitation of proposed method which will be even more enhanced in last Case 4 with significant amount of generation.

- Case 4: feeder 3 – load 225 kW, generation 550 kW - disturbed operation (Table 4.12 and Table 4.13)

Table 4.12: Case 4: without residual manipulation – disturbed operation

Error [%]	P_{T1}	P_{T2}
AVERAGE	3.36E+00	3.36E+00
MIN	1.76E-02	1.76E-02
MAX	2.27E+01	2.27E+01
STD DEVIATION	3.17E+00	3.17E+00

Error [%]	Q_{T1}	Q_{T2}
AVERAGE	3.40E+00	3.40E+00
MIN	1.79E-02	1.79E-02
MAX	2.27E+01	2.27E+01
STD DEVIATION	3.24E+00	3.24E+00

Error [%]	V_{MV}
AVERAGE	8.28E-03
MIN	5.88E-05
MAX	3.67E-02
STD DEVIATION	6.52E-03

Error [%]	I_{T1}	I_{T2}
AVERAGE	3.33E+00	3.33E+00
MIN	1.78E-02	1.78E-02
MAX	2.28E+01	2.28E+01
STD DEVIATION	3.15E+00	3.15E+00

Error [%]	$I_{feederMT1}$	$I_{feederMT2}$	$I_{feederMT3}$	$I_{feederMT4}$
AVERAGE	8.28E-03	8.27E-03	1.17E-02	9.38E-03
MIN	5.89E-05	8.08E-07	8.84E-05	4.75E-06
MAX	3.67E-02	3.68E-02	4.45E-02	4.09E-02
STD DEVIATION	6.52E-03	6.53E-03	8.89E-03	7.29E-03

Table 4.13: Case 4: with residual manipulation – disturbed operation

Error [%]	P_{T1}	P_{T2}
AVERAGE	2.73E+00	2.73E+00
MIN	3.44E-05	3.44E-05
MAX	2.27E+01	2.27E+01
STD DEVIATION	3.37E+00	3.37E+00

Error [%]	Q_{T1}	Q_{T2}
AVERAGE	1.17E+00	1.17E+00
MIN	1.16E-04	1.16E-04
MAX	1.68E+01	1.68E+01
STD DEVIATION	2.18E+00	2.18E+00

Error [%]	V_{MV}
AVERAGE	2.78E-03
MIN	3.32E-07
MAX	2.97E-02
STD DEVIATION	4.47E-03

Error [%]	I_{T1}	I_{T2}
AVERAGE	1.82E+00	1.82E+00
MIN	7.72E-05	7.72E-05
MAX	1.84E+01	1.84E+01
STD DEVIATION	2.55E+00	2.55E+00

Error [%]	$I_{feederMT1}$	$I_{feederMT2}$	$I_{feederMT3}$	$I_{feederMT4}$
AVERAGE	8.75E-01	8.77E-01	7.59E-01	9.09E-01
MIN	1.39E-02	1.35E-02	2.01E-03	9.73E-03
MAX	1.00E+00	1.00E+00	1.02E+00	1.09E+00
STD DEVIATION	2.52E-01	2.53E-01	3.18E-01	2.79E-01

Case 4 introduces significant amount of generation in the third feeder and as the effect of that reader can see that errors on all the estimates have grown

significantly. As a result of larger uncertainty of load, errors are much higher than in Case 2. As an effect of using proposed procedure of residual manipulation, errors on reactive power of the transformers have been decreased for roughly 2.2% which is an considerable amount (average value), but as a result of that not much could be done regarding real power, from 3.36% to 2.73%. But, maximal errors of power estimates on transformers are much higher than 1%, even with using proposed procedure of residual manipulation.

This leads to acknowledging the limitation of the SSE. It can be used well in normal conditions with very high performances regarding results and time consumption but in case of very bad initial data, optimization procedure must be used. It should be also pointed that the computational time needed for this procedure is insignificant with respect to a PF computation. Therefore, from computation point of view, two PF computations are dominant (the average time is less than 0.005 seconds).

4.3.3.2 The Optimization Approach

In this subchapter, the results of the optimization procedure for some cases in which the simple, non-optimization, approach gives bad results in terms of errors between the estimated and the measured values will be provided. These tests were made using the same network and assumptions as previously (Fig. 4.16). The computational time depends on the number of variables and constraints of the problem. In the following tests the optimization model consists of 28 variables and 14 constraints.

In the first case, we considered the network containing no generation and an uncertainty of the load profiles of 80% and of the power factor of each load of 10%. The results of the 1000 simulations are reported in Table 4.14. As it can be seen, the errors are very small and due only to the approximation of the final power losses in the feeders and transformers. The average simulation time for the optimization procedure is 0.054 s, much longer than the simple method, but still contained.

Table 4.14: Case 1. only load - optimization method

Error [%]	I_{T1}	I_{T2}	I_{T3}	I_{T4}
AVERAGE	2.25E-03	2.25E-03	5.09E-03	5.09E-03
MIN	5.39E-06	5.39E-06	8.32E-06	8.34E-06
MAX	9.41E-03	9.41E-03	2.10E-02	2.10E-02
STD DEVIATION	1.80E-03	1.80E-03	3.84E-03	3.84E-03

Error [%]	P_{T1}	P_{T2}	P_{T3}	P_{T4}
AVERAGE	2.25E-03	2.25E-03	5.09E-03	5.09E-03
MIN	5.39E-06	5.39E-06	8.32E-06	8.34E-06
MAX	9.41E-03	9.41E-03	2.10E-02	2.10E-02
STD DEVIATION	1.80E-03	1.80E-03	3.84E-03	3.84E-03

Error [%]	Q_{T1}	Q_{T2}	Q_{T3}	Q_{T4}
AVERAGE	3.80E-03	3.80E-03	6.94E-03	6.95E-03
MIN	9.09E-06	9.09E-06	5.41E-06	5.47E-06
MAX	1.80E-02	1.80E-02	2.79E-02	2.79E-02
STD DEVIATION	3.21E-03	3.21E-03	5.27E-03	5.27E-03

Error [%]	I_{f1}	I_{f2}	I_{f3}	I_{f4}
AVERAGE	5.30E-04	3.50E-03	2.38E-04	5.49E-03
MIN	1.18E-06	1.70E-08	2.05E-07	5.55E-06
MAX	1.54E-03	9.62E-02	1.40E-03	2.24E-02
STD DEVIATION	3.50E-04	6.88E-03	2.52E-04	4.14E-03

Next, generators were introduced in one of the feeders and many cases where simulated. Further, the most severe case is going to be reported. In this case the uncertainty of the load and generation profiles is 80% and of the power factor of each load and generator is 10%. Table 4.15 depicts the results of the 1000 simulations. Also this time the errors are very small. However,

one can notice a slightly high error in the maximum value of P_{T1} and P_{T2}. This is because in this situation the real generated power almost balances the real load, so the real power flows in the AT/MT transformers are almost null. In the same time, the feeders are highly loaded and therefore the error introduced by the approximation of the losses in the feeders has a high impact on the very small real power flow in the transformers. However, the difference in kW between the measured and the computed P_{T1} and P_{T2} is very small, i.e. 0.2 kW of difference with respect to $P_{T1\_m} = P_{T2\_m} \approx 40$ kW.

Table 4.15: Case 2. generation and load - optimization method

Error [%]	I_{T1}	I_{T2}	I_{T3}	I_{T4}
AVERAGE	3.47E-02	3.47E-02	5.04E-03	5.04E-03
MIN	6.93E-03	6.93E-03	2.76E-06	2.76E-06
MAX	7.28E-02	7.28E-02	2.25E-02	2.25E-02
STD DEVIATION	1.16E-02	1.16E-02	3.86E-03	3.86E-03

Error [%]	P_{T1}	P_{T2}	P_{T3}	P_{T4}
AVERAGE	1.07E-01	1.07E-01	4.66E-03	4.66E-03
MIN	1.88E-02	1.88E-02	2.15E-05	2.15E-05
MAX	4.25E-01	4.25E-01	2.13E-02	2.13E-02
STD DEVIATION	6.73E-02	6.73E-02	3.59E-03	3.59E-03

Error [%]	Q_{T1}	Q_{T2}	Q_{T3}	Q_{T4}
AVERAGE	2.34E-02	2.34E-02	6.39E-03	6.39E-03
MIN	2.35E-03	2.35E-03	1.83E-06	1.81E-06
MAX	5.53E-02	5.53E-02	2.67E-02	2.67E-02
STD DEVIATION	9.04E-03	9.04E-03	4.84E-03	4.85E-03

Error [%]	I_{f1}	I_{f2}	I_{f3}	I_{f4}
AVERAGE	5.46E-02	3.51E-03	2.41E-04	5.04E-03
MIN	3.30E-02	7.05E-05	1.99E-07	2.76E-06
MAX	7.51E-02	1.02E-01	1.27E-03	2.25E-02
STD DEVIATION	7.20E-03	6.67E-03	2.28E-04	3.86E-03

This time, the average simulation time of the optimization procedure was 0.059 s, a value similar to the previous one. Generally, the average simulation time for all the tests made with this network was ≈ 0.06 s, so well contained.

These tests, allow us to conclude that the optimization can provide very good results in all the situations. However, since the simulation time of the optimization procedure is much higher than the simple method (≈ 0.06 s over ≈ 0.005 s) and since the simple method gives good results in many situations, it was chosen as a general strategy to perform the optimization only when the simple approach gives unacceptable results. With the tests done here, the maximum admissible error between computed values by the simple method and the measurements was set to 1%.

4.3.4 Implementation Aspects Regarding the SSE

The previously presented function was implemented in the MATLAB environment. The SSE cannot be run if one or more of previously stated measurements is/are missing:

- If V_{HV}^{m} is missing, both PF and SE functions cannot be run correctly because they would lack the real setting of slack bus voltage;
- If one of the following quantities is missing: V_{HV}^{m} or $V_{MV1/2}^{m}$ it is impossible to estimate the position of HV/MV transformer's tap changer which is crucial for obtaining good PF and as a consequence SE solution;
- If $V_{MV1/2}^{m}$ is missing it is impossible to obtain high quality SE solution since it becomes impossible to compute the actual apparent power absorbed by the feeder ($A_{f,p/q}^{m} = \sqrt{3} V_{MV1/2}^{m} \cdot I_{f,p/q}^{m}$) and, hence, it is impossible to adjust $P_{f,p/q}$ and $Q_{f,p/q}$ such to obtain $A_{f,p/q}^{m}$ and P_{T}^{m} and Q_{T}^{m}, respectively;

- If P_T^m or Q_T^m is missing, SE cannot give the solution of the problem because powers obtained as a solution in feeder level cannot be compared to a measured value on transformer level and changed accordingly;
- If some of the values from $I_{f,p/q}^m$ are missing, solutions obtained by SE function on feeder level can turn the solution with a very large error as it will not match the values of powers on MV level of transformer.

4.3.5 Advanced State Estimation (ASE) function

The presence of measurements at the secondary substations of the DS forces the change of the approach as now it is required to constraint the state estimation procedure with the PF equations, making the procedure more computationally burdened. In these regards, an optimization based procedure is proposed to improve the observability of the DS in the presence of measurements in the secondary substations. In brief, the optimization problem is defined as the minimization of the sum of the squares of the differences between measured and estimated values – the slack variables α_i – so as to satisfy the PF equations. The mathematical model of the optimization problem can be generally written as follows [68]:

$$\begin{aligned} &\min \sum_{i=1}^{N_m} \left(\frac{\alpha_i}{x_i^m}\right)^2 \\ &\text{Subject to:} \\ &f_P(V_M, V_A, \mathbf{x^{est}}) = 0 \\ &f_Q(V_M, V_A, \mathbf{x^{est}}) = 0 \\ &\mathbf{x^m} - \mathbf{x^{est}} + \boldsymbol{\alpha} = 0 \end{aligned} \tag{4.56}$$

where:

α_i	contained in the vector $\boldsymbol{\alpha}$, are the slack variables;
N_m	is the number of available measurements;
f_P and f_Q	are the PF equations;
x_i^m	contained in the vector $\mathbf{x^m}$, are the available measurements in the considered DN;
$\mathbf{x^{est}}$	is the vector of the state variables;
V_M and V_A	are the vectors of the bus voltage magnitudes and phases, excluding the slack bus.

In the objective function (OF) of Eq. (4.56), the slack variables, α_i, are scaled with respect to the measured quantities: in the absence of any statistical information regarding the quality of the measurements, in particular the type of distribution and the standard deviation of the measurements with respect to the exact value, it is very difficult to properly weight the slack variables in the OF. Introducing typical values for the standard deviations may force the optimization solver to give unrealistic results in many cases. If particular network measurement $x_i^m \to 0$, α_i cannot be scaled according to the value of the measurement (as it would have potentially infinite value), so in this case measurement value is replaced with properly chosen small reference value which depends on which particular quantity it is.

Moreover, defining an OF as the sum of the squares of α_i may give many bad results since the absolute errors would be minimized without taking into account that various measurements in the DN can be very different in terms of numerical values, i.e. 10 to 1000 times different. This could give very high relative errors between the estimates and corresponding measurements. Thus, minimizing the OF in Eq. (4.), which ideally is zero, will minimize the relative error between the measured and the estimated values in a balance manner.

4.3.5.1 Vector of State Variables and Objective Function Definition

In defining the particular shape of model given by Eq. (4.56) one can observe from Figs. (4.) and (4.) that the types of measurements that are available in the secondary substations coincide with the ones available in the primary substation. Thus, a unified set of measurements can be considered and the vector of variables associated with this set can be defined as:

$$\mathbf{x^{est}} = \begin{bmatrix} V_M & V_A & I_{ft\_re} & I_{ft\_im} & I_{tf\_re} & I_{tf\_im} & P_{ft} & Q_{ft} & P_{tf} & Q_{tf} \end{bmatrix} \quad (4.57)$$

where:

V_M the vector of bus voltage magnitudes in p.u. excluding the slack bus;

V_A the vector of bus voltage phase angles in p.u. excluding the slack bus;

I_{ft_re} the vector of real parts of branch currents with existing current measurements in p.u. in from – to direction;

I_{ft_im} the vector of imaginary parts of branch currents with existing current measurements in p.u. in from – to direction;

I_{tf_re} the vector of real parts of branch currents with existing current measurements in p.u. in to – from direction;

I_{tf_im} the vector of imaginary parts of branch currents with existing current measurements in p.u. in to – from direction;

P_{ft} the vector of branch real powers with existing power measurements in p.u. in from – to direction;

Q_{ft} the vector of branch reactive powers with existing power measurements in p.u. in from – to direction;

P_{tf} the vector of branch real powers with existing power measurements in p.u. in to – from direction;

Q_{tf} the vector of branch reactive powers with existing power measurements in p.u. in to – from direction.

Thus, the vector of slack variables consists of:

$$\boldsymbol{\alpha} = [\alpha_P \quad \alpha_Q \quad \alpha_V \quad \alpha_{I_{ft}} \quad \alpha_{I_{tf}} \quad \alpha_{P_{ft}} \quad \alpha_{Q_{ft}} \quad \alpha_{P_{tf}} \quad \alpha_{Q_{tf}}] \quad (4.58)$$

where:

α_P the vector of slack variables associated with the measured real power injections of the non-empty busses;

α_Q the vector of slack variables associated with the measured reactive power injections of the non-empty busses;

α_V the vector of slack variables pertaining to the voltage magnitude of the busses with voltage measurement equipment;

$\alpha_{I_{ft}}$ the vector of slack variables pertaining to the current in from – to direction of the busses with current measurement equipment;

$\alpha_{I_{tf}}$ the vector of slack variables pertaining to the current in to – from direction of the busses with current measurement equipment;

$\alpha_{P_{ft}}$ the vector of slack variables pertaining to the real power in from – to direction of the busses with power measurement equipment;

$\alpha_{Q_{ft}}$ the vector of slack variables pertaining to the reactive power in from – to direction of the busses with power measurement equipment;

$\alpha_{P_{tf}}$ the vector of slack variables pertaining to the real power in to – from direction of the busses with power measurement equipment;

$\alpha_{Q_{tf}}$ the vector of slack variables pertaining to the reactive power in to – from direction of the busses with power measurement equipment.

The solution of DSSE problem is obtaining an accurate as possible picture of the network which means in ideal case equaling estimates with measured values of different quantities throughout the network. The difficulty is that number of measurements is limited so the differences between estimated and measured values will exist. The task is that differences be as small as possible so this is why the estimator's objective function is the minimization of sum of squares of these differences which are represented by the slack variables. The objective function is the following:

$$\min f = \min \sum_{k=1}^{N_{m\_bus}} \left(\frac{\alpha_{P_k}}{P_{G_k}^m - P_{L_k}^m} \right)^2 + \sum_{k=1}^{N_{m\_bus}} \left(\frac{\alpha_{Q_k}}{Q_{G_k}^m - Q_{L_k}^m} \right)^2 + \sum_{k=1}^{N_{m\_VIPQ}} \left(\frac{\alpha_{VIPQ_k}}{VIPQ_k^m} \right)^2 \tag{4.59}$$

where:

N_{m_bus} the number of buses with completely measured injected powers (see Fig. 4., d);

N_{m_VIPQ} the total number of voltage and branch powers and currents measurements (see Fig. 4.);

α_{VIPQ} vector holding α_V, $\alpha_{I_{branch}}$, $\alpha_{P_{branch}}$, $\alpha_{Q_{branch}}$;

$VIPQ^m$ vector holding the voltage and branch measurements.

The other quantities have been defined in subchapter 4.3.1.

It should be noted that regarding the real and reactive power injections, only the slacks pertaining to buses with completely known load and generation are included into Eq. (4.59) since only these measurements can be matched.

4.3.5.2 Equality Constraints of the Problem

Every optimization problem is a subject to a certain number of linear and/or nonlinear constraints. These constraints ensure the technical or physical limitations of the problem so the problem itself represents as real as possible the picture of the system. Following are the constraints adopted in our SE problem.

4.3.5.2.1 Power Flow Equations

SE uses the initial values of the problem obtained directly from the PF which means that PF equations represent the first constraint of the problem. This is a nonlinear constraint. We have to distinguish between:

1. Buses without connected load and generation, i.e. empty buses:

$$\begin{aligned} f_{P_k}(V_M, V_A) &= 0 \\ f_{Q_k}(V_M, V_A) &= 0 \end{aligned} \tag{4.60}$$

2. Buses with connected loads and/or generators but partially measured or not measured at all, such that the resulted nodal injected power is not known:

$$\begin{aligned} P_k^0 - f_{P_k}(V_M, V_A) + \alpha_{P_k} &= 0 \\ Q_k^0 - f_{Q_k}(V_M, V_A) + \alpha_{Q_k} &= 0 \end{aligned} \tag{4.61}$$

   In this case the slack variables are not present in the OF given by Eq. (4.59) since the injected powers are not completely measured; however their lower bounds (LB) and upper bounds (UB) are defined in accordance to the measured data. These bounds can be find in Table 4.15. In Eqs. (4.60) and (4.61):

   $f_{P_k}(V_M, V_A)$ real power of the *k*-th bus which is the result of the state estimation's appropriate iteration and is the function of bus voltage magnitude and phase angle;

   $f_{Q_k}(V_M, V_A)$ reactive power of the *k*-th bus which is the result of the state estimation's appropriate iteration and is the function of bus voltage magnitude and phase angle;

   P_k^0 initial real power of the *k*-th bus corresponding to the initial estimated profiles. Power injection stands for the difference between generation and load of the network buses;

   Q_k^0 initial reactive power of the *k*-th bus gained as the result of the computation of complex bus power injection matrix;

   α_{P_k} slack variables of real power of the *k*-th bus;

   α_{Q_k} slack variables of reactive power of the *k*-th bus.

3. Buses with connected loads and/or generation which are all measured. In this case, the nodal injected power can be considered completely known: P_k^m and Q_k^m:

$$\begin{aligned} P_k^{\mathbf{m}} - f_{P_k}(V_M, V_A) + \alpha_{P_k} = 0 \\ Q_k^{\mathbf{m}} - f_{Q_k}(V_M, V_A) + \alpha_{Q_k} = 0 \end{aligned} \tag{4.62}$$

Accordingly, the slack variables are present in the objective function and are subject of upper and lower bounds determined by the errors of the measurement apparatus:

$$\begin{aligned} -\varepsilon_{P_k}^{\mathbf{m}} \cdot P_k^{\mathbf{m}} \leq \alpha_{P_k} \leq \varepsilon_{P_k}^{\mathbf{m}} \cdot P_k^{\mathbf{m}} \\ -\varepsilon_{Q_k}^{\mathbf{m}} \cdot Q_k^{\mathbf{m}} \leq \alpha_{Q_k} \leq \varepsilon_{Q_k}^{\mathbf{m}} \cdot Q_k^{\mathbf{m}} \end{aligned} \tag{4.63}$$

where $\varepsilon_{P_k}^{\mathbf{m}}$ and $\varepsilon_{Q_k}^{\mathbf{m}}$ are the errors that take into account the total measurement errors.

4.3.5.2.2 Measured Voltage Constraints

For the buses of the network where a voltage measurement equipment is present, the following constraint must be respected:

$$V_{M,k} - V_k^{\mathbf{m}} + \alpha_{V_k} = 0 \tag{4.64}$$

where:

$V_{M,k}$ - voltage magnitude of the *k*-th bus which is the result of the state estimation's appropriate iteration;

$V_k^{\mathbf{m}}$ - measured voltage of the *k*-th bus;

α_{V_k} - slack variable of voltage of the *k*-th bus.

4.3.5.2.3 Measured Current Constraints

For the buses of the network where there is present current measurement equipment (from-to and/or to-from direction), following constraints must be respected:

$$\begin{aligned} I_{ft\_re} - Re\big(Y_f \cdot V\big) = 0 \\ I_{ft\_im} - Im\big(Y_f \cdot V\big) = 0 \\ I_{tf\_re} - Re(Y_t \cdot V) = 0 \\ I_{tf\_im} - Im(Y_t \cdot V) = 0 \end{aligned} \tag{4.65}$$

Eqs. (4.65) which pertain to the branch current constraints are then used to compute the current measurement constraints given by Eqs. (4.66) as follows:

$$\begin{aligned} \sqrt{I_{ft\_re}^2 + I_{ft\_im}^2} - I_{ft}^{\mathbf{m}} + \alpha_{I_{ft}} = 0 \\ \sqrt{I_{tf\_re}^2 + I_{tf\_im}^2} - I_{tf}^{\mathbf{m}} + \alpha_{I_{tf}} = 0 \end{aligned} \tag{4.66}$$

where:

V the vector of the complex bus voltages; $V = V_M e^{jV_A}$;

Y_f the branch admittance matrix computed according to the from buses of the considered branches;

Y_t the branch admittance matrix computed according to the "to" buses of the considered branches;

$I_{ft}^{\mathbf{m}}$ measured branch current in from-to direction;

$I_{tf}^{\mathbf{m}}$ measured branch current in to-from direction.

For the structure of Y_f and Y_t, it is suggested to refer to MATPOWER software package [140].

The set of constraints given by Eqs. (4.65) and (4.66) is defined only for the branches where measurements are available.

4.3.5.2.4 Measured Power Constraints

For the buses of the network where there is present real and reactive power measurement equipment (from-to and/or to-from direction), following constraints must be respected:

$$\begin{aligned} P_{ft} - Re\left(V_f \cdot conj\left(Y_f \cdot V\right)\right) = 0 \\ Q_{ft} - Im\left(V_f \cdot conj\left(Y_f \cdot V\right)\right) = 0 \\ P_{tf} - Re\left(V_t \cdot conj(Y_t \cdot V)\right) = 0 \\ Q_{tf} - Im\left(V_t \cdot conj(Y_t \cdot V)\right) = 0 \end{aligned} \tag{4.67}$$

Eqs. (4.67) which pertain to the branch power constraints are then used to compute power measurement constraints given by Eqs. (4.68) as follows:

$$\begin{aligned} P_{ft} - P_{ft}^{\mathbf{m}} + \alpha_{P_{ft}} = 0 \\ Q_{ft} - Q_{ft}^{\mathbf{m}} + \alpha_{Q_{ft}} = 0 \\ P_{tf} - P_{tf}^{\mathbf{m}} + \alpha_{P_{tf}} = 0 \\ Q_{tf} - Q_{tf}^{\mathbf{m}} + \alpha_{Q_{tf}} = 0 \end{aligned} \tag{4.68}$$

where:

$P_{ft}^{\mathbf{m}}$ - measured real power of the branch in from-to direction;

$Q_{ft}^{\mathbf{m}}$ - measured reactive power of the branch in from-to direction;

$P_{tf}^{\mathbf{m}}$ - measured real power of the branch in to-from direction;

$Q_{tf}^{\mathbf{m}}$ - measured reactive power of the branch in to-from direction.

Constraints given by Eqs. (4.67) are nonlinear while constraints (4.68) constraints are linear. The set of constraints given by Eqs. (4.67) and (4.68) is defined only for the branches where measurements are available.

4.3.5.2.5 Upper and Lower Bounds

To prevent the convergence of the defined optimization problem (OP) to technically unfeasible operating points (e.g. operating points in which the DN would be disconnected from the main grid due to the protection actions) appropriate lower and upper bounds have been adopted for the variables of the OP as shown in Table 4.16. These values are set according to the DSO criteria and expressed in per. Since the powers in DN buses are generally at maximum few hundreds of kVA, the limits in Table 4.16 were set such to provide large margins for any DN.

Table 4.16: Upper and lower bounds for the optimization problem variables

Variable	Lower Bound	Upper Bound
V_M	1.1 p.u.	0.9 p.u.
V_A	$-\pi/2$	$\pi/2$
I_{ft_re}, I_{ft_im} , I_{tf_re}, I_{tf_im}, P_{ft}, Q_{ft}, P_{tf}, Q_{tf}	-0.05	0.05
α_P, α_Q	-10 or $-\varepsilon_{P_k}^{\mathbf{m}} \cdot P_k^{\mathbf{m}}/Q_k^{\mathbf{m}}$	10 or $\varepsilon_{P_k}^{\mathbf{m}} \cdot P_k^{\mathbf{m}}/Q_k^{\mathbf{m}}$
α_{VIPQ}	$-$ 0.05	0.05

4.3.6 Implementation Aspects Regarding the ASE

The proposed optimization model was implemented in MATLAB and the "fmincon" native function was used to find the solution to the OP. In order to facilitate and reduce the computation time, the constraints and OF gradients and hessians were defined.

It should be noted that at least one voltage measurement and branch current or power measurement is required to run the ASE. In the absence of this minimum required information, running the ASE is meaningless.

4.3.7 Advanced State Estimation Simulation Results

To evaluate the performances of the optimization model many different DNs were tested in various measurement configurations. The test procedure involved generating a large number of measurement scenarios: large deviations were introduced in the standard load/generation profiles using a standard uniform distribution set to generate random numbers in the range of ±80% of the initial quantities; then PF were run to obtain the measurements. Once the set of measurements was obtained, noise was added to the measured values using a standard uniform distribution set to generate random numbers in various ranges with respect to the initial quantities. In the following subchapters, representative tests are reported.

4.3.7.1 9-bus Test System

The first investigated DN is the small grid depicted in Fig. 4.17. This test system was chosen to emphasize in details the features of the proposed

procedure. The network consists of a 7 bus feeder with load distributed among its buses and with a secondary substation where a generation plant is connected. The primary and secondary substations are measured as shown in Fig. 4.17.

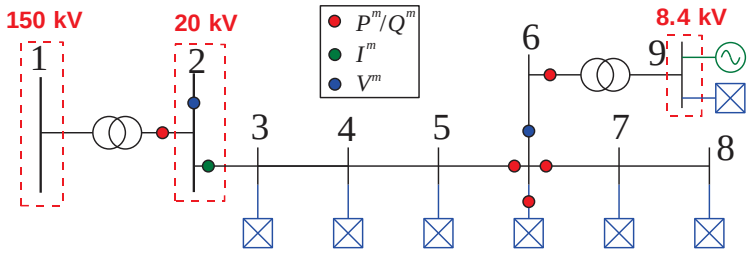

Figure 4.17: *The 9-bus distribution network*

To test the proposed procedure a set of 500 operation scenarios were generated as described above. In the absence of any procedure to improve the observability of the network, the DSO would have to rely on the results of the PF computed using the standard load/generation profiles. Table 4.17 shows the mean values and standard deviations of the estimation errors for the bus voltage magnitudes and phases in % when the standard profiles are used.
The voltage angles estimation error is at least 20%, while the voltage magnitude estimation error reaches an average of 1.5% and a standard deviation of 1% for the bus at the end of the feeder (bus 8).

Table 4.17: 9-bus DN observability based on the standard profiles in %

V_M	2	3	4	5	6	7	8	9
Mean	0.3	0.7	0.7	0.7	0.8	1.1	1.5	0.8
Std.	0.2	0.5	0.5	0.5	0.5	0.7	1.0	0.6
V_A	2	3	4	5	6	7	8	9
Mean	28.3	22.0	21.6	21.5	21.3	18.4	18.5	32.1
Std.	52.6	24.9	23.9	23.7	23.3	17.4	16.5	79.0

Fig. 4.18 shows the real and the standard profiles for the voltage magnitude of bus 8. The real voltage magnitude is below 0.96 p.u. in 43% of the cases and bellow 0.95 p.u. in 26% of the cases, while the values given by the standard profiles are ≈ 0.98 p.u.: in almost half of the cases control actions to improve the voltage magnitude would be required, but the results of the standard profiles are unreliable.

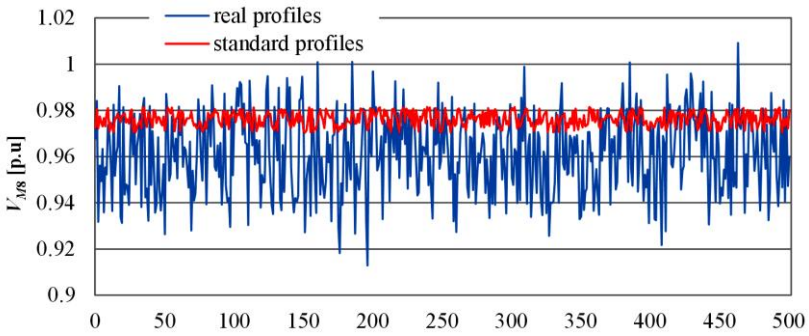

Figure 4.18: *Voltage magnitude at bus 8: real vs standard profiles*

Table 4.18 shows the mean values and standard deviations of the estimation errors for the power injections at bus 1 and 9 in % when the standard profiles are used. The values of Table 4.18 are very high as the error of the standard profiles in terms of load and generation are up to 80% for each single load or generator. Table 4.18 shows that the estimation of both the power exchange with the HV grid and the power produced by the generator plant is very bad and, in consequence, no control action is possible to improve the voltage profile of the feeder.

Table 4.18: Power injections observability based on the standard profiles in %

P	**1**	**9**
Mean	27.9	398.5
Std.	52.1	1595.2
Q	**1**	**9**
Mean	174.7	303.5
Std.	462.2	1063.7

In conclusion, the DN is unobservable and uncontrollable if only the standard profiles are considered. The proposed OP is run for the 500 scenarios in three cases:

1. Case I: the exact measurements are used;
2. Case II: the voltage measurements are perturbed by maximum ±1% while the remaining measurements by maximum ±3%;
3. Case III: the voltage measurements are perturbed by maximum ±2% while the remaining measurements by maximum ±5%.

The voltage measurement is generally more precise than other measurements, hence the values reported above. Table 4.19 depicts the mean values and standard deviations of the estimate errors for the measured quantities with respect to the exact values of the measures for all the cases. In Case I, when the measurements are exact, the estimates match very well the measured values, the errors being insignificant. When noise is introduced in the measurement profile (Case II and III), the procedure converges to a point where the estimate errors are as close as possible to the exact measurements, the errors being congruent with the introduced noise.

Table 4.19: 9-bus DN estimate errors with respect to the exact measurements

%	**Case I**		**Case II**		**Case III**	
Measure	**Mean**	**Std.**	**Mean**	**Std.**	**Mean**	**Std.**
V_{M2}	2E-7	7E-7	5E-3	5E-3	8E-3	8E-3
V_{M6}	5E-3	6E-3	6E-2	4E-2	7E-2	5E-2
$I_{2,3}$	8E-5	6E-4	1.0	0.7	1.7	1.2
$P_{6,7}$	3E-5	3E-4	1.2	0.8	1.9	1.3
$P_{2,1}$	8E-5	6E-4	1.1	0.7	1.8	1.2
$P_{6,5}$	3E-5	2E-4	1.1	0.7	1.8	1.3
$P_{6,9}$	2E-5	3E-4	1.3	0.9	2.2	1.4
$Q_{6,7}$	1E-5	1E-4	1.2	0.8	2.0	1.4
$Q_{2,1}$	4E-5	2E-4	1.5	0.9	2.6	1.4
$Q_{6,5}$	1E-5	8E-5	1.2	0.8	2.0	1.3
$Q_{6,9}$	7E-6	5E-5	1.4	0.9	2.2	1.4
P_6	3E-5	2E-4	1.4	0.8	2.3	1.4
Q_6	3E-5	3E-4	1.3	0.8	2.1	1.4

In what regards the network observability, Table 4.20 reports the major improvements in the states of the system while Fig. 4.19 illustrates the dramatic improvements in the observability of bus 8 voltage magnitude. The voltage magnitude and angle errors are reported for the worst observable and most critical bus (bus 8). Expressed in absolute errors, for Case III, the average error of V_{M8} is ≈ 0.004 p.u. and the maximum value is ≈ 0.011 p.u., value reached in less than 1% of the measurement scenarios; while the average error of V_{A8} is ≈ 0.5° and the maximum value is ≈ 1.6°. Clearly, the observability of the voltage profile has improved up to the point where reliable control actions can be applied.

Table 4.20: 9-bus DN observability based on the optimization procedure

%	Case I		Case II		Case III	
Measure	**Mean**	**Std.**	**Mean**	**Std.**	**Mean**	**Std.**
V_{M8}	0.39	0.28	0.40	0.28	0.41	0.29
V_{A8}	4.60	1.57	4.68	1.86	4.71	2.22
P_1	8E-5	6E-4	1.07	0.70	1.77	1.21
Q_1	2E-5	3E-4	1.98	5.83	3.19	5.97
P_9	1E-4	5E-4	1.32	0.87	2.24	1.41
Q_9	7E-4	4E-3	1.34	0.88	2.17	1.55

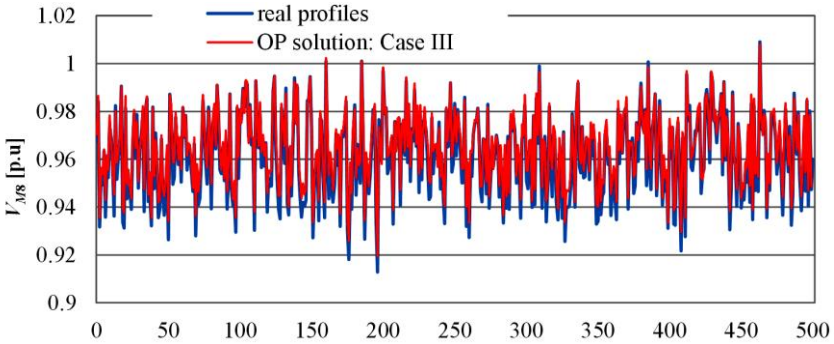

Figure 4.19: *Voltage magnitude at bus 8: real vs OP solution (Case III)*

In what regards the controllability of the network, Table 4.20 shows that now the estimation of both the power exchange with the HV grid and the power produced by the generator plant are within acceptable limits and hence control actions regarding the voltage profile of the feeder and the power flows injected into the TN are now possible. Concerning the injected powers along the feeder (at buses 3, 4, 5, 7 and 8), their observability is not improved at all as there is no information available regarding their actual values and they are free variables in the OP. However, it can be generally concluded that the proposed procedure majorly improves the observability of the DN up to render it controllable in various variables. Of course, in the lack of redundancy, the DN state cannot be completely known.

4.3.7.2 69-bus Test System

Figure 4.20 depicts the second investigated DN. It is a 69 bus network containing 10 generation plants. The figure also shows the measurement locations and their types: the measured substations are depicted in detail. As with the previous DN, 500 measurement scenarios were defined and run for

the 3 defined cases. Moreover, 3 configurations for the measurement types and locations were defined:

1. Configuration I: the base case depicted in Fig. 4.20;
2. Configuration II: same as Configuration I, but with the current measurements changed to power measurements;
3. Configuration III: same as Configuration III, but with branch power measurements added at substations 57, 59 and 62.

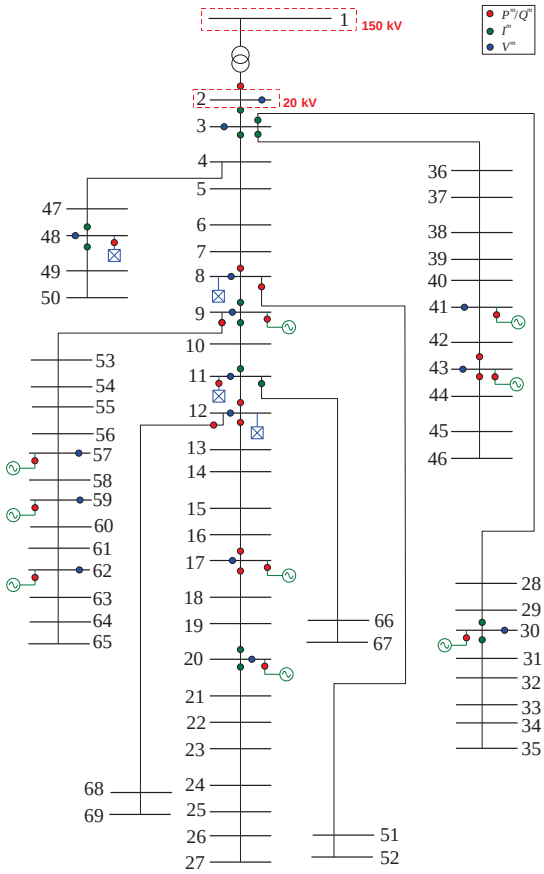

Figure 4.20: *The 69-bus distribution network: Configuration I*

Table 4.21 shows the results of the OP for all the defined measurement configurations and cases in terms of mean relative errors of the estimates with respect to the measurements and their standard deviations. Since there is a large number of measurements, only the worst results are shown for each type of measurements: generally, the estimate errors are much smaller than the reported maximum case. The results of Table 4.21 show that the procedure has found very good solutions where the estimates are as close as possible to the exact measurements, the errors being congruent with the introduced noise.

Table 4.21: 69-bus DN estimate errors with respect to the exact measurements

	Configuration I					
%	**Case I**		**Case II**		**Case III**	
Measure	**Mean**	**Std.**	**Mean**	**Std.**	**Mean**	**Std.**
V_{M62}	2E-2	1E-2	0.3	0.2	0.4	0.3
$I_{3,36}$	1E-3	5E-4	1.6	0.9	2.6	1.4
$P_{8,51}$	1E-4	7E-5	1.5	0.8	2.5	1.4
$Q_{8,51}$	2E-4	6E-5	1.6	0.9	2.5	1.4
P_{62}	5E-5	4E-5	1.5	0.9	2.7	1.5
Q_{62}	4E-5	3E-5	1.5	0.8	2.4	1.4
Configuration II						
V_{M62}	2E-2	2E-2	0.3	0.2	0.4	0.3
$P_{8,51}$	2E-4	5E-5	1.5	0.8	2.5	1.4
$Q_{8,51}$	2E-4	5E-5	1.5	0.9	2.6	1.4
P_{62}	6E-5	4E-5	1.5	0.9	2.5	1.5
Q_{62}	5E-5	3E-5	1.5	0.9	2.4	1.5
Configuration III						
V_{M62}	4E-2	3E-2	1E-1	1E-1	1E-1	1E-1
$P_{8,51}$	1E-4	6E-5	1.5	0.9	2.3	1.4
$Q_{8,51}$	1E-4	6E-5	1.5	0.9	2.4	1.5
P_{43}	2E-5	4E-5	1.5	0.9	2.6	1.4
Q_{43}	1E-5	1E-5	1.5	0.9	2.5	1.5

Regarding the observability of the network, Figs. 4.21 ÷ 4.24 depict the estimation errors in terms of means and standard deviation for the voltage magnitudes and phases of the buses at the end of the main feeder, i.e. bus 27, and of its deviations (secondary feeders), i.e. buses 35, 46, 50, 52, 65, 67, 69. The results are shown for all the measurement configurations, including also the results given by the standard profiles, for the case with the most severe measurement noise (Case III).

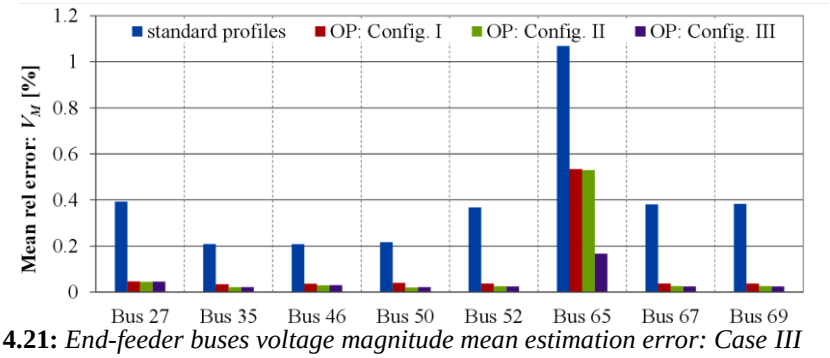

Figure 4.21: *End-feeder buses voltage magnitude mean estimation error: Case III*

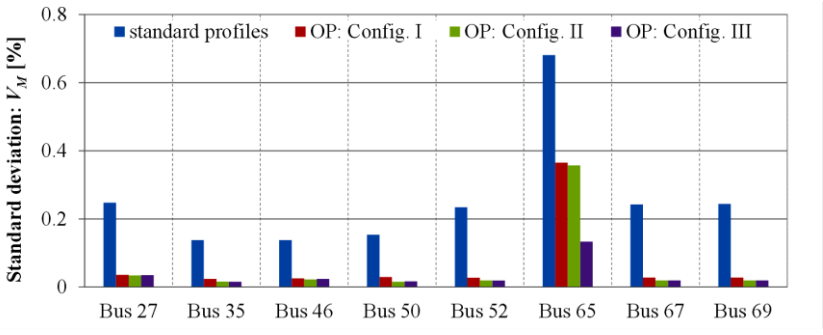

Figure 4.22: *End-feeder buses voltage magnitude standard deviation: Case III*

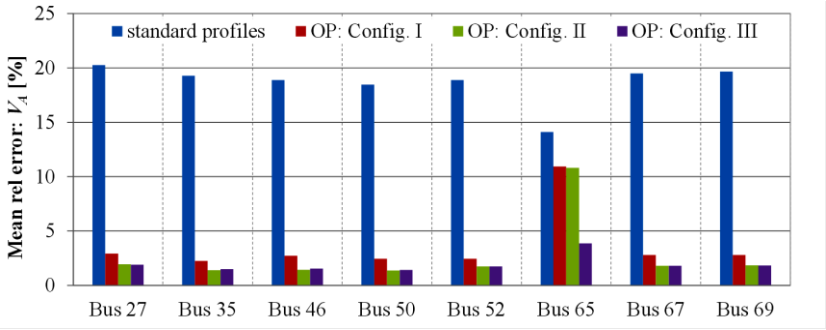

Figure 4.23: *End-feeder buses voltage angle mean estimation error: Case III*

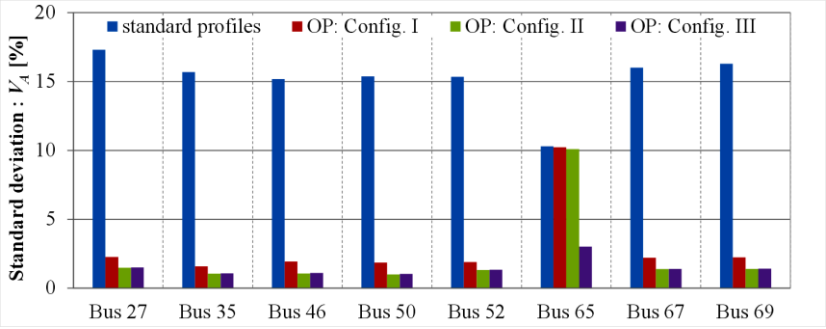

Figure 4.24: *End-feeder buses voltage angle standard deviation: Case III*

When branch measurements in the feeders are available (all buses except bus 65 in Figs. 4.21 ÷ 4.24) the estimation of the voltage magnitudes and angles are very good up to render the voltage profile observable and, hence, make control actions possible. Strictly referring to the feeders where branch measurements are available, an improvement in the voltage angle observability is noticed when changing the branch measurements from currents to powers, but no improvement in the voltage magnitude observability. This happens as the voltage drops in the lines are strongly dependent on the current magnitudes, already well estimated in Configuration I, while the voltage angles are more sensitive to real/reactive power flows transmitted by the network which are better estimated in Configuration II.

Moreover, the estimation of the nodal powers for the buses located in the vicinity of the branch measurements are improved when the type of branch measurement is changed from current magnitude to powers. Table 4.22 depicts the errors in absolute values for the nodal powers of the buses in the vicinity of the measured bus 30 (buses 29 and 31 are transit buses). The major improvement when the measurement type is changed can be seen in the buses nearest to bus 30: buses 28 and 32; for the rest of the buses, no major improvement is achieved. Moreover, even if buses 28 and 32 are almost equally electrically distant with respect to bus 30 ($Z_{28,30}\approx0.18$ p.u. and $Z_{30,32}\approx0.14$ p.u.) the major improvement is achieved for bus 28 as this bus is located between measured buses: 3 and 30, while bus 32 is not.

For the feeder where the branch measurements are initially missing (buses 53÷65), the voltage profile estimation is much worse, especially regarding the voltage angle: for Configuration I and II, the estimation of the voltage angle of bus 65 is more or less as bad as using the standard profiles; then, when the power branch measurements are available, it improves up to observable values.

Table 4.22: 69-bus DN estimate errors with respect to the exact measurements

Case II				
kW/kVar	**Configuration I**		**Configuration II**	
Measure	**Mean**	**Std.**	**Mean**	**Std.**
P_{28}	15.8	13.8	2.2	1.6
Q_{28}	13.5	9.0	1.6	1.1
P_{32}	7.2	5.7	4.7	3.6
Q_{32}	7.0	5.5	3.7	2.7
P_{33}	9.5	7.9	7.3	4.9
Q_{33}	6.0	4.3	5.3	3.5
P_{34}	10.4	4.8	8.8	5.6
Q_{34}	8.9	5.7	7.6	3.4

Regarding the controllability of the network, all the generation plants and the power exchange with the HV network are measured and the estimation of their output is very good (see Fig. 4.20 and Table 4.21). Therefore, the voltage profile and the power exchange with the HV grid are controllable through the adjustment of the generation plants output.

CHAPTER 5

5. Optimization of Measurement Equipment Placement

5.1 Problem Definition and Importance

The operation philosophy for power systems has been changing in the deregulated business environment. A key objective is now to improve operational efficiency through better utilization of network capacity. Another important goal is to accommodate a considerable portion of the DG within an overall MW/MVAr transaction portfolio. This requires the monitoring and control of the network by means of a modern DMS at substation level. DSSE should obviously be at the center of the DMS technology. However, a large part of the system, particularly the distribution segment, continues to operate in an unmonitored fashion, adversely affecting the accuracy and quality of the SE and therefore its usefulness. This introduces bottlenecks in carrying out a range of substation and feeder automation tasks that rely on the quality of the DSSE.

Voltage, current and power flows are typically measured in a secondary busbar of primary substation; virtually no monitoring is carried out further down at the secondary substation level. The loads are not measured; instead they are modeled as pseudo-measurements constructed from the historical and sample load profiles [56],[70]. Since pseudo-measurements are high-variance estimates of the loads, the quality of the estimated voltages and angles at each bus is poor if the number of pseudo-measurements is large.

Therefore, an innovative tool that improves the observability of the DNs considering few measurements has been proposed by the authors in [68],[69]. The developed algorithm bypasses the lack of redundancy and statistical information regarding the measurements in the DN, but, the quality of the results strongly depends on the quality of the measurements and location of the equipment.

As the investments into measurement equipment are low compared to the increase of DG penetration [68], the DN infrastructure of today has not changed much with respect to the past: a limited set of measurements in the

primary substations and in some secondary substations are available. The equipment is mostly old and the precision class is inappropriate for classical state estimation as it was installed for other purposes, (e.g. input signal for the protection systems). Moreover, the measurements are not synchronized but averaged and collected at different moments. Improvement of the observability of the DN in a way to obtain as accurate as possible representation of the network state can give results but its impact is still not sufficient with the perspective of further penetration of DGs and increased need to make automatic control actions. So, even though DSOs are reluctant to do so because of the expenses, investments into the new measurement equipment are the matter of necessity. The measurement equipment should be placed optimally throughout the network to ensure the best possible attainable observability with the least possible number of new measurement locations to diminish the expenses.

The problem of the determination of the best locations of the measurement equipment for state estimation is known as the problem of Optimal Measurement Equipment Placement (OMEP). With every additional instrument, assessment of state is improved, but there are economical and physical boundaries related to the number of additional equipment: it is necessary to find the minimum number of additional instruments that, when placed in optimal locations, enable maximal network observability. These issues have been addressed in the literature, at transmission level. But little attention has been paid to measurement equipment placement at the distribution level. Research reported in the literature concerning measurement placement fall, broadly speaking, into two categories:

- the improvement of the network observability;
- the minimization of the errors in the estimates.

5.2 Bibliography review

The topic of this chapter is not a new one, but as with SE, little attention in the past was dedicated to the problem of OMEP in DS. The reason is that, in the past, operators knew the behavior of the DN well enough to render control actions and most of the issues regarding DN were solved by the manipulations on the primary substation, in most of the cases by adapting voltage to ensure normal operation of the network. However, this is no longer sufficient and new equipment must be installed to ensure the observability of the larger portion of the DS and also to make possible automatic control actions that are crucial for the optimal operation of the network.

Highly precise and automated actions needed nowadays in DN are the result of the increased penetration of DGs that completely changed the picture of the system as known before. Also, changes already described in Chapter 2, regarding the functionalities of DS are further pointing out that with other investments in DN, measurement equipment needs to have a central position.

The description of the proposed approaches will start with the ones that are developed for TS, and then proceed to a few pioneering approaches, specially designed for DS.

The research of B. Gou and A. Abur [71] proposes a fast method for multiple measurement placement for systems that are found to be unobservable. The method uses a test matrix whose leading dimension is determined by the rank deficiency of the gain matrix.

Authors notice that observability analysis of power systems involves checking the rank of the state estimation gain matrix **G**, which is sparse, symmetric and positive definite for observable systems. This can be accomplished by topological [34] or by numerical [43] methods. If the gain matrix is found to be singular, then all observable islands need to be identified and power injection pseudo-measurements will have to be introduced in order to merge these islands into a single observable island for the entire system. The process of choosing the right set of additional measurements for this purpose is referred to as the measurement equipment placement.

Pseudo-measurements are typically generated from load forecasts, scheduled generation data, or some other source with a degree of uncertainty. Hence, pseudo-measurements are usually of injection type.

The main idea behind the proposed method is the use of the test matrix, in order to simultaneously process the candidate measurements and make the final selection in a noniterative and fast manner.

The measurement placement algorithm presented in this research is based on the observability analysis method. One should consider the real power versus phase angle part of the linearized and decoupled measurement equation. This is obtained by using the first order approximation of the decoupled nonlinear measurement equation around the operating point:

$$z = \mathbf{H}\theta + e \tag{5.1}$$

where:

- z mismatch between the measured and calculated real power measurements;
- H decoupled Jacobian of the real power measurements versus all bus phase angles;
- θ incremental change in the bus phase angles at all buses including the slack bus;
- e measurement error vector.

The decoupled gain matrix for the real power measurements can be formed as:

$$\mathbf{G} = \mathbf{H}^{\mathrm{T}}\mathbf{H} \tag{5.2}$$

where measurement covariance error matrix is assumed to be the identity matrix without loss of generality.

The symmetric matrix **G** can be decomposed into its Cholesky factors $\mathbf{LDL}^{\mathrm{T}}$ where the diagonal factor **D**, may have one or more zeros on its diagonal. Taking the inverse of **L** and collecting only those rows of $\mathbf{L}^{-1}$ corresponding to the zero diagonals of **D**, we can form a rectangular submatrix which is called the “test” matrix and denoted by **W**.

The following algorithm can then be used to determine all the observable islands simultaneously:

Step 1. Form the gain matrix **G** and perform the triangular factorization;
Step 2. Check if **D** has only one zero pivot. If yes, stop. If not, compute the test matrix **W** from **L**;
Step 3. Compute the matrix $\mathbf{C} = \mathbf{A}\mathbf{W}^T$, where **A** is the branch-node incidence matrix. If at least one entry in a row is not zero, then the corresponding branch will be unobservable;
Step 4. Remove all the unobservable branches, to obtain the observable islands;
Step 5. Stop.

After the determination of the observable islands, authors propose the following algorithm for the multiple measurement placement:

Step 1. Form the gain matrix **G** and perform the triangular factorization;
Step 2. Check if **D** has only one zero pivot. If yes, stop. If not, form the test matrix **W**;
Step 3. Using the test matrix **W**, find the observable islands;
Step 4. Form the candidate list. Those injection measurements, which connect at least two different observable islands, should be included in the list if those pseudo-measurements are available;
Step 5. Form the rectangular matrix $\mathbf{B} = \mathbf{H}_c\mathbf{W}^T$ and reduce it to its Echelon form **E**. The candidates will correspond to the linearly indipendent columns in **E**. **H**c is the Jacobian matrix of the pseudo-measurements chosen from the candidate measurements.

This approach makes use of small dimension test matrix in deciding on the placement of measurements. The dimension of the test matrix is equal to the rank deficiency of the existing gain matrix, and therefore is typically only a small fraction of the total number of buses in the system. This makes the method computationally very attractive, yet simple to implement in existing state estimators.

Authors in [72] present the method for an optimal measurement placement of PMUs for PSSE. The proposed method considers two types of contingency conditions (i.e., single measurement loss and single-branch outage) in order to obtain a reliable measurement system. In order to minimize the number of PMU placement sites, a heuristic technique to rearrange measurement positions is also proposed.

Authors point out that the PMU placement method should be performed under three considerations: 1) the accuracy of estimation, 2) the reliability of estimated state under measurements failure and change of network topology, and 3) the investment cost.

PMU placement method for PSSE is based on the minimum condition number of the normalized measurement matrix. The proposed method finds an optimal measurement set necessary for complete numerical observability and single measurement loss and single-branch outage contingency of the system. Then, the positions of these measurements are rearranged by a heuristic algorithm in order to minimize the number of PMU placement sites.

The proposed placement algorithm consists of four stages. In the first stage, a measurement set for a completely determined condition is searched. It is called an essential measurement set. Next, a redundant measurement set is selected from the candidate measurements under each contingency condition. Both stages use the minimum condition number of normalized measurement matrix as criteria in selecting the measurement positions. Then, from these measurements, the optimal redundant set is selected by using the binary integer programming technique [127]. The essential measurements and the optimal redundant measurements are rearranged by the proposed heuristic method in order to minimize the number of PMU placement sites in the final stage.

The algorithm starts by searching the essential measurement set, in other words, the positions and types of measurements under the completely determined condition (i.e., the number of the measurements is equal to the number of estimated states).

The sequential addition method is used to search the redundant measurements for each contingency condition. This step is used to find the necessary measurements from candidate measurements of each contingency condition such that SE is still solvable under these conditions.

In case of measurement loss, the measurement matrix would be modified by removing the row corresponding to the lost measurement. However, when the network topology changes, it is necessary to rebuild the measurement matrix according to the outage condition. Candidate measurements that yield normalized measurement matrices with condition number below a predefined threshold are selected as redundant measurements.

The output from the sequential addition contains the list of redundant measurements to be added into the essential measurements to ensure the completely observable condition of the power network when the contingency occurs.

A binary integer programming has been applied to solve the placement problem of the conventional measurements and is used to find the optimal redundant measurements for the contigency. The redundant measurements according to the nonzero elements are considered as the optimal redundant measurements.

The number of PMU placement sites should be minimized in order to reduce the communication costs. The measurement positions obtained from the minimum condition number criteria can be rearranged to minimize the number of PMU placement sites by the following heuristic algorithm:

Step 1. Based on the placement position list, obtained from the measurement placement algorithm, the bus where either an injection current or a bus voltage measuring device is installed should be determined. These buses are called major buses. Other buses are called minor buses;

Step 2. If there is a branch current measuring device on the branch connected to the major buses, the device is moved close to the major buses;

Step 3. From the branches with branch current measurement devices, which are not connected to major buses, the minor bus with the maximum connection number of those branches with branch current measurements should be determined. Then, the branch current measurement device on the connected branches moves close to the

selected bus. Note that this minor bus will not be considered again in the next iteration.

Step 4. Repeat Step 3. until the maximum connection number of branches with branch current measuring devices is equal to one.

Numerical results on the IEEE test systems indicate that the proposed placement method satisfactorily provides the reliable measurement system that ensures the SE to be solvable under the given contingency conditions. Furthermore, due to the well-conditioned measurement matrix, SE accuracy is also improved.

While the previous methods were hard to apply for DSs as they fit the operation of the TSs, the following refferences concern DSs. In their work, M. E. Baran and others [73] write about the identification of the data requirements for real-time monitoring and control of DSs. The research points out that in addition to having supervisory control and data acquisition on switches and control equipment, methods are necessary to obtain an accurate estimation of data needed for feeder automation functions. A meter placement method is proposed for this purpose.

Real-time data required for real-time monitoring and control of a DS is mainly determined by the functions to be automated in the system. Economic considerations usually put limits on the number of the functions that can be automated.

Meters and monitoring devices need to be placed at various points in the system and integrated in a SCADA system so that the real-time data obtained from these devices can be communicated to the dispatch center. Unfortunately, economics put very strong limits on the scale of such SCADA systems in DS monitoring and control applications.

Besides providing a more reliable real-time load data for feeder automation functions, SE can also be used to check the consistency of the measurements and the network model and hence provide data for the following real-time monitoring functions:

1. Switch Status Monitoring: Since most of the switching in a DS is done manually and not telemetered, SE can help the dispatchers to keep the network topology information up-to-date by detecting the status changes in switches.
2. Locating Faults: The pre-fault and post-fault load distribution data from SE can also be used to identify the protection device (fuse or recloser) that operated to isolate a fault.
3. Monitoring the Operation of Control Devices: Any change in the status of a capacitor bank, a voltage regulating transformer or a third party generation unit will affect the operation of a feeder appreciably. By measuring appropriate quantities in a feeder, SE can detect the changes in the status of these devices.

The main goal of meter placement is determining the number, place, and type of meters that need to be placed on a given feeder such that the SE with these measurements will have the desired performance [73]. However, as pointed out before, the cost considerations usually limit the number of meters that can be placed on distribution feeders; usually below the minimum needed

for SE. To overcome this observability problem, forecasted load data needs to be added as pseudo-measurements. Therefore, the main goal of meter placement in DSs becomes supplementing the forecasted load data with real-time measurements such that the SE with these measurements will satisfy the performance requirements outlined in previous part of the research. Meter placement is a complex problem. This is not only due to size of the problem (number of choices available), but also often due to the conflicting requirements between the SE performance and the cost of the measurement system necessary to achieve the desired performance.

In this work, Rule Based Meter Placement Scheme, as a simple set of rules, is developed. It consists of few steps as follows:

Rule 1. Put meters at all the main switch and fuse locations that need to be monitored. These measurements will provide data especially for feeder switching and switch monitoring functions;

Rule 2. Put additional meters along the feeder line sections such that the total loads in the zones defined by the meters are similar in magnitude. These measurements can be of current type;

Rule 3. Put meters on normally open tie switches that are used for feeder switching. These meters can also be of current type. Voltage measurements at both ends of these tie switches are also desirable for monitoring and control of volt/var control devices from the substation and/or dispatch center.

The proposed method is a good compromise between the accuracy and the computational simplicity; it does not guarantee the optimality of the solution, but it is computationally simple.

Since in feeder operation, data needed for feeder switching is considered more important than the load distribution data, it may be hard to justify economically placing all the meters the above method will suggest. To help user eliminate some of the meters from this basic metering scheme, the authors adapted Koglin's method to rank these meters. The ranking will indicate the order with which the meters are to be eliminated. Ranking is based on the contribution of a measurement to the accuracy of the quantities that need to be estimated which are called interesting quantities, *y*. Authors define system accuracy index *a(z)* as:

$$a(z) = \sum_{i=1}^{k} \sigma_{yi}^{2}(z) \tag{5.3}$$

and use it to rank the measurements in the basic measurement set Z_0. In the previous equation, $\sigma_{yi}(z)$ is the variance of the *i*-th interesting quantity, *z* is the given metering scheme and *k* is total number of interesting quantities.

First measurements are taken out of the available measurement list one at a time and the resulting change in $a(z)$ is calculated. The measurement which causes the least change in $a(z)$ is then actually eliminated from the measurement set and the elimination process is repeated until all the measurements are eliminated and ranked.

The proposed meter placement and meter ranking methods are very effective in helping the user to identify these meters. The methods are also computationally simple and exploit the special features of radial feeders and feeder monitoring functions.

Work brought by H. Wang and N. Schulz [74] takes into consideration the development of automation in DSs, distribution SCADA and the fact that many automated meter reading (AMR) systems have been installed on DSs. Authors also explain that DMS has advanced and includes more sophisticated analysis tools. The combination of these developments is providing a platform for development of DSSE. A branch-current-based three-phase DSSE algorithm has been developed and tested. This method chooses the magnitude and phase angle of the branch current as the state variables. Because of the limited number of real-time measurements in the DS, the SE cannot acquire enough real-time measurements for convergence and authors conclude that pseudo-measurements are necessary for DSSE. The load estimated at every node from the AMR systems is used as a pseudo-measurement for the SE.

Authors point out that various constraints make it impossible to have a perfect picture of the system. First, because of the economic constraints, measurement instruments cannot be installed every place where the measurements are needed, so the data is incomplete. Second, because of the nature of the measurement instruments and the communication problems in transmitting the data back to the control center, the measured data are subject to error or lost communication, so the data may be inaccurate, unreliable and delayed.

The proposed DSSE algorithm uses the magnitude and phase angle of the branch current as the state variables. The measurements that are widely used on the DSs are incorporated. They are real and reactive branch power measurements, current magnitude measurements, power injection measurements and voltage magnitude measurements. The algorithm is implemented as the following steps:

Step 1. Initialization: Initialization of the current magnitude and phase angle has a great impact on the convergence speed of the algorithm. In this implementation, a two-step approach is used:
   a) Use a backward approach to get the initial value of current. In this step, set the initial value of voltage at every node to be a per unit value, and using the injected power at every node to calculate the branch current.
   b) Use a forward approach to get the initial value of voltage. In this step, using the branch current value calculated in a) and the root node voltage calculate the voltage at every node.

Step 2. Calculate the updates of the system state (branch current) using the following expression for the three phases separately:

$$\Delta x^{(n)} = \left[\mathbf{H}^{\mathrm{T}}(x^{(n)})\mathbf{R}^{-1}\mathbf{H}(x^{(n)})\right]^{-1} \times \mathbf{H}^{\mathrm{T}}(x^{(n)})\mathbf{R}^{-1}\left[z - h(x^{(n)})\right] \qquad (5.4)$$

where:

z measurements;

$h()$ measurement function;

$\mathbf{H}(x)$ the Jacobian of the measurement function $h(x)$;
R the covariance matrix of the measurement errors.

Step 3. Update the branch current using following expression and using the forward approach to calculate the node voltage:

$$x^{(n+1)} = x^{(n)} + \Delta x^{(n)} \tag{5.5}$$

Step 4. If it is smaller than a convergence tolerance (stop criterion), then stop. Otherwise, if the number of iteration is smaller than the pre-set maximum iteration number, go to step 2, if it is not, it does not converge.

From the above algorithm and test cases, some rules of meter placement for this proposed DSSE algorithm can be found:

- The results of the branch power measurements are the best. The current magnitude measurement comes the second. They are much better than the voltage magnitude measurement.
- Branch power and current magnitude measurements can provide better results when they are installed near the source and in the main feeder which has many downstream nodes, while the voltage magnitude measurement can provide better results when it is installed far from the primary substation.
- When meters are placed at different locations, the results are better.

Group of authors in [75] proposes an optimization algorithm suitable to choose the optimal number and position of the measurement devices needed to mitigate management and control issues, such as energy dispatching and protection coordination, in modern electric DNs. The goal of the proposed procedure, which is based on the dynamic programming, is to guarantee at the same time the minimum cost and the accuracy required to the measured data.

Authors point out that DSs are subject to deep changes arising from economic and technological reasons, such as the liberalization and the increasing integration of DG, i.e. small production plants located in several points of the distribution grid. The impact of such changes on the power system configuration creates new management, control and monitoring issues. The critical role of such operations requires the reliability of the results provided by the measurement devices in the network and reliable algorithms for the DSSE.

A system is observable whether it can be known in each own feature, e.g. if the relevant SE has a solution. A power system with a measurement device on each node can be totally known, but it is economically unacceptable.

The same solutions proposed for TSs usually cannot be directly applied to DNs, because of the different features of the two systems. Indeed, the number of the available measurements in DS is generally much smaller than the number of the state variables in the SE problem. The lack of enough real time measurements implies the requirement of numerous pseudo-measurements to obtain the observability of the system. On the other hand, the concept of distribution active network inherently requires accurate SE to perform on-line

network reconfiguration, to operate DG and renewable energy sources, and to implement load response policies with the final goal to exploit novel technologies deferring or avoiding network investments. As a consequence, for DSs it is necessary an *ad hoc* estimator able to give a good SE by reducing the number of measurement devices to as low as possible and this approach sustains the approach proposed by the authors in [68] and [69].

The main goal of a meter placement technique is to establish number, position and type of meters to be placed on a given system to achieve an observable system. The aim of a minimal meter placement is to obtain a DS that is observable with established accuracy and cost. The constraint on the maximum uncertainty, acceptable for the results means that, in each one of the B selected branches and/or nodes of the network, the estimated standard deviation (σ_{yi}, for i=1,…,B) of the quantity of interest y must not overcome the limit λ_{yi} imposed for that quantity in that node. Since these constraints could be met for different measurement sets, having the same minimum number of measurement units, the optimal set is the one that minimizes the function J, which is the weighted mean value of the variances of the quantities of interest:

$$J = \sum_{i=1}^{B} \left(\frac{\sigma_{yi}}{\lambda_{yi}} \right)^2 \qquad (5.6)$$
$$\text{subject to: } \sigma_{yi} < \lambda_{yi}, \forall i = 1, \dots, B$$

From a mathematical point of view, this is a non-linear combinatorial optimization problem.

Fig. 5.1 depicts the whole optimization algorithm. The procedure starts with a definition of those network nodes that are candidates to have a meter device. The inputs are the network topology, the line impedances and the real and reactive powers drawn by each node, along with their variances. A solution of the optimization problem is represented by a set of measurement devices allocated in a certain set of network nodes.

Preliminarily, for each load, a set of N possible values for real and reactive power is defined by means of a Gaussian distribution centered on the nominal values and having a prefixed standard deviation. Then, a Monte Carlo approach is used to define, by extracting a power value from each set, a set of N possible network conditions. The DSSE is performed on each of these situations, in order to achieve N reference conditions.

Then the algorithm starts by assuming that measurement devices are located only at the substation and DG bus bars. In the remaining nodes only pseudo-measurement can be considered.

On each one of the N networks, a Monte Carlo procedure is applied to take into consideration uncertainties in the measured data. Thus, M tests are performed in which the DSSE is run by using measured data randomly extracted from the sets defined by their nominal values and their uncertainty. As a consequence, for each branch current the distribution probability of the output values can be evaluated.

Then, the quality index J is calculated for each network, and the mean of such values:

$$Q = \frac{1}{N}\sum_{i=1}^{N} J_i \tag{5.7}$$

calculated over all the *N* network configurations, represents the *metric* by means of which the *quality* of the solution is synthetically evaluated. If the accuracy constraints are met for all current branches, such a solution represents the optimal one. Otherwise, additional measurement devices should be positioned, according to the optimization algorithm based on the dynamic programming.

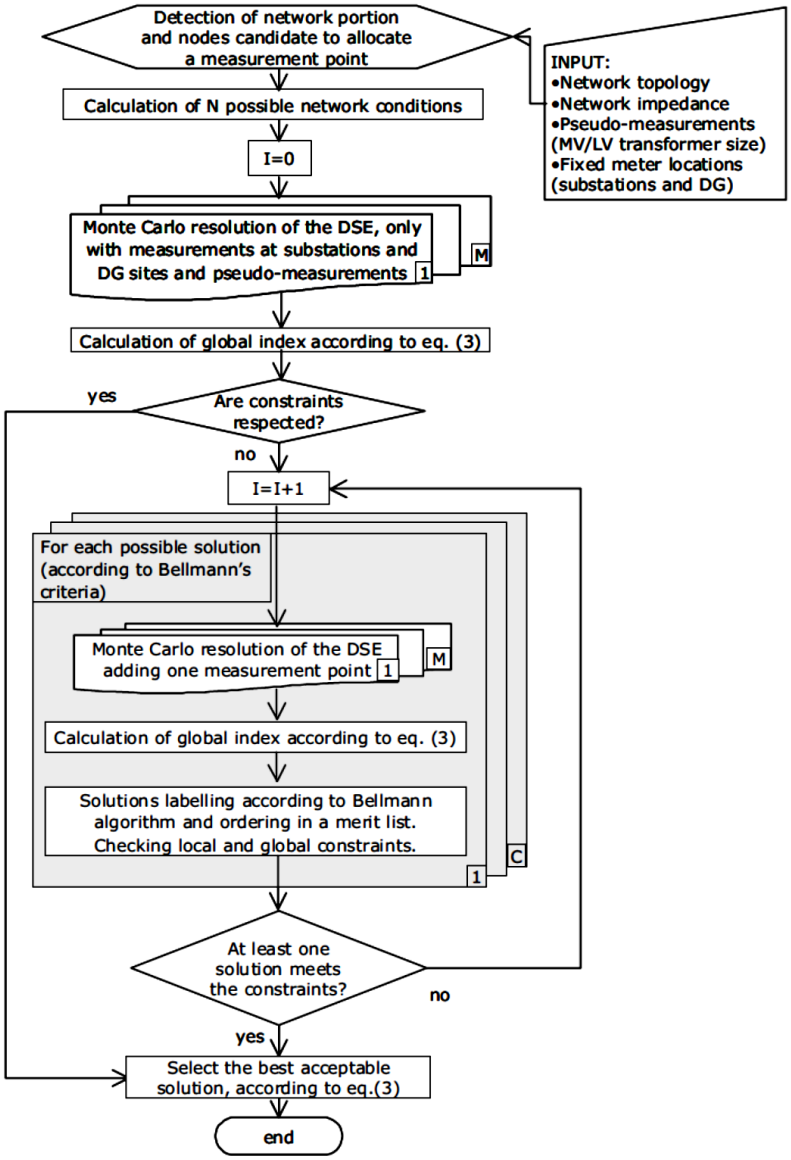

Figure 5.1: *Flow chart of the optimization algorithm for the OMEP in DNs [75]*

In this research the evaluation of the uncertainty affecting the results of the DSSE applied to the *N* network conditions is performed by means of a methodology based on a Monte Carlo statistical approach. This approach is based on the propagation of distributions: the entire probability density

functions (pdf) assigned to the input quantities, rather than only their variances, are used in the calculations. Monte Carlo methods exploit the capability of commercial software packages to generate sequences of random numbers, characterized by prefixed statistical parameters. The applied procedure can be summarized in the following three steps:

1) Characterizing the uncertainty on the measured data: all the relevant information available is used. A suitable probability distribution is then assigned to these uncertainty terms, which can be numerically represented by sets of random variables defined by the software package.
2) Performing a large number of simulated tests: in each test the measured data are corrupted by different contributions, whose values are extracted from the above sets, and the DSSE algorithm is applied by using this set of input data.
3) Processing the set of the obtained output values, which could be considered as the probability density function of the measurement result, whose standard deviation represents the standard uncertainty of the result.

Results of this study bring the following: it is not possible to understand *a priori* the effect of DG on the final optimal solution, thus justifying the resort to optimization tools. Indeed, DG in certain nodes allows reducing the number of measurements required by the SE in one part of the open loop network thanks to the small size of generator in comparison to loads and the particular allocation. On the other hand, if the generator has a much more significant impact in the part of the open loop network then SE algorithm may need more information on branch currents. This particular behavior is caused by the imposition of the injected power at some nodes, that modifies the PF equations.

Authors in [76] present a heuristic approach to identify potential points for location of voltage measurements for SE as part of a proposed DMS controller. The developed technique identifies measurement locations to reduce the voltage standard deviation of the bus bars which do not have a measurement. It addresses the problems of classical transmission meter placement methods, which are not directly applicable to DS due to limited measurements, and unobservability of the network.

The technique assumes that the voltages at those bus bars selected for a measurement are known within the accuracy of the measurement system. The location and number of these measurements are then adjusted so that the standard deviations of voltages at the unmeasured bus bars (caused by random load changes) are reduced to an acceptable minimum.

The algorithm uses the following equation to calculate the error between voltage magnitudes obtained initially from a PF using an estimate of maximum demands and results from series of PFs using random changes in the same loads.

$$\mathcal{E} = \sum_{m=1}^{M} (V_0^m - V_{rand}^m)^2 \tag{5.8}$$

The standard deviation of the voltage magnitudes resulting from these random variations in the loads for each bus bar is calculated using following Eq. 5.9. Fig. 5.2 shows a flowchart of the technique used to implement the algorithm. Standard deviation of the voltage magnitude at bus is:

$$w = \sqrt{\frac{\sum_{n=1}^{N}(V_{rand(w)}^{n} - \mu_{V_{rand(w)}})^2}{N-1}} \qquad \mu_{V_{rand(w)}} = \frac{\sum_{n=1}^{N} V_{rand(w)}^{n}}{N} \tag{5.9}$$

In the last two equations:

V_0^m voltage measurement at bus *m* obtained from initial PF;
V_{rand}^m voltage measurement at bus *m* resulting from random variation in loads;
$V_{rand(w)}^n$ *n*-th random voltage within *N* voltage sets at bus *w*;
$\mu_{V_{rand(w)}}$ mean voltage at bus *w*;
N number of voltage sets;
M total number of measurements;
w = 1,2,… all bus bars in the system (including the measurement bus bars).

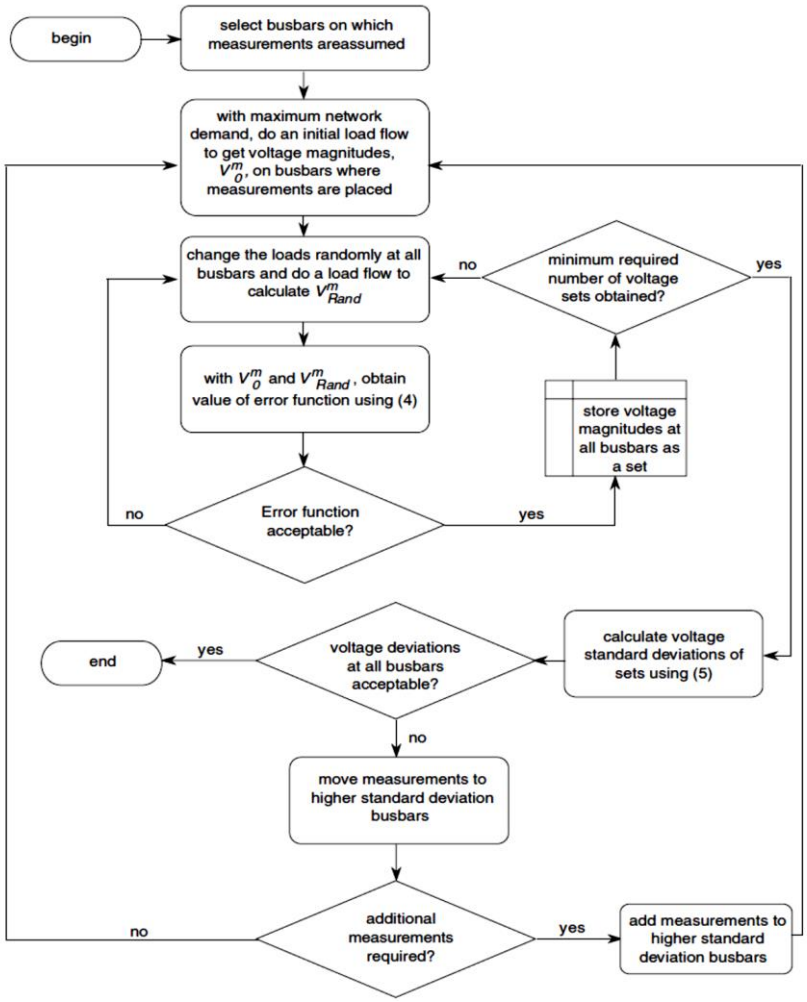

Figure 5.2: *Flow chart to locate potential measurement points for SE [76]*

The results of the study have shown that the topology of the network is important in placing the measurements. Measurement placement techniques for TSSE cannot be directly applied to DNs for the purpose of DSSE. This is both due to non-redundancy of measurements on these networks and the unobservable nature of the estimation process with the addition of few pseudo-measurements.

The authors conclude also that the technique does not obtain the global optimal measurement system for the network as is done in TSs and neither does it allocate measurements to overcome observability problems but identifies those points on the network with the higher voltage variations. The process provides a methodical approach to placing measurements on DSs for SE rather than relying only on engineering judgment.

The research developed in [77] is also concerned with improvement of the quality of voltage and angle estimates across a network, similar to the previous reference. The proposed technique is based on the sequential improvement of a bivariate probability index governing relative errors in voltage and angle at each bus. The meter placement problem is simplified by transforming it into a probability bound reduction problem [128], with the help of the two sided-Chebyshev inequality. A straightforward solution technique is proposed for the latter problem, based on the consideration of 2-σ error ellipses.

In this research, three types of measurements were considered. The voltage and flow measurements at the main substation and the substations with DGs were taken as real measurements. Zero injections, with a very low variance 10^{-8}, were modeled as virtual measurements. The error in the pseudo-measurements was chosen on the basis of the uncertainty in the load estimates of various classes of customers, like industrial, domestic and commercial. The loads of the industrial customer can be estimated fairly accurately. The load of the domestic customers is very difficult to estimate and will give rise to a large estimation error. The uncertainty in the commercial load estimates lies between the two. For a Gaussian distribution, a $\pm 3\sigma$ deviation about the mean accounts for more than 99.73% of the area under the Gaussian curve. For a given % of maximum error about the mean μ_{zi}, the standard deviation of the error was computed as follows:

$$\sigma_{zi} = \frac{\mu_{zi} \times \%error}{3 \times 100} \tag{5.10}$$

Observing the relative voltage and angle errors at different buses, authors concluded that when the measurement errors are small, the relative estimation errors in the voltages and angles, in more than 95% of simulation cases, are below their respective thresholds (i.e., 1% for voltage error and 5% for angle error). With the increase in errors in the pseudo-measurements from 20% to 50%, the voltage estimate errors do not violate their threshold in all the simulations, while the angle estimate errors violate their threshold in significant number of simulation cases. With increase in the errors in the real measurements from 1% to 3% both the errors in the voltage and the angle estimates violate the threshold limits. This violation is significantly more for

the voltage estimate errors than it is for the angle estimate errors. It can be understood that the errors in the voltage estimates are highly influenced by the errors in the real measurements and less influenced by the errors in the pseudo-measurements (loads). On the other hand, the errors in angle estimates are influenced by both. In the case when the errors in both real and pseudo-measurements are high, the errors in voltage and angle estimates significantly violate the limits. An efficient way to overcome this problem is to increase the number of real measurements, although it may not be economical to place large number of meters. Hence, a cost effective strategy for meter placement should take account of the following factors:

- location of meters;
- type of measurements;
- number of measurements;

The problem of meter placement is to identify the effective locations and the number of real measurements, so that the following probability indices:

$$p_i = Pr\left\{\left|\frac{\hat{V}^i - \hat{V}_t^i}{\hat{V}_t^i}\right| \leq \varepsilon_1, \left|\frac{\hat{\delta}^i - \hat{\delta}_t^i}{\hat{\delta}_t^i}\right| \leq \varepsilon_2\right\}, \text{ for } i = 2,\ldots,n \qquad (5.11)$$

In the previous equation:

$\hat{V}_t^i$, $\hat{\delta}_t^i$ true value of voltage and angle at the *i*-th bus, respectively;
$\hat{V}^i$, $\hat{\delta}^i$ estimated value of voltage and angle at the *i*-th bus, respectively;
ε_1 , ε_2 voltage and angle prespecified thresholds, respectively;
n number of the buses of DN.

Measurement Placement – The voltage measurements can efficiently bring down the relative errors in the voltage estimates below threshold, but in some cases the same may not be achieved for the angle estimates even with the help of a large number of voltage meters. The reasons for this are evident from Fig. 5.3(a) and (b). As shown in Figure 5.3(a), at a given bus, the two axes of the error ellipse are not aligned in the direction of coordinate axes. This implies that the errors in voltage and angle estimates are correlated. In this case the error reduction in the voltage estimate consequently reduces the error in angle estimate and vice versa. The reduction of the error estimate in one variable with respect to the other depends upon the degree of correlation between the two. A stronger correlation implies that the error reduction in one variable significantly reduces the error in the other.

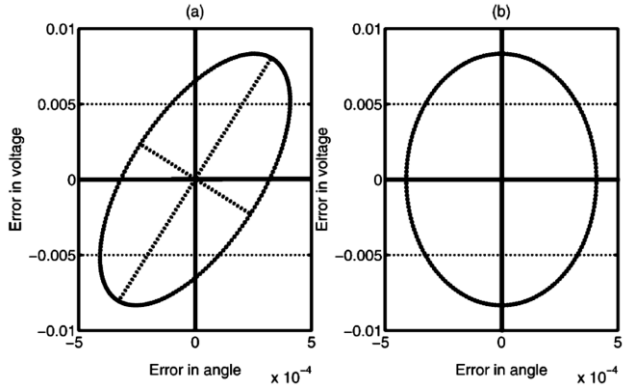

Figure 5.3: *Voltage and angle error ellipse: errors are (a) correlated, (b) uncorrelated [77]*

In Figure 5.3(b), the ellipse axes are in the direction of coordinate axes. This means the errors in voltage and angle estimates are uncorrelated and hence the reduction of one does not influence the other.

The process for the location and number of these measurements is as follows:

Step 1. Run WLS over a set of Monte Carlo simulations and observe the relative errors in voltages and angles in each simulation at all the buses.

Step 2. If in more than 95% of the cases the relative errors in the voltages and angles are below their specified thresholds, respectively (i.e., 1% for voltage (ε_1) and 5% for angle (ε_2)), stop; else go to Step 3.

Step 3. If only the relative errors in voltage estimates satisfy the criterion in Step 2, go to Step 6; else Step 4.

Step 4. Take the mean of the state error covariance matrix over all the Monte Carlo simulations and extract the sub-matrices corresponding to the voltage and angle at each bus.

Step 5. At every bus compute the area of the error ellipse from the determinant of sub-matrix and identify the bus with the largest area and place the voltage measurement at this bus. If measurement is already present choose the bus with the next largest area. Go to Step 1.

Step 6. Compute the mean of error covariance matrix corresponding to the real and reactive power flow, in each line.

Step 7. For each line compute the area of the line flow error ellipse and place the flow measurement in the line with the largest area. If the measurement is already present choose the line with the next largest area. Go to Step 1.

The procedure is sequential and stops when the desired level of accuracy in estimates is achieved. The advantage of the method is that it reduces the errors in both voltage and angles by exploiting the error correlations under a wide range of uncertainty in the pseudo-measurements. However, authors notice that it produces feasible but not necessarily optimal solution. The performance of the technique needs further investigation in view of the possible presence of the leverage points in the network.

Finally, multi-objective optimization by implementing genetic algorithms was used in research conducted by B. Milosevic and M. Begovic [78]. This research considers PMU placement problem requiring simultaneous optimization of two conflicting objectives, such as minimization of the number of PMUs and maximization of the measurement redundancy.

The problem considered is the placement of a minimum set of PMUs, so that the system is topologically observable (all of the bus voltage phasors can be estimated) during its normal operation and following any single-line contingency:

$$\min_{x \in S}\{K, -R\} \quad \text{Subject to: U = 0} \tag{5.12}$$

where:

S search space;
K total number of PMUs to be placed in the system;
R system single line-outage redundancy, expressed as a number of buses that are observable following any single-line outage;
U total number of unobservable buses.

This is a typical multi-objective optimization problem requiring simultaneous optimization of two objectives with different individual optima. Objectives are such that none of these can be improved without degradation of another. Therefore, instead of a unique optimal solution, there exists a set of optimal trade-offs between the objectives, the so-called Pareto-optimal solutions.

The concept of Pareto optimality may be explained in terms of a *dominance relation* [79]. For a multi-objective problem having *k* objective functions to be simultaneously minimized, a solution *x* is said to dominate the other solution *y* if is better than *y* for at least one objective f_i and is not worse for any other f_j, where $j = 1,\ldots,k$ and $j \neq i$.

$$f_i(x) < f_i(y) \text{ and } f_j(x) \leq f_j(y) \text{ then } x \succ y \tag{5.13}$$

Here, the symbol $\succ$ denotes domination operator; $x, y \in P$, where $P \subseteq S$ and *S* denote the entire search space. The above concept is used to find a set of non-dominated solutions in *P*. These solutions are equally optimal when all objectives are considered, for none of them is dominated by any other solution in *P*. The solutions that are non-dominated regarding the entire search space are called *Pareto-optimal solutions*. The hypersurface connecting those defines the *Pareto-optimal front*.

A minimum set of PMUs to ensure system topological observability $\widehat{K}_{min}$ is estimated by building a spanning measurement tree of full rank across the system. Since the PMU provides measurements of voltages, as well as all incident current phasors at the buses where it is located, a calculated current phasor is assigned to any branch connecting two buses with known voltage phasors, and to any branch whose current can be found by using Kirchoff's current law. A bus is considered observable ("covered") if its voltage phasor is either directly measured or calculated by using the available measured/calculated voltage and current phasors.

The algorithm iterates two main steps until a set of unobservable buses is exhausted: 1) bus ranking; and 2) selection of PMU locations among the highest ranked buses by using a simple GA.

To reduce the number of PMU candidate locations, buses where PMUs need and need not be placed are identified so that the system topological observability is possible with minimum number of PMUs. These buses are then removed from the initial set that comprises all system buses.

Buses are ranked in decreasing order of their *coverage index C*, where *C(i)* is defined as the number of buses that become observable after a PMU has been placed at bus *i*. Nodes with the highest coverage index are then identified. If the total number of such buses, denoted as *m*, is equal to 1, a PMU is placed at the corresponding bus, and the bus-ranking step is repeated.

Otherwise, these m buses represent the candidate locations for PMU placement and a simple GA is used to select the optimal ones among them.

The algorithm starts with a set of PMUs that ensures the system topological observability. The additional PMUs are then added by iterating the bus-ranking step and the GA step, until maximum measurement redundancy R_{max} has been achieved. In the bus-ranking step, the buses are ranked based on the modified coverage index C_R which is defined as the number of buses that are observable following any single-line outage, after a PMU has been placed at the corresponding bus. In the GA step, the chromosomes are evaluated based on the objective function R_R, given as a total number of buses in the system "covered" by PMUs more than twice.

The population is classified into subsets (fronts) of individuals sharing the same non-dominance properties, as shown in Fig. 5.4.

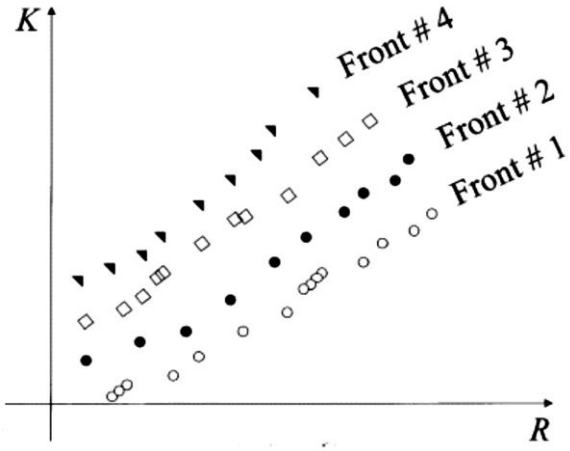

Figure 5.4: *Population classification into fronts [78]*

The infeasible solutions are repaired by removing the non-optimally placed PMUs, and adding the additional ones, until the topological observability is obtained. A PMU is considered non-optimally located if the number of (un)observable buses remains the same when removed from the system.

The algorithm terminates when the number of generations reaches the predetermined maximum value G_{max}. However, it could end in a number of ways depending of decision maker's satisfaction criteria.

The analysis of the computational complexity of the algorithm reveals that most of the overhead is due to the solution repair (correction of infeasible solutions). This imposes a limitation on the size of the problems that can practically be handled using the proposed technique.

The important advantage of the algorithm and the justification for its complexity are that it provides the entire Pareto-optimal front instead of a single point solution, and could lend itself to application in an entire class of problems where multi-objective optimization on a prohibitively large enumerative search space is required.

5.2.1 Critical review of the proposed bibliography

Approaches reported in [71] and [72] address the problem of OMEP or similar approaches at transmission level. Unfortunately, as already stated, mechanisms used in TS are not applicable in DS, firstly because of the topological differences between them, further, because regarding observability there are completely different. TN is in much better situation then DN regarding observability with significantly larger number of measurements present. TNs satisfy the conditions of redundancy, while DNs no.

Approach and results provided in [73] bring an interesting perspective of the problem but the limitations are reflected in the fact that the approach is designed for simple test DNs that do not correspond to complex real systems of today and advanced DSOs requirements. Also, approach proposes the placement of too many measurement equipment from the point of economic criteria.

Work elaborated in [74] is based on three-phase model for SE. This is not applicable for real MV grids: the loads are generally balanced and the cables parameters (especially mutual coupling) are not known.

Approach proposed by [75] is interesting because it includes DG in the problem of OMEP in DSs. However, the major problem in this case as well as in [77] is using of Monte Carlo simulations for the solution of the problem and its practical inability to face the large scale problems such as DSSE and DS OMEP. To elaborate on this, one should assume that the real and reactive power flows in a line are measured together. The complete measurement set Ω consists of $n + 2l$ elements, where n is the number of voltage magnitudes, and l is the number of line real and reactive power pairs (which coincides with the number of line current magnitudes). The number of combinations of deploying k meters is then:

$$N = \binom{n+2l}{k} = \frac{(n+2l)!}{k!\,(n+2l-k)!} \tag{5.14}$$

This is typically a very large number. Bearing in mind that Monte Carlo evaluation of the cost is computationally expensive, one can see that exhaustive search that is yield by implementing Monte Carlo simulations is not a practical option [80].

For instance, if the DN has $n = 95$, $l = 94$ and $k = 5$ (and this is a small DN compared to real size DNs), there are 1.45×10^{10} possible choices to be examined. Although the number of choices can be reduced by exploiting the structure of the problem, for example by excluding measurements on lines which are connected to zero-injection buses, exhaustive search still may not be a viable option for large-scale problems.

Work reported in [76] presents one of the first attempts in DN to solve the problem of OMEP. However, authors themselves note that their solution does not present the optimal solution of the problem nor it allocate measurements to overcome observability problems but identifies those points on the network with the higher voltage variations. Also, only voltage measurements are considered.

Approach reported in [77] brought a new view on the problem of OPM. The problem of implementation with Monte Carlo simulations is already addressed. To continue, authors assume a Gaussian distribution for the load profile uncertainties. This is, however, inconsistent with real situation, due to the fact that loads are estimated according to energy curves. So, although the paper is very interesting from the point of view of the information it provides, it does not correspond to real life situation. One more limitation is that the research deals only with voltage measurements, which makes it very limited. To conclude, authors themselves notice that the solution produces feasible but not necessarily optimal solution and that further investigation is necessary.

Finally, work reported in [78] is quite a pioneering approach but its practical usefulness is limited due to the fact that it uses PMUs to solve the problem of OMEP. As it was already discussed in Chapter 4, the introduction of PMUs in a realistic DN is very rare nowadays. The other problem of this solution is that it covers only topological observability and not both topological and numerical, nor it explores the state of the network by SE. This is definitely a limiting factor.

In conclusion, the works presented here do not take into account some important aspects of the present DNs:

- the size and complexity of modern DNs;
- requirements of DSOs;
- available information of the realistic networks;
- adequacy of the approaches for the realistic DNs;
- economic burden of proposed solutions…

5.3 Optimization of Measurement Equipment Placement Mathematical Model

The mathematical model of the OMEP problem can be formally defined as a generalization of the advance state estimation model described by Eq. (4.56) in subchapter 4.3.5, including the possibility to change and add or eliminate various measurement equipment. For this, it is necessary to consider all the possible measurement locations and types for the entire DN and associate a new variable to each of them; this variable quantifies if a certain quantity, located in a certain point in the network, is measured or not. Moreover, the objective function needs to also take into account the quality of DN observability. Therefore, the OMEP model can be defined as:

$$\min \sum_{i=1}^{N_t} \left(\frac{\alpha_i}{x_i^m}\right)^2 \cdot Y_i - f_{obs}(V_M, V_A, \mathbf{x^{est}}, \alpha) \tag{5.15a}$$

$$s.t.\ f_P(V_M, V_A, \mathbf{x^{est}}) = 0 \tag{5.15b}$$

$$f_Q(V_M, V_A, \mathbf{x^{est}}) = 0 \tag{5.15b}$$

$$\mathrm{Y}_i(\mathbf{x^m} - \mathbf{x^{est}} + \boldsymbol{\alpha}) = 0 \tag{5.15c}$$

$$\sum_{i=1}^{N_t} Y_i \leq N_p \tag{5.15d}$$

where:

Y_i binary variable that models the existence of a measurement equipment for the *i*-th measurable quantity, be it *V*, *I*, *P*, *Q*; when Y_i is 1, the *i*-th quantity is measured, when it is 0, it is not;
f_{obs} function quantifying the quality of DNs observability;
N_t total number of measurements that can be considered in the DN;
N_p maximum number of measurement equipment to install in the network;
The rest of the quantities have been already defined in subchapter 4.3.5.

As with the DSSE model (4.56), the first term in the objective function (5.15, a) minimizes the estimation errors for the measured quantities, i.e. for the quantities for which $Y_i = 1$. In details, for all the $Y_i = 1$ equations (5.15, b) and (5.15, c) together with the first term of (5.15, a) constitute the previously formulated DSSE model (4.56), and hence, the estimation of networks state for a certain measurement configuration is thus assured. Further, constraint (5.15, d) provides that a limited number of measurement equipment is installed in the network; at limit this number can be strictly imposed by converting this constraint into an equality constraint. Finally, in order to guide the search of the optimal set of measurement locations, the second term in the objective function (5.15, a), i.e. $f_{obs}(V_M, V_A, \mathbf{x^{est}}, \alpha)$, quantifies the quality of the observability of the DN in its whole. Since the electric state of a bus is completely described by *V*, *φ*, *P* and *Q*, in its most general form, this function should sum the estimation errors of *V*, *φ*, *P* and *Q* in all the buses:

$$f_{obs} = \sum_{i=1}^{N_{bus}} \left(\left| \frac{V_i^{act} - V_i^{est}}{V_i^m} \right|^2 + \left| \frac{\varphi_i^{act} - \varphi_i^{est}}{\varphi_i^m} \right|^2 + \left| \frac{P_i^{act} - P_i^{est}}{P_i^m} \right|^2 + \left| \frac{Q_i^{act} - Q_i^{est}}{Q_i^m} \right|^2 \right) \qquad (5.16)$$

where:
V_i^{act} actual value of the voltage magnitude of *i*-th bus;
V_i^{est} estimated value of the voltage magnitude of *i*-th bus computed by DSSE;
φ_i^{act} actual value of the phase angle of *i*-th bus;
φ_i^{est} estimated value of the phase angle of *i*-th bus computed by DSSE;
P_i^{act} actual value of the real power of *i*-th bus;
P_i^{est} estimated value of the real power of *i*-th bus computed by DSSE;
Q_i^{act} actual value of the reactive power of *i*-th bus;
Q_i^{est} estimated value of the reactive power of *i*-th bus computed by DSSE.

This is a mix integer non-linear programming (MINLP) problem, including strongly non-linear PF constraints, for which is not so simple to write and solve a convex relaxation. . However, much harder to deal with with when solving this model is the combinatorial dimension of the problem. For a realistic DN the problem becomes very large in terms of possible feasible discrete solutions. In particular, for a radial network consisting of *N* buses (so, *N*-1 branches), as presented in Chapter 4, it is possible to install *N* voltage measurements, *N* real and *N* reactive power measurements of the loads as well as *N* real and *N* reactive power measurements of the generation in each bus of the system, and *N*-1 real, *N*-1 reactive power flow and *N*-1 current flow

measurements, resulting a total of $7N$-3 possible measurements to install in all the network. For a specified maximum number of measurement equipment N_p the total number of feasible combination is:

$$\binom{7N-3}{N_p} = \frac{(7N-3)!}{N_p!\,(7N-3-N_p)}$$

This means that for an average size DN of 500 buses with N_p = 100 measurements, there are approximately 3500 discreet variables and the number of possible feasible values of Y is given by the following number of combinations:

$$\binom{3500}{100} = 6.56 \cdot 10^{195}$$

Therefore, it is hard to imagine that a combinatorial problem of this size can be solved using traditional relaxation techniques such as Branch and bound [147] or Lagrange relaxations [148].

At this point it is important to notice that this problem can be separated into two distinctive sub-problems:

- discreet problem i.e. finding the optimal measurement equipment configuration – the optimal Y_i obtained by minimizing f_{obs}; and
- for each possible configuration - Y_i - there is a continuous sub-problem, i.e. the SE.

Therefore, a more computationally simple alternative is to efficiently explore a sub-space of the solution space by a heuristic search technique to find a sub-optimal solution for the vector Y and solving, in the same time, the already developed state estimation algorithm to correctly evaluate f_{obs} for each possible Y.

Generally, finding the solution in this way can be made according to the flow chart of Fig. 5.5. Firstly, one possible discrete solution, configuration $Y_{possible}$ is chosen. $Y_{possible}$ refers to feasible solution i.e. the solution that satisfies the constraints, but not necessarily optimal. Then ASE algorithm, developed in Chapter 4, is run, function f_{obs} is computed and the convergence criterion is checked. It can be maximum number of iterations allowed, maximum computation time or some other criteria. If the solution satisfies the criteria, the optimization is finished, otherwise, another feasible configuration is found according to the considered heuristic search algorithm and the process is repeated until convergence.

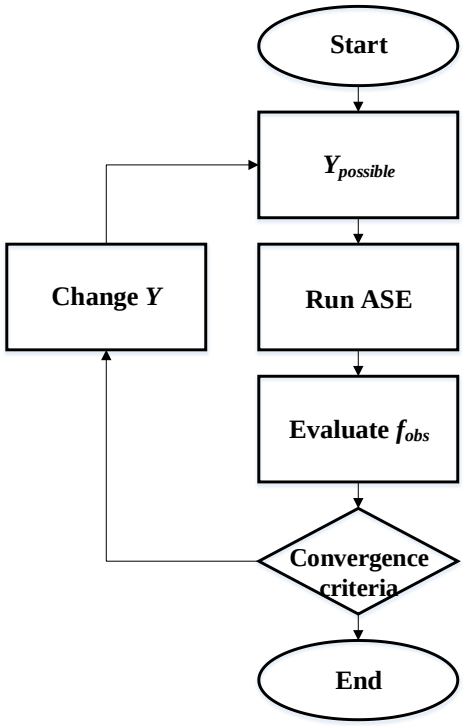

Figure 5.5: *Flow chart of the problem solution*

In this dissertation, the use of evolutionary techniques, in particular genetic algorithms, was selected for the heuristic search part. This optimization approach uses the good properties of the possible solutions and combines them together to produce better offspring. In the following subchapters, these techniques will be explained in detail. Moreover, the particular form of the OMEP problem (5.15) adapted for the use of evolutionary techniques will be detailed. Lastly, various considerations will be made concerning the reduction of the search space.

5.4 Evolutionary Algorithms for Large-Scale Problems

5.4.1 Evolutionary Algorithms vs. Classical Techniques

This part of the dissertation is dedicated to the solution of OMEP problem. As the title already states, the aim is to optimize a large-scale problem as the planning of DN definitely is. Solving the real-life large problems of efficiently allocating limited resources, as well as developing and managing complicated systems, and designing strategies for decision makers to cope with different conflicting situations have always been demanding for individuals and organizations [81]. To cope with these kinds of hard problems, optimization is the key discipline that can facilitate the operators with quantitative decision-making and decision analysis by applying scientific methods and technologies. Optimization is the sub-discipline of applied mathematics, where the aim is either to minimize or maximize the output of a function over a set of input variables subject to a set of constraints.

Many of the optimization problems are combinatorial optimization [82], where the desired optimal solutions are certain combinations of variable settings (possibilities) from a finite pool [83]. Though some combinatorial

optimization problems have well-known polynomial time algorithms, there is a family of combinatorial optimization problems which is NP-hard. The NP-hard [84] problems are very complex with huge search spaces and no exact algorithm is known to solve them in polynomial time.

Many of the real-life NP-hard optimization problems are planning problems. Planning problems can be defined in different ways depending on the related field. The research covered by this chapter of the dissertation is on planning the future distribution grid or extending the existing one with the installation of the measurement equipment. As already said, this problem is to be one of the central points of Smart Grid managing already today and even more in a near future [129].

When a choice is made regarding the optimization tool for the solution of the problem, one has to realize that in the large-scale realistic problems, it is rarely possible to find the optimal solution which is offered by implementation of the exhaustive search. This is because this type of search needs to cover the entire search space at a time. Also, in order to model the data, some techniques like Monte Carlo simulations need to be utilized. OMEP for realistic DNs cannot be solved in this manner.

Classical optimization techniques, like exhaustive search, are incapable of solving multi-objective problems. This group of problems is computationally highly demanding and even if the computational time is not considered as an obstacle, which obviously is, classical techniques show significant convergence problems.

On the other side, Evolutionary Algorithms (EAs) are powerful and sophisticated tools for optimization of the large-scale problems like this one. The advantage of this method over many others is that it looks for the solution over the group of possible solutions rather than whole search space at the time and it combines the good properties of the individuals to produce better offspring. Other multiple advantages of EAs over other methods are: conceptual simplicity, proven broad applicability, outperformance of the classical methods on real problems, potential to use knowledge and hybridize with other methods, parallelism, robustness to dynamic changes, capability for self-optimization, ability to solve problems that have no known solutions etc.

Another important characteristic of EA is that it is possible to apply EA even if the gradient and the Hessian of the OF and constraints do not exist (due to the presence of binary/integer variables).

5.4.2 Introduction to Evolutionary Algorithms

An EA is a stochastic iterative procedure for generating tentative solutions for a certain problem. The algorithm manipulates a collection P of individuals (the *population*), each of which comprises one or more chromosomes. These chromosomes represent a potential solution for the problem under consideration. An encoding/decoding process is responsible for performing this mapping between chromosomes and solutions. Chromosomes are divided into smaller units termed *genes*. The different values a certain gene can take are called the *alleles* for that gene [130].

Initially, the population is generated at random or by means of some heuristic seeding procedure. Each individual in P receives a *fitness* value: a

measure of how good the solution is for the problem being considered. Subsequently, this value is used within the algorithm for guiding the search. The whole process is sketched in Figure 5.6.

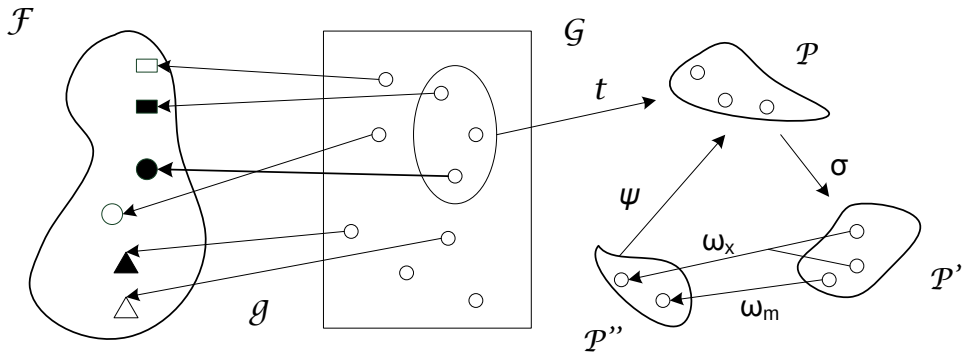

Figure 5.6: *Illustration of the evolutionary approach to optimization [130]*

As it can be seen, it is assumed the existence of a set *F* (also known as *phenotype space*) comprising the solutions for the problem at hand. Associated with *F*, there also exists a set *G* (known as *genotype space*). These sets *G* and *F* respectively constitute the domain and codomain of a function *g* known as the *growth* (or *expression*) function. It could be the case that *F* and *G* were actually equivalent, being *g* a trivial identity function. However, this is not the general situation. As a matter of fact, the only requirement posed on *g* is surjectivity. Furthermore, *g* could be undefined for some elements in *G*.

After having defined these two sets *G* and *F*, one should notice the existence of a function *t* selecting some elements from *G*. This function is called the *initialization* function, and these selected solutions (also known as *individuals*) constitute the so-called *initial population*. This initial population is in fact a pool of solutions onto which the EA will subsequently work, iteratively applying evolutionary operators to modify its contents. More precisely, the process comprises three major stages: *selection* (promising solutions are picked from the population by using a selection function σ), *reproduction* (new solutions are created by modifying selected solutions using some reproductive operators ω_i), and replacement (the population is updated by replacing some existing solutions by the newly created ones, using a replacement function ψ). This process is repeated until a certain termination criterion (usually reaching a maximum number of iterations) is satisfied. Each iteration of this process is commonly termed a *generation*.

5.4.3 Diversification of Evolutionary Algorithms

EAs, as we know them now, began their existence during the late 1960s and early 1970s (some earlier references to the topic exist [85]). In these years, and almost simultaneously, scientists from different places in the world began the task of putting nature at work in algorithmics, and more precisely in search or problem solving duties. The existence of these different primordial sources originated the rise of three different EA models. These classical families are:

- *Evolutionary Programming* (EP): this EA family originated in the work of Fogel *et al.* [86]. EP focuses in the adaption of individuals rather than in the evolution of their genetic information. This implies a much more abstract view of the evolutionary process, in which the behavior of individuals is directly modified (as opposed to manipulating its genes). This behavior is typically modeled by using complex data structures such as finite automata or as graphs (see Figure 5.7-left). Traditionally, EP uses asexual reproduction, also known as mutation, i.e. introducing slight changes in an existing solution and selection techniques based on direct competition among individuals.

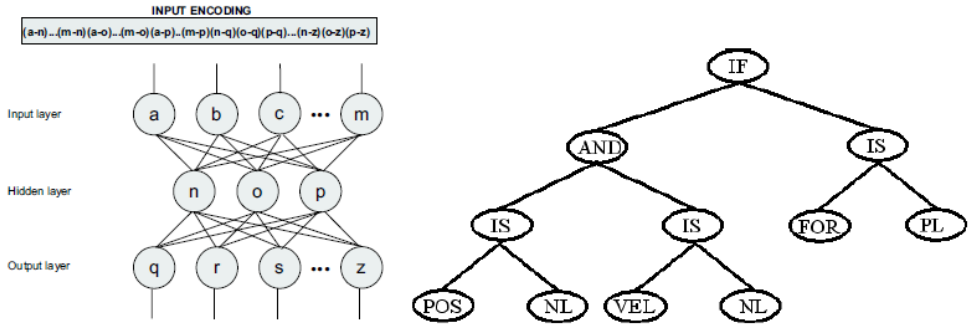

Figure 5.7: *Two examples of complex representations - (Left) A graph representing a neural network. (Right) A tree representing a fuzzy rule. [130]*

- *Evolution Strategies* (ES): these techniques were initially developed in Germany by Rechenberg and Schwefel [88],[89]. Their original goal was serving as a tool for solving engineering problems. With this goal in mind, these techniques are characterized by manipulating arrays of floating-point numbers (there exist versions of ES for discrete problems, but they are much more popular for continuous optimization). As EP, mutation is sometimes the unique reproductive operator used in ES; it is not rare to also consider Crossover (i.e. the construction of new solutions by combining portions of some individuals) though. A very important feature of ES is the utilization of self-adaptive mechanisms for controlling the application of mutation. These mechanisms are aimed at optimizing the progress of the search by evolving not only the solutions for the problem being considered, but also some parameters for mutating these solutions (in a typical situation, an ES individual is a pair $(\vec{x}, \vec{\sigma})$, where $\vec{\sigma}$ is a vector of standard deviations used to control the Gaussian mutation exerted on the actual solution $\vec{x}$).
- *Genetic Algorithms* (GA): GAs are possibly the most widespread variant of EAs. They were conceived by Holland [90]. His work has had a great influence in the development of the field, to the point that some portions, arguably extrapolated, of it were taken almost like dogmas (i.e. the ubiquitous use of binary strings as chromosomes). The main feature of GAs is the use of a recombination (or *crossover*) operator as the primary search tool. The rationale is the assumption that different parts of the optimal solution can be independently discovered, and be later combined to create better solutions. Additionally, mutation is also used, but it was usually considered a secondary background operator whose purpose is merely "keeping the pot boiling" by introducing new information in the

population (this classical interpretation is no longer considered valid though).

These families have not grown in complete isolation from each other. On the contrary, numerous researchers built bridges among them. As a result of this interaction, the borders of these classical families tend to be fuzzy, and new variants have emerged. The following can be cited:

- *Evolution Programs*: this term is due to Michalewicz [91], and comprises those techniques that, while using the principles of functioning of GAs, evolve complex data structures, as in EP. Nowadays, it is customary to use the acronym GA, or more generally EA, to refer to such an algorithm, leaving the term "traditional GA" to denote classical bit-string based GAs.
- *Genetic Programming (GP)*: the roots of GP can be traced back to the work of Cramer [92], but it is undisputable that it has been Koza [93] the researcher who promoted GP to its current status. Essentially, GP could be viewed as an evolution program in which the structures evolved represent computer programs. Such programs are typically encoded by trees (see Figure 5.7-right). The final goal of GP is the automatic design of a program for solving a certain task, formulated as a collection of (input, output) examples.
- *Memetic Algorithms (MA)*: these techniques owe their name to Moscato [94]. Some widespread misconception equates MAs to EAs augmented with local search; although such an augmented EA could be indeed considered a MA, other possibilities exist for defining MAs. In general, a MA is problem-aware EA [95]. This problem awareness is typically acquired by combining the EA with existing algorithms such as hill climbing, branch and bound, etc.

5.4.4 Detailed Structure of Evolutionary Algorithm

Once the general structure of an EA has been presented, more detail on the different components of the algorithm will be provided.

5.4.4.1 Fitness Function

This is an essential component of the EA, to the point that some early (and nowadays discredited) views of EAs considered it as the unique point of interaction with the problem that is intended to be solved. This way, the fitness function measured how good a certain tentative solution is for the problem of interest. This interpretation has given rise to several misconceptions, the most important being the equation "fitness = quality of a solution". There are many examples in which this is simply not true [87], e.g., tackling the satisfability problem with EAs (that is, finding the truth assignment that makes a logic formula in conjunctive normal form be satisfied). If quality is used as fitness function, then the search space is divided into solutions with fitness 1 (those satisfying the target formula), and solutions with fitness 0 (those that do not satisfy it). Hence, the EA would be essentially looking for a needle in a haystack (actually, there may be more

than one needle in that haystack, but that does not change the situation). A much more reasonable choice is making fitness be the number of satisfied clauses in the formula by a certain solution. This introduces a gradation that allows the EA "climbing" in search of near-optimal solutions.

The existence of this gradation is thus a central feature of the fitness function, and its actual implementation is not that important as long this goal is achieved. Of course, implementation issues are important from a computational point of view, since the cost of the EA is typically assumed to be that of evaluating solutions. In this sense, it must be taken into account that fitness can be measured by means of a simple mathematical expression, or may involve performing a complex simulation of a physical system. Furthermore, this fitness function may incorporate some level of noise, or even vary dynamically. The remaining components of the EA must be defined accordingly so as to deal with these features of the fitness function, e.g., using a non-haploid representation [96] (i.e., having more than one chromosome) so as to have a genetic reservoir of worthwhile information in the past, and thus be capable of tackling dynamic changes in the fitness function.

It should be noticed that there may even exist more than one criterion for guiding the search (e.g., we would like to evolve the shape of a set of pillars, so that their strength is maximal, but so that their cost is also minimal). These criteria will be typically partially conflicting. In this case, a *multi-objective* problem is being faced. This can be tackled in different ways, such as performing an aggregation of these multiple criteria into a single value, or using the notion of Pareto dominance (i.e., solution x dominates solution y if, and only if, $f_i(x)$ yields a better or equal value than $f_i(y)$ for all i, where the f_i's represent the multiple criteria being optimized).

5.4.4.2 Initialization

In order to have the EA started, it is necessary to create the initial population of solutions. This is typically addressed by randomly generating the desired number of solutions. When the alphabet used for representing solutions has low cardinality, this random initialization provides a more or less uniform sample of the solution space. The EA can subsequently start exploring the wide area covered by the initial population, in search of the most promising regions.

In some cases, there exists the risk of not having the initial population adequately scattered all over the search space (e.g., when using small populations and/or large alphabets for representing solutions.) It is then necessary to resort to systematic initialization procedures [99], so as to ensure that all symbols are uniformly present in the initial population.

This random initialization can be complemented with the inclusion of heuristic solutions in the initial population. Thus, the EA can benefit from the existence of other algorithms, using the solutions they provide. This is termed *seeding*, and it is known to be very beneficial in terms of convergence speed, and quality of the solutions achieved [97],[98]. The potential drawback of this technique is having the injected solutions taking over the whole population in a few iterations, provoking the stagnation of the algorithm. This problem can be remedied by tuning the selection intensity by some means (e.g., by making an adequate choice of the selection operator).

5.4.4.3 Selection

In combination with replacement, selection is responsible for the competition aspects of individuals in the population. In fact, replacement can be intuitively regarded as the complementary application of the selection operation.

Using the information provided by the fitness function, a sample of individuals from the population is selected for breeding. This sample is obviously biased towards better individuals, i.e., good, according to the fitness function, solutions should be more likely in the sample than bad solutions and this is the function of the selection.

The most popular techniques are fitness-proportionate methods. In these methods, the probability of selecting an individual for breeding is proportional to its fitness, i.e.:

$$p_i = \frac{f_i}{\sum_{j \in P} f_j} \tag{5.17}$$

where f_i is the fitness of individual i, and p_i is the probability of i getting into the reproduction stage. This proportional selection can be implemented in a number of ways. For example, *roulette-wheel selection* rolls a dice with $|P|$ sides, such that the i-th side has probability p_i. This is repeated as many times as individuals are required in the sample. A drawback of this procedure is that the actual number of instances of individual i in the sample can largely deviate from the expected $|P| \cdot p_i$. *Stochastic Universal Sampling* [100] (SUS) does not have this problem, and produces a sample with minimal deviation from expected values.

Fitness-proportionate selection faces problems when the fitness values of individuals are very similar among them. In this case, p_i would be approximately $|P|^{-1}$ for all $i \in P$, and hence selection would be essentially random. This can be remedied by using fitness scaling. Typical options are [90]:

- Linear scaling: $f_i' = a \cdot f_i + b$ for some real numbers a, b;
- Exponential scaling: $f_i' = (f_i)^k$, for some real number k;
- Sigma truncation: $f_i' = \max(0, f_i - (\bar{f} - c \cdot \sigma))$, where $\bar{f}$ is the mean fitness of the individuals, σ is the fitness standard deviation and c is a real number.

Another problem is the appearance of an individual whose fitness is much better than the remaining individuals. Such *super-individuals* can quickly take over the population. To avoid this, the best option is to use non-fitness-proportionate mechanism. A first possibility is *ranking selection* [101]: individuals are ranked according to fitness (best first, worst last), and later selected, e.g. by means of SUS, using the following probabilities:

$$p_i = \frac{1}{|P|}\left[\eta^- + (\eta^+ - \eta^-)\frac{i-1}{|P|-1}\right] \tag{5.18}$$

where p_i is the possibility of selecting the i-th best individual, and $\eta^+ + \eta^- = 2$

Another possibility is using *tournament selection* [102]. A direct competition is performed whenever an individual needs be selected. To be precise, α individuals are sampled at random, and the best of them is selected for reproduction. This is repeated as many times as needed. The parameter α is termed the *tournament size*; the higher this value, the stronger the selective pressure. These non-proportionate selection methods have the advantage of being insensitive to fitness scaling problems and to the sense of optimization (maximization or minimization). For a theoretical analysis of the properties of different selection operators more can be found in [101],[102].

Regardless of the selection operator used, it was implicitly assumed in the previous discussion that any two individuals in the population can mate, i.e., all individuals belong to an unstructured centralized population. However, this is not necessarily the case. There exists a long tradition in using structured populations in evolutionary algorithms, especially associated to parallel implementations. Among the most widely known types of structured EAs, *distributed* (dEA) and *cellular* (cEA) algorithms are very popular optimization procedures [103].

Decentralizing a single population can be achieved by partitioning it into several subpopulations, where component EAs are run performing sparse exchanges of individuals (distributed EAs), or in the form of neighborhoods (cellular EAs). The main difference is that a distributed EA has a large subpopulation, usually much larger than the single individual and cEA has typically small size subpopulations. In a dEA, the subpopulations are loosely coupled, while for a cEA they are tightly coupled. Additionally, in a dEA, there exist only a few subpopulations, while in a cEA there is a large number of them [114].

The use of decentralized populations has a great influence in the selection intensity, since not all individuals have to compete among them. As a consequence, diversity is often better preserved.

5.4.4.4 Crossover

Crossover is a process that models information exchange among several individuals (typically two of them, but a higher number is possible [103]). This is done by constructing new solutions using the information contained in a number of selected *parents*. If it is the case that the resulting individuals (the *offsprings*) are entirely composed of information taken from the parents, then the crossover is said to be *transmitting* [104],[105]. This is the case of classical crossover operators for bit-strings such as *single-point crossover*, or *uniform crossover* [108], among others. Figure 5.8 shows an example of the application of these operators.

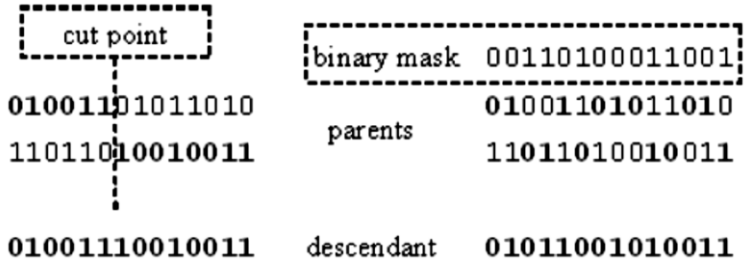

Figure 5.8: *Two examples of crossover on bit-strings: single-point crossover (left) and uniform crossover (right)*

This property captures the *a priori* role of crossover: combining good parts of solutions that have been independently discovered. It can be difficult to achieve for certain problem domains though (the *Traveling Salesman Problem* (TSP) is a typical example). In those situations, it is possible to consider other properties of interest such as *respect* or *assortment*. The former refers to the fact that the crossover operator generates descendants carrying all features common to all parents; thus, this property can be seen as a part of the *exploitative* side of the search. On the other hand, *assortment* represents the exploratory side of crossover. A crossover operator is said to be *properly assorting* if, and only if, it can generate descendants carrying any combination of compatible features taken from the parents. The assortment is said to be *weak* if it is necessary to perform several crossovers within the offspring to achieve this effect.

5.4.4.5 Mutation

From a classical point of view (at least in the GA [79]), this was a secondary operator whose mission is to *keep the pot boiling*, continuously injecting new material in the population, but at a low rate (otherwise the search would degrade to a random walk in the solution space). Evolutionary-programming practitioners [87] would disagree with this characterization, claiming a central role for mutation. Actually, it is considered the crucial part of the search engine in this context. This later vision has nowadays propagated to most EC researchers (at least in the sense of considering mutation as important as crossover).

As it was the case for crossover, the choice of a mutation operator depends on the representation used. In bit-strings (and in general, in linear strings spanning Σ^n, where Σ is arbitrary alphabet) mutation is done by randomly substituting the symbol contained at a certain position by a different symbol. If a permutation representation is used, such a procedure cannot be used for it would not produce a valid permutation. Typical strategies in this case are swapping two randomly chosen positions, or inverting a segment of the permutation.

5.4.4.6 Replacement

The role of replacement is keeping the population size constant. To do so, some individuals from the population have to be substituted by some of the individuals created during reproduction. This can be done in several ways:

- *Replacement-of-the-worst*: the population is sorted according to fitness, and the new individuals replace the worst ones from the population;
- *Random replacement*: the individuals to be replaced are selected at random;
- *Tournament replacement*: a subset of α individuals is selected at random, and the worst one is selected for replacement. Notice that if α = 1 we have random replacement;
- *Direct replacement*: the offspring replace their parents.

Some variants of these strategies are possible. For example, it is possible to consider the *elitist* versions of these, and only perform replacement if the new individual is better than the individual it has to replace. The described approach was adopted in this dissertation.

Two replacement strategies (*comma* and *plus*) are also typically considered in the context of ES and EP. Comma replacement is analogous to replacement of the worst, with the addition that the number of new individuals $|P''|$ (also denoted by λ) can be larger than the population size $|P|$ (also denoted by μ). In this case, the population is constructed using the best μ out of the λ new individuals. As for the plus strategy, it would be the elitist counterpart of the former, i.e., pick the best new μ individuals out of the μ old individuals plus the λ new ones. The notation (μ, λ) – EA and $(\mu + \lambda)$ – EA is used to denote these two strategies [113].

It must be noted that the term elitism is often used as well to denote replacement-of-the-worst strategies in which $|P''| < |P|$. This strategy is very commonly used, and ensures that the best individual found so far is never lost.

An extreme situation takes place when $|P''| = 1$, i.e. just a single individual is generated in each iteration of the algorithm. This is known as *steady-state* reproduction, and it is usually associated with faster convergence of the algorithm. The term *generational* is used to designate the classical situation in which $|P''| = |P|$.

5.4.5 Genetic Algorithms as Optimization Tool

GA principles are different from classical optimization methodologies in the following main ways [79]:

- GA procedure does not usually use gradient information in its search process. Thus, GA methodologies are direct search procedures, allowing them to be applied to a wide variety of optimization problems.
- GA procedure uses more than one solution (a population approach) in an iteration, unlike in most classical optimization algorithms which updates one solution at each iteration (a point approach). The use of a population has a number of advantages: (i) it provides the GA with a parallel processing power achieving a computationally quick overall search; (ii) it allows the GA to find multiple optimal solutions, thereby facilitating the solution of multi-modal and multi-objective optimization problems, and (iii) it provides the GA with the ability to normalize decision variables (as well as objective and constraint functions) within an evolving population using the population-best minimum and maximum values.

- GA procedure uses stochastic operators, unlike deterministic operators used in most classical optimization methods. The operators tend to achieve a desired effect by using higher probabilities towards desirable outcomes, as opposed to using predetermined and fixed transition rules. This allows the GA algorithm to negotiate multiple optima and other complexities better and provide them with a global perspective in their search.

The initialization procedure usually involves a random creation of solutions. If in a problem the knowledge of some good solutions is available, it is better to use such information in creating the initial population. Elsewhere [106], it is highlighted that for solving complex real-world optimization problems, such a customized initialization is useful and also helpful in achieving a faster search. After the population members are evaluated, the selection operator chooses above-average (in other words, better) solutions with a larger probability to fill an intermediate mating pool. For this purpose, several stochastic selection operators exist in the GA literature. In its simplest form, two solutions can be picked at random from the evaluated population and the better of the two (in terms of its evaluated order) can be picked. This is called tournament selection [107].

The "variation" operator is a collection of a number of operators (such as crossover, mutation etc.) which are used to generate a modified population. The purpose of the crossover operator is to pick two or more solutions (parents) randomly from the mating pool and create one or more solutions by exchanging information among the parent solutions. The crossover operator is applied with a crossover probability ($p_c \in [0,1]$), indicating the proportion of population members participating in the crossover operation. The remaining $(1 - p_c)$ proportion of the population is simply copied to the modified (child) population.

Each child solution, created by the crossover operator, is then perturbed in its vicinity by a mutation operator [79]. Every variable is mutated with a mutation probability p_m, usually set as $1/n$ (n is the number of variables), so that on an average one variable gets mutated per solution.

The elitism operator combines the old population with the newly created population and chooses to keep better solutions from the combined population. Such an operation makes sure that an algorithm has a monotonically non-degrading performance. Reference [107] proved an asymptotic convergence of a specific GA but having elitism and mutation as two essential operators.

On one hand, the GA procedure is flexible, thereby allowing a user to choose suitable operators and problem-specific information to suit a specific problem. On the other hand, the flexibility comes with a burden on the part of a user to choose appropriate and tangible operators so as to create an efficient and consistent search [110]. However, the benefits of having a flexible optimization procedure, over their more rigid and deterministic optimization algorithms, provide hope in solving difficult real-world optimization problems involving non-differentiable objectives and constraints, non-linearities, discreteness, multiple optima, large problem sizes, uncertainties in

computation of objectives and constraints, uncertainties in decision variables, mixed type of variables, and others.

A wiser approach to solving optimization problems of the real world would be to first understand the niche of both GA and classical methodologies and then adopt hybrid procedures employing the better of both worlds as the search progresses over varying degrees of search-space complexity from start to finish. There are two phases in the search of a GA. First, the GA exhibits a more global search by maintaining a diverse population, thereby discovering potentially good regions of interest. Second, a more local search takes place by bringing the population members closer together.

5.5 Optimization of Measurement Equipment Placement Method

Considering what was already discussed in subchapter 5.2.1, the proposed OMEP algorithm is now defined and discussed. The algorithm uses the DSSE algorithm described and tested in detail in Chapter 4. The problems related to DNs are already mitigated.

First part of the OMEP problem is dedicated to the solution with the single-objective technical fitness function – minimization of the sum of the square differences between measured and estimated values of DN's bus voltage magnitudes, voltage angles and injected real and reactive powers. The core of this part of the dissertation is devoted to the development of the different single-objective GAs and comparing them in order to find the best one to solve OMEP problem. In the following subchapters, the mechanism of GAs for single-objective problems, coding techniques and different genetic operators will be described in detail.

5.5.1 Structure of the OMEP algorithm

5.5.1.1 Candidate Bus and Measurement Configuration

A first step in designing the OMEP algorithm consists in defining the fundamental element of measurement equipment location: it is possible to consider each particular measurement apparatus (voltage, current etc.) for each network element (bus, branch etc.) or group the measurements into larger elements and consider these measurements as possible locations. Since the major investment into the measurement equipment is given by the acquisition unit, the second option was adopted: the fundamental unit for measurement location that was considered is the electric substation (bus). Therefore, if bus i is selected as a candidate (see Fig. 5.9), it means that measurement equipment is installed for all the network elements connected to bus i: the busbar voltage (V_i) branch powers (P_{ji} and Q_{ji}, P_{ik} and Q_{ik}, P_{il} and Q_{il}) that are joined to neighboring buses j, k and l respectively, generator injections (P_{Gi} and Q_{Gi}) and load (P_{Li} and Q_{Li}).

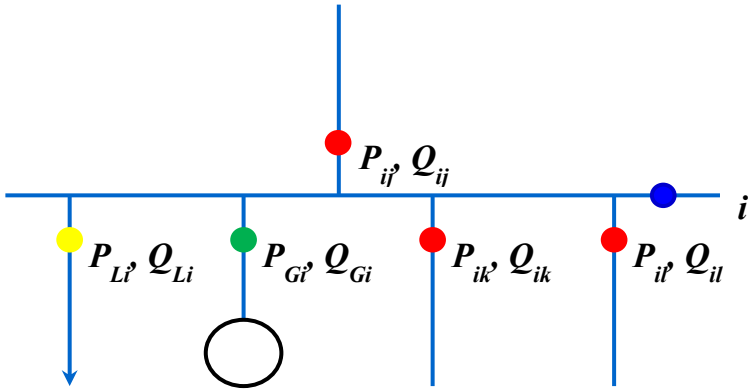

Figure 5.9: *Bus candidate*

The measurement configuration is a set of bus candidates with predefined length. This length is set by the user's needs. Each individual of the population that is processed by GA is actually one measurement configuration. Initial population can be formed in a randomized way or with *a priori* seeding. Both cases were considered in this study. To quantify the differences between individuals, to each of them, in the initialization step of the algorithm, fitness is joined. The fitness is quantitatively different, of course, because each configuration is composed of different bus candidates. Fitness is the measure of how close to the optimal solution is the certain solution and it is obtained as the result of running DSSE [69], which was explained in details in Chapter 4.

5.5.1.2 Coding Approaches

The most important part of any genetic process is the design strategy of the population. The first step is the selection of the possible bus candidates for the placement of new measurement equipment. Some buses are not the appropriate bus candidates:

- They already contain measurement equipment;
- They are buses with no load – "empty buses";
- They are buried welded junctions between various cables.

These buses have to be discarded from the set of available measurement locations and the rest of the buses are defined as search space. From it, algorithm randomly chooses the predefined number of the bus candidates. To incorporate this information into the algorithm and, at the same time, update the network structure accordingly, three coding techniques have been evaluated.

5.5.1.2.1 Integer Coding Technique

The integer coding technique was introduced as the most straight-forward approach. Information about each individual of the population regarding measurement locations needs to be propagated to the physical buses of the search space. The procedure of information propagation is depicted in Figure 5.10.

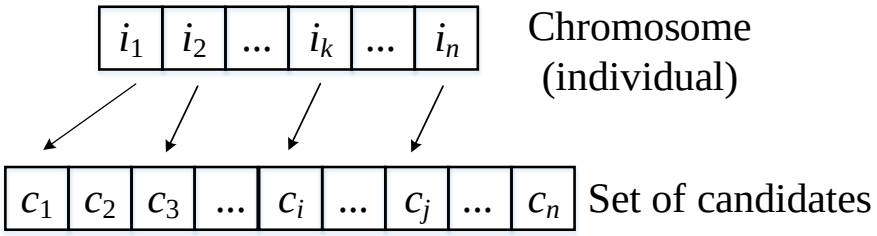

Figure 5.10: *Integer coding GA*

Figure shows one individual of the population (gen) during initialization or inside generation process before obtaining fitness. Values i_1, i_2,…,i_m are integer numbers that can have values from 1 to S where S is the length of the search space and m is the length of chromosome i.e. predefined number of measurement locations. Values $i_1 \neq i_2 \neq ... \neq i_k \neq ... \neq i_m$ which is important as repeating buses are not desired in the generation process because these individuals would automatically have worse fitness values.

Set of candidates is denoted by c_1, c_2,…,c_n and these values are also integer numbers but this time they represent physical buses of the DN, not necessarily starting with bus 1 (e.g. bus 1 might not be appropriate candidate). Upper bound (UB) for values of this vector is the index of the last bus in the DN. Length of the vector is not the same as the length of chromosome.

5.5.1.2.2 Binary Coding Technique

Binary coding technique has been implemented in order to try to broaden the abilities of genetic operators compared to integer ones. In this approach number of bits (alleles) of the gen is dependable on the search space size. If the size of search space is S, then a vector A is defined as follows:

$$A = \left[\underbrace{2^1}_{1} \quad \underbrace{2^2}_{2} \quad \cdots \quad \underbrace{2^k}_{k} \quad \cdots \quad \underbrace{2^S}_{S}\right] \tag{5.19}$$

In binary coding strategy, number of bits necessary to map one measurement location in a binary chromosome is equal to the first index in vector A such that the value given by that index is bigger than the size of the search space S. In details, the number of the bits necessary to code one possible measurement location is k if $2^k \geq S$ and $2^{k-1} < S$. Using the stated rules, information propagation is shown on following Fig. 5.11.

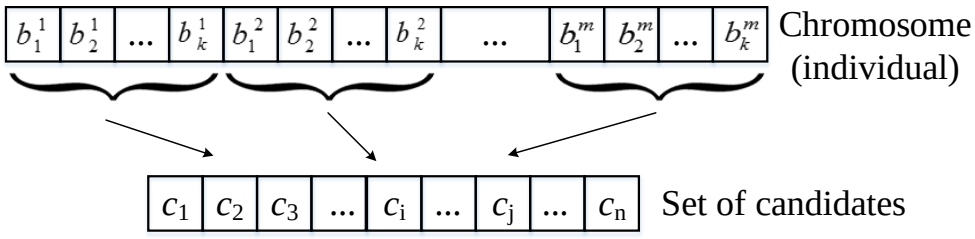

Figure 5.11: *Binary coding GA*

Subvectors $[b_1^i \quad b_2^i \quad ... \quad b_k^i]$ in binary notation represent one measurement location with respect to previously stated strategy. The information they carry corresponds to certain bus of network's search space.

The length of the gen is $k \times m$. In what regards the set of candidates, same conclusions are valid as for integer notation.

Decoding process is necessary before the end of each generation cycle because fitness values of the child population must be obtained using physical buses as in initialization process. However, it is possible that after decoding, locations that are not feasible occur in certain individuals of the child population [c_1 c_2 … c_i … c_n] (where c_i < LB or c_i > UB, LB stands for 1 and UB stands for the size of search space) or that one individual has repeating locations [c_1 c_2 c_2 … c_n]. This is the result of using binary crossover and mutation operators. The repeating measurement locations in the individual do not pose the problem for the algorithm as such individuals will be probably discarded from the population in the next cycle after the fitness evaluation since the repeating locations are treated as a single physical location and the fitness of these individuals would be worse (i.e. configurations are treated as having fewer than desired physical measurement locations). "Out of bound" locations are first altered to UB (or LB depending on the case) locations so they do not pose the problem to the algorithm and after that these individuals are treated the same as the other individuals. This is the trade-off of using the binary coding GA.

5.5.1.2.3 Binary Coding Technique with Whole Search Space Approach

Binary coding GA with whole search space approach has been implemented in order to try to exploit the search space as best as possible (i.e. to avoid creating situations with repeating locations or locations out of bounds). Each individual of the population is represented as a binary vector of ones and zeros and has a size of the search space - S. In the initialization process, random individuals are created which means that most of them will have more or less then the predefined number of measurement location. As the consequence, this type of coding requires the use of penalty factor in order to force the convergence to a feasible solution where the number of measurements is equal to the predefined desired number. In what regards the set of candidates, same conclusions are valid as for integer notation. The information propagation is shown on the Fig. 5.12.

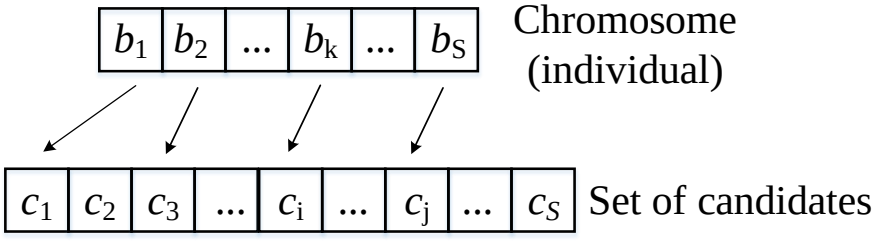

Figure 5.12: *Binary coding GA with whole search space approach*

Neither special coding nor decoding procedure is necessary in this case as the algorithm simply maps the locations with ones in chromosome structure to physical buses of the network.

5.5.1.3 Fitness Function

Value of the fitness that is joined to each individual in the initialization process as well as during each generation cycle is the measure of the quality of each measurement configuration (individual) and therefore it is the essential part of the GA technique. OMEP problem is directly related to the DSSE function as the information about the state of the system is essential to compute the fitness function. DSSE was implemented in GAMS environment for the sake of faster and more reliable computations.

Once the measurement locations had been set by the GA, the DSSE has been solved using the ASE solution described in Chapter 4. Then, in order to quantify the quality of the estimation for the particular configuration, the estimation of the network states of all the buses (V, φ, P and Q) is evaluated against the actual values for all the buses. Therefore, fitness function is computed in the following manner for integer and binary coding GA corresponds to the most general form of observability function defined in Eq. (5.16):

$$F_k = f_{obs} = \sum_{i=1}^{N_{bus}} \left(\left| \frac{V_i^{act} - V_i^{est}}{V_i^m} \right|^2 + \left| \frac{\varphi_i^{act} - \varphi_i^{est}}{\varphi_i^m} \right|^2 + \left| \frac{P_i^{act} - P_i^{est}}{P_i^m} \right|^2 + \left| \frac{Q_i^{act} - Q_i^{est}}{Q_i^m} \right|^2 \right) \quad (5.20)$$

All the quantities have been defined in subchapter 5.3.

In case of binary coding GA with whole search space approach, individuals with higher or lower number of measurement locations than desired (predefined) one can appear because the initialization is randomized and crossover and mutation can produce number of locations different from predefined. As a predefined number of measurement locations is desired, fitness function has to be penalized:

$$p_k = e^{k_p \cdot \frac{N_k - N_p}{N_p}}, \text{ if } N_k \neq N_p \quad (5.21)$$

where:

p_k penalty of the k-th individual of the population, $k = 1, 2, \ldots, pop$;

k_p factor that defines the penalty pressure and is set to be smaller in the beginning of GA process (in the first generations of GA) and as the number of generations is increasing, so is the factor in order to discard the individuals with a number larger or smaller than the set one. This factor has to be set very carefully in order not to discard the certain solutions too fast as it can lead to local minimum of the algorithm. Use of penalty is a trade-off from the use of this type of coding;

N_k number of the measurement locations of the k-th individual of the population;

N_p predefined number of the measurement locations.

After the computation of the penalty, fitness of the k-th individual of the population is computed in the following manner:

$$F_k = \sum_{i=1}^{N_{bus}} \left(\left| \frac{V_i^{act} - V_i^{est}}{V_i^m} \right|^2 + \left| \frac{\varphi_i^{act} - \varphi_i^{est}}{\varphi_i^m} \right|^2 + \left| \frac{P_i^{act} - P_i^{est}}{P_i^m} \right|^2 + \left| \frac{Q_i^{act} - Q_i^{est}}{Q_i^m} \right|^2 \right) + p_k \quad (5.22)$$

5.5.1.4 Sorting Procedure

After the initialization procedure, in which initial population is created, equipped with fitness value and coded in one of the stated ways, population is sorted. Sorting is based on a non-dominance property of the individuals. An individual is said to dominate another if the objective functions of it is no worse than the other and at least in one of its objective functions it is better than the other. The fast sort algorithm is described as:

- for each individual p in main population P do the following:
  - initialize $S_p = \{\}$. This set would contain all the individuals that is being dominated by p;
  - initialize $n_p = 0$. This would be the number of individuals that dominate p;
  - for each individual q in P:
    - if p dominated q then:
      - ✓ add q to the set S_p i.e. $S_p = S_p \cup \{q\}$;
    - else, if q dominates p then:
      - ✓ increment the domination counter for p i.e. $n_p = n_p + 1$;
  - if $n_p = 0$ i.e. no individuals dominate p, then p belongs to the first front; Set rank of individual p to one i.e. $p_{rank} = 1$. Update the first front set by adding p to front one i.e. $F_1 = F_1 \cup \{p\}$;
- this is carried out for all the individuals in main population P;
- initialize the front counter to one: $i = 1$;
- following is carried out while the i^{th} front is nonempty i.e. $Fi \neq \{\}$:
  - $Q = \{\}$. The set for storing the individuals for $(i + 1)^{th}$ front;
  - for each individual p in front F_i:
    - for each individual q in S_p (S_p is the set of individuals dominated by p):
      - ✓ $n_q = n_q - 1$, decrement the domination count for individual q;
      - ✓ if $n_q = 0$ then none of the individuals in the subsequent fronts would dominate q. Hence set $q_{rank} = i + 1$. Update the set Q with individual q i.e. $Q = Q \cup \{q\}$;
  - increment the front counter by one;
  - now the set Q is the next front and hence $F_i = Q$.

This algorithm utilizes the information about the set that an individual dominate (S_p) and number of individuals that dominate the individual (n_p).

5.5.1.5 Crowding Distance

Although in this part of the dissertation the attention is on single-objective optimization and crowding distance is the property of the multi-objective optimization, it will be described in detail in this place as it is the part of the sorting procedure and also because later attention will be on the multi-objective problems.

Once the non-dominated sort is complete the crowding distance is assigned. Since the individuals are selected based on rank and crowding distance all the individuals in the population are assigned a crowding distance value. Crowding distance is assigned front wise and comparing the crowding distance between two individuals in different front is meaningless. The crowing distance is calculated as follows:

- for each front F_i, n is the number of individuals:
  - initialize the distance to be zero for all the individuals i.e. $F_i(d_j) = 0$, where j corresponds to the j^{th} individual in front F_i.
  - for each objective function m:
    - sort the individuals in front F_i based on objective m i.e. $I = sort(F_i, m)$;
    - Assign infinite distance to boundary values for each individual in F_i i.e. $I(d_1) = \infty$ and $I(d_n) = \infty$
      - ✓ $I(d_k) = I(d_k) + \frac{I(k+1).m - I(k-1).m}{f_m^{max} - f_m^{min}}$;
      - ✓ $I(k).m$ is the value of the m^{th} objective function of the k^{th} individual in I.

The basic idea behind the crowing distance is finding the Euclidian distance between each individual in a front based on their m objectives in the m dimensional hyper space. The individuals in the boundary are always selected since they have infinite distance assignment.

5.5.1.6 Selection

In this dissertation, a number of selection approaches were adopted: fixed size tournament, fitness scaling – based roulette wheel, fine grained tournament selection and stochastic universal sampling.

5.5.1.6.1 Tournament Selection

Tournament selection is probably the most popular selection method in GA due to its efficiency and simple implementation [103]. In tournament selection, n individuals out of N (the size of the population) are selected randomly and placed in a mating pool from the larger population, and the selected individuals compete against each other. Based on the replacement strategy, in this dissertation, size of the pool was half of the population, if the replacement is implicit, and whole population if the replacement is explicit which will be further explained in the subsequent chapters.

The individual with the best fitness or the best ranking wins and will be included as one of the next generation population. The number of individuals competing in each tournament is referred to as tournament size, commonly set to 2 (also called binary tournament). For testing purposes, in this dissertation, tournament size was set to different values and it was proven that the best results are obtained with the size 4.

Tournament selection also gives a chance to all individuals to be selected and thus it preserves diversity, although keeping diversity may degrade the convergence speed. Fig. 5.13 illustrates the mechanism of tournament selection.

The tournament selection has several advantages which include efficient time complexity, especially if implemented in parallel, low susceptibility to takeover by dominant individuals, and no requirement for fitness scaling or sorting [103], [111].

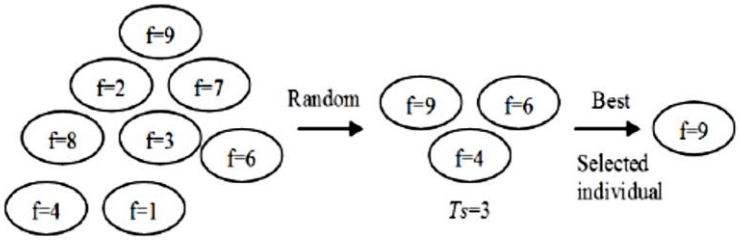

Figure 5.13: *Selection strategy with tournament mechanism [103]*

In the above example, the tournament size, T_s, is set to three, which means that three individuals compete against each other. Only the best chromosome among them is selected to reproduce. In tournament selection, larger values of tournament size lead to higher expected loss of diversity [111],[112]. The larger tournament size means that a smaller portion of the population actually contributes to genetic diversity, making the search increasingly greedy in nature. There might be two factors that lead to the loss of diversity in regular tournament selection; some individuals might not get sampled to participate in a tournament at all while other individuals might not be selected for the intermediate population because they lost a tournament.

5.5.1.6.2 Fitness scaling-based Roulette Wheel Selection

Fitness scaling-based roulette wheel selection is the selection strategy where the probability of an individual being selected is based on its fitness relative to the entire population. Fitness scaling -based selection schemes first sort individuals in the population according to their fitness and then computes selection probabilities according to their fitness values. Hence fitness scaling - based roulette wheel selection can maintain a constant pressure in the evolutionary search where it introduces a uniform scaling across the population and is not influenced by super-individuals or the spreading of fitness values at all as in proportional selection. Fitness scaling - based roulette wheel selection uses a function to map the indices of individuals in the sorted list to their selection probabilities. Although this mapping function can be linear (linear ranking) or non-linear (non-linear ranking), the idea of fitness scaling - based roulette wheel selection remains unchanged. The performance of the selection scheme depends greatly on this mapping function.

In this dissertation, linear based ranking was used [115]. For linear fitness scaling - based selection, the biasness could be controlled through the selection pressure (*SP*), such that the expected sampling rate of the best individual is *SP* and the expected sampling rate of the worst individual is 2-*SP* and the selective pressure of all other population members can be interpreted by linear interpolation of the selection pressure according to rank. Consider *n* the number of individuals in the population and *Pos* the position of an individual in the population (least fit individual has *Pos* = 1, the fittest

individual *Pos* = *n*). Instead of using the fitness value of an individual, the scaled fitness of individuals is used. The fitness for an individual may be scaled linearly using the following formula:

$$Rank(Pos) = 2 - SP + 2 \cdot \left((SP - 1) \cdot \frac{Pos - 1}{n - 1} \right) \tag{5.23}$$

Fitness scaling - based selection schemes can avoid premature convergence, but can be computationally expensive because of the need to sort populations. Once selection probabilities have been assigned, sampling method using roulette wheel is required to populate the mating pool. Fitness scaling - based selection scheme helps prevent premature convergence due to "super" individuals, since the best individual is always assigned the same selection probability, regardless of its objective value. However, this method can lead to slower convergence, because the best chromosomes do not differ so much from other ones. The difference between roulette wheel selection without and with fitness scaling - based fitness is depicted in Fig. 5.14-left and Fig. 5.14-right respectively.

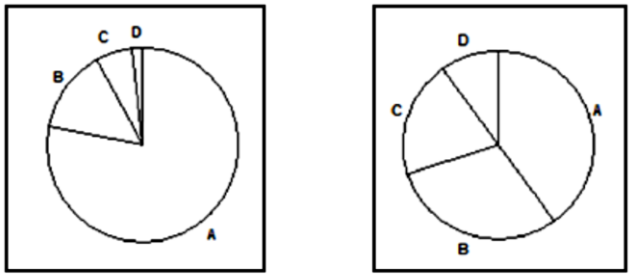

Figure 5.14: *Roulette – wheel selection; without fitness scaling- left and with fitness scaling- right*

As it can be seen from the figures, implementation of the fitness scaling provides fairer share of the roulette wheel compared to the case without fitness scaling.

5.5.1.6.3 Fine Grained Tournament Selection

Fine-grained Tournament Selection (FGTS) is an attempt to improve the tournament selection. FGTS is controlled by real value parameter F_{tour} (the desired average tournament size) instead of the integer parameter T_s (the tournament size). Similarly to the tournament selection, an individual is chosen if it is the best individual on the tournament. However, unlike tournament selection, size of the tournament is not unique in the whole population, i.e., tournaments with different number of competitors can be held within one step of the selection [116].

The parameter F_{tour} governs the selection procedure; therefore, average tournament size in population should be as close to F_{tour} as possible.

Sizes of the tournaments are $F_{tour}^{-} = [F_{tour}]$, $F_{tour}^{+} = [F_{tour}] + 1$ where $[\cdot]$ denotes the rounding of the real to the integer value. The size of all of n held tournaments is either F_{tour}^{-} or F_{tour}^{+}. The number of tournaments with size F_{tour}^{-} (denoted as n^{-}) and the number of tournaments with size F_{tour}^{+}

(denoted as n^+), have to fulfill two conditions: their sum should be n and average tournament size should be as close to real value F_{tour} as possible:

$$\begin{cases} n^+ + n^- = n \\ n^+ F_{tour}^+ + n^- F_{tour}^- = nF_{tour} \end{cases} \tag{5.24}$$

The explicit formulas for n^+ and n^- are obtained by solving these equations.

5.5.1.6.4 Stochastic Universal Sampling Selection

Stochastic Universal Sampling (SUS) developed by Baker [117] is a single-phase sampling algorithm with minimum spread and zero bias. Instead of a single selection pointer employed in roulette wheel methods (repetition of the procedure until there are enough selected individuals), SUS uses *N* equally spaced pointers, where *N* is the number of selections required. The population is shuffled randomly and a single random number *pointer1* in the range [0, 1/*N*] is generated. The *N* individuals are then chosen by generating the *N* pointers, starting with *pointer1* and spaced by 1/*N*, and selecting the individuals whose fitness spans the positions of the pointers. If *et*(*i*) is the expected number of trials of individual *i*, $\lfloor et(i) \rfloor$ is the floor of $et(i)$ and $\lceil et(i) \rceil$ is the ceiling, an individual is thus guaranteed to be selected a minimum of times $\lfloor et(i) \rfloor$ and no more than $\lceil et(i) \rceil$, thus achieving minimum spread. In addition, as individuals are selected entirely on their positions in the population, SUS has zero bias. For these reasons, SUS has become one of the most widely used selection algorithms in current GAs.

Figure 5.14 demonstrates the SUS. The individuals are mapped to contiguous segments of a line, such that each individual's segment is equal in size to its fitness exactly as in roulette wheel selection. Equally spaced pointers are placed over the line as many as there are individuals to be selected (*N*). For 6 individuals (*N* = 6) to be selected, the distance between the pointers is 1/6 = 0.167. Figure 5.15 shows the selection for the sample of the random number 0.1 in the range [0, 0.167].

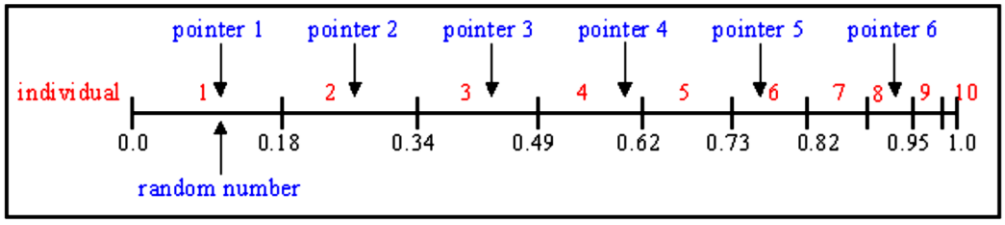

Figure 5.15: *Stochastic universal sampling*

After selection, the mating population consists of the individuals 1, 2, 3, 4, 6 and 8. Stochastic universal sampling ensures a selection of offspring which is closer to what is desired than roulette wheel selection.

5.5.1.7 Crossover

Choice of crossover operators used in this dissertation depends on the type of coding. For integer coding GAs, partially matched crossover was used while, for the remaining two types of coding, scattered crossover was utilized.

In all the approaches, the crossover operator probability is 0.9, which is the standard value found in the majority of bibliography. This value has also backed up good convergence property of OMEP algorithm.

5.5.1.7.1 Partially Matched Crossover

Partially matched crossover (PMX) is one of the most popular and effective crossovers for order-based GAs to deal with combinatorial optimization problems. In view of the operation, PMX can be regarded as a modification of two-point crossover but additionally uses a mapping relationship to legalize offspring that have duplicate numbers.

Goldberg and Lingle [118] developed partially matched crossover (PMX) that preserves absolute position using two cut points in parents. This operator first randomly selects two cut points on both parents. In order to create an offspring, the substring between the two cut points in the first parent replaces the corresponding substring in the second parent. Then, the inverse replacement is applied outside of the cut points, in order to eliminate duplicates and recover all cities.

PMX is executed following the steps:

- *Substring selection*: Cut two substrings of equal size on each parent at the same positions;
- *Substring exchange*: Exchange the two selected substrings to produce proto-child;
- *Mapping list determination*: Determine the mapping relationship based on the selected substrings;
- *Offspring legalization*: Legalize proto-child with the mapping relationship.

For instance, two parent chromosomes P_1 and P_2 are considered:

$$P_1 = [1\ 2\ 3 \mid 5\ 4\ 6\ 7 \mid 8\ 9]$$
$$P_2 = [4\ 5\ 2 \mid 1\ 8\ 7\ 6 \mid 9\ 3]$$

The first step is to immediately create the part of children C_1 and C_2 between the cut points:

$$C_1 = [*\ *\ * \mid 5\ 4\ 6\ 7 \mid *\ *]$$
$$C_2 = [*\ *\ * \mid 1\ 8\ 7\ 6 \mid *\ *]$$

The two initialized sections C_1 and C_2 of define a mapping:

$$5 \rightarrow 1,\ 4 \rightarrow 8,\ 6 \rightarrow 7,\ 7 \rightarrow 6$$

Next, the vacant places of C_1 are filled (if possible) with vertices from P_2 that happen to be in the same positions. Following is obtained:

$$C_1 = [*\ *\ 2 \mid 5\ 4\ 6\ 7 \mid 9\ 3]$$

The two remaining positions should be filled with 4 and 5. But since 4 and 5 are already present in C_1, they are being replaced according to the above mapping with 8 and 1 respectively. Thus, the completed first child is:

$$C_1 = [8\ 1\ 2 \mid 5\ 4\ 6\ 7 \mid 9\ 3]$$

The second child C_2 is completed by an analogous procedure, and it looks as follows:

$$C_2 = [5\ 2\ 3 \mid 1\ 8\ 7\ 6 \mid 4\ 9]$$

K. Deep and H. Mebrahtu [119] offered the variation of PMX (VPMX) algorithm cutting two substrings of equal size on each parent at randomly chosen positions. In this dissertation, both approaches, PMX and VPMX, were implemented and tested. It was proven, however, that VPMX for OMEP problem does not bring any improvements regarding convergence rate compared to PMX.

5.5.1.7.2 Scattered Crossover

Unlike many traditional crossover techniques that are position oriented, which means positioning has a great deal of relevance in deciding the crossover's efficiency, scattered crossover is position independent. This means that the position and the ordering of the bits do not carry any importance [120].

In this technique, random vector of binary values (the mask) is created first (Fig. 5.16).

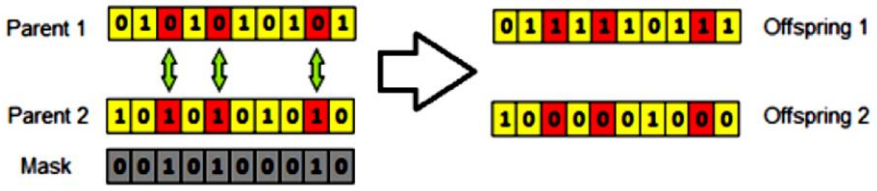

Figure 5.16: *Scattered crossover*

The length of the vector is the length of individuals. Each element of vector is either 0 or 1, which denotes the parent. If the vector contains 0 at any position, the gen corresponding to this position is taken from the first parent, and vice versa. Thus position has no relevance in this; and hence this solution is position independent. This characteristic is important because of the highly interconnected nature of the genes and the attributes in deciding the fitness.

It should also be noted that the scattered crossover cannot be used for integer coding GA because it could produce identical genes in the offspring due to the mapping according to the mask.

5.5.1.8 Mutation

As with the crossover, the choice of mutation operator also depends of the type of coding used. For integer coding GA, Mutation Matrix approach was developed and for the other two types of coding, uniform mutation was used.

5.5.1.8.1 Mutation Matrix Approach

This type of mutation was specially designed for the OMEP problem. First mutation matrix of the parent population size is created. This matrix is a binary matrix, composed of either ones or zeros. Ones are in the positions where random number created by program was higher than mutation probability - 0.05 and zeros in remaining locations. In most of the sources found in bibliography, the value of the mutation probability is given by inverse value of the population size (which in the most of the simulations ran in case of OMEP is 200). Therefore, this value is 0.005 for the binary coding GA. The reason why the 10 times higher value was used in case of integer coding GA is because the integer coding crossover might not produce satisfactory results regarding the variety of the offsprings, so additional probability of the mutation needed to be adopted.

Program sweeps through the rows (individuals) of the parent population one by one and changes the alleles of the individuals that correspond to the position of ones in mutation matrix. The mutation, however, is not completely random in order to avoid creating integer duplicates within the same individual and therefore deteriorate the individual.

5.5.1.8.2 Uniform Mutation

Similar to mutation matrix approach, this type of mutation creates the Mutation Points matrix which is binary and composed of ones and zeros. Ones are in the locations where the random value is higher than mutation probability (0.1 for binary approaches) and zeros in remaining locations.

Program sweeps through the rows (individuals) of the parent population one by one and changes the alleles of the individuals that correspond to the position of ones in mutation matrix. This time it is simpler than in mutation matrix approach, as simply ones become zeros in appropriate locations and vice versa.

5.5.1.9 Replacement

In this dissertation, two types of replacements were considered. The classical approach, Replacement-of-the-worst or explicit elitist approach is designed in a way that the population is sorted according to fitness and *m* best individuals of population are stored before each generation cycle. All the individuals of the population are then subjected to genetic operators. At the end of each cycle, *m* best individuals stored before replace *m* worst individuals obtained after the generation cycle.

Implicit elitism functions differently. To start with, not the entire population of size *N* is subjected to genetic operators. After the population is sorted according to fitness, only a part of population (in this dissertation *N*/2) is selected into matting pool and later crossovered and mutated.

Once selection, crossover, and mutation have occurred, the child population (size *N*/2) is combined with the entire parent population (size *N*) to create an intermediate population (size 3*N*/2). This combined population is subject to another non-dominated sorting and *N* solutions are chosen for the

next population using rank and crowding comparison operator to compare solutions in the same front, in case of multi-objective optimization. Therefore, the resulting population consists of the best solutions from the newly formed population as well as best solutions from the previous population that may have been lost through the selection, crossover, and mutation operations.

The newly formed population undergoes selection, crossover, and mutation and then recombination and reevaluation in subsequent generations to eventually arrive at the optimal solution of the problem.

The implicit elitism involves a reduced computation time but may affect the diversity of the population with respect to the explicit elitism.

5.5.2 Single-objective OMEP Results

5.5.2.1 Test of the Algorithm Convergence Quality

A set of pre-tests was conducted in order to check the convergence quality of diverse approaches regarding coding and genetic operator types. This particular test checks if the OMEP algorithm finds the optimal solution. The test was conducted on different DNs and with different starting conditions. These include:

- random initialization of the measurement configuration population;
- *a priori* seeding of the initial population with at least one super-individual. i.e. configuration with fitness close to the optimal one;
- *a priori* seeding of the initial population with a number of individuals with poor fitness and no super-individuals.

These tests made with the algorithm of following characteristics:

- integer coding GA;
- tournament selection;
- PMX crossover;
- mutation matrix approach;
- explicit replacement;
- population size 200 individuals;
- number of generations 200.

Test DN is shown in Fig. 5.17. It is a simple system with 29 buses and 28 branches, with distribution generation plant in bus 10 and three “empty” buses. The available information of the network is previously described in subchapter 4.3.1 and it concerns primary TS. When these buses are discarded from the possible measurement equipment set, 23 out of 29 buses comprise search space.

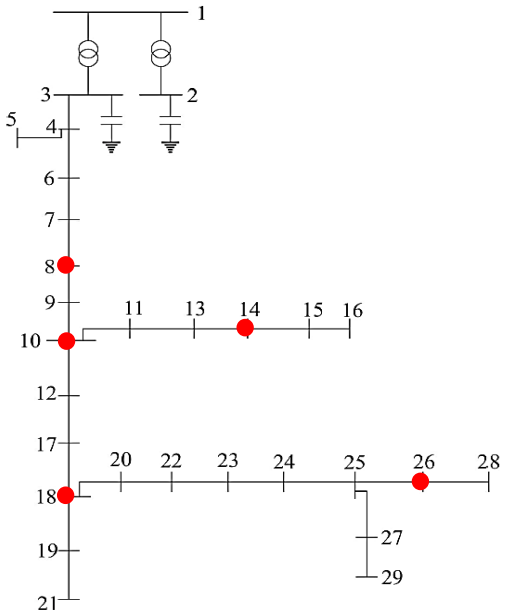

Figure 5.17: *29-bus test DN with optimal measurement configuration*

First, the algorithm was completed, thus providing the optimal configuration of the OMEP problem. The reported configuration is the following (Fig 5.17): 8, 10, 14, 18 and 26 with the fitness (according to Eq. 5.20) 5,8866. This configuration and fitness value were checked by multiple runs of the algorithm.

In order to check if this configuration is really optimal, series of tests were made by changing the position measurement equipment from optimal buses to their neighboring buses and precomputing the fitness of these new configurations. Here will be presented just some of these (Fig 5.18):

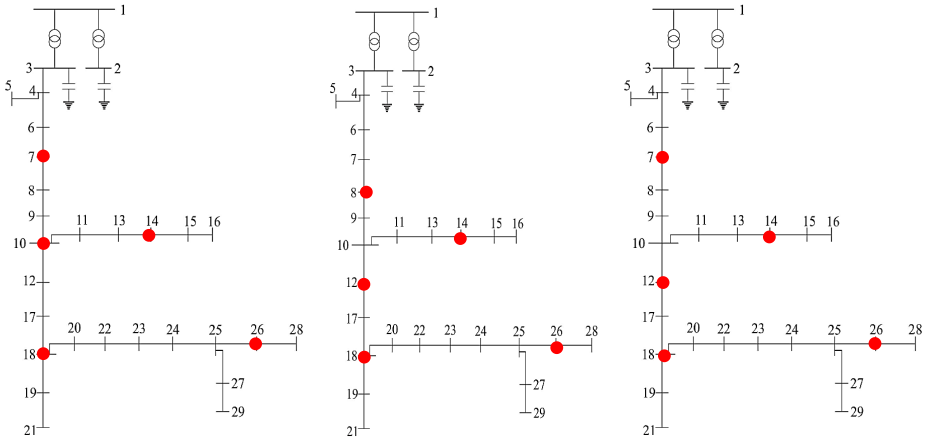

(a) *(b)* *(c)*

Figure 5.18: *Manipulations of the optimal configuration*

The manipulations are the following:

a) Replace the measurement equipment from bus 8 to bus 7;
b) Replace the measurement equipment from bus 10 to bus 12;
c) Replace the measurement equipment from bus 8 to bus 7 and bus 10 to bus 12.

New obtained configurations and appropriate fitness values are reported in Table 5.1:

Table 5.1: Test of the Algorithm Convergence Quality

Manipulation	Configuration					Fitness
a)	7	10	14	18	26	6.3266
b)	8	12	14	18	26	7.1012
c)	7	12	14	18	26	8.2241

As it can be seen, all of the stated configurations in Table 5.1 are worse than optimal configuration obtained by the OMEP algorithm which can be clearly seen from the values of fitness that were obtained. This test proves the convergence quality of the developed OMEP algorithm.

5.5.2.2 Test of the Algorithm Properties

The following test was made in order to distinguish how the algorithm corresponds to different degrees of freedom set by the problem. Same algorithm and network properties were used as in the first test. The test was firstly run with 5 optimal measurement locations obtained in the previous test and 5 new ones that algorithm should place in optimal places. Then the algorithm was used to optimally place 10 new acquisition units in the same DN. The situation is depicted in Fig. 5.19.

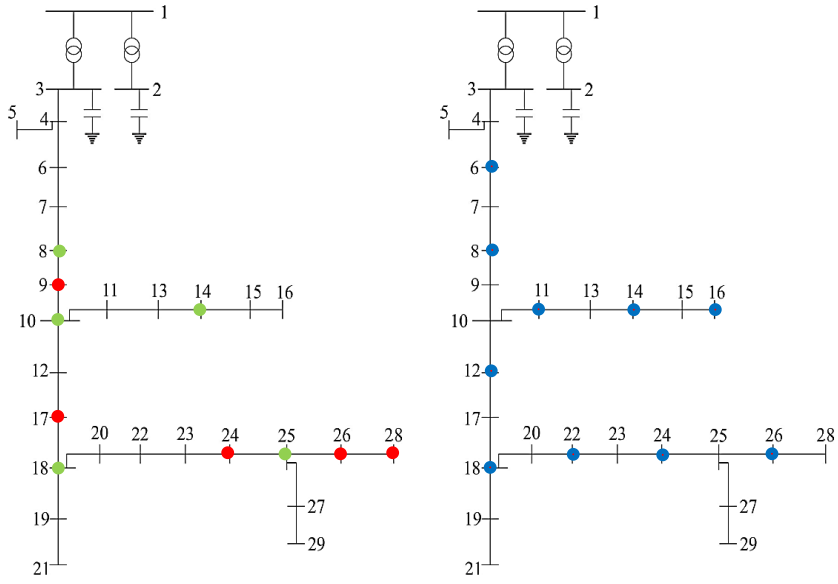

(a) *(b)*

Figure 5.19: *DN with (a) 5 old and 5 new optimally placed units and (b) 10 new units*

Fig. 5.19 (a) shows the previous 5 optimal locations set by the algorithm in the first step (red dots) and 5 new optimally chosen locations (green dots). Fig. 5.19 (b) shows completely new optimally located measurement equipment (light blue dots). It is obvious that the configurations are topologically different. Table 5.2 shows these configurations and their fitness values.

Table 5.2: Test of the Algorithm Properties

Type	Configuration										Fitness
(a)	8	9	10	14	17	18	24	25	26	28	1.7415
(b)	6	8	11	14	16	12	18	22	24	26	0.2060

Results show that the algorithm provides far better results if it can optimize 10 locations at the time than if it optimizes 5 and then additional 5 locations. This is because the first option provides more degrees of freedom to the algorithm and it can arrange the units more optimally.

However, this test also demonstrated the possibilities of the algorithm to be used to planning new network but also improvement of the existing ones thus showing its flexibility as the part of some future DMS software solution apart from its main function – optimization of the measurement equipment placement.

5.5.2.3 Comparison of Integer and Binary Approaches

While the previously described pre-tests are important to prove the convergence capabilities of the different OMEP algorithms that were developed, the core of this part of dissertation is to find the type of OMEP algorithm with the best convergence characteristics with the variety of input data regarding DN types, nature and parameters.

The ultimate goal was to design the algorithm that can provide (sub)optimal solution for the realistic large-scale DNs in computationally acceptable time frame. As many different approaches were developed, to decide the best one, they were compared in different environments – smaller to larger DNs, randomized or *a priori* initialization, different population sizes and generation cycle number etc.

5.5.2.3.1 29-bus DN Tests

First group of tests was conducted on small size 29-bus test DN (Fig. 5.20) that was previously described. The aim was to prove the convergence of the various GA approaches but also to make first conclusions about the speed of convergence. Following algorithms were tested:

1. Integer coding GA with tournament selection, PMX crossover, mutation matrix approach and implicit elitist replacement;
2. Integer coding GA with tournament selection, PMX crossover, mutation matrix approach and explicit elitist replacement;
3. Integer coding GA with fitness scaling-based roulette wheel selection, PMX crossover, mutation matrix approach and explicit elitist replacement;
4. Integer coding GA with fine grained tournament selection, PMX crossover, mutation matrix approach and explicit elitist replacement;
5. Binary coding GA with tournament selection, scattered crossover, uniform mutation and explicit elitist replacement;
6. Binary coding GA with stochastic universal sampling selection, scattered crossover, uniform mutation and explicit elitist replacement;
7. Binary coding GA with fine grained tournament selection, scattered crossover, uniform mutation and explicit elitist replacement;

8. Binary coding GA with whole search space approach, fine grained tournament selection, scattered crossover, uniform mutation and explicit elitist replacement.

These diverse algorithms are summarized in the following Table 5.3:

Table 5.3: Types of the approaches used for tests – 29-bus DN

Algorithm type		1.	2.	3.	4.	5.	6.	7.	8.
Coding type	Integer	●	●	●	●				
	Binary					●	●	●	
	Binary with whole SS								●
Selection type	Tournament	●	●			●			
	Roulette wheel			●					
	FGTS				●			●	●
	SUS						●		
Crossover type	PMX	●	●	●	●				
	Scattered					●	●	●	●
Mutation type	Mutation matrix	●	●	●	●				
	Uniform					●			
Elitism type	Implicit	●							
	Explicit		●	●	●	●	●	●	●

In order to obtain the average behavior, each of the stated approaches was run 5 times and results are reported for averaged fitness in each generation per approach. Algorithm settings are the following:

- Population size 200 individuals;
- Number of generation cycles 200;
- *A priori* initialization with super-individual(s) and poor-individuals independently. This was done in order to have the same starting points for all the runs of the algorithms. Also, it is important to observe if and how much quantitatively starting point interferes with the convergence rate of the algorithm.

Although the algorithm was run each time for 200 generations, it converged much faster, so only the first 20 generations will be reported on the following Figures 5.20 and 5.21. This is done in order to have the clearer picture of the convergence rate of approaches.

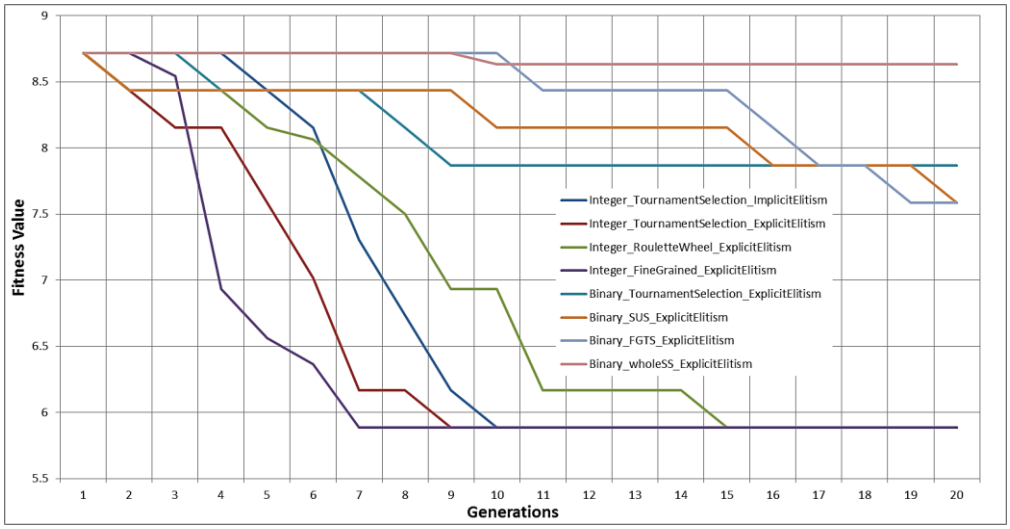

Figure 5.20: *Comparison of algorithms – good initial fitness of the population*

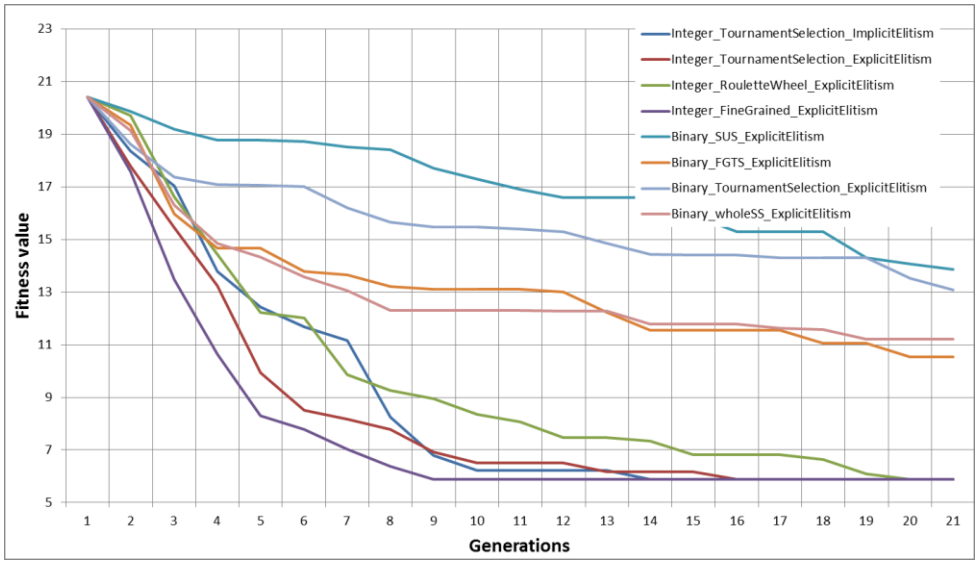

Figure 5.21: *Comparison of algorithms – bad initial fitness of the population*

Graphs show the obvious superiority of integer coding GAs compared to binary ones. This conclusion is the same for both types of initial populations. When comparing particular integer approaches, it can be concluded that all of them converge quite fast (from 7^{th} to 15^{th} generation for good starting point or 9^{th} to 20^{th} generation for bad starting point) and that they converge in almost same time. The algorithm with the best properties for the small network is Integer coding GA with fine grained tournament selection, PMX crossover, mutation matrix approach and explicit elitist replacement.

Another important conclusion that can be drawn from this test is that *a priori* seeding of the initial population didn't interfere in a great manner with the rate of convergence of the algorithm. For example, the algorithm with the best properties converged in 7 generations with the good starting fitness of the population, while it took 9 generations to reach the optimal solution with the bad starting fitness of the initial population.

The average simulation time with the previously stated algorithm settings is 28 minutes on Intel(R) Core(TM) i7-2600 CPU @ 3.4 GHz and 8 GB of RAM.

Binary coding GAs did not demonstrate desired convergence rate although they converged to optimal fitness value. Figures 5.22 and 5.23 show the convergence rate of binary approaches. 100 generations have been shown in the figures.

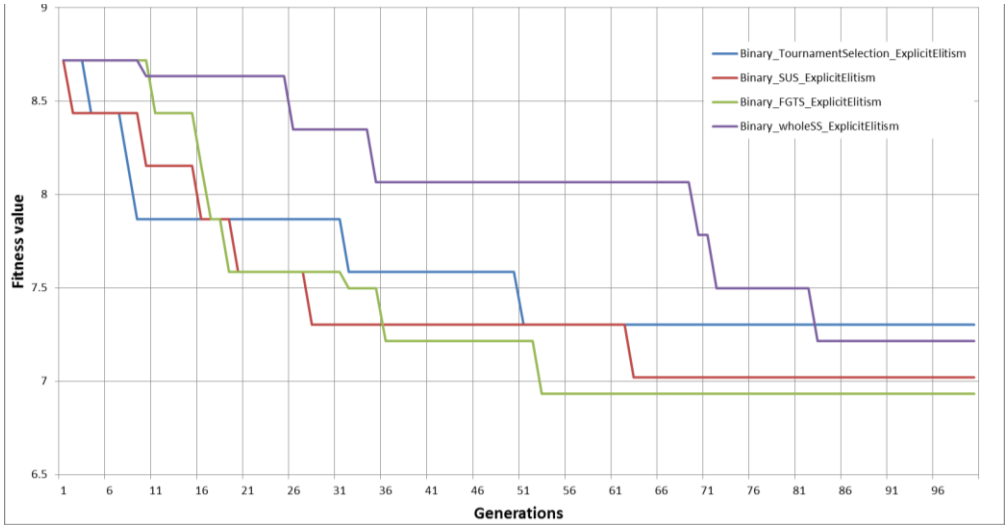

Figure 5.22: *Comparison of binary coding GAs – good initial fitness of the population*

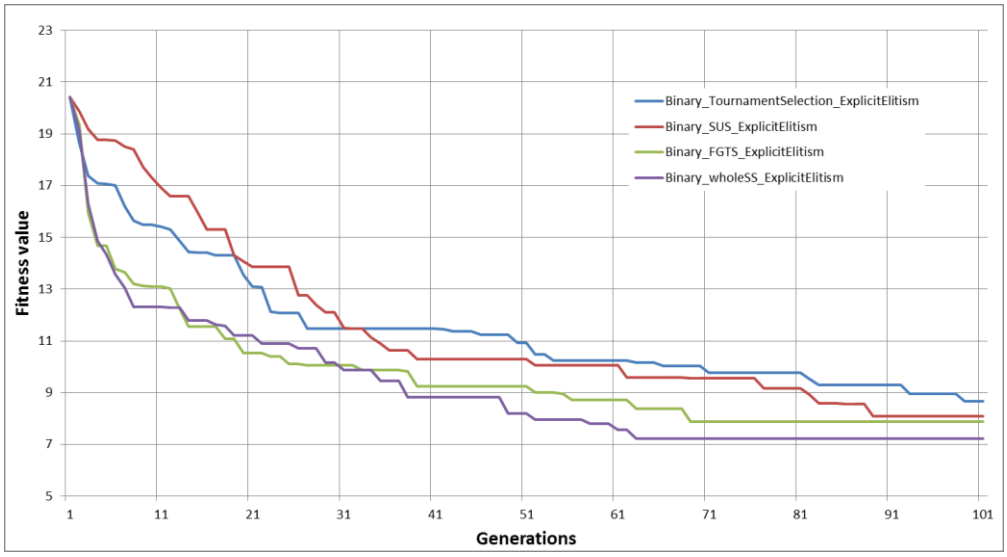

Figure 5.23: *Comparison of binary coding GAs – bad initial fitness of the population*

Figures show that binary coding GAs converge quite slower compared to integer ones. Moreover, even after 100 generations, none of the algorithms managed to converge to optimal solution, whether using good or bad starting fitness of the population. Among binary approaches, overall best quality was recorded with binary coding GA with fine grained tournament selection, scattered crossover, uniform mutation and explicit elitist replacement.

5.5.2.3.2 69-bus DN Tests

Last results have proven the superiority of integer coding GAs for solving of the OMEP problem over the binary coding ones. This is why only the results with the following types of integer coding GA will be published:

1. Integer coding GA with tournament selection, PMX crossover, mutation matrix approach and implicit elitist replacement;
2. Integer coding GA with tournament selection, PMX crossover, mutation matrix approach and explicit elitist replacement;
3. Integer coding GA with fitness scaling-based roulette wheel selection, PMX crossover, mutation matrix approach and explicit elitist replacement;
4. Integer coding GA with fine grained tournament selection, PMX crossover, mutation matrix approach and explicit elitist replacement.

This diverse algorithms are summarized in the following Table 5.4:

Table 5.4: Types of the approaches used for tests – 69-bus DN

Algorithm type		1.	2.	3.	4.
Coding type	Integer	●	●	●	●
	Binary				
	Binary with whole SS				
Selection type	Tournament	●	●		
	Roulette wheel			●	
	FGTS				●
	SUS				
Crossover type	PMX	●	●	●	●
	Scattered				
Mutation type	Mutation matrix	●	●	●	●
	Uniform				
Elitism type	Implicit	●			
	Explicit		●	●	●

Test network is the medium sized realistic DN (Fig. 5.24) which is quite active with DG in buses 9, 17, 20, 30, 41, 43, 57, 59 and 62. As with the 29-bus network, this one is also measured only in primary TS. After removal of the empty buses, size of the search space is 65.

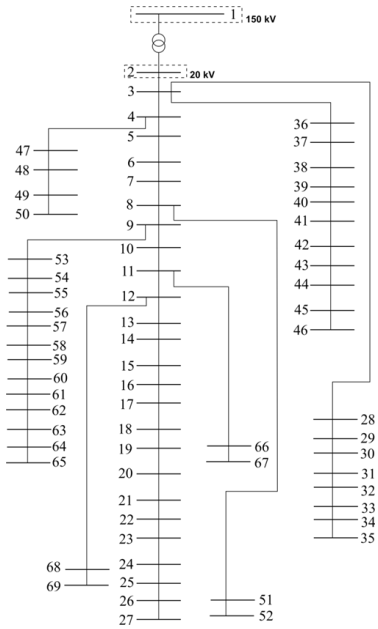

Figure 5.24: *69-bus distribution network*

In order to obtain the average behavior, each of the stated approaches was run 5 times and results are reported for averaged fitness in each generation per approach. Algorithm settings are the following:

- Population size 250 individuals;
- Number of generation cycles 200;
- Random initialization of the population;
- Three measurement configurations: 15, 22 and 30 measurement locations.

Figure 5.25 depicts the DN with the optimally located measurement equipment for 15, 22 and 30 measurement configurations respectfully.

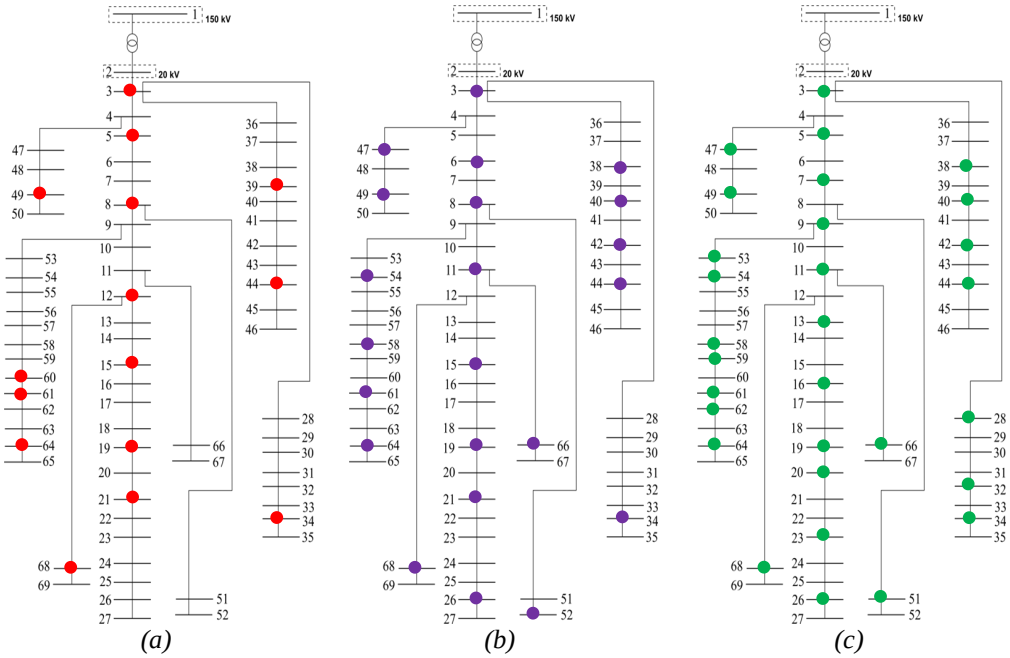

Figure 5.25: *Optimal locations for (a) 15, (b) 22 and (c) 30 measurement equipment*

The average simulation time with the previously stated algorithm settings is 2 h 38 min on Intel(R) Core(TM) i7-2600 CPU @ 3.4 GHz and 8 GB of RAM.

Figures 5.26, 5.27 and 5.28 show the convergence rate of integer approaches during 200 generations for 15, 22 and 30 measurements configuration respectively in 69-bus DN.

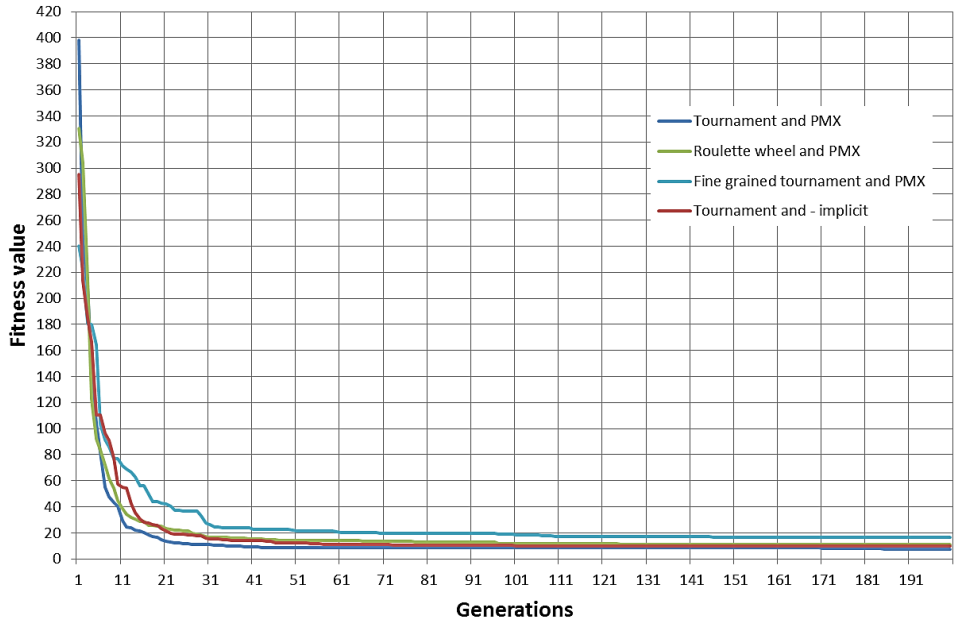

Figure 5.26: *Comparison of integer coding GAs – 15 measurements configuration*

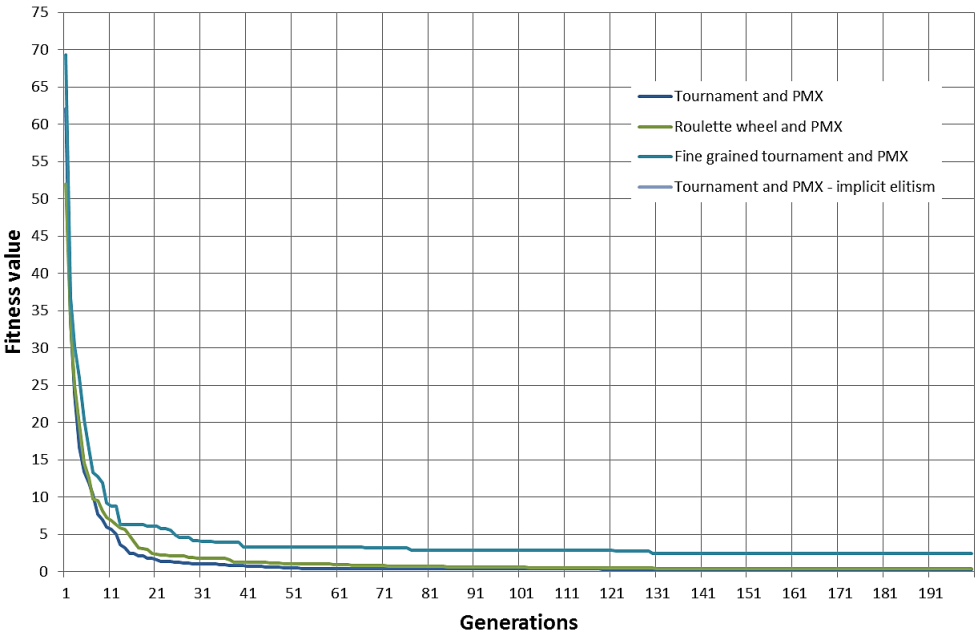

Figure 5.27: *Comparison of integer coding GAs – 22 measurements configuration*

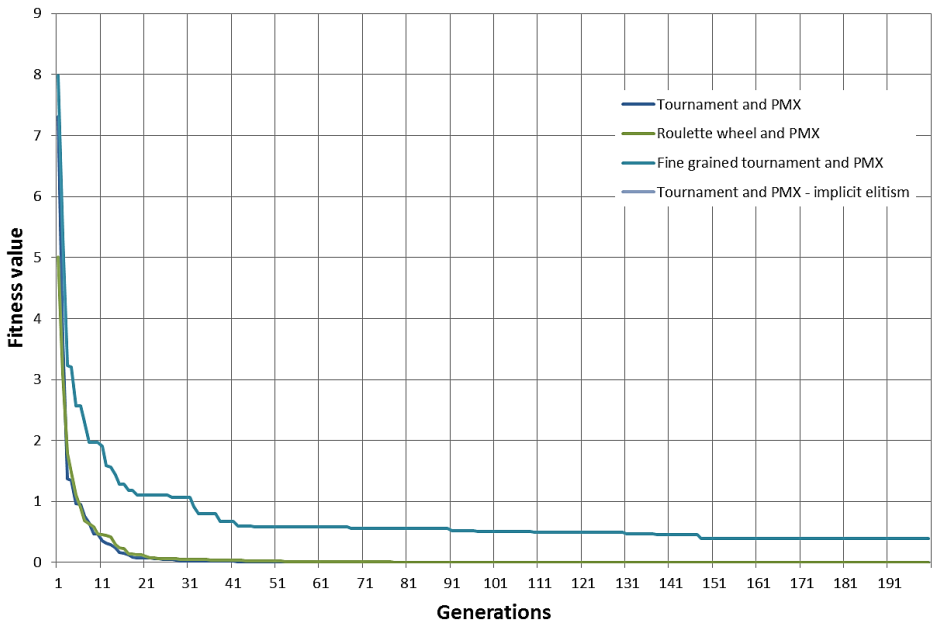

Figure 5.28: *Comparison of integer coding GAs – 30 measurements configuration*

Graphs demonstrate that all the approaches except integer coding GA with fine grained tournament selection, PMX crossover, mutation matrix approach and explicit elitist replacement converge to near-optimal region of solution in a limited number of generations (in all the cases around 70th generation. Near-optimal region of solutions is the solution region of the problem whose fitness values are significantly less than the starting fitness and without significant numerical improvements over many generations. In order to explore furtherly in how many cases out of 5 runs algorithms reach (sub)optimal solution and their pace of convergence, the results of the simulations are shown in the following Tables 5.5, 5.6 and 5.7.

Table 5.5: Convergence quality of the algorithms – 15 measurements configuration

Type of the algorithm	Number of generations to reach sub(optimal) solution	Number of attempts to reach (sub)optima solution /out of 5
1.	53	3
2.	39	2
3.	76	2
4.	More than 200	0

Table 5.6: Convergence quality of the algorithms – 22 measurements configuration

Type of the algorithm	Number of generations to reach sub(optimal) solution	Number of attempts to reach (sub)optima solution /out of 5
1.	77	3
2.	197	3
3.	More than 200	0
4.	More than 200	0

Table 5.7: Convergence quality of the algorithms – 30 measurements configuration

Type of the algorithm	Number of generations to reach sub(optimal) solution	Number of attempts to reach (sub)optima solution /out of 5
1.	86	4
2.	84	4
3.	125	2
4.	More than 200	0

As it can be seen from the previous tables, further examination of the approaches on 69-bus network has shown that Integer coding GA with tournament selection, PMX crossover, mutation matrix approach and implicit elitist replacement and Integer coding GA with tournament selection, PMX crossover, mutation matrix approach and explicit elitist replacement give the best results. Both approaches are well designed for OMEP problem in different problem environments.

As the last step in deciding which approach is the best, two of the best candidate algorithms were tested on 272-bus real DN and the results of this study can be summed in the following subchapter.

5.5.2.3.3 272-bus DN Tests

This is a larger size realistic DN with three voltage levels. It is highly active with 44 buses that contain DG. The only measured data correspond from the equipment installed on primary TS and DN transformers. Search space that was defined according to the rules from the subchapter 5.4.2.2 is of size 187.

As all the binary approaches did not demonstrate promising convergence quality and also, in last subchapter, two more approaches were discarded, the following tests were run only with the two best integer coding GAs:

1. Integer coding GA with tournament selection, PMX crossover, mutation matrix approach and implicit elitist replacement;
2. Integer coding GA with tournament selection, PMX crossover, mutation matrix approach and explicit elitist replacement.

In order to obtain the average behavior, the approaches were run 5 times and results are reported for averaged fitness in each generation per approach. Algorithm settings are the following:

- Population size 300 individuals;
- Number of generation cycles 200;
- Random initialization of the population;
- 25 measurement locations.

Figure 5.29 shows the comparison of convergence rate of the two best GA approaches. Figure 5.30 show the same comparison but on the scale of last 200 generations to distinguish better the difference between convergence curves.

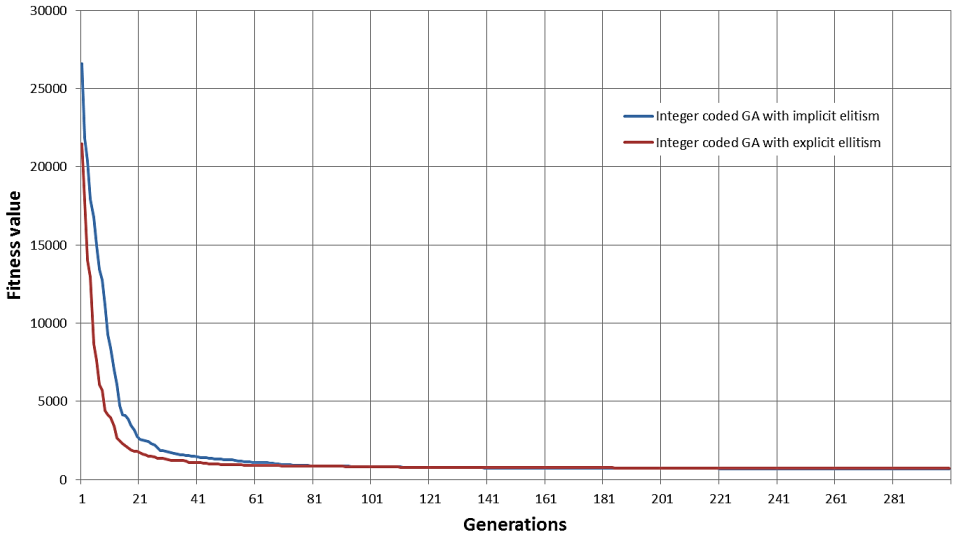

Figure 5.29: *Comparison of the two best integer approaches – 272-bus DN*

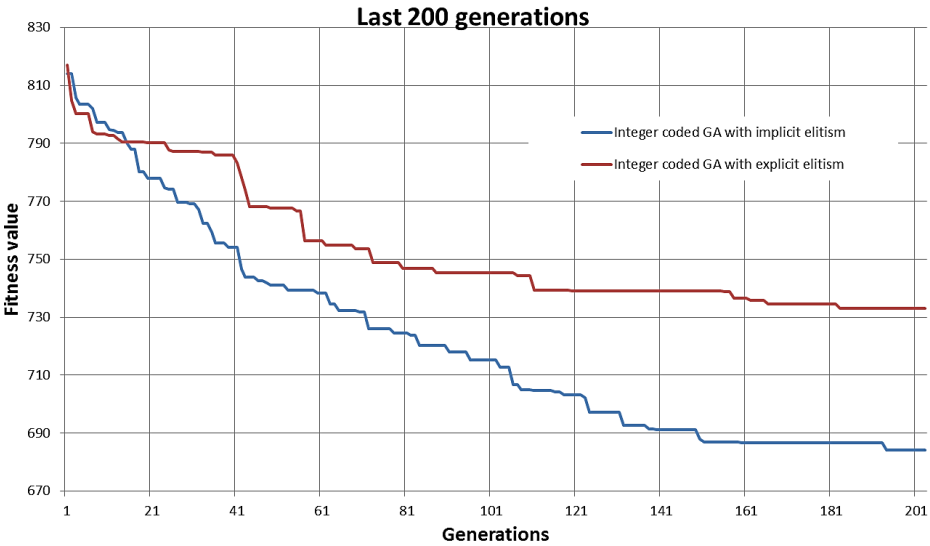

Figure 5.30: *Comparison of the two best integer approaches – last 200 generations*

From the Fig. 5.29, it can be concluded that both approaches have good convergence capabilities and reach near-optimal region of solutions in about 85 generations. Fig. 5.30 depicts the last 200 generations of generation process and offers the zoomed representations of parts of convergence curves.

From this figure we can finally conclude that the best approach for the OMEP problem is Integer coding GA with tournament selection, PMX crossover, mutation matrix approach and implicit elitist replacement.

5.5.3 General Design Strategy of OMEP in DNs

This subchapter is dedicated to the study that was conducted in order to design a general strategy for placement of the measurement equipment in various DNs. This is important, firstly, because if such a general recommendation can be made, *a priori* seeding of the initial population can be made in a way that the algorithm might converge faster and produce a solution of higher quality at the end of genetic process. Secondly, the

conclusions made in this way could offer DSOs or owners of the DN general guidelines about planning of new or improving of the existing DNs.

Hundred randomly generated measurement scenarios were created per test by altering load following a standard uniform distribution (± 60%). After that, GA was run as previously described. For the sake of this study, two DNs were created. First test DN is shown in Fig. 5.31. It is 48-bus DN with 5 distribution feeders.

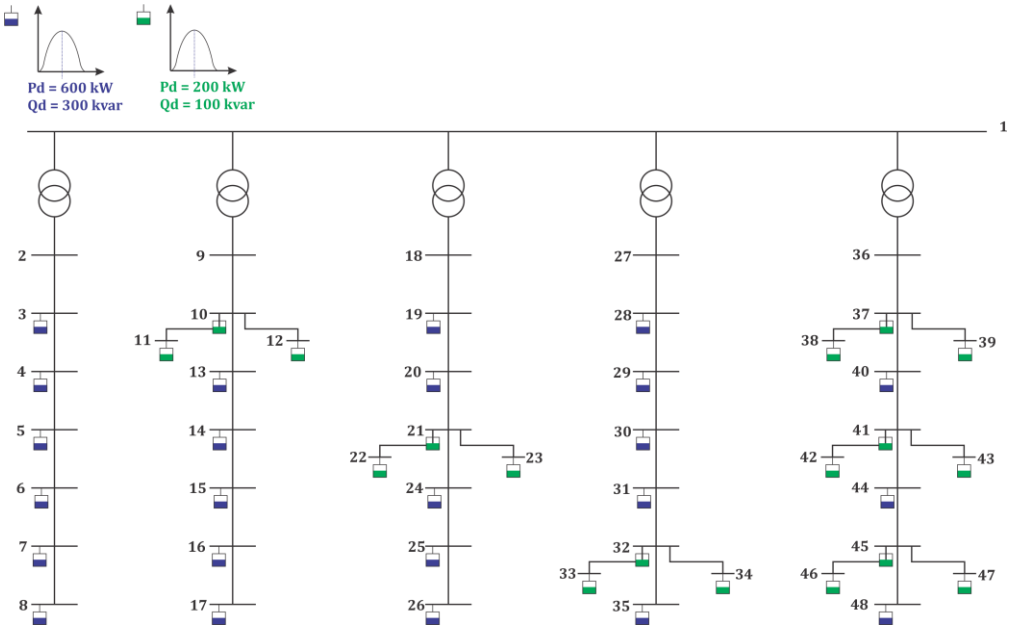

Figure 5.31: *48-bus test DN with equal loads*

All the primary substations have the same electrical characteristics. Branches do not have the same characteristics i.e. electrical distance between buses is different. First feeder is without *branching*, i.e. without secondary feeders. All the base values of the bus loads without branching are the same as noted by white-blue squares on the Fig. 5.31. The rest of the feeders contain the branching – second feeder at its beginning, third feeder at the middle, fourth feeder close to the end and last one contains all three previously described branching. Base bus loads at primary feeder with branching as well as base loads of the buses of the secondary feeders are the same and quantitatively less than the ones without branching (noted by white-green squares at the previous figure).

For each bus and each scenario, following sets have been defined:

V^{real} set of real scenario voltage magnitudes;
V^{est} set of voltage magnitudes after the completion of SE;
V^{error} set of voltage magnitude errors;
φ^{real} set of real scenario voltage angles;
φ^{est} set of voltage angles after the completion of SE;
φ^{error} set of phase angle errors.

Previously mentioned V^{error} and φ^{error} are computed in the following way:

$$V^{error} = \max_{k \epsilon bus} \left| \frac{V^{est} - V^{real}}{V^{real}} \right|^2$$
$$\varphi^{error} = \max_{k \epsilon bus} \left| \frac{\varphi^{est} - \varphi^{real}}{\varphi^{real}} \right|^2 \quad (5.25)$$

where:
k index of buses, k = 1,…,N_{bus}

After this step, i.e. finding the maximal errors of the estimates for each scenario, objective function is minimize the sum of V^{error} and φ^{error} on the scope of all scenarios. However, in the objective function, it is necessary to scale the terms for voltage magnitude and angle in order to make them comparable.

The first set of results (see Fig. 5.32) is corresponding to installing 5 measurement devices on a blank network (i.e. network without primary substation measurements).

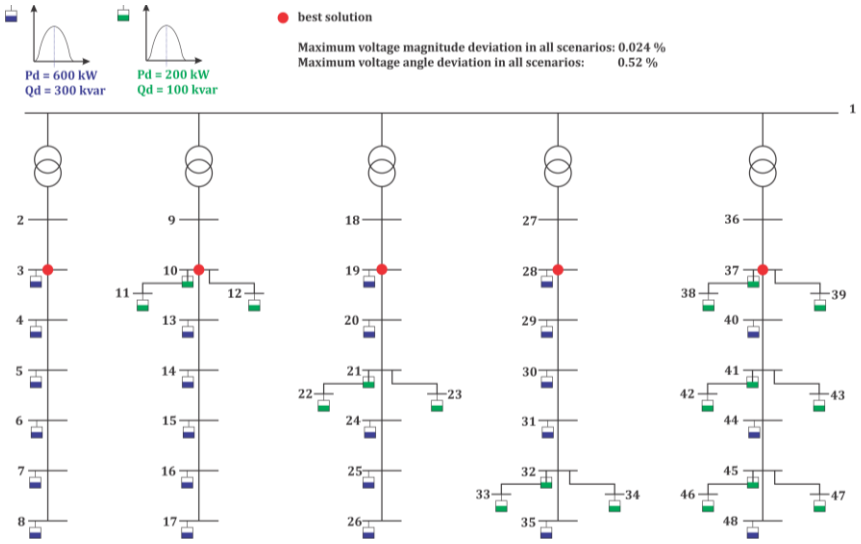

Figure 5.32: *Voltage objective function without primary substation measurements (5 meas. points)– equal loads*

As it can be seen from the figure, algorithm found that the best solution is obtained when placing 5 measurements at the beginning of each feeder of the DN. The explanation is the following: If the voltage at the beginning of the feeder is known, then both voltage magnitude and current of the feeder will be known. Algorithm chooses second and not the first bus of the feeder because this bus also contains load so in this way also the load will be measured (refer to subchapter 5.4.2.1 about the bus candidate) and therefore this offers better observability of the appropriate feeder.

In what regards the other results of this test case, one can see that the maximum voltage magnitude deviation of all the scenarios is 0.024%, while the maximum phase angle deviation of all the scenarios is 0.52%.

The second set of the results (see Fig. 5.33) corresponds to installing 5 measurement devices on a network with primary substation measurements (noted by blue dots in the figure).

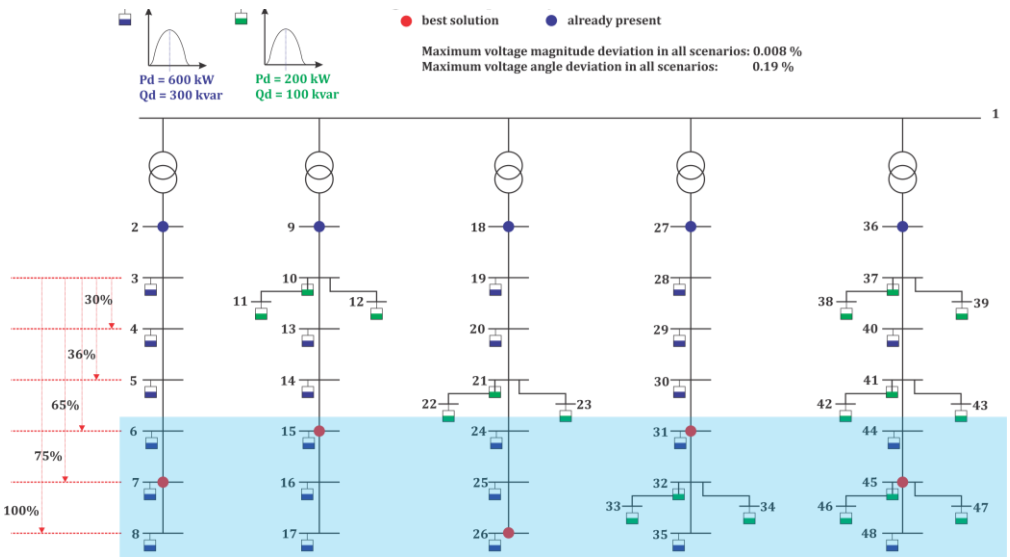

Figure 5.33: *Voltage objective function with primary substation measurements (5 meas. points) – equal loads*

Averagely, the feeder is equally loaded. Figure also shows relative electrical distance of appropriate buses from the first loaded bus in the primary feeder. Electrical distance between first bus with load and the remaining buses of that feeder is defined as relative impedance value between them.

In this case the algorithm cannot distinguish single clear position in terms of the topology and size of the load that would be common for each feeder. Rather, region of potential good solutions can be selected. This is because the feeder is equally loaded and therefore solution is influenced by the particular configuration of the scenario. To back up this conclusion, in next test 5 more measurement locations have been considered.

In what regards the other results of this test case, one can see that the maximum voltage magnitude deviation of all the scenarios is 0.008%, while the maximum phase angle deviation of all the scenarios is 0.19%.

The third set of the results (see Fig. 5.34) corresponds to installing 10 measurement devices on a network with primary substation measurements (noted by blue dots in the figure).

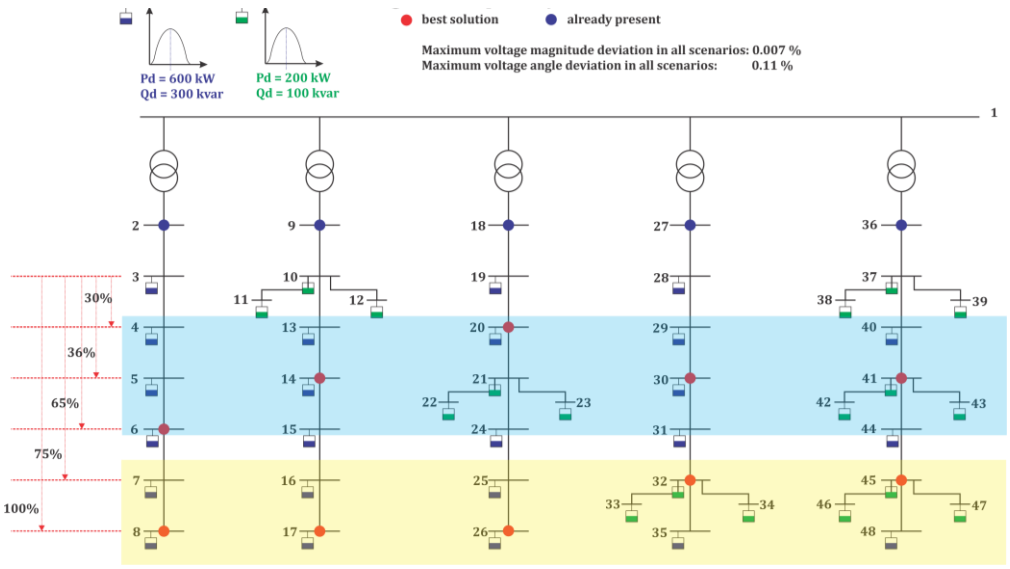

Figure 5.34: *Voltage objective function with primary substation measurements (10 meas. points) – equal loads*

As it can be seen, also in this case, solution is influenced by the particular configuration of the scenario. The algorithm does not find one clear location but rather two regions of possibly good solution. It is interesting, however, that the difference in fitness value given by solutions within the same region, e.g. bus 7 and 8 of the first feeder, are similar so deciding to place the equipment in bus 7 instead of bus 8 does not deteriorate the solution a lot.

In what regards the other results of this test case, one can see that the maximum voltage magnitude deviation of all the scenarios is 0.007%, while the maximum phase angle deviation of all the scenarios is 0.11%.

The second test DN is shown in Fig. 5.35. As the first one, this is also 48-bus DN with 5 distribution feeders. However, the feeders of this network are not equally loaded.

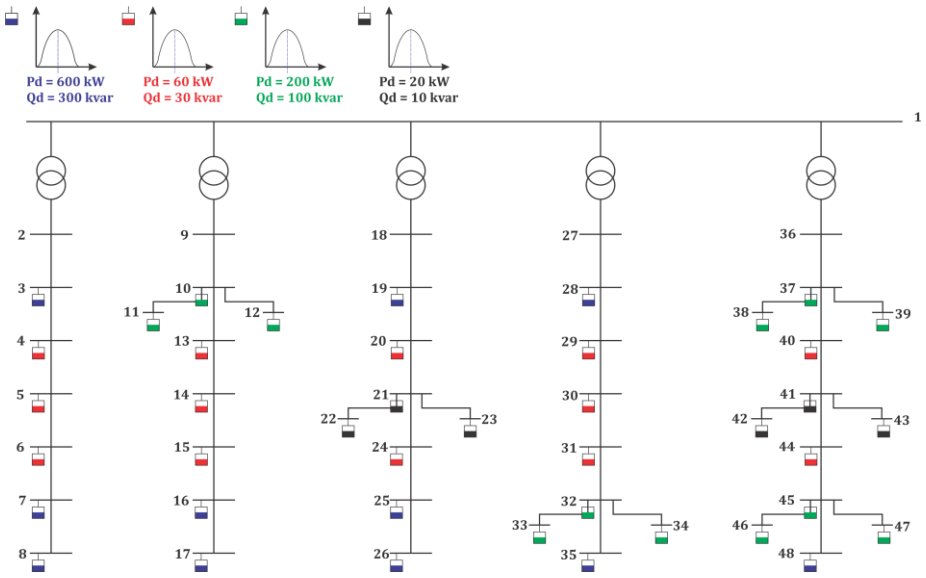

Figure 5.35: *48-bus test DN with unequal loads*

The primary substations have the same electrical characteristics and electrical distances between buses are different. The configuration of the feeders regarding branching is the same as in first DN as well. In this case, however, feeders are not equally loaded. It can be observed that each feeder contains more and less loaded buses. Heavily loaded buses are depicted with white-blue and white-green (in case of branching) squares while less loaded buses are depicted by white-red and white-black (in case of branching) squares in previous figure.

The first set of results (see Fig. 5.36) is corresponding to installing 5 measurement devices on a blank network (i.e. network without primary substation measurements).

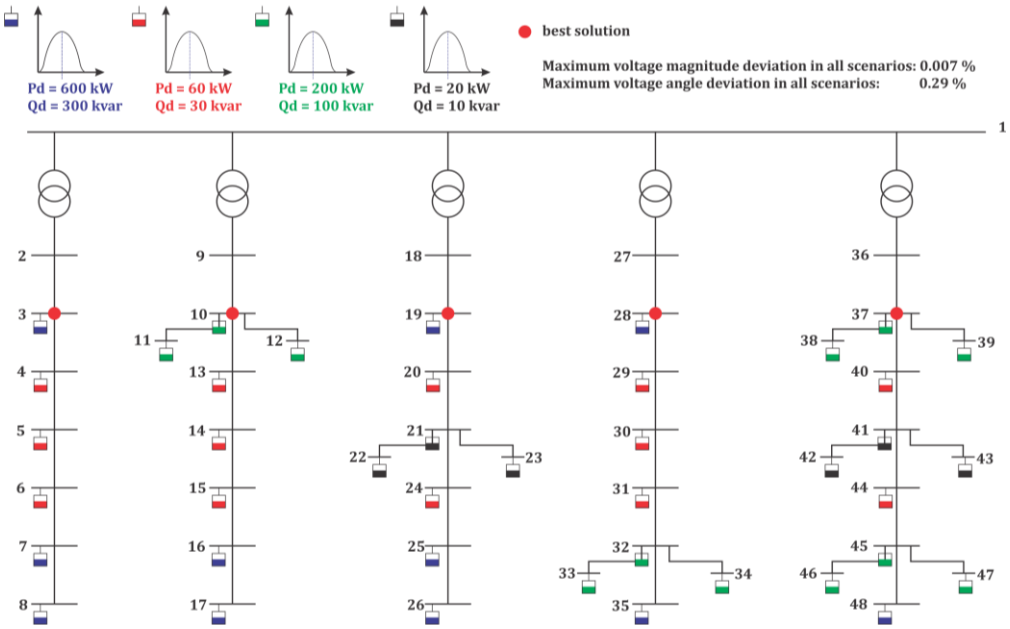

Figure 5.36: *Voltage objective function without primary substation measurements (5 meas. points) – unequal loads*

The first set of results corresponds to the ones already stated for the first DN, i.e. the best solution is obtained when placing 5 measurements at the beginning of each feeder of the DN.

In what regards the other results of this test case, one can see that the maximum voltage magnitude deviation of all the scenarios is 0.007%, while the maximum phase angle deviation of all the scenarios is 0.29%.

The second set of the results (see Fig. 5.37) corresponds to installing 5 measurement devices on a network with primary substation measurements (noted by blue dots in the figure).

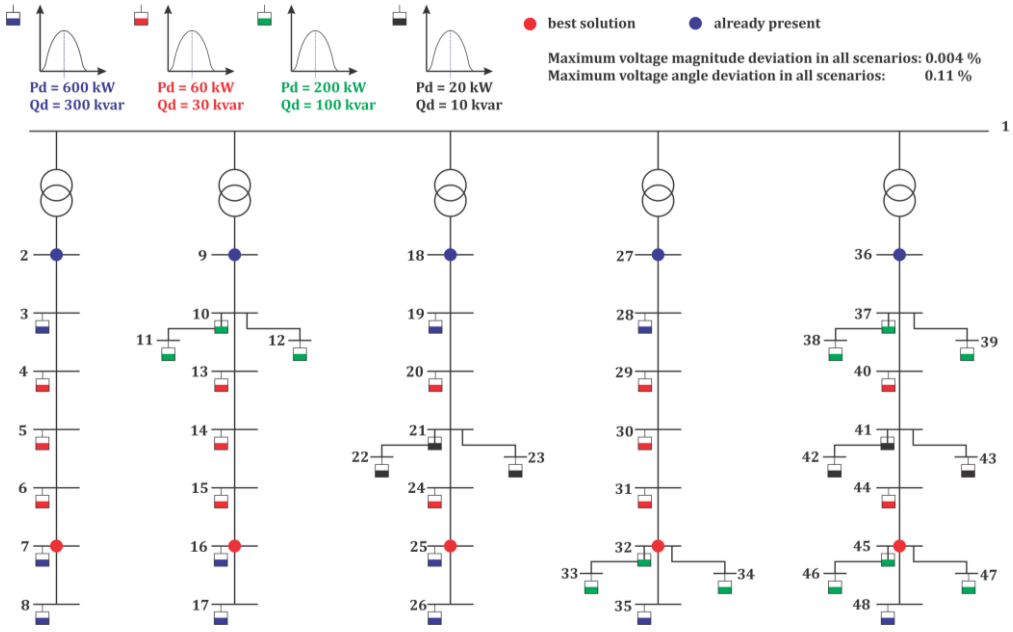

Figure 5.37: *Voltage objective function with primary substation measurements (5 meas. points) – unequal loads*

Unlike the case of the first DN, algorithm was capable to propose the same unique position for measurement placement in each feeder (red dots) and the solution is no more influenced by the particular configuration of the scenario. This position is close to highly loaded buses. The question of why is optimal location on penultimate and not ultimate bus of the feeder can arise. The answer is that measurement on penultimate bus (e.g. bus 7) ensures that the power flows between this bus and buses 6 and 8 are known. As the bus 8 is the ultimate bus, all the flow from bus 7 is going to load of bus 8. In return, very quality estimation of this load can be made. On the other side, buses 4, 5 and 6 are "less important" regarding estimator as the values of the load are much less but the estimates of these loads and the larger load in bus 3 can still be made with a fair quality thanks to measurements in buses 2 and 7.

In what regards the other results of this test case, one can see that the maximum voltage magnitude deviation of all the scenarios is 0.007%, while the maximum phase angle deviation of all the scenarios is 0.29%.

The last set of the results (see Fig. 5.37) corresponds to installing 10 measurement devices on a network with primary substation measurements (noted by blue dots in the figure).

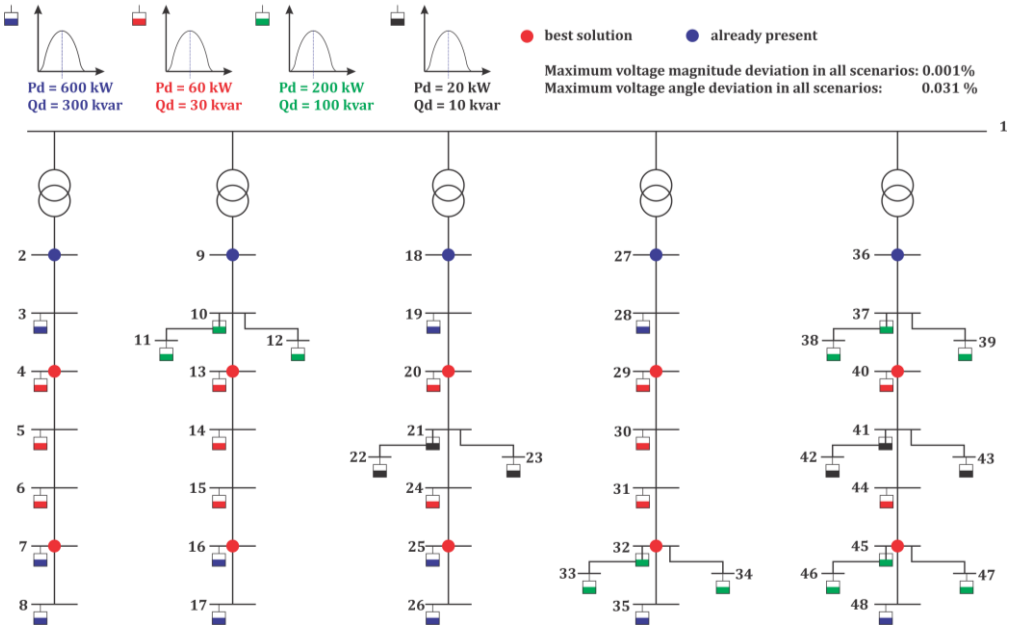

Figure 5.38: *Voltage objective function with primary substation measurements (10 meas. points) – unequal loads*

Also in this case algorithm was capable to propose the same unique position for measurement equipment in each feeder (red dots). Observing the optimal locations, following can be concluded: one optimal measurement location is proposed at the second bus with load and the other at penultimate bus of the feeder (observing from the top of the feeder). The conclusion about choice of the penultimate bus is the same as in previous case. Similar is with second bus with load of the feeder, e.g. bus 4. Although the size of the load corresponding to this bus is much less than the neighboring bus 3, algorithm proposes the placement of the equipment in bus 4. This ensures the knowledge of the power flow of line 3 – 4 and, as there is measurement equipment at primary substation, consecutively, the knowledge of the power flow of line 2 – 3. Therefore, also the load of the bus 3 is well estimated. It can be further concluded that with 3 measurement equipment, state of the 7 out of 5 buses can be very well estimated. Among these 7 buses, all heavily loaded buses can be well estimated.

5.6 Advanced Optimization of Measurement Equipment Placement Method

The core of this part of the dissertation is on the development of the multi-objective GA that could be used to optimize vast family of OMEP related realistic problems. This study can have a great importance for DSOs as it can be used to take into account different limitations or requests that are posed by DSOs when planning new network or improving the existing one. As developed OMEP software solution is highly modular, it can also be used to solve wider group of planning problems.

In the following subchapters, the mechanism of Genetic Multi-Objective Optimization (GMOO), specific GA for multi-objective optimization, NSGA-II, and a study regarding DN voltage observability will be explained.

5.6.1 Genetic Multi-Objective Optimization (GMOO)

A multi-objective optimization problem involves a number of objective functions which are to be either minimized or maximized. As in a single-objective optimization problem, the multi-objective optimization problem may contain a number of constraints which any feasible solution (including all optimal solutions) must satisfy. Since objectives can be either minimized or maximized, we state the multi-objective optimization problem in its general form [146]:

$$\begin{gathered} \min[\boldsymbol{f}_1(\mathbf{x}), \boldsymbol{f}_2(\mathbf{x}), \ldots, \boldsymbol{f}_j(\mathbf{x}), \ldots, \boldsymbol{f}_p(\mathbf{x})] \\ \text{subject to: } \boldsymbol{g}(\mathbf{x}) \leq 0 \\ \mathbf{x} \in \mathrm{X} \end{gathered} \tag{5.26}$$

where:

$\boldsymbol{f}_j(\mathbf{x})$ j-th OF considered (to be minimized);
$\boldsymbol{g}(\mathbf{x})$ the constraint vector (m elements);
$\mathbf{x}$ the control variable vector (n elements) and X is the feasibility region.

One of the striking differences between single-objective and multi-objective optimization is that in multi-objective optimization the objective functions constitute a multi-dimensional space, in addition to the usual decision variable space. This additional P-dimensional space is called the *objective space*. To make the descriptions clear, we refer a "solution" as a variable vector and a "point" as the corresponding objective vector.

The optimal solutions in multi-objective optimization can be defined from a mathematical concept of *partial ordering*. In the parlance of multi-objective optimization, the term domination is used for this purpose. In this subchapter, the stress is on the unconstrained (without any equality, inequality or bound constraints) optimization problems. The domination between two solutions is defined as follows [84],[119]:

Definition 5.1 *A solution $x^{(1)}$ is said to dominate the other solution $x^{(2)}$, if both the following conditions are true:*

1. *The solution $x^{(1)}$ is no worse than $x^{(2)}$ in all objectives. Thus, the solutions are compared based on their objective function values (or location of the corresponding points ($\mathbf{z}^{(1)}$ and $\mathbf{z}^{(2)}$) on the objective space).*
2. *The solution is $x^{(1)}$ strictly better than $x^{(2)}$ in at least one objective.*

For a given set of solutions (or corresponding points on the objective space, for example, those shown in Fig. 5.39(a)), a pair-wise comparison can be made using the above definition and whether one point dominates the other can be established. All points which are not dominated by any other member of the set are called the non-dominated points of class one, or simply the non-dominated points. For the set of six solutions shown in the figure, they are points 3, 5, and 6. One property of any two such points is that a gain in an objective from one point to the other happens only due to a sacrifice in at least one other objective. This *trade-off* property between the non-dominated points

makes the practitioners interested in finding a wide variety of them before making a final choice. These points make up a front when viewed them together on the objective space; hence the non-dominated points are often visualized to represent a non-domination front [121].

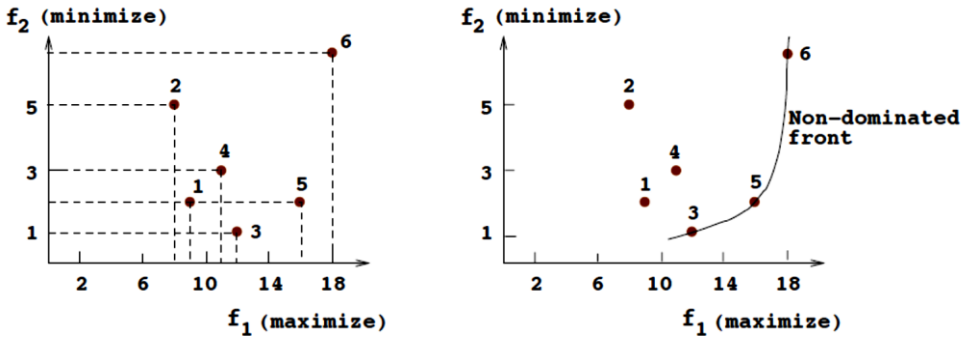

Figure 5.39: *A set of points and the first non-dominated front*

With the above concept, now it is easier to define the Pareto-optimal solutions in a multi-objective optimization problem. If the given set of points for the above task contain all points in the search space (assuming a countable number), the points lying on the non-domination front, by definition, do not get dominated by any other point in the objective space, hence are Pareto-optimal points (together they constitute the Pareto-optimal front) and the corresponding pre-images (decision variable vectors) are called Pareto-optimal solutions. However, more mathematically elegant definitions of Pareto-optimality (including the ones for continuous search space problems) exist in the multi-objective optimization literature [122],[123].

5.6.1.1 Principle of GMOO's Search

In the context of multi-objective optimization, the extremist principle of finding the optimum solution cannot be applied to one objective alone, when the rest of the objectives are also important. Different solutions may produce trade-offs (conflicting outcomes among objectives) among different objectives. A solution that is extreme (in a better sense) with respect to one objective requires a compromise in other objectives. This prohibits one to choose a solution which is optimal with respect to only one objective. This clearly suggests two ideal goals of multi-objective optimization:

1. Find a set of solutions which lie on the Pareto-optimal front, and
2. Find a set of solutions which are diverse enough to represent the entire range of the Pareto-optimal front.

Although one fundamental difference between single and multiple objective optimizations lies in the cardinality in the optimal set, from a practical standpoint a user needs only one solution, no matter whether the associated optimization problem is single or multi-objective. The user is now in a dilemma. Since a number of solutions are optimal, the obvious question arises: Which of these optimal solutions must one choose? This is not an easy question to answer. It involves higher-level information which is often non-

technical, qualitative and experience-driven. However, if a set of many trade-off solutions are already worked out or available, one can evaluate the pros and cons of each of these solutions based on all such non-technical and qualitative, yet still important, considerations and compare them to make a choice.

Thus, in a multi-objective optimization, ideally the effort must be made in finding the set of trade-off optimal solutions by considering all objectives to be important. After a set of such trade-off solutions are found, a user can then use higher-level qualitative considerations to make a choice. Since the GMOO procedure deals with a population of solutions in every iteration, it makes them intuitive to be applied in multi-objective optimization to find a set of non-dominated solutions. The GMOO based procedure works with the following principle in handling multi-objective optimization problems:

Step 1. Find multiple non-dominated points as close to the Pareto-optimal front as possible, with a wide trade-off among objectives;
Step 2. Choose one of the obtained points using higher-level information.

Since GMOO procedures are heuristic based, they may not guarantee in finding Pareto-optimal points, as a theoretically provable optimization method would do for tractable (for example, linear or convex) problems. But GMOO procedures have essential operators to constantly improve the evolving non-dominated points (from the point of view of convergence and diversity discussed above) similar to the way most natural and artificial evolving systems continuously improve their solutions.

In the first step of the GMOO-based multi-objective optimization, multiple trade-off, non-dominated points are found. Thereafter, in the second step, higher-level information is used to choose one of the obtained trade-off points. This dual task allows an interesting feature, if applied for solving single-objective optimization problems. It is easy to realize that a single-objective optimization is a degenerate case of multi-objective optimization [124]. In the case of single-objective optimization, having only one globally optimal solution, the first step will ideally find only one solution, thereby not requiring us to proceed to the second step. However, in the case of single-objective optimization having multiple global optima, both steps are necessary to first find all or multiple global optima, and then to choose one solution from them by using a higher-level information about the problem. Thus, although seems ideal for multi-objective optimization, the proposed framework can be ideally thought as a generic principle for both single and multiple objective optimization.

5.6.1.2 Generating Classical Methods and GMOO

In the generating Multi-Criteria Decision Making (MCDM) approach, the task of finding multiple Pareto-optimal solutions is achieved by executing many independent single-objective optimizations, each time finding a single Pareto-optimal solution. A parametric scalarizing approach (such as the weighted-sum approach, ϵ-constraint approach, and others) can be used to convert multiple objectives into a parametric single-objective function [125].

By simply varying the parameters (weight vector or ϵ-vector) and optimizing the scalarized function, different Pareto-optimal solutions can be found. In contrast, in the GMOO, multiple Pareto-optimal solutions are attempted to be found in a single simulation by emphasizing multiple non-dominated and isolated solutions [129].

Fig. 5.40 depicts how multiple independent parametric single-objective optimizations may find different Pareto-optimal solutions. The Pareto-optimal front corresponds to global optimal solutions of several scalarized objectives. However, during the course of an optimization task, algorithms must overcome a number of difficulties, such as infeasible regions, local optimal solutions, at regions of objective functions, isolation of optimum, etc., to converge to the global optimal solution. Moreover, due to practical limitations, an optimization task must also be completed in a reasonable computational time.

This requires an algorithm to strike a good balance between the extent of these tasks its search operators must do to overcome the above-mentioned difficulties reliably and quickly. When multiple simulations are performed to find a set of Pareto-optimal solutions, the above balancing act must be performed in every single simulation. Since simulations are performed independently, no information about the success or failure of previous simulations is used to speed up the process. In difficult multi-objective optimization problems, such memory-less *a posteriori* methods may demand a large overall computational overhead to get a set of Pareto-optimal solutions. Moreover, even though the convergence can be achieved in some problems, independent simulations can never guarantee finding a good distribution among obtained points.

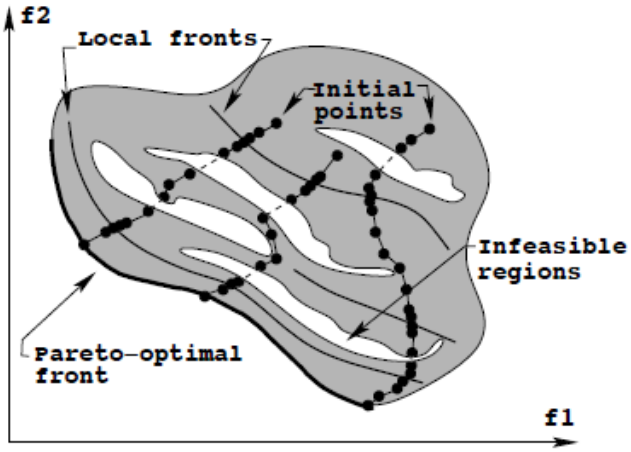

Figure 5.40: *Generative MCDM methodology employs multiple, independent single-objective optimizations*

GMOO, as mentioned earlier, constitutes an inherent parallel search. When a population member overcomes certain difficulties and make a progress towards the Pareto-optimal front, its variable values and their combination reflect this fact. When a recombination takes place between this solution and other population members, such valuable information of variable value combinations gets shared through variable exchanges and blending, thereby making the overall task of finding multiple trade-off solutions a parallelly processed task.

5.6.2 Elitist Non-dominated Sorting GA or NSGA-II

The NSGA-II procedure [125] is one of the popularly used GMOO procedures which attempt to find multiple Pareto-optimal solutions in a multi-objective optimization problem and has the following three features:

1. it uses an implicit elitist principle;
2. it uses an explicit diversity preserving mechanism;
3. it emphasizes non-dominated solutions.

Initially, a random parent population P_0 is created. The population is sorted based on the non-domination. Each solution is assigned a fitness (or rank) equal to its non-domination level (1 is the best level, 2 is the next-best level, and so on). Thus, minimization of fitness is assumed. At first, the tournament selection, crossover, and mutation operators are used to create an offspring population Q_0 of size N. Since elitism is introduced by comparing current population with previously found best nondominated solutions, the procedure is different after the initial generation. The t-th generation of the proposed algorithm is considered below.

The step-by-step procedure shows that NSGA-II algorithm is simple and straightforward. First, a combined population $R_t = P_t \cup Q_t$ is formed. The population R_t is of size $2N$. Then, the population R_t is sorted according to non-domination. Since all previous and current population members are included in R_t, elitism is ensured. Now, solutions belonging to the best nondominated set F_1 are of best solutions in the combined population and must be emphasized more than any other solution in the combined population. If the size of F_1 is smaller than N, all members of the set F_1 for the new population P_{t+1} are chosen. The remaining members of the population P_{t+1} are chosen from subsequent nondominated fronts in the order of their ranking. Thus, solutions from the set F_2 are chosen next, followed by solutions from the set F_3, and so on. This procedure is continued until no more sets can be accommodated. Say that the set F_l is the last nondominated set beyond which no other set can be accommodated. In general, the count of solutions in all sets from F_1 to F_l would be larger than the population size. To choose exactly N population members, we sort the solutions of the *last* front F_l using the crowded-comparison operator $\prec_n$ in descending order and choose the best solutions needed to fill all population slots. The NSGA-II procedure is also shown in Fig. 5.41. The new population P_{t+1} of size N is now used for selection, crossover, and mutation to create a new population Q_{t+1} of size N. It is important to note that we use a tournament selection operator but the selection criterion is now based on the crowded-comparison operator $\prec_n$. Since this operator requires both the rank and crowded distance of each solution in the population, we calculate these quantities while forming the population P_{t+1}.

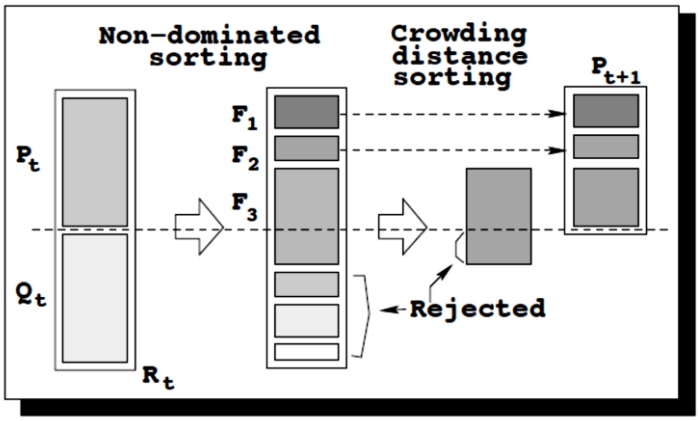

Figure 5.41: *Schematic of the NSGA-II procedure*

The diversity among nondominated solutions is introduced by using the crowding comparison procedure, which is used in the tournament selection and during the population reduction phase. Since solutions compete with their crowding-distance (a measure of density of solutions in the neighborhood), no extra niching parameter is required. Although the crowding distance is calculated in the objective function space, it can also be implemented in the parameter space, if so desired.

The crowded-sorting of the points of the last front which could not be accommodated fully is achieved in the descending order of their crowding distance values and points from the top of the ordered list are chosen. The crowding distance d_i of point i is a measure of the objective space around i which is not occupied by any other solution in the population. Here, quantity d_i is simply calculated by estimating the perimeter of the cuboid (Fig. 5.42) formed by using the nearest neighbors in the objective space as the vertices.

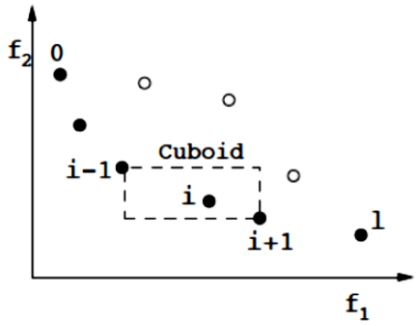

Figure 5.42: *The crowding distance calculation*

5.6.3 Application of Advanced OMEP – Voltage Observability

The DMS software development is in line with the DSOs requirements towards more advanced ways to control and manage the DN and also to plan the future networks or improve the existing ones in an optimal way.

Complete observability of the DN is hard to accomplish because of the poor number of measurement equipment and the other limitations that were already underlined. However, knowledge of the system state, e.g. voltage characteristic in some buses of the network is more crucial than in some other buses. In other words, DSO's requirement in this case is sharp observation of

voltages in some buses and a good (permissible) observation of the remaining ones.

The voltage observability requirement can be further explained observing the Fig. 5.43. It is obvious that the best observability is obtained by introducing the measurement equipment in all the buses of the network. For the DSO, knowledge of the voltage might be more important in buses 1 and 3 because bus 1 is the source of DN i.e. first bus of the distribution feeder and bus 3 contains generation unit. But what happens if we cannot install the equipment in both buses 1 and 3? We need to use OMEP algorithm. In this case, however, there are two sets of buses – buses 1 and 3 where the objective is $\Delta V_{1,3} \rightarrow 0$ ($\Delta V_i = \frac{V_i^m - V_i^{est}}{V_i^m}$) while $\Delta V_{2,4}$ should be reduced as much as possible.

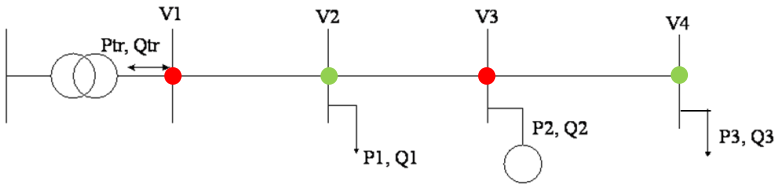

Figure 5.43: *Voltage observability in DN*

It is obvious that this is multi-objective problem. It can be solved by adapting it into single-objective problem or using the developed NSGA-II algorithm that gives the Pareto-optimal front in a single run.

In this study, one classical approach – weighted single objective GA and NSGA-II have been compared. Weighted single objective function was constructed in a following manner:

$$F_k = w_1 \, \Delta V_i + w_2 \, \Delta V_j \tag{5.27}$$

where:

F_k fitness of the *k*-th individual of the population;
w_1, w_2 weights of the objectives;
ΔV_i relative error (voltage objective) of the *i*-th measurement configuration;
ΔV_j relative error (voltage objective) of the *j*-th measurement configuration;
i index of the set of buses where exact observability is required;
j index of the set of buses where permissible observability is required.

There are two objectives of this study:

1. To find the optimal locations taking into account both objectives or more precisely in this case – sets of data
2. To compare the quality of NSGA-II solution with the classical GA.

5.6.3.1 Voltage Observability: 29-bus DN Test

First test case is the small test DN (depicted in Fig. 5.17) which was modified by adding 2 more generation plants – in buses 15 and 22. First set of buses includes the terminal buses of all the feeders (5, 16, 21, 28, and 29) and

buses with the generation plants (10, 15 and 22). The rest of the buses (excluding the buses with measurements previously installed – primary TS buses) are the members of the second set.

Algorithms settings are the following:

- Number of generation cycles is 200;
- Size of the population is 200;
- 5 measurement units;
- Successive changes of w_1 and w_2 by 0.1 steps (i.e. running classical GA eleven times starting from $w_1 = 1$ and $w_2 = 0$ until $w_1 = 0$ and $w_2 = 1$) to obtain the complete Pareto-optimal front as explained in the previous subchapter.

Resulting Pareto – optimal front using both weighted GA approach and NSGA-II approach are shown in Fig. 5.44.

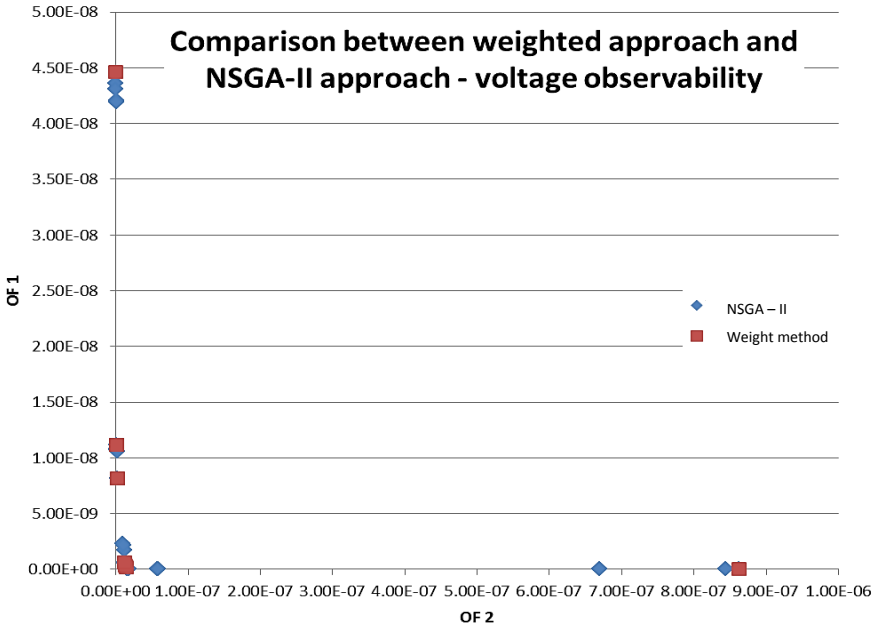

Figure 5.44(a): *Comparison of weighted and NSGA-II approach for voltage observability (29-bus DN)*

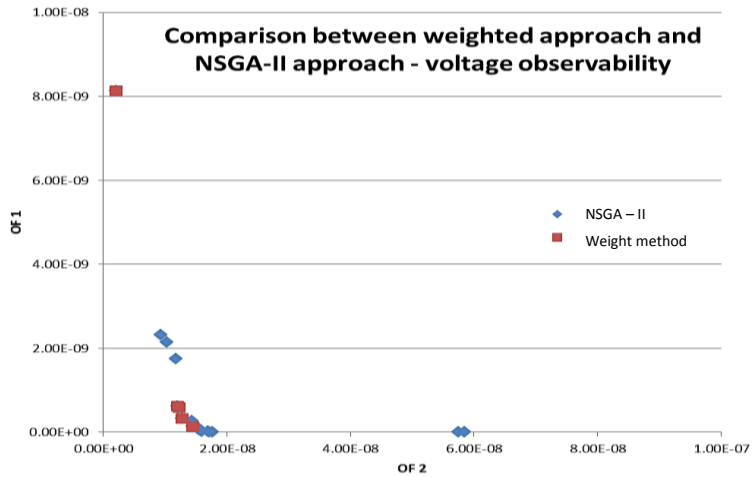

Figure 5.44(b): *Comparison of weighted and NSGA-II approach for voltage observability (29-bus DN)*

It can be seen from the Fig. 5.44(a) that using NSGA-II algorithm ensured high-quality solution compared to classical GA. Pareto-optimal front obtained in this way corresponds to the solution given by 11 successive runs of classical GA. Two best individuals (i.e. rank 1 individuals with infinite crowding distance) are exactly the same whether obtained running NSGA-II algorithm once or with critical values of weighted classical GA i.e. first and eleventh run ($w_1 = 1$, $w_2 = 0$ and $w_2 = 0$, $w_1 = 1$)

Fig. 5.44(b) offers the zoomed view of the Fig. 5.44(a) in order to further exam and conclude that the Pareto-optimal fronts really correspond one to another.

This is a very important conclusion as it offers the possibility to use NSGA-II algorithm for Advanced OMEP family of problems. It is ensured that the quality of the results obtained this way will be preserved. This is also important from the computational point of view. One simulation with the NSGA-II algorithm takes approximately the same amount of time as one simulation with the weighted method [125] so the solution is obtained 11 times faster. This is especially important for large-scale realistic DNs.

To sum up, the average simulation time with the weighted approach is 28 minutes per run, which summed up means 11·28 min = 308 min, while for the completion of NSGA-II simulation, only 28.2 min is required, on Intel(R) Core(TM) i7-2600 CPU @ 3.4 GHz and 8 GB of RAM per run.

5.6.3.2 Voltage Observability: 69-bus DN Test

Second test is used as the confirmation test for the conclusions made on small network. Therefore, the cause of the test is the same. It is necessary to conduct voltage observability study with two sets and compare the results obtained with classical weighted GA and special multi-objective NSGA-II algorithm.

Test network is depicted in Fig. 5.24 and its properties were previously described. First set of buses includes the terminal buses of all the feeders (27, 35, 46, 50, 52, 65, 67 and 69) and buses with the generation plants (9, 17, 20, 30, 41, 43, 57, 59 and 62). The rest of the buses (excluding the buses with measurements previously installed – primary TS buses) are the members of the second set.

Algorithms settings are the following:

- Number of generation cycles is 260;
- Size of the population is 200;
- 10 measurement units;
- Successive changes of w_1 and w_2 by 0.1 steps (i.e. running classical GA eleven times starting from $w_1 = 1$ and $w_2 = 0$ until $w_1 = 0$ and $w_2 = 1$) to obtain the complete Pareto-optimal front.

Resulting Pareto – optimal front using both weighted GA approach and NSGA-II approach are shown in Fig. 5.45.

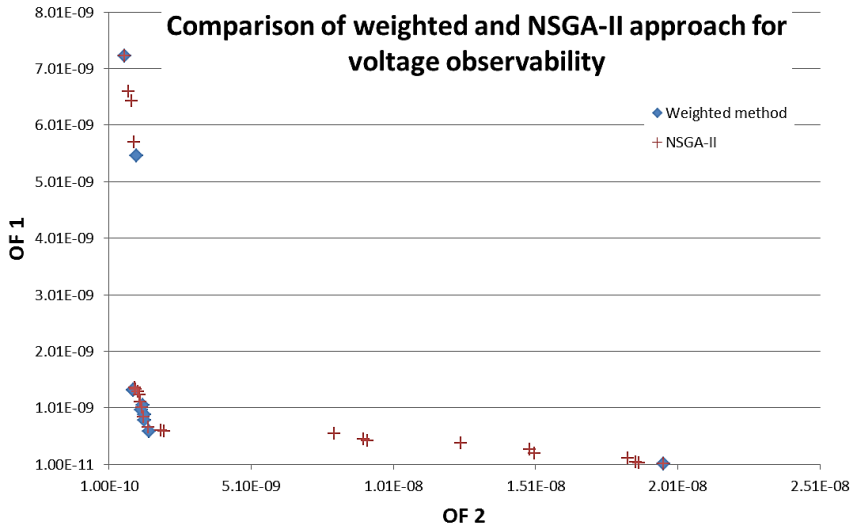

Figure 5.45: *Comparison of weighted and NSGA-II approach for voltage observability (69-bus DN)*

It can be seen from the Fig. 5.44 that the conclusions of the previous tests were confirmed also with the bigger DN.

To sum up, the average simulation time with the weighted approach is 2 h 38 min per run, which summed up means 11·2 h 38 min ≈ 29 h, while for the completion of NSGA-II simulation, only 2h 40 min is required, on Intel(R) Core(TM) i7-2600 CPU @ 3.4 GHz and 8 GB of RAM per run.

CHAPTER 6

6. Conclusion and Future Work

6.1 Conclusion

Power systems of today are the subject of one of the biggest structural, functional but also ethical change since the massive electrification started. From vertically oriented, they are changing to Smart Grids. From big concentrated generation plants, the global movement is towards dispersed generation plants that are mostly connected to MV and LV networks. This, indeed, changes the entire idea of not only the structure of power network but also its management. Many new technologies are introduced in power systems; they are interconnected with information technology now more than ever because the stakes are higher – information about the status of the network needs to be propagated in the optimal way and new management strategies need to be developed and used. Power systems are also going through ethical changes because of the rise of the consciousness about the planet and depletion of conventional energy sources.

In this massive movement, distribution systems are probably revolutionized the most as the major part of changes takes place here. Motivated by the need to improve distribution system management, operation and planning, this dissertation offers detailed mathematical models and applications of distribution system state estimation and optimization of measurement equipment placement. As discussed in the introduction, fields covered by this dissertation already are and will increasingly continue to be in the center of DMS software solutions as they are crucial for smart grid environment.

The main empirical findings of this dissertation are concentrated in Chapter 4 – Distribution System State Estimation and Chapter 5 – Optimization of Measurement Equipment Placement.

The first motivation to develop the DSSE was triggered by limited success in applying transmission system state estimation approach to

distribution environment; and additionally, specific approaches that have been developed for distribution systems experienced problems related to limitations of the distribution grids.

The second motivation is due to the fact that the increased penetration of dispersed generation is one of the main contributors to the new management mechanisms that are being developed. To improve the hosting capacity of the DN and to reduce the impact of DG on the regulation requirements of the bulk power system, the DG has to provide ancillary services (to solve local and global issues – frequency, reserve, voltage regulation, congestion management). Therefore the distribution system will assume the role of DSO. Premise of this is the knowledge of the network. For this reason, SE applied to DN is a main tool to improve the effects of DG penetration.

The aim was to develop computationally fast, robust and adaptable DSSE solution. For this reason, two SE modules have been developed and tested on vast number of test DNs and on different scenarios. While the Simplified SE can be used in most of the DN of today and provide satisfactory results with impressive computational speed, Advanced SE is aimed for DNs with more measurement points and it incorporates the power flow equations as constraints. It has lower speed than the simplified module, but it provides more accurate results in cases with high penetration of DG.

Both modules significantly improve the observability of the DN with a little information currently present and are suitable for real-time operational applications, which is a huge leap forward in DMS technology and reliable base for numerous functionalities that rely on SE. Practicability and reliability of the proposed SE is proven by the fact that it is operational in a number of nationwide DNs: Smart Grid ACEA, ASM – Terni, Grid4EU – ENEL (co-founded by the EU under the 7^{th} Framework Program), HERA – Modena (in operation from June 2014), and A2A – Milan (finalizing stage) [149].

On the other side, planning of the DNs has to be conducted much more carefully than in the past and therefore optimization procedures have to be enforced in the early stages of development of new networks. Chapter 5 of this dissertation is concerned with a very important planning functionality – optimization of the measurement equipment placement. Having elaborated on the fact that the knowledge of the network state is crucial for its operation, it is not hard to understand why the installation of the new measurement equipment has a central part in planning of the new or improvement of the existing DNs.

The proposed solution strongly reckons on genetic algorithms that have proven to possess good properties with large-scale problems like this one. Many different implementation approaches have been developed, tested and compared on large number of realistic test DNs for this dissertation and the best approach is recorded. Apart from the fact that the OMEP algorithm provides (sub)optimal solutions for all the tested systems, it is also robust, highly modular and easily implementable in DMS solutions.

One another empirical finding of this dissertation is the general design strategy of measurement equipment placement in DNs. Important guidelines for the planners of the DNs regarding the good practices of measurement placement are provided and backed up by a large number of tests.

Lastly, multi-objective genetic algorithm has been developed and tested with the specific DSO requirements in order to show the broad applicability of

the proposed OMEP solution. There are many more specific DSO requirements regarding planning of future networks that can be exploited with the proposed algorithm.

6.2 Future Work

This work opens several avenues for further investigation. The first involves the improvements of the developed DSSE software solution. As this solution is already used in a number of distribution control centers, the particularities of specific networks bring out the possible points of improvement of the solution itself as it needs to be globally operational, i.e. on a vast number of different realistic DNs. The developers of this functionality are already improving the algorithm in order to offer better estimate of the network state and enable even better observability which is, as many times underlined, crucial for other automated actions necessary in DNs.

Larger number of modern measurement equipment will also offer better utilization of DSSE software solution. This is where the second functionality described in this dissertation will find its place. SE techniques enable just the limited performance if the number of the measurement equipment is poor. The future field of study would be further implementation of the Advanced OMEP problem to different DSOs requirements.

One of the avenues is also further utilization of Advanced OMEP algorithm to similar families of problems. Exploitation of the algorithm can offer multiple breakthroughs in similar fields.

Of course, work can be done in continuous improvement of the algorithm itself, proposing other types of genetic operators and further interpretation of the results in order to make a generalized pattern for measurement equipment placement in distribution systems. These *a priori* solutions could also fasten the generation process by diminishing the number of generations necessary for the solution of the problem.

Bibliography

[1] National Academy of Engineering, "Greatest Engineering Achievements of the 20th Century", 2014. [Online]. Available: http://www.greatachievements.org/.

[2] Council of European Energy Regulators ASBL, "Guidelines of Good Practice on Estimation of Costs due to Electricity Interruptions and Voltage Disturbances", Brussels, 2010. [Online]. Available: http://www.ceer.eu/portal/page/portal/EER_HOME/EER_PUBLICATIONS/

[3] P. Donalek, R. Farmer, N. Hatziargyriou, I. Kamwa, P. Kundur, N. Martins, J. Paserba, P. Pourbeik, J. Sanchez-Gasca, R. Schulz, A. Stankovic, C. Taylor, V. Vittal, G. Andersson, "Causes of the 2003 major grid blackouts in North America and Europe and recommended means to improve system dynamic performance", *IEEE TRANSACTIONS ON POWER SYSTEMS*, vol. 20, no. 4, pp. 1922-1928, 2005.

[4] The Board of Directors of Enel SpA, "Preliminary Consolidated Results for 2013", ENEL, Rome, 2014. [Online]. Available: https://www.enel.com/en-gb/media/press_releases/

[5] V. P. Morano, "Aggregated Management of Distributed Energy Resources: Impact on the Electrical System", 2014. [Online]. Available: http://www.iit.upcomillas.es/pfc/resumenes/538a238fbf55a.pdf

[6] Eurelectric, "Active Distribution System Management", Eurelectric, 2013. [Online]. Available: http://www.eurelectric.org

[7] M. R. Mozayyani, Z. Modarres, H. S. Farmad, "Challenges Of Implementing Active Distribution System Management", in *CIRED Workshop*, Rome, 11-12 June 2014.

[8] The European Parliament and the council of the European Union, "Directive 2009/28/EC on the promotion of the use of energy from renewable sources", *Official Journal of the European Union*, pp. 1-47, 2009.

[9] The European Parliament and the Council of the European Union, "Directive 2012/27/EU on energy efficiency", *Official Journal of the European Union*, pp. 1-56, 2012.

[10] The European Parliament and the Council of the European Union, "Directive 2009/72/EC concerning common rules for the internal market in electricity", *Official Journal of the European Union*, pp. 1-39, 2009.

[11] R. van Gerwent, Distributed Generation and Renewables, Copper Development Association, Brussels, 2006.

[12] P. Birkner, Smart Grid in Practice, Mainova, Frankfurt, 2012. [Online]. Available: http://phoenix-forums.com/

[13] European Distribution Systems Operators for Smart Grids, "Flexibility: The role of DSOs in tomorrows' electricity market", European Distribution Systems Operators for Smart Grids, Brussels, 2014. [Online]. Available: http://www.edsoforsmartgrids.eu/

[14] E. Binda Zane, R. Bruckmann, D. Bauknecht, F. Jirous, R. Piria, N. Trennepohl, J. Bracker, R. Frank, J. Herling, "Integration of Electricity from Renewables to the Electricity Grid and to the Electricity Market", Ecleron, Berlin, 2012. [Online]. Available: http://www.oeko.de

[15] Eurelectric, "RES Integration and Market Design", Eurelectric, Brussels, 2011. [Online]. Available: http://www.eurelectric.org

[16] Autorita per l'energia elettrica e il gas, "Consultazioni", 1 August 2013. [Online]. Available: http://www.autorita.energia.it/it/index.htm.

[17] Expert Group for Regulatory Recommendations for Smart Grid Deployment, "Options on Handling Smart Grids Data", Expert Group for Regulatory Recommendations for Smart Grid Deployment, Brussels, 2013. [Online]. Available: http://ec.europa.eu/energy/

[18] Union Fenosa Distribucion & other entities, "Development of technological solutions for the Spanish Electricity Network of 2025", Union Fenosa Distribucion & other entities, Madrid, 1012. [Online]. Available: http://www.gasnaturalfenosa.com/es/1285338501612/inicio.html

[19] A. Becker, J. Schmiesing, E. Wehrmann, B. Werther, "Voltage control in low voltage systems with controlled low voltage Transformer (CLVT)", in *CIRED Workshop*, Lisbon, 29-30 May 2012.

[20] M. Zdrallek, J. Schmiesing, M. Schneider, H. H. Thies, "Future Structure of Rural Medium-voltage Grids for Sustainable Energy Supply", in *CIRED Workshop*, Lisbon, 29-30 May 2012.

[21] F. Gangale, G. Fulli, M. S. Jimenez, I. Onyeji, A. Colta, I. Papaioannou, A. Mengolini, C. Alecu, T. Ojala, I. Maschio, V. Giordano, "Smart Grid Projects in Europe: Lessons learned and current developments", Publications Office of the European Union, Luxembourg, 2013. [Online]. Available: http://ses.jrc.ec.europa.eu

[22] F. C. Schweppe, J. Wildes, "Power System Static-State Estimation, Part I: Exact Model", *IEEE Transactions on Power Apparatus and Systems*, vol. 89, no. 1, pp. 120-125, 1970.

[23] F. C. Schweppe, D. B. Rom, "Power System Static-State Estimation, Part II: Approximate Model", *IEEE Transactions on Power Apparatus and Systems*, vol. 89, no. 1, pp. 125-130, 1970.

[24] F. C. Schweppe, "Power System Static-State Estimation, Part III: Implementation", *IEEE Transactions on Power Apparatus and Systems*, vol. 89, no. 1, pp. 130-135, 1970.

[25] A. Abur, A. G. Exposito, Power System State Estimation - Theory and Implementation, New York: Marcel Dekker, Inc, 2004.

[26] A. J. A. S. Costa, Power System State Estimation: Orthogonal Methods for Estimation, Bad Data Processing and Techniques for Topological Observability, Waterloo: University of Waterloo, 1981. [Online]. Available: https://www.wpi.edu

[27] D. Denzel, G. Schellstedem, F. Aschmoneit, "Optimal Power System Static State Estimation" in *Proceedings of the 5th Power Systems Computation Conference*, Cambridge, 1-5 September 1975.

[28] A. Monticelli, P. Abreu, A. Garcia, "Fast Decoupled State Estimator and Bad Data Processing" *IEEE Trans. on Power Apparatus and Systems*, vol. 98, no. 5, pp. 1645-1652. 2007.

[29] K. L. Lo, P. S. Ong, R. D. McColl, A. M. Moffatt, J. L. Sulley, "Development of a Static State Estimation Part I: Estimation and Bad data Suppression", *IEEE Transactions on Power Apparatus and Systems*, vol. 7, no. 3, pp. 1378-1385, 1983.

[30] A. Garcia, A. Monticelli, "Reliable bad data processing for real-Time state Estimation", *IEEE Transactions on Power Apparatus and Systems*, vol. 102, no. 5, pp. 1126-1139, 1983.

[31] F. C. Schweppe, J. Kohlas, A. Fiechter, E. Handschin, "Bad data analysis for power system state estimation," *IEEE Transactions on Power Apparatus and Systems*, vol. 94, no. 2, pp. 329-337, 1975.

[32] S. Wang, E. Yu, N. Xiang, "A New Approach for Detection and Identification of Multiple Bad Data in Power System State Estimation", *IEEE Transactions on Power System State Estimation*, vol. 101, no. 2, pp. 454-462, 1982.

[33] T. Van Cutsem, L. Mili, M. Ribbens-Pavella, "Hypothesis testing identification: a new method for bad data analysis in power system state estimation", *IEEE Transactions on Power Apparatus and Systems*, vol. 101, no. 2, pp. 3239-3252, 1984.

[34] K. A. Clements, P. W. Davis, G. R. Krumpholz, "Power system observability: a

practical algorithm using network observability", *IEEE Transactions on Power Apparatus and Systems*, vol. 99, no. 4, pp. 1534-1542, 1980.

[35] A. Monticelli, F. F. Wu, "Network observability: identification of observable islands and measurement placement - parts 1 and 2", *IEEE Transactions on Power Apparatus and Systems*, vol. 103, no. 5, pp. 1035-1048, 1985.

[36] G. Golub, V. Klema, G. W. Stewart, "Rank degeneracy and least squares problems", Stanford University, Stanford, 1976. [Online]. Available: http://www.nber.org/papers/w165

[37] K. A. Clements, B. F. Wollenberg, "An Algorithm for Observability Determination in Power System State Estimation", in *IEEE Summer Power Meeting*, San Francisco, 20-25 July 1975.

[38] T. V. Cutsem, P. J. Gailly, "A simple algorithm for power system observability analysis and related functions", in *IFAC Symposium on Control Applications to Power System Security*, Florence, 5-8 Septmeber 1983.

[39] G. R. Krumpholz, P. W. Davis, K. A. Clements, "Power system state estimation with measurement deficiency - an algorithm that determines the maximal observable subnetwork", *IEEE Transactions on Power Apparatus and Systems*, vol. 101, no. 9, pp. 3044-3052, 1982.

[40] A. Simoes-Costa, A. Mandel, V. H. Quintana, "Power system topological observability using a direct graph - theoretic approach", *IEEE Transactions on Power Apparatus and Systems*, vol. 101, no. 3, pp. 617-626, 1982.

[41] A. Shaifu, V. Thornley, N. Jenkins, G. Strbac, A. Maloyd, "Control of Active Networks", in *18th International Conference on Electricity Distribution*, Turin, 6-9 June 2005.

[42] K. A. Clements, G. R. Krumpholz, P. W. Davis, J. W. Gu, "The solution of ill-conditioned power system state estimation problems", *IEEE Transactions on Power Apparatus and Systems*, vol. 102, no. 10, pp. 3473-3480, 1983.

[43] C. A. F. Murari, F. F. Wu, A. Monticelli, "A hybrid state estimator: solving normal equations by orthogonal transformations", *IEEE Transactions on Power Apparatus and Systems*, vol. 104, no. 12, pp. 3460-3468, 1985.

[44] N. Peterson, E. Adrian, F. Aschmoneit, "State estimation with equality constraints", in *Power Industry Computer Applications Conference*, Toronto, 24-27 May 1977.

[45] D. S. Watkins, Fundamentals of Matrix Computations, 2nd edition, New York: Wiley, 2002.

[46] R. Hoffman, "Practical State Estimation for Electric Distribution Networks", in *Power Systems Conference and Exposition*, Atlanta, 15-20 March 2006.

[47] P. P. Barker, R. W. De Mello, "Determining the impact of distributed generation on power systems: Part I - Radial Distribution Systems", in *IEEE Power Engineering Society Summer Meeting*, Seattle, 16-20 July 2000.

[48] F. C. Schweppe, J. Wildes, "Power system static state estimation - Part I, II & III", *IEEE Transaction on Power Apparatus and Systems*, vol. 89, no. 1, pp. 120-135, 1970.

[49] R. Critchley, E. Catz, M. Bazargan, P. Favre-Perrod, "New participants in smartgrids and associated challenges in the transition towards the grid of the future", in *IEEE Powertech*, Bucharest, 28 June - 2 July 2009.

[50] M. E. Baran, A. W. Kelley, "State estimation for real-time monitoring of distribution systems", *IEEE Transactions on Power Systems*, vol. 9, no. 3, pp. 1601-1609, 1994.

[51] S. Civanlar, J. J. Grainger, "Forecasting distribution feeder loads: modeling and application to volt/VAr control", *IEEE Transactions on Power Delivery*, vol. 3, no. 1, pp. 255 - 264 , 1988.

[52] A. J. Wood, B. F. Wollenberg, Power Generation, Operation and Control, New York: John Wiley & Sons, 1978.

[53] M. E. Baran, A. W. Kelley, "A branch-current-based state estimation method for

distribution systems", *IEEE Transactions on Power Systems*, vol. 10, no. 1, pp. 483-491, 1995.

[54] J. H. Teng, W. H. E. Liu, C. N. Lu, "Distribution System State Estimation", *IEEE Transactions on Power Systems*, vol. 10, no. 1, pp. 229-240, 1995.

[55] D. I. H. Sun, *Distribution System Loss Analysis and Optimal Planning - PhD Dissertation*, Arlington: University of Texas, 1980. [Online]. Available: www.uta.edu

[56] K. Li, "State estimation for power distribution system and measurement impact", *IEEE Transactions on Power Systems*, vol. 11, no. 2, pp. 911-916, 1996.

[57] A. P. Sakis Meliopoulos, F. Zhang, "Multiphase Power Flow and State Estimation for Power Distribution Systems", *IEEE Transactions on Power Systems*, vol. 11, no. 2, pp. 939-946, 1996.

[58] S. Lee, K. Vu, C.C. Liu, "Loss Minimization of Distribution Feeders: Optimality and Algorithms", *IEEE Transactions on Power Delivery*, vol. 4, no. 2, pp. 1281-1289, 1989.

[59] J. Jerome, "Network observability and bad data processing algorithm for distribution networks", in *Power Engineering Society Summer Meeting*, Vancouver, 15-19 July 2001.

[60] B. C. Pal, R. A. Jabr, R. Singh, "Choice of estimator for distribution system state estimation", *IET Generation, Transmission and Distribution*, vol. 3, no. 7, pp. 666-678, 2008.

[61] S. S. Blackman, Multiple target tracking with radar applications, Dedham: Artech House, Inc., 1986.

[62] H. Singh, F. L. Alvarado, "Weighted Least Absolute Value state estimation using interior point methods", *IEEE Transactions on Power Systems*, vol. 9, no. 3, pp. 1478-1484, 1994.

[63] P. J. Huber, Robust Statistics, New York: John Wiley & Sons, 1981.

[64] T. Kozubowski, K. Podgorski, S. Kotz, The Laplace Distribution and Generalizations, Basel: Birkhäuser, 2001.

[65] S. K. Salman, S. F. Tan, "Investigation into Protection of Active Distribution Network with High Penetration of Embedded Generation Using Radial and Ring Operation Mode", *Proceedings of the 41st International Universities Power Engineering Conference UPEC '06*, vol. 3, pp. 841-845, Newcastle-upon-Tyne, 6-8 September 2006.

[66] M. Bigoloni, I. Rochira, M. Rodolfi, F. Zanellini, C. Bovo, V. Ilea, M. M. Subasic, Merlo, G. Monfredini, R. Bonera, M. Arigoni, "The InGrid project and the evolution of supervision & control systems for Smart Distribution System management", in *Convegno Nazionale AEIT*, Mondello, 3-5 October 2013.

[67] I. Rochira, M. Bignoli, M. Rodolfi, F. Zanellini, C. Bovo, M. Merlo, V. Ilea, G. Monfredini, M. Subasic, R. Bonera, "Smart distribution system the ingrid project and the evolution of supervision & control systems for smart distribution system management", in *AEIT Annual Conference*, Mondello, 3-5 October 2013.

[68] A .Berizzi, C. Bovo, V. Ilea, M. Merlo, G. Monfredini, M. Subasic, C. Arrigoni, F. Zanellini, F. Corti, I. Rochira, "Advanced Functions for DSOs Control Center", in *IEEE Powertech*, Grenoble, 16-20 June 2013.

[69] C. Bovo, V. Ilea, M. Subasic, F. Zanellini, C. Arrigoni, R. Bonera, "Improvement of Observability in Poorly Measured Distribution Networks", *PSCC 2014*, Wroclaw, 17-23 August 2014.

[70] D. L. Lubkeman, M. J. Downey, R. H. Jones, A. K. Ghosh, "Distribution circuit state estimation using a probabilistic approach", *IEEE Transactions on Power Systems*, vol. 12, no. 1, pp. 45-51, 1997.

[71] A. Abur, B. Gou, "An Improved Measurement Placement Algorithm for Network Observability", *IEEE Transactions on Power Systems*, vol. 16, no. 4, pp. 819-824, 2001.

[72] S. Premrudeepreechacharn, C. Rakpenthai, "An Optimal PMU Placement Method Against Measurement Loss and Branch Outage", *IEEE Transactions on Power Delivery*, vol. 22, no. 1, pp. 101-107, 2007

[73] J. Z. A. W. K. M. E. Baran, "Meter Placement for Real-Time Monitoring of Distribution Feeders", *IEEE Transactions on Power Systems*, vol. 11, no. 1, pp. 332-337, 1996.

[74] N. Schulz, H. Wang, "A Revised Branch Current-Based Distribution System State Estimation Algorithm and Meter Placement Impact", *IEEE Transactions on Power Systems*, vol. 19, no. 1, pp. 207-213, 2004.

[75] F. Pilo, G. Pisano, S. Sulis, C. Muscas, "Optimal Placement of Measurement Devices in Electric Distribution Systems", in *Instrumentatiton and Measurement Technology Conference IMTC 2006*, Sorrento, 24-27 April 2006.

[76] N. Jenkins, G. Strbac, A. Shafiu, "Measurement location for state estimation of distribution networks with generation", *IEEE Proceedings on Generation, Transmission and Distribution*, vol. 152, no. 2, pp. 240-246, 2005.

[77] B. Pal, R. Vinter, R. Singh, "Measurement Placement in Distribution System State Estimation", *IEEE Transactions on Power Systems*, vol. 24, no. 2, pp. 668-675, 2009.

[78] M. Begovic, B. Milosevic, "Nondominated Sorting Genetic Algorithm for Optimal Phasor Measurement Placement", *IEEE Transactions on Power Systems*, vol. 18, no. 1, pp. 69-75, 2003.

[79] D. E. Goldberg, Genetic Algorithms in Search, Optimization, and Machine Learning, Reading: Addison-Wesley, 1989.

[80] B. C. Pal, R. A. Jabr, R. B. Vinter, R. Singh, "Meter Placement for Distribution System State Estimation: An Ordinal Optimization Approach", *IEEE Transactions on Power Systems*, vol. 26, no. 4, pp. 2328-2335, 2011.

[81] U. Derigs, Optimization and Operations Research, Cologne: Eolss Publishers Company Limited, 2009.

[82] P. M. Pardalos, D.Z. Du, R. L. Graham, "Combinatorial optimization", in *Handbook of Combinatorics*, Cambridge, MA, MIT Press, 1995, pp. 1541-1597.

[83] A. Schrijver, "A course in combinatorial optimization," TU Delft, Delft, 2000.

[84] D. S. Johnson, M. R. Garey, Computers and Intractability; A Guide to the Theory of NP-Completeness, New York: W. H. Freeman & Co., 1990.

[85] K. Deb, "Multi-objective optimization using evolutionary algorithms", in *Multi-objective optimization*, New York, John Wiley & Sons, 2001, pp. 13-46.

[86] D. B. Fogel, Evolutionary Computation: The Fossil Record, Piscataway, NJ: Wiley-IEEE Press, 1998.

[87] A. Owens, M. Walsh, L.J. Fogel, Artificial Intelligence Through Simulated Evolution, New York: Wiley and Sons, 1966.

[88] I. Rechenberg, Evolutionsstrategie: Optimierung technischer Systeme nach Prinzipien der biologischen Evolution, Stuttgart: Frommann-Holzboog Verlag, 1973.

[89] H. Schwefel, Numerische Optimierung von Computer - Modellen mittels der Evolutionsstrategie, Basel: Birkhauser, 1977.

[90] J. Holland, Adaptation in Natural and Artificial Systems, Ann Harbor: University of Michigan Press, 1975.

[91] Z. Michalewicz, Genetic Algorithms + Data Structures = Evolution Programs, Berlin: Springer-Verlag, 1992.

[92] M. L. Cramer, "A representation for the adaptive generation of simple seqential programs", in *Proceedings of the First International Conference on Genetic Algorithms*, Hillsdale, NJ, 1-6 August 1985.

[93] J. R. Koza, Genetic Programming, Cambridge, MA: MIT Press, 1992.

[94] P. Moscato, "On Evolution, Search, Optimization, Genetic Algorithms and Martial Arts: Towards Memetic Algorithms", California Institute of Technology, Pasadena, CA, 1989.

[95] C. Cotta, P. Moscato, "A gentle introduction to memetic algorithms", *Handbook of Metaheuristics*, Boston, MA, Kluwer Academic Publishers, 2003, pp. 105-144.

[96] R. E. Smith, "Diploid genetic algorithms for search in time varying environments", in *Annual Southeast Regional Conference of the ACM*, New York, NY, 10-19 April 1987.

[97] C. R. Reeves, "Using genetic algorithms with small populations", in *Proceedings of the Fifth International Conference on Genetic Algorithms*, San Mateo, CA, 1993.

[98] C. Cotta, "On the evolutionary inference of temporal boolean networks", in *Computational Methods in Neural Modeling*, Berlin, Springer-Verlag, 2003, pp. 494-501.

[99] J. Grefenstette, C. Ramsey, "Case-based initialization of genetic algorithms", in *Proceedings of the Fifth International Conference on Genetic Algorithms*, San Mateo, CA, 1993.

[100] J. E. Baker, "Reducing bias and inefficiency in the selection algorithm", in *Proceedings of Second International Conference on Genetic Algorithms*, Hillsdale, NJ, 1987.

[101] D. L. Whitley, "Using reproductive evaluation to improve genetic search and heuristic discovery", in *Proceedings of Second International Conference on Genetic Algorithms*, Hillsdale, NJ, 1987.

[102] L. Thiele, T. Bickle, "A mathematical analysis of tournament selection", in *Proceedings of Sixth International Conference on Genetic Algorithms*, San Francisco, CA, 1995.

[103] D. Goldberg, K. Deb, "A comparative analysis of selection schemes used in genetic algorithms", in *Foundations of Genetic Algorithms*, San Mateo, CA, Morgan Kaufman Publishers, Inc., 1991, pp. 69-93.

[104] E. Cantu-Paz, "Order statistics and selection methods of evolutionary algorithms", *Information Processing Letters*, vol. 82, no. 1, pp. 15-22, 2002.

[105] P. E. Raue, Z. Ruttkay, A.E. Eiben, "Genetic algorithms with multi-parent recombination", in *Lecture Notes in Computer Science*, Berlin, Springer-Verlag, 1994, pp. 78-87.

[106] J. Troya, C. Cotta, "Information processing in transmitting recombination", *Applied Mathematics Letters*, vol. 16, no. 6, pp. 945-948, 2003.

[107] N. J. Radcliffe, "The algebra of genetic algorithms", *Annalss of Mathematics and Artificial Intelligence*, vol. 10, no. 4, pp. 339-384, 1994.

[108] G. Syswerda, "Uniform crossover in genetic algorithms", in *Third International Conference on Genetic Algorithms*, San Mateo, CA, 1989.

[109] A. R. Reddy, G. Singh, K. Deb, "Optimal scheduling of casting sequence using genetic algorithms", *Journal of Materials and Manufacturing Processes*, vol. 18, no. 3, pp. 409-432, 2003.

[110] K. Deb, "An introduction to genetic algorithms", *Sadhana*, vol. 24, no. 4, pp. 293-315, 1999.

[111] G. Rudolph, "Convergence analysis of canonical genetic algorithms", *IEEE Transactions on Neural Networks*, vol. 5, no. 1, pp. 96-101, 1994.

[112] I. Wegener, T. Jensen, "On the utility of populations", in *Proceedings of Genetic and Evolutionary Computation Conference*, San Mateo, CA, 2001.

[113] N. J. Radcliffe, "Forma analysis and random respectful recombination", in *Proceedings of Fourth International Conference on Genetic Algorithms*, San Diego, CA, 1991.

[114] L. Thiele, T. Blickle, "A Comparison of Selection Schemes used in Genetic Algorithms", TIK-Zurich, Zurich, 1995, [Online]. Available: www.tik.ee.ethz.ch

[115] D. Whitley, "The genitor algorithm and selection pressure: Why rank-based allocation of reproductive trials is the best", in *Proceedings of 3rd International Conference on Genetic Algorithms*, Fairfax, 1989.

[116] V. Filipovic, "Fine-grained Tournament Selection Operator in Genetic Algorithms", *Computing and Informatics*, vol. 22, no. 3, pp. 143-161, 2003.

[117] J. Baker, "Reducing Bias and Inefficiency in the Selection Algorithm", *Proceedings of the Second International Conference on Genetic Algorithms and their Application*, Hillsdale, NJ, 1987.

[118] R. Lingle, D. E. Goldberg, "Alleles, Loci and the Traveling Salesman Problem", in *Proceedings of the First International Conference on Genetic Algorithms*, Pittsburg, 1985.

[119] K. Deep, H. Mebrahtu, "Novel GA for metropolitan stations of Indian railways when modelled as a TSP", in *International Journal of Combinatorial Optimization Problems and Informatics*, vol. 3, no. 1, pp. 47-69, 2012.

[120] R. Tiwari, R. Kala, A. Shukla, Real Life Applications of Soft Computing, Boca Raton, FL: Taylor & Francis Group, 2002.

[121] K. Miettinen, Nonlinear Multiobjective Optimization, Boston: Kluwer, 1999.

[122] F. Luccio, F. P. Preparata, H. T. Kung, "On finding the maxima of a set of vectors", *Journal of the Association for Computing Machinery*, vol. 22, no. 4, pp. 469-476, 1975.

[123] M. Ehrgott, Multicriteria Optimization, Berlin: Springer, 2000.

[124] S. Tiwari, K. Deb, "Omni-optimizer: A generic evolutionary algorithm for global optimization", *European Journal of Operations Research*, vol. 185, no. 3, pp. 1062-1087, 2008.

[125] K. Deb, A. Pratap, S. Agarwal, T. Meyarivan, "A fast and Elitist multi-objective Genetic Algorithm: NSGA-II", *IEEE Transactions on Evolutionary Computation*, vol. 6, no. 2, pp. 182-197, 2002.

[126] Eurelectric, "Power Distribution in Europe - Facts and Figures", Eurelectric, 2013. [Online]. Available: http://www.eurelectric.org

[127] J. W. Chinneck, Practical Optimization: A Gentle Introduction, Ottawa, Carleton University, 2004. [Online]. Available: http://www.sce.carleton.ca

[128] D. Bertsimas, I. Popescu, "Optimal Inequalities in Probability Theory: A Convex Optimization Approach", *Society for Industrial and Applied Methematics*, vol. 15, no. 3, pp 780-804, 2005

[129] K. Deb, "Multi-Objective Optimization Using Evolutionary Algorithms: An Introduction", *KanGAL Report*, Kanpur, 2011. [Online]. Available: http://www.iitk.ac.in

[130] E. Alba, C. Cotta, "Evolutionary Algorithms", Universidad de Malaga, Malaga, 2004. [Online]. Available: www.lcc.uma.es

[131] Terna, "Piano di sviluppo 2014 (in Italian)," Rome, 2013. [Online]. Available: www.terna.it

[132] EirGrid, "Winter Outlook 2013-2014," Belfast, 2013. [Online]. Available: www.eirgrid.com

[133] F. Coffele, M. Dolan, C. Booth, G. Ault, G. Burt, "Coordination of protection and active network management for smart distribution networks", in *CIRED Workshop*, Lisbon, 29-30 May 2012.

[134] Eurelectric, "Active Distribution System Management - A key tool for the smooth integration of distributed generation", Eurelectric, 2013. [Online]. Available: http://www.eurelectric.org

[135] D. Pudjianto, M. Castro, G. Strbac, E. Gaxiola, "Transmission infrastructure investment requirements in the future European low carbon electricity sytem", *International Conference on the European Energy Market*, Stockholm, 27-31 May 2013

[136] F. C. Schweppe, D. B. Rom, "Power system static state estimation, part 2: approximate model", *IEEE Transactions on Power Apparatus and Systems*, vol. 89, no. 1, pp. 125-130, 1970.

[137] International Electrotechnical Comission, "International Standard IEC60909", IEC, Geneva, 2001.

[138] The Department of Mathematical Sciences at The University of Alabama in Huntsville, "The Chi-Square Distribution", [Online]. Available: http://www.math.uah.edu/stat/special/ChiSquare.html

[139] U. N. Khan, "Impact of Distributed Generation on Distributed Network", University of Technology, Wroclaw, 2008 [Online]. Available: http://www.dwm.pwr.wroc.pl

[140] R. D. Zimmerman, C. E. Murillo-Sánchez & D. Gan, "MATPOWER - A MATLAB Power System Simulation Package", Power Systems Engineering Research Center - Arizona State University, [Online].
Available: http://www.pserc.cornell.edu//matpower/#docs.

[141] M. Merlo, N. Scordino, F. Zanellini, "Optimal Power Flow approach to manage Dispersed Generation rise and passive load energy needs over distribution grid", *International Review of Electrical Engineering*, vol. 8, no. 5, pp. 1482-1493, 2013.

[142] CEI EN 50160 *Voltage Characteristics of Electricity Supplied by Public Distribution Networks*, May 2011

[143] G. Beaulineu, M. Bollen, S. Malgarotti, R. Ball, "Power Quality Indices and Objectives", *International Conference and Exhibition on Electricity Distribution - CIRED*, Turin, 6-9 June 2005.

[144] C. Bovo, M. Baioni, A. Berizzi, "Power quality impact of cogeneration modules in urban networks", *International Conference on Harmonics and Quality of Power*, Bergamo, 26-29 September 2010.

[145] L. Kumpulainen, K. Kauhaniemi, "Analysis of the impact od distributed generation on automatic reclosing", *IEEE Power System Conference and Exposition*, Hong Kong,10-13 October 2004.

[146] A. Berizzi, C. Bovo, M. Innorta, P. Marannino, "Multiobjective optimization techniques applied to modern power systems", *IEEE Power Engineering Society Winter Meeting*, vol. 3, Columbus, 28. January - 1. February 2004.

[147] A. H. Land, A. G. Doig, " An Automatic Method of Solving Discrete Programming Problems", *Econometrica*, vol. 28, no. 3, pp. 497-520, 1960.

[148] R. K. Ahuja, T. L. Magnanti, J. B. Orlin, Network Flows: Theory, Algorithms, and Applications, Prentice Hall, Upper Saddle River, 1993.

[149] A. Berizzi, C. Bovo, V. Ilea, M. Merlo, G. Monfredini, M. Subasic, M. Bigoloni, I. Rochira, R. Bonera, "Architecture and functionalities of a smart Distribution Management System", *IEEE International Conference on Harmonics and Quality of Power (ICHQP)*, Bucharest, 25-28 May, 2014.